Climate-driven shifts in abundance, distribution, and composition of the pelagic fish community in a rapidly changing Pacific Arctic

Robert Max Levine

A dissertation

submitted in partial fulfillment of the

requirements for the degree of

Doctor of Philosophy

University of Washington

2021

Reading Committee:

Daniel Grünbaum, Chair

Rebecca Woodgate

Alex De Robertis

Program Authorized to Offer Degree:

Oceanography

University of Washington

Abstract

Climate-driven shifts in abundance, distribution, and composition of the pelagic fish community in a rapidly changing Pacific Arctic

Robert Max Levine

Chair of the Supervisory Committee:
Professor Emeritus Daniel Grünbaum
Oceanography

The Chukchi Sea is experiencing rapid environmental change due to warming temperatures, reductions in sea ice, and increases in transport of warm southern-origin waters into the region. Continued changes in the physical environment may further alter the marine ecosystem, resulting in changes in the community structure and composition. This dissertation examines the role of the environment in structuring the distribution and composition of the pelagic fish community in the eastern Chukchi Sea. Using a multi-platform approach centered around the use of fisheries acoustics, I investigate the impact of changing climate on the distribution of age-0 gadids that have historically dominated the pelagic fish community in the Chukchi Sea in summer. Chapter 2 uses repeat acoustic surveys conducted using autonomous surface vehicles and particle tracking simulations to examine potential movement of the age-0 gadid population in summer. During summer, the size of fishes increased during a period of wind-driven retention on the shelf, indicating that the Chukchi shelf may serve as an important nursery region for these age-0 fishes. Chapter 3 investigates the changes in the abundance and distribution of pelagic fishes observed in

summer acoustic-trawl surveys in 2012, 2013, 2017, and 2019. While age-0 Arctic cod (*Boreogadus saida*) remain the dominant pelagic fish, walleye pollock (*Gadus chalcogrammus*), a boreal species, have become increasingly abundant in recent years, driven by increases in temperature and transport on the Chukchi Sea shelf. This suggests that environmental conditions now allow pollock to extend their northern range into the southern and central Chukchi Sea, at least on a seasonal basis. In Chapter 4, two years of seafloor-mounted moored echosounder observations are used to identify the seasonal abundance and movement of the age-0 fishes observed in summer. The moorings identify strong seasonal trends in fish abundance and pelagic community composition driven by the advective transport of fishes from the south. The cumulative flux of fishes to the northeast suggests that these age-0 fishes are likely exported off the shelf in late fall and winter. Chapter 5 presents a classroom activity on underwater acoustics for use in elementary to undergraduate education, emphasizing the importance of hands-on experiential learning and ocean technology.

Together, these findings indicate that the composition of the pelagic fish community in the Chukchi Sea is primarily structured by transport. Changes in the transport of Pacific-origin water is increasing the abundance of boreal species in the Chukchi Sea, with the potential to further alter the composition of the pelagic community in the future. This dissertation provides insight into how the integration of observations across a wide range of spatial and temporal scales can help identify the mechanisms that drive the distribution and composition of pelagic fishes. These findings further our understanding of the mechanisms that drive fish abundance and distribution in the Chukchi Sea, and the identification of the role of transport in shaping fish distributions in the region provides us with information that will help to predict the future state of Arctic fish communities.

TABLE OF CONTENTS

LIST OF FIGURES

LIST OF TABLES

ACKNOWLEDGEMENTS

Thank you to Danny Grünbaum, my advisor, for his support, guidance, and advice over the past 5+ years. Danny has continuously told me to think with my feet while being a steadfast example of how to do so. Danny has both encouraged me and provided the opportunities to explore new skills and experiences, from my interests in education and outreach to going full speed into (potentially ill-advised) side projects. Throughout my degree, he has been able to filter and reflect my incoherent ramblings into insightful guidance and taught me to embrace the entire research process.

Thank you to my committee members Rebecca Woodgate, Julie Keister, Alex De Robertis, Franz Mueter, and Kristin Laidre for your feedback, research insights, collaborations, and for keeping me moving forward throughout this process.

I owe many thanks to Alex, who along with Chris Wilson, took a chance on hiring me 7 years ago. Alex has been instrumental in my development as a researcher and my success as a graduate student and scientist, providing never-ending support and guidance in navigating my research and career. Alex and Chris have made sure that every moment of my time since I arrived in Seattle was a learning opportunity, from how to break a hammer lock to including me in the proposal that would become my dissertation, all while putting in countless hours behind the scenes to set me up for success.

To go back even further, I would never have ended up in Seattle if it were not for Chuck Greene, who a decade ago guided me into the world of bioacoustics. Chuck gave me the opportunity to attend what would turn out to be the penultimate bioacoustics workshop at Friday Harbor Labs, my first ever course credits at UW, and my first real dive into oceanography. That

workshop led me to my future network of mentors: Gareth Lawson, Peter Wiebe, and Andone Lavery who adopted me into their labs and, along with Chuck, provided me with invaluable hands-on experience in my first stint in grad school that led me to where I am today.

I have had the privilege of being part of an incredible lab group and community here at UW. Thank you to my lab mates Sasha, Amy, Deana, Katie, and Tansy for making lab meetings, celebrations (and commiserating over failures) a family event. Thank you to my incredible friends: Zac, Max, and the MSB/Waffle Wednesday crew, Ann, Isaiah, Anna, David, Hannah, Hannah, Brendan, Tess, Erik, Ryan, Jiwoon, and the rest of my 2016 cohort, and the entire Oceanography graduate student community.

Thank you to the North Pacific Research Board for funding my dissertation. Thank you to NOAA and PMEL for the additional support that made it possible to further expand the scope of this research and providing the space and facilities to do so. Thank you to all of the Arctic Integrated Ecosystem Research Program investigators, Danielle, Matt, and NPRB staff for making me feel included and valued as a member of the program.

My dissertation research would not have been possible without the incredible network of people who have helped me along the way. Thank you to all of my coauthors for the time and guidance you've provided, and of course your patience. Thank you to Sandy, Patrick, Rick, Kresimir, Scott, and the rest of the MACE division for giving me your time and space, helping me with equipment, code, and data, and holding doors open, no questions asked, as I mysteriously wheeled equipment around Sand Point. I also owe a lot to everyone who has spent time on a ship with me in the past five years. Over the course of three field seasons of Arctic cruises during my PhD, I've had the chance to work with some incredible people at sea from whom I've learned so much and have been incredible resources in addition to becoming great friends.

I've been fortunate to have a committee that has allowed me to deviate into side projects, whether knowingly or not, which has led me to friends and colleagues I otherwise would not have had the chance to work with. In particular, thank you to Kristin, Johna, Chris, Dax, Tina, Wu-Jung, Sophie, and the entire OOI-ECS community for welcoming me and for your mentorship.

Thank you to my family, Mom, Dad, Jen, Ryann, and Ralph. You've always made me feel safe to pursue my passions, and regardless of whether you've understood what I'm actually doing at any given point, have made me feel loved and supported at all times. And to my west coast family, Linda, Audrey, Nigel, McKinley, Cindy, Stephen, Tom, Jodene, and Anne: thank you for making me feel at home since that very first summer at Friday Harbor. Finally, thank you to my wife Claire. We've been by each other's side through a combined five degrees, seven institutions, and too much sea time to count. You're my best friend, biggest cheerleader, and greatest source of motivation. At this point, you are also likely one of the world-leading experts in Arctic gadid ecology. You've been an inspiring example of how to act true to your values and show love and care to those around you.

DEDICATION

To Claire, for always leading by example.

CHAPTER 1. INTRODUCTION

The shallow continental shelf of the Chukchi and northern Bering Seas function as a transition zone between the Pacific and Arctic Oceans (Figure 1.1). The region serves as the Pacific gateway to the Arctic Basin, concentrating the flow of heat, freshwater (Woodgate and Peralta-Ferriz, 2021), and nutrients (Mordy et al., 2020) through the Bering Strait and across the Chukchi Sea shelf by northward currents, driven by local winds and the pressure head between the two basins (Coachman and Aargaard, 1966; Woodgate et al., 2005; Danielson et al., 2014; Woodgate, 2018). The marine environment of the continental shelf exhibits high seasonal variability, with cool water and sea ice cover for as much as half of the year, and rapid warming in summer as sea ice retreats. The enhanced flushing of Pacific water across the shallow Chukchi Sea in summer drives strong seasonal dynamics, triggering ice melt (Woodgate et al., 2010) and sparking productivity that supports a large Pacific Arctic ecosystem (Grebmeier et al., 2006). This seasonal productivity also supports a large pelagic fish community present on the shelf in summer (De Robertis et al., 2017).

The Arctic has been undergoing rapid changes associated with surface warming and loss of sea ice (Frey et al., 2015; Bliss et al., 2019; Danielson et al., 2020). The Chukchi Sea is one of the seasonally ice-covered areas where this decrease is clearly observed (Duarte et al., 2012; Frey et al., 2015; Wood et al., 2015). With sea ice in the Chukchi Sea melting earlier by 2.3 days decade^{-1} (Stroeve et al., 2014), more extensive phytoplankton blooms in open water may shift the balance of the benthic-pelagic coupling towards a pelagic-dominated ecosystem (Wassman and Reigstad, 2011; Moore and Stabeno, 2015; Hunt et al., 2016). The region is predicted to experience further warming (Overland et al., 2019) and sea ice loss (Wang et al., 2018), the ecological consequences of which are unclear. Observations indicate that the Pacific Arctic may be on the cusp of a major

shift in the region across all levels of the ecosystem as a result of these physical changes (Huntington et al., 2020; Mueter et al., 2021), as evidenced by northward shifts in the distribution of zooplankton (Spear et al., 2020), benthic fauna (Waga et al., 2020), and seabirds (Kuletz et al., 2020), and delays in the migration timing of marine mammals (Druckenmiller et al., 2018).

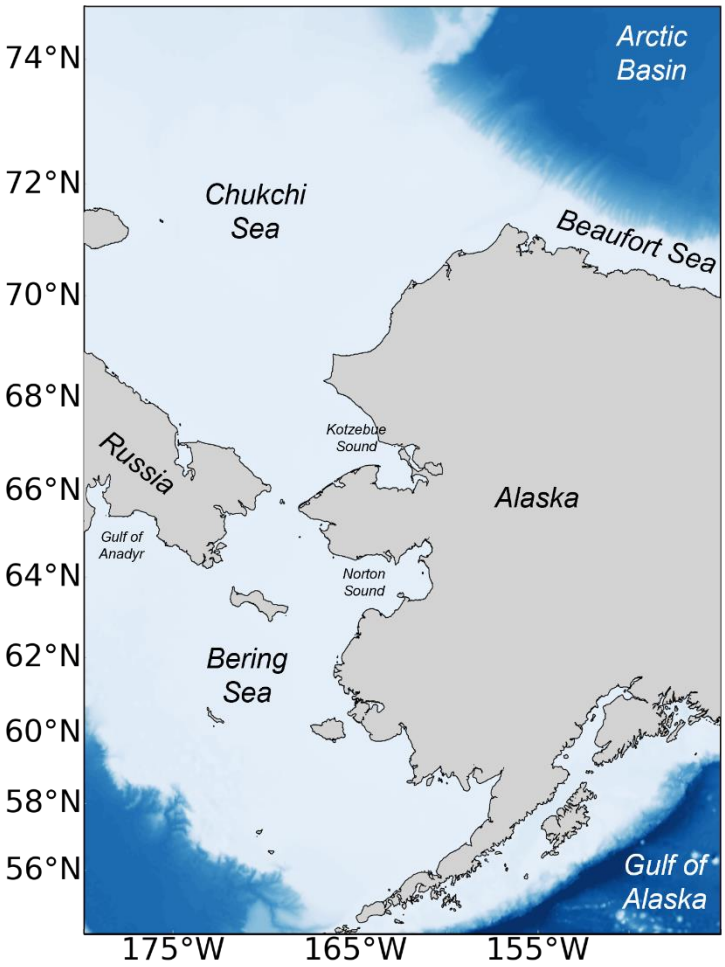

Figure 1.1 Map of the Pacific Arctic. The shallow continental shelves of the Bering, Chukchi, and Beaufort Seas are indicated by the lighter colors.

The presence of sea ice and the remoteness of the Pacific Arctic have historically limited our ability to study pelagic fishes. The eastern and western portions of the region lie in the U.S. and Russian exclusive economic zones, respectively, neither of which operate large-scale

commercial fisheries in the Chukchi Sea. Until recent decades, efforts to characterize the ecosystem have been limited (Logerwell et al., 2015). Recent investment in the Arctic has led to increased research and efforts to evaluate the ecological impact of further disturbance and changes in climate (Hopcroft et al., 2013; Grebmeier et al., 2015a; Logerwell et al., 2015; Mueter et al., 2017). The region is considered a benthic-dominated system where relatively low grazing pressure results in a large amount of carbon export to the seafloor, supporting a benthic-based food web (Grebmeier et al., 2006; Hunt et al., 2013; Moore and Stabeno, 2015). In response to increased interest in the region, much of the sampling effort has been focused on the benthic fauna and demersal fish community (Norcross et al., 2013; Goddard et al., 2014; Grebmeier et al., 2015b; Logerwell et al., 2015). There are also large numbers of small pelagic fishes in the region (De Robertis et al., 2017). However, sampling of pelagic species in the Chukchi Sea has been sparse, and we do not yet know the mechanisms that structure their abundance and distribution in the region. Thus, a main motivating objective of this dissertation is to understand how pelagic fishes are responding to these current and projected changes in the environment.

The pelagic fish community is likely to be impacted by the rapidly changing environment of the region, but we lack the data to quantify this. The pelagic fish community is dominated by a few species, the most abundant of which is Arctic cod *(Boreogadus saida*). Previous sampling conducted in 1970 using midwater trawls found an abundance of age-0 Arctic cod in the northeast Chukchi Sea (Quast, 1974). Midwater sampling across the U.S. continental region of the Chukchi Sea conducted in 2012 and 2013 found midwater fishes throughout the region to be dominated by age-0 Arctic cod (De Robertis et al., 2017). These fish help to support large migratory populations of seabirds (Matley et al., 2012) and marine mammals (Bradstreet et al., 1986; Laidre et al., 2008).

Growth and survival of Arctic cod is highly temperature-dependent and species-specific (Laurel et al., 2017; Koenker et al., 2018). Environmental conditions are particularly important for early life stages, for which maximizing growth in summer is necessary for survival through winter (Bouchard et al., 2017). Continued loss of sea ice and warming thus has the potential to inhibit Arctic cod growth and survival in this region and their role in energy transfer within Arctic food webs. Under future warming, Arctic species may be negatively impacted by reduced habitat (Baker, 2021) and increased competition (Bouchard et al., 2017) due to changing species distributions.

Globally, warming has led to the northward expansion in distributions of boreal species in the Arctic (Wassman et al., 2011). In the Barents Sea, a shallow marginal sea of the Atlantic Arctic, warming has altered the distribution of fish communities. Subarctic species have expanded northward (Fossheim et al., 2015), potentially altering the efficiency of energy transfer due to changes in food web structure (Kortsch et al., 2015). In the Pacific Arctic, similar transitions have already been observed in the Bering Sea, where boreal species such as pollock and Pacific cod have expanded their range northwards and further onto the inner shelf (Eisner et al., 2020; Spies et al., 2020), with pollock biomass increasing as much as 65-fold in the northern Bering Sea. The alterations in temperature driving these expansions have simultaneously restricted the distributions of Arctic species such as Arctic cod, shifting their southern boundary further north (Marsh and Mueter, 2020; Baker, 2021).

Understanding the environmental mechanisms that influence fish distribution will improve our ability to predict the consequences of continued warming in the Chukchi Sea and potential for such ecosystem transitions. Changes in water mass transport have led to northwards shifts in the distribution of other pelagic organisms – e.g., zooplankton distributions have shifted northward

(Eisner et al., 2013; Spear et al., 2020) which, in turn, has influenced distribution shifts of their mobile predators (e.g., seabirds, Kuletz et al., 2020). These population shifts have yet to be documented in the pelagic fish community of the Chukchi Sea, but the environmental mechanisms that alter zooplankton distributions are likely to drive similar changes in other pelagic organisms, particularly small larval and juvenile fishes. Mooring-, satellite-, and shore-based observations as well as model-based predictions of ice, temperature, and transport are well established in the region (Frey et al., 2015; Woodgate, 2018; Janzen et al., 2019; Wang et al., 2018; Danielson et al., 2020) which are the basis for the predictions of anticipated future changes. Since 1990, long-term increases have been observed in the transport of Pacific water (~0.01 Sv $year^{-1}$; Woodgate, 2018) into the Chukchi Sea, bringing additional heat and contributing to the increase in summer and fall temperatures (0.43 ± 0.35 °C $decade^{-1}$; Danielson et al., 2020). Developing a mechanistic understanding of how the anticipated rapid increases in warming and transport in the Chukchi Sea will affect fishes is key to understanding future impacts on pelagic fish communities and their role in the ecosystem, and is vital to effective management of the ecosystem.

The gaps in our knowledge of fishes stem primarily from the difficulties sampling in the region. From November to June, access to the Chukchi Sea is restricted by the seasonal ice cover. During the ice-free summer, long transit times and limited resources for vessel support create additional impediments, making regular shelf-wide surveys costly. Thus, autonomous technologies may expand our ability to collect observations in such remote environments. Mobile autonomous platforms capable of long-duration operations create an opportunity for less costly operations over large, remote areas. Recent integration of ship-equivalent acoustic instrumentation on autonomous surface vehicles provides opportunities to collect oceanographic and biological data deeper than the upper 1-2 meters of the water column (Mordy et al., 2017; De Robertis et al.,

2019). Similarly, as sea ice extends to the south in winter and limits vessel traffic and surface-based observations, moored instrumentation can continue to collect samples year-round. Continuous measurements of the water column have been used to describe the physical oceanography of the Bering Strait and Chukchi shelf (Woodgate et al., 2005, 2015; Stabeno et al., 2018), and moored passive acoustic instrumentation has been established as a viable method of tracking marine mammals in the region (Woodgate et al., 2015; Stafford et al., 2018). However, sampling of the ecosystem, particularly fishes, has continued to be limited by the inability to survey during periods of ice cover.

In the low diversity pelagic ecosystem of the Chukchi shelf, acoustic backscatter is dominated by few species which improves our ability to infer the dominant sound scatterers observed in autonomous acoustic observations. Autonomous or moored echosounders are effective tools for measuring the abundance and behavior of fish and zooplankton on temporal scales of days to years (Kaartvedt et al., 2009; Urmy et al., 2012; Ross et al., 2013; Sato et al., 2013; De Robertis et al., 2018). Deployments of autonomous echosounders for observations of zooplankton and fishes have been conducted in the Chukchi Sea, including the use of acoustic doppler current profilers and autonomous multi-frequency echosounders (Miksis-Olds et al., 2013; Kitamura et al., 2017; Gonzalez et al., 2021). Recent advances in technology have improved the quality of data and battery life, allowing for multi-year deployments, and expanding the range of applications (De Robertis et al., 2018), including the ability to track individual fishes (Kaartvedt et al., 2009) to investigate patterns in movement and behavior.

This dissertation investigates the inter- and intra-annual variability of the pelagic community in the eastern Chukchi Sea using observations from acoustic-trawl surveys and autonomous sampling platforms. By understanding the seasonal dynamics on the shelf that drive

the summer variability in fish distribution, we can better predict how continued environmental changes will alter this ecosystem. In Chapter 2, I present results from repeat acoustic surveys using autonomous surface vehicles. The goal of these surveys was to investigate the movement of the pelagic fish population during summer in order to constrain the source and fate of this age-0 population. Observations of population retention were validated using particle tracking simulations. The integration of the model with the survey observations indicate that the age-0 gadids observed on the Chukchi shelf in summer 2018 were likely retained during a period of growth until late fall before being advected farther north toward the Chukchi and Beaufort shelf breaks.

In Chapter 3, I expand upon previous summer acoustic-trawl surveys of the eastern Chukchi Sea to classify the composition of the pelagic community in 2017 and 2019, two recent years of extreme warming. The connection between species and water mass compositions is used to investigate the drivers of shifting species distributions, which suggest that recent increases in transport of warm water from the Bering Sea is transporting higher abundances of boreal species onto the Chukchi shelf in summer. In Chapter 4, I use two years (2017-2019) of observations from seafloor-mounted moored echosounders to determine seasonality in the pelagic community and its relation to the physical environment. Fish tracking is used to determine the movement of the pelagic fishes and the role of currents and wind in displacement of the population. The velocity and direction of fish displacement is strongly correlated with currents and net transport of fishes is to the northeast, suggesting that the appearance of age-0 fishes in summer is tied to the seasonal advection of waters from southern spawning grounds and the low densities of age-1+ fishes is the result of continued transport of the fish population to the northeast in fall. The work presented in

Chapters 2, 3, and 4 provides new insights into the relationship between the physical environment and the age-0 fishes observed on the eastern Chukchi shelf in summer.

Chapter 5 is developed from interest in STEM education and teaching experiences in which I developed a sensor-based classroom activity for students to engage with the principles of underwater acoustics. In this chapter, I present a hands-on sensor building activity in which students build and calibrate an ultrasonic distance sensor (i.e., echosounder) and evaluate sensor accuracy and precision while mapping the bathymetry of the seafloor. Finally, in Chapter 6, I present conclusions and considerations outside the scope of this dissertation, summarize the open questions that still remain, and identify priorities for future research.

References

Baker, M.R., 2021. Contrast of warm and cold phases in the Bering Sea to understand spatial distributions of Arctic and sub-Arctic gadids. Polar Biol. 44, 1083–1105. https://doi.org/10.1007/s00300-021-02856-x

Bliss, A.C., Steele, M., Peng, G., Meier, W.N., Dickinson, S., 2019. Regional variability of Arctic sea ice seasonal change climate indicators from a passive microwave climate data record. Environ. Res. Lett. 2, 1–2. https://doi.org/10.1088/1748-9326/aafb84

Bouchard, C., Geoffroy, M., LeBlanc, M., Majewski, A., Gauthier, S., Walkusz, W., Reist, J.D., Fortier, L., 2017. Climate warming enhances polar cod recruitment, at least transiently. Prog. Oceanogr. 156, 121–129. https://doi.org/10.1016/j.pocean.2017.06.008

Bradstreet, M.S.W., Finley, K.J., Sekerak, A.-D., Griffiths, W.B., Evans, C.R., Fabijan, M.F., Stallard, H.E., 1986. Aspects of the Biology of Arctic Cod (*Boreogadus saida*) and its Importance in Arctic Marine Food Chains, Canadian Technical Report of Fisheries and Aquatic Sciences. https://doi.org/10.1002/aic.12482

Coachman, L.K., Aagaard, K., 1966. On the water exchange through Bering Strait. Limnol. Oceanogr. 11, 44–59. https://doi.org/10.4319/lo.1966.11.1.0044

Danielson, S.L., Ahkinga, O., Ashjian, C., Basyuk, E., Cooper, L.W., Eisner, L., Farley, E., Iken, K.B., Grebmeier, J.M., Juranek, L., Khen, G., Jayne, S.R., Kikuchi, T., Ladd, C., Lu, K., McCabe, R.M., Moore, G.W.K., Nishino, S., Ozenna, F., Pickart, R.S., Polyakov, I., Stabeno, P.J., Thoman, R., Williams, W.J., Wood, K., Weingartner, T.J., 2020. Manifestation and consequences of warming and altered heat fluxes over the Bering and Chukchi Sea continental shelves. Deep. Res. Part II Top. Stud. Oceanogr. 177. https://doi.org/10.1016/j.dsr2.2020.104781

Danielson, S.L., Weingartner, T.J., Hedstrom, K.S., Aagaard, K., Woodgate, R., Curchitser, E., Stabeno, P.J., 2014. Coupled wind-forced controls of the Bering-Chukchi shelf circulation and the Bering Strait throughflow: Ekman transport, continental shelf waves, and variations of the Pacific-Arctic sea surface height gradient. Prog. Oceanogr. 125, 40–61. https://doi.org/10.1016/j.pocean.2014.04.006

De Robertis, A., Lawrence-Slavas, N., Jenkins, R., Wangen, I., Mordy, C.W., Meinig, C., Levine, M., Peacock, D., Tabisola, H., 2019. Long-term measurements of fish backscatter from Saildrone unmanned surface vehicles and comparison with observations from a noise-reduced research vessel. ICES J. Mar. Sci. 76, 2459–2470. https://doi.org/10.1093/icesjms/fsz124

De Robertis, A., Taylor, K., Wilson, C.D., Farley, E. V., 2017. Abundance and distribution of Arctic cod (*Boreogadus saida*) and other pelagic fishes over the U.S. Continental Shelf of the Northern Bering and Chukchi Seas. Deep. Res. Part II Top. Stud. Oceanogr. 135, 51–65. https://doi.org/10.1016/j.dsr2.2016.03.002

Druckenmiller, M.L., Citta, J.J., Ferguson, M.C., Clarke, J.T., George, J.C., Quakenbush, L., 2018. Trends in sea-ice cover within bowhead whale habitats in the Pacific Arctic. Deep. Res. Part II Top. Stud. Oceanogr. 152, 95–107. https://doi.org/10.1016/j.dsr2.2017.10.017

Duarte, C.M., Lenton, T.M., Wadhams, P., Wassmann, P., 2012. Abrupt climate change in the Arctic. Nat. Clim. Chang. 2, 60–62. https://doi.org/10.1038/nclimate1386

Eisner, L.B., Zuenko, Y.I., Basyuk, E.O., Britt, L.L., Duffy-Anderson, J.T., Kotwicki, S., Ladd, C., Cheng, W., 2020. Environmental impacts on walleye pollock (*Gadus chalcogrammus*) distribution across the Bering Sea shelf. Deep. Res. Part II Top. Stud. Oceanogr. 181–182, 104881. https://doi.org/10.1016/j.dsr2.2020.104881

Eisner, L., Hillgruber, N., Martinson, E., Maselko, J., 2013. Pelagic fish and zooplankton species assemblages in relation to water mass characteristics in the northern Bering and southeast Chukchi seas. Polar Biol. 36, 87–113. https://doi.org/10.1007/s00300-012-1241-0

Fossheim, M., Primicerio, R., Johannesen, E., Ingvaldsen, R.B., Aschan, M.M., Dolgov, A. V., 2015. Recent warming leads to a rapid borealization of fish communities in the Arctic. Nat. Clim. Chang. 5, 673–677. https://doi.org/10.1038/nclimate2647

Frey, K.E., Moore, G.W.K., Cooper, L.W., Grebmeier, J.M., 2015. Divergent patterns of recent sea ice cover across the Bering, Chukchi, and Beaufort seas of the Pacific Arctic Region. Prog. Oceanogr. 136, 32–49. https://doi.org/10.1016/j.pocean.2015.05.009

Goddard, P., Lauth, R., Armistead, C., 2014. Results of the 2012 Chukchi Sea Bottom Trawl Survey of Bottomfishes, Crabs, and Other Demersal Macrofauna. U.S. Dep. Commer. NOAA Tech. Memorandum, 110.

Gonzalez, S., Horne, J.K., Danielson, S.L., 2021. Multi-scale temporal variability in biological-physical associations in the NE Chukchi Sea. Polar Biol. 44, 837–855. https://doi.org/10.1007/s00300-021-02844-1

Grebmeier, J.M., Bluhm, B.A., Cooper, L.W., Denisenko, S.G., Iken, K., Kedra, M., Serratos, C., 2015a. Time-series benthic community composition and biomass and associated environmental characteristics in the Chukchi Sea during the RUSALCA 2004-2012 Program. Oceanography 28, 116–133. https://doi.org/10.5670/oceanog.2015.61

Grebmeier, J.M., Bluhm, B.A., Cooper, L.W., Danielson, S.L., Arrigo, K.R., Blanchard, A.L., Clarke, J.T., Day, R.H., Frey, K.E., Gradinger, R.R., Kedra, M., Konar, B., Kuletz, K.J., Lee, S.H., Lovvorn, J.R., Norcross, B.L., Okkonen, S.R., 2015b. Ecosystem characteristics and processes facilitating persistent macrobenthic biomass hotspots and associated benthivory in the Pacific Arctic. Prog. Oceanogr. 136, 92–114. https://doi.org/10.1016/j.pocean.2015.05.006

Grebmeier, J.M., Cooper, L.W., Feder, H.M., Sirenko, B.I., 2006. Ecosystem dynamics of the Pacific-influenced Northern Bering and Chukchi Seas in the Amerasian Arctic. Prog. Oceanogr. 71, 331–361. https://doi.org/10.1016/j.pocean.2006.10.001

Hopcroft, R.R., Day, R.H., 2013. Introduction to the special issue on the ecology of the northeastern Chukchi Sea. Cont. Shelf Res. 67, 1–4. https://doi.org/10.1016/j.csr.2013.06.017

Hunt, G.L., Blanchard, A.L., Boveng, P., Dalpadado, P., Drinkwater, K.F., Eisner, L., Hopcroft, R.R., Kovacs, K.M., Norcross, B.L., Renaud, P., Reigstad, M., Renner, M., Skjoldal, H.R., Whitehouse, A., Woodgate, R.A., 2013. The barents and chukchi seas: Comparison of two Arctic shelf ecosystems. J. Mar. Syst. 109–110, 43–68. https://doi.org/10.1016/j.jmarsys.2012.08.003

Hunt, G.L., Drinkwater, K.F., Arrigo, K., Berge, J., Daly, K.L., Danielson, S., Daase, M., Hop, H., Isla, E., Karnovsky, N., Laidre, K., Mueter, F.J., Murphy, E.J., Renaud, P.E., Smith, W.O., Trathan, P., Turner, J., Wolf-Gladrow, D., 2016. Advection in polar and sub-polar environments: Impacts on high latitude marine ecosystems. Prog. Oceanogr. 149, 40–81. https://doi.org/10.1016/j.pocean.2016.10.004

Huntington, H.P., Danielson, S.L., Wiese, F.K., Baker, M., Boveng, P., Citta, J.J., De Robertis, A., Dickson, D.M.S., Farley, E., George, J.C., Iken, K., Kimmel, D.G., Kuletz, K., Ladd, C., Levine, R., Quakenbush, L., Stabeno, P., Stafford, K.M., Stockwell, D., Wilson, C., 2020. Evidence suggests potential transformation of the Pacific Arctic ecosystem is underway. Nat. Clim. Chang. https://doi.org/10.1038/s41558-020-0695-2

Janzen, C.D., McCammon, M., Danielson, S.S.L., Weingartner, T., Statscewich, H., Page, E., Heim, B., 2019. Innovative real-time observing capabilities for remote coastal regions. Front. Mar. Sci. 6, 1–8. https://doi.org/10.3389/fmars.2019.00176

Kaartvedt, S., Røstad, A., Klevjer, T.A., Staby, A., 2009. Use of bottom-mounted echo sounders in exploring behavior of mesopelagic fishes. Mar. Ecol. Prog. Ser. 395, 109–118. https://doi.org/10.3354/meps08174

Kitamura, M., Amakasu, K., Kikuchi, T., Nishino, S., 2017. Seasonal dynamics of zooplankton in the southern Chukchi Sea revealed from acoustic backscattering strength. Cont. Shelf Res. 133, 47–58. https://doi.org/10.1016/j.csr.2016.12.009

Koenker, B.L., Copeman, L.A., Laurel, B.J., 2018. Impacts of temperature and food availability on the condition of larval Arctic cod (*Boreogadus saida*) and walleye pollock (*Gadus chalcogrammus*). ICES J. Mar. Sci. 75, 2370–2385. https://doi.org/10.1093/icesjms/fsy052

Kortsch, S., Primicerio, R., Fossheim, M., Dolgov, A. V., Aschan, M., 2015. Climate change alters the structure of arctic marine food webs due to poleward shifts of boreal generalists. Proc. R. Soc. B Biol. Sci. 282. https://doi.org/10.1098/rspb.2015.1546

Kuletz, K., Cushing, D., Labunski, E., 2020. Distributional shifts among seabird communities of the Northern Bering and Chukchi seas in response to ocean warming during 2017–2019. Deep. Res. Part II Top. Stud. Oceanogr. 181–182, 104913. https://doi.org/10.1016/j.dsr2.2020.104913

Laidre, K.L., Stirling, I., Lowry, L.F., Wiig, Ø., Peter Heide-Jørgensen, M., Ferguson, S.H., Heide-Jørgensen, M.P., Ferguson, S.H., 2008. Quantifying the Sensitivity of Arctic Marine Mammals To Climate-Induced Habitat Change. Ecol. Appl. 18, S97–S125. https://doi.org/10.1890/06-0546.1

Laurel, B.J., Copeman, L.A., Spencer, M., Iseri, P., 2017. Temperature-dependent growth as a function of size and age in juvenile Arctic cod (*Boreogadus saida*). ICES J. Mar. Sci. 74, 1614–1621. https://doi.org/10.1093/icesjms/fsx028

Logerwell, E.A., Busby, M., Mier, K.L., Tabisola, H., Duffy-Anderson, J., 2020. The effect of oceanographic variability on the distribution of larval fishes of the northern Bering and Chukchi seas. Deep. Res. Part II Top. Stud. Oceanogr. 177, 104784. https://doi.org/10.1016/j.dsr2.2020.104784

Marsh, J.M., Mueter, F.J., 2020. Influences of temperature, predators, and competitors on polar cod (*Boreogadus saida*) at the southern margin of their distribution. Polar Biol. 43, 995–1014. https://doi.org/10.1007/s00300-019-02575-4

Matley, J.K., Fisk, A.T., Dick, T.A., 2012. Seabird predation on Arctic cod during summer in the Canadian Arctic. Mar. Ecol. Prog. Ser. 450, 219–228. https://doi.org/10.3354/meps09561

Miksis-Olds, J.L., Stabeno, P.J., Napp, J.M., Pinchuk, A.I., Nystuen, J.A., Warren, J.D., Denes, S.L., 2013. Ecosystem response to a temporary sea ice retreat in the Bering Sea: Winter 2009. Prog. Oceanogr. 111, 38–51. https://doi.org/10.1016/j.pocean.2012.10.010

Moore, S.E., Stabeno, P.J., 2015. Synthesis of Arctic Research (SOAR) in marine ecosystems of the Pacific Arctic. Prog. Oceanogr. 136, 1–11. https://doi.org/10.1016/j.pocean.2015.05.017

Mordy, C.W., Bell, S., Cokelet, E.D., Ladd, C., Lebon, G., Proctor, P., Stabeno, P., Strausz, D., Wisegarver, E., Wood, K., 2020. Seasonal and interannual variability of nitrate in the eastern Chukchi Sea: Transport and winter replenishment. Deep. Res. Part II Top. Stud. Oceanogr. 177, 104807. https://doi.org/10.1016/j.dsr2.2020.104807

Mordy, C., Cokelet, E., De Robertis, A., Jenkins, R., Kuhn, C., Lawrence-Slavas, N., Berchok, C., Crance, J., Sterling, J., Cross, J., Stabeno, P., Meinig, C., Tabisola, H., Burgess, W., Wangen, I., 2017. Advances in Ecosystem Research: Saildrone Surveys of Oceanography, Fish, and Marine Mammals in the Bering Sea. Oceanography 30, 113–115. https://doi.org/10.5670/oceanog.2017.230

Mueter, F.J., Planque, B., Hunt Jr, G.L., Alabia, I.D., Hirawake, T., Eisner, L., Dalpadado, P., Drinkwater, K.F., Harada, N., Arneberg, P., Saitoh, S.-I., 2021. Possible future scenarios in the Gateways to the Arctic for Subarctic and Arctic marine systems: Prey resources, food webs, fish, and fisheries. ICES J. Mar. Sci.

Mueter, F.J., Weems, J., Farley, E. V., Sigler, M.F., 2017. Arctic Ecosystem Integrated Survey (Arctic Eis): Marine ecosystem dynamics in the rapidly changing Pacific Arctic Gateway.

Deep. Res. Part II Top. Stud. Oceanogr. 135, 1–6. https://doi.org/10.1016/j.dsr2.2016.11.005

Norcross, B.L., Raborn, S.W., Holladay, B.A., Gallaway, B.J., Crawford, S.T., Priest, J.T., Edenfield, L.E., Meyer, R., 2013. Northeastern Chukchi Sea demersal fishes and associated environmental characteristics, 2009-2010. Cont. Shelf Res. 67, 77–95. https://doi.org/10.1016/j.csr.2013.05.010

Overland, J., Dunlea, E., Box, J.E., Corell, R., Forsius, M., Kattsov, V., Olsen, M.S., Pawlak, J., Reiersen, L.O., Wang, M., 2019. The urgency of Arctic change. Polar Sci. 21, 6–13. https://doi.org/10.1016/j.polar.2018.11.008

Quast, J.C., 1974. Density distribution of juvenile Arctic cod, *Boreogadus saida*, in the eastern Chukchi Sea in the fall of 1970. Fish. Bull. 72, 1094–1105.

Ross, T., Keister, J.E., Lara-Lopez, A., 2013. On the use of high-frequency broadband sonar to classify biological scattering layers from a cabled observatory in Saanich Inlet, British Columbia. Methods Oceanogr. 5, 19–38. https://doi.org/10.1016/j.mio.2013.05.001

Sato, M., Dower, J.F., Kunze, E., Dewey, R., 2013. Second-order seasonal variability in diel vertical migration timing of euphausiids in a coastal inlet. Mar. Ecol. Prog. Ser. 480, 39–56. https://doi.org/10.3354/meps10215

Spear, A., Napp, J., Ferm, N., Kimmel, D., 2020. Advection and in situ processes as drivers of change for the abundance of large zooplankton taxa in the Chukchi Sea. Deep. Res. Part II Top. Stud. Oceanogr. 177, 104814. https://doi.org/10.1016/j.dsr2.2020.104814

Spies, I., Gruenthal, K.M., Drinan, D.P., Hollowed, A.B., Stevenson, D.E., Tarpey, C.M., Hauser, L., 2020. Genetic evidence of a northward range expansion in the eastern Bering Sea stock of Pacific cod. Evol. Appl. 13, 362–375. https://doi.org/10.1111/eva.12874

Stabeno, P., Kachel, N., Ladd, C., Woodgate, R., 2018. Flow Patterns in the Eastern Chukchi Sea: 2010–2015. J. Geophys. Res. Ocean. 123, 1177–1195. https://doi.org/10.1002/2017JC013135

Stafford, K.M., Castellote, M., Guerra, M., Berchok, C.L., 2018. Seasonal acoustic environments of beluga and bowhead whale core-use regions in the Pacific Arctic. Deep. Res. Part II Top. Stud. Oceanogr. 152, 108–120. https://doi.org/10.1016/j.dsr2.2017.08.003

Stroeve, J.C., Markus, T., Boisvert, L., Miller, J., Barrett, A., 2014. Changes in Arctic melt season and implications for sea ice loss. Geophys. Res. Lett. 41, 1216–1225. https://doi.org/10.1002/2013GL058951

Urmy, S.S., Horne, J.K., Barbee, D.H., 2012. Measuring the vertical distributional variability of pelagic fauna in Monterey Bay. ICES J. Mar. Sci. 69, 184–196. https://doi.org/10.1093/icesjms/fsr205

Waga, H., Hirawake, T., Grebmeier, J.M., 2020. Recent change in benthic macrofaunal community composition in relation to physical forcing in the Pacific Arctic. Polar Biol. 43, 285–294. https://doi.org/10.1007/s00300-020-02632-3

Wang, M., Yang, Q., Overland, J.E., Stabeno, P., 2018. Sea-ice cover timing in the Pacific Arctic: The present and projections to mid-century by selected CMIP5 models. Deep. Res. Part II Top. Stud. Oceanogr. 152, 22–34. https://doi.org/10.1016/j.dsr2.2017.11.017

Wassmann, P., Duarte, C.M., Agustí, S., Sejr, M.K., 2011. Footprints of climate change in the Arctic marine ecosystem. Glob. Chang. Biol. 17, 1235–1249. https://doi.org/10.1111/j.1365-2486.2010.02311.x

Wassmann, P., Reigstad, M., 2011. Future Arctic Ocean Seasonal Ice Zones and Implications for Pelagic-Benthic Coupling. Oceanography 24, 220–231. https://doi.org/10.5670/oceanog.2011.74

Wood, K., Wang, J., Salo, S., Stabeno, P., 2015. The Climate of the Pacific Arctic During the First RUSALCA Decade 2004–2013. Oceanography 28, 24–35. https://doi.org/10.5670/oceanog.2015.55

Woodgate, R.A., Peralta-Ferriz, C., 2021. Warming and Freshening of the Pacific Inflow to the Arctic from 1990-2019 implying dramatic shoaling in Pacific Winter Water ventilation of the Arctic water column. Geophys. Res. Lett. https://doi.org/10.1029/2021GL092528

Woodgate, R.A., 2018. Increases in the Pacific inflow to the Arctic from 1990 to 2015, and insights into seasonal trends and driving mechanisms from year-round Bering Strait mooring data. Prog. Oceanogr. 160, 124–154. https://doi.org/10.1016/j.pocean.2017.12.007

Woodgate, R.A., Aagaard, K., Weingartner, T.J., 2005. Monthly temperature, salinity, and transport variability of the Bering Strait through flow. Geophys. Res. Lett. 32, 1–4. https://doi.org/10.1029/2004GL021880

Woodgate, R.A., Weingartner, T., Lindsay, R., 2010. The 2007 Bering Strait oceanic heat flux and anomalous Arctic sea-ice retreat. Geophys. Res. Lett. 37, 1–5. https://doi.org/10.1029/2009GL041621

Woodgate, R.A., Aagaard, K., Weingartner, T.J., 2005. A year in the physical oceanography of the Chukchi Sea: Moored measurements from autumn 1990-1991. Deep. Res. Part II Top. Stud. Oceanogr. 52, 3116–3149. https://doi.org/10.1016/j.dsr2.2005.10.016

Woodgate, R., Stafford, K., Prahl, F., 2015. A Synthesis of Year-Round Interdisciplinary Mooring Measurements in the Bering Strait (1990–2014) and the RUSALCA Years (2004–2011). Oceanography 28, 46–67. https://doi.org/10.5670/oceanog.2015.57

CHAPTER 2. AUTONOMOUS VEHICLE SURVEYS INDICATE THAT FLOW REVERSALS RETAIN JUVENILE FISHES IN A HIGHLY ADVECTIVE HIGH-LATITUDE ECOSYSTEM

This manuscript has been previously published as:

Levine, R.M., De Robertis, A., Grünbaum, D., Woodgate, R., Mordy, C.W., Mueter, F., Cokelet, E., Lawrence-Slavas, N. and Tabisola, H. (2021). Autonomous vehicle surveys indicate that flow reversals retain juvenile fishes in a highly advective high-latitude ecosystem. Limnol. Oceanogr., 66: 1139-1154. https://doi.org/10.1002/lno.11671

2.1 ABSTRACT

Summer surveys of the Chukchi Sea indicate that high densities of age-0 gadid fishes, historically Arctic cod (*Boreogadus saida*) but recently also walleye pollock (*Gadus chalcogrammus*), dominate the pelagic fish community. Adults are comparatively scarce, suggesting that either overwinter survivorship of age-0 gadids is low, or that they emigrate to other areas of the Pacific Arctic. To examine population movement, we conducted repeat acoustic surveys with saildrone autonomous surface vehicles equipped with echosounders throughout summer 2018. The saildrones' range and endurance enabled two large-scale surveys of the U.S. Chukchi shelf. Acoustic backscatter, a proxy for fish density, was highest in regions with sea surface temperatures of 6–8°C, and lowest in areas influenced by recent ice melt. A subarea of the central Chukchi was surveyed a total of four times; backscatter in this subarea increased by > 85% from late-July to mid-September. As summer progressed, fish developed more extensive diel vertical migrations and backscatter from individuals doubled. Both changes suggest increases in backscatter were

driven primarily by increasing body size. Particle tracking simulations indicated age-0 gadids were likely retained over the Chukchi shelf by extended periods of wind-driven southward flow during the survey period before strong northward flow in late fall transported them to the north. These findings suggest that in summer 2018, age-0 gadids were advected northward to the Chukchi shelf from the northern Bering Sea, where they were retained during a period of growth until late fall before being advected farther north toward the Chukchi and Beaufort shelf breaks.

2.2 INTRODUCTION

Arctic gadids, particularly Arctic cod (*Boreogadus saida*), dominate the pelagic fish community in the Pacific Arctic ecosystem of the northern Bering, Chukchi, East Siberian, and Beaufort Seas. Arctic cod have a circumarctic distribution and are abundant throughout the shallow shelves of the Arctic marginal seas as well as the Arctic Basin (Mecklenburg et al., 2018). Arctic cod are key pelagic secondary consumers that serve as a central trophic link between plankton and higher trophic levels (Bradstreet et al., 1986; Whitehouse and Aydin, 2016), supporting large migratory populations of seabirds (Matley et al., 2012) and marine mammals (Bradstreet et al., 1986). The Pacific Arctic is undergoing rapid changes associated with surface warming and loss of sea ice (Steele et al., 2008; Frey et al., 2015; Woodgate, 2018). These changes have the potential to negatively impact Arctic cod growth and survival in this region and alter species distributions.

Recent studies suggest that the warming conditions in the Pacific Arctic are becoming increasingly hospitable for more boreal species such as walleye pollock (*Gadus chalcogrammus*) (Laurel et al., 2016; Huntington et al., 2020). Historically, trawl surveys conducted in the Chukchi Sea have found that pelagic biomass is dominated by age-0 (born within the past year) Arctic cod (Quast, 1974; Norcross et al., 2010; Logerwell et al., 2015). Acoustic-trawl surveys conducted in 2017 and 2019 indicate that age-0 walleye pollock have become more abundant on the Chukchi

shelf (R. M. Levine unpubl.). As the region changes due to increasing temperatures, walleye pollock distributions may expand to the north and become a potentially significant component of the gadid community on the Chukchi shelf.

Little is known about the distribution and movements of pelagic fish populations in the region, particularly in the Chukchi Sea. Acoustic-trawl surveys conducted in summer 2012 and 2013 established a baseline of distributions of pelagic fishes in the U.S. northern Bering and Chukchi Seas (De Robertis et al., 2017). These surveys documented large numbers of pelagic age-0 Arctic cod, with the highest abundances in the northern Chukchi Sea where the average length was 3.5 cm and < 0.3% were greater than 6.5 cm (De Robertis et al., 2017). However, this and other surveys in the area indicate that older Arctic cod are comparatively rare on the U.S. Chukchi shelf (Logerwell et al., 2015; De Robertis et al., 2017).

Estimates of the reproductive potential of the Arctic cod population in the survey region indicate that observed densities of adults are likely insufficient to produce the large numbers of age-0 fish observed in the acoustic-trawl surveys (Marsh et al., 2019). It is likely that age-0 Arctic cod observed on the Chukchi shelf in summer are produced by adults that seasonally migrate into the region to spawn, or from eggs and larvae spawned in other areas and subsequently transported into the region. Large-scale horizontal migration of Arctic cod to spawning aggregation sites has been observed in the Barents Sea (Gjøsæter, 1995) and Russian Arctic (Ponomarenko, 1968). Recent work has hypothesized that a similar pattern of seasonal migration may occur in the Pacific Arctic (Forster et al., 2020). Similarly, walleye pollock have recently become more abundant in the northern Bering Sea (Stevenson and Lauth, 2019), and this may have increased the supply of walleye pollock larvae that enter the Chukchi Sea from the south in recent years. The low densities of age-1+ relative to age-0 gadids found on the Chukchi shelf indicate that either overwinter

survival of age-0s retained in the area is very low, or that the Chukchi shelf serves only as a summer nursery area, after which age-0s subsequently emigrate or are transported to other areas (De Robertis et al., 2017).

The likelihood of these scenarios is partially constrained by local advective regimes. The Chukchi Sea is a region of seasonally high advection, with strong northward currents that may transport eggs and larvae from the south (Figure 2.1). High northward transport across the shelf occurs during the summer and fall (Woodgate et al., 2005; Stabeno et al., 2018), yielding residence times of Pacific Waters in the Chukchi of 4–5 months, although this residence time has likely decreased in recent years (Woodgate et al., 2005; Woodgate, 2018). This movement of Pacific water toward the Arctic structures the species composition and distribution of plankton communities in the Chukchi Sea, with many species being transported into the Chukchi Sea from the Bering Sea (Eisner et al., 2013; Ershova et al., 2015; Sigler et al., 2017). Interannual variability in phytoplankton, zooplankton and ichthyoplankton communities is strongly influenced by changes in oceanographic forcing, as indicated by associations between water masses of southern origin and community composition (Norcross et al., 2010; Danielson et al., 2017; Pinchuk and Eisner, 2017; Spear et al., 2019).

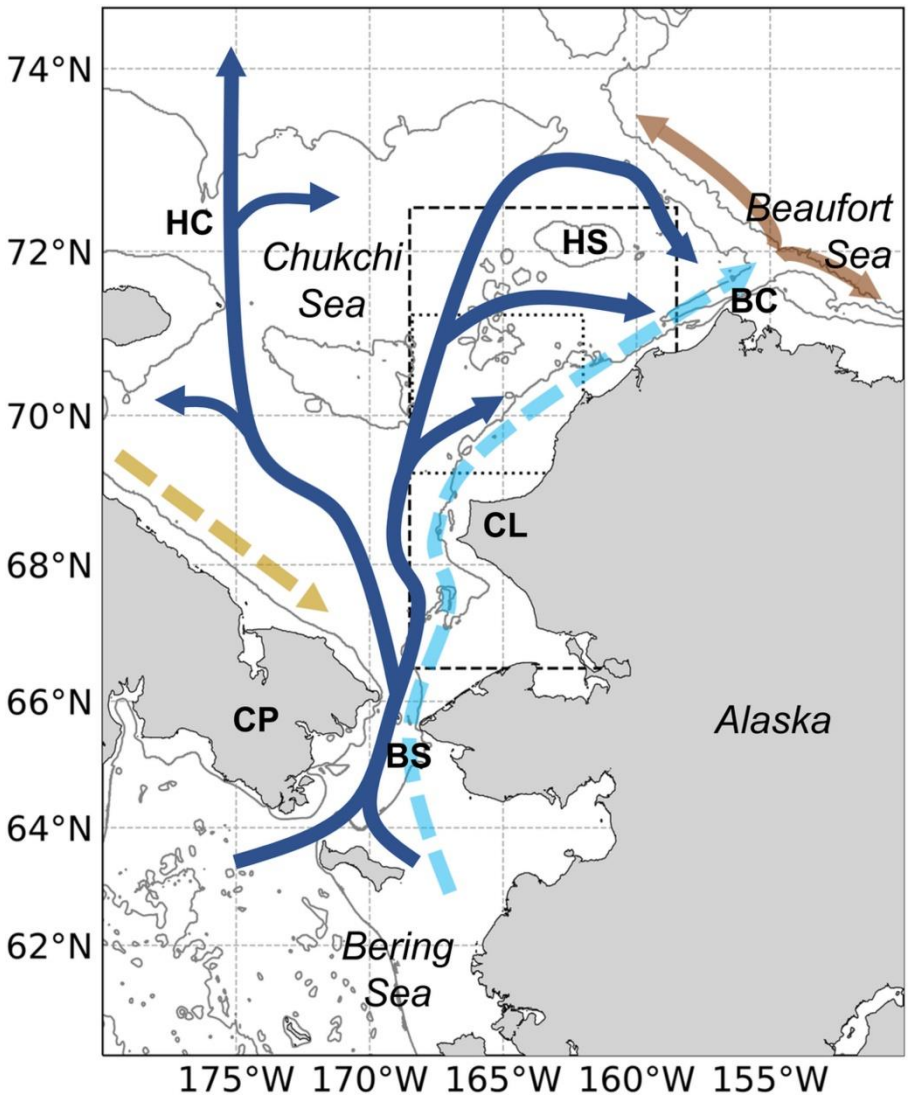

Figure 2.1 Map of the study region, showing the primary transport pathways through the Chukchi Sea based on Corlett and Pickart (2017): Alaskan coastal current (light blue), Bering Sea water (dark blue), Siberian coastal current (gold), slope current (brown, westward) and shelf break jet (brown, eastward). Dashed lines indicate seasonal currents. Survey regions are indicated for the large-scale survey (dashed box) and small-scale survey (dotted box). Geographic features referred to in the text are indicated in bold: Bering Strait (BS), Chukotka Peninsula (CP), Cape Lisburne, (CL), Herald Canyon (HC), Hanna Shoal (HS), and Barrow Canyon (BC). The 40-, 100-, and 1000-m depth contours are shown.

The reproductive biology of Arctic cod and walleye pollock in the context of the advective regime provides additional clues to the origins of fish observed on the Chukchi shelf. Arctic cod are known to spawn in fall and winter under sea ice on the shallow shelves of the Arctic marginal seas (Ponomarenko, 2000). Fertilized eggs are buoyant and develop under ice cover at the ice–water interface (Ponomarenko, 2000). Pollock similarly produce pelagic eggs and, as larvae, remain close to the surface (Spencer et al., 2020). Development time in both species is temperature dependent, with time to 50% hatching of Arctic cod in laboratory studies ranging from 31 d at 3.8°C to 67 d at −0.4°C and approximately half of that time across these temperatures for walleye pollock (Laurel et al., 2018). Arctic cod hatching has been observed from December through August, with a peak during May/June (Bouchard and Fortier, 2011). Ichthyoplankton surveys and otolith aging of larval and juvenile Arctic cod in other regions of the Arctic indicates that spawning occurs over a period of months, producing an extended distribution of larval fish throughout the summer rather than a single short pulse or a set of discrete pulses (Bouchard and Fortier, 2011; Bouchard et al., 2016). The spawning period of walleye pollock in the Bering Sea extends from early winter into early fall, with spawning in the northern Bering shelf highest in early summer (Hinckley, 1987).

It is hypothesized that age-0 gadids on the Chukchi shelf are spawned to the south and are advected northward onto the Chukchi shelf in summer. Particle tracking simulations suggest that variations in wind and current patterns drive the interannual variability observed in late-summer distribution in the Chukchi Sea (Vestfals et al., 2021). The age-0 gadids are then advected further to the north in the fall. Observations and modeled transport of larval Arctic cod suggest that spawning occurs at multiple locations in the Pacific Arctic (Vestfals et al., 2019; Vestfals et al., 2021). Three key areas have been proposed as spawning areas for age-0 Arctic cod on the Chukchi

shelf: the northern Bering Sea, along the Chukotka Peninsula in western Bering Strait, and the Beaufort Sea (Figure 2.1; Kono et al., 2016; Vestfals et al., 2019). Acoustic-trawl abundance estimates in 2012 were lower than those in 2013 which is consistent with the hypothesis that lower annual northward transport in 2012 (e.g., Woodgate, 2018) resulted in fewer age-0 Arctic cod originating in the Bering Sea were advected to the northeast Chukchi Sea by the time of the survey (Vestfals et al., 2021). Larval Arctic cod have also been found in the northern Chukchi and western Beaufort Seas, in particular near Barrow Canyon. These fish may have been transported southward via up-canyon advection from aggregations of adult Arctic cod distributed to the north along the Beaufort shelf break (Geoffroy et al., 2011; Parker-Stetter et al., 2011; Vestfals et al., 2021). Although Arctic cod are historically the most abundant species, advective transport is likely the main process driving the presence of all age-0 gadids on the Chukchi shelf. Walleye pollock and saffron cod (*Eleginus gracilis*) are abundant in the northern Bering and southern Chukchi Seas, respectively (De Robertis et al., 2017; Stevenson and Lauth, 2019). Eggs and larvae of these species are likely to follow transport pathways similar to Arctic cod on the Chukchi shelf.

In this study, we sought to test the hypothesis that age-0 gadids in the Chukchi Sea are typically advected north during the summer, and that their distribution would shift northward during the open-water season. We used uncrewed surface vehicles (USVs) to conduct repeat acoustic surveys of the northeastern Chukchi Sea to quantify the intraseasonal variability in the spatial distribution of gadids in summer 2018. By conducting repeat surveys, we aimed to: (1) infer the source location of the age-0 gadid population in the northeastern Chukchi Sea in summer; (2) evaluate what movements of the fish population may reveal about the role of the northeastern Chukchi Sea as a nursery area for age-0 Arctic cod and other gadid fishes; and (3) ascertain whether, when, and how fish were transported out of the study area.

2.3 METHODS

2.3.1 *Survey design and data collection*

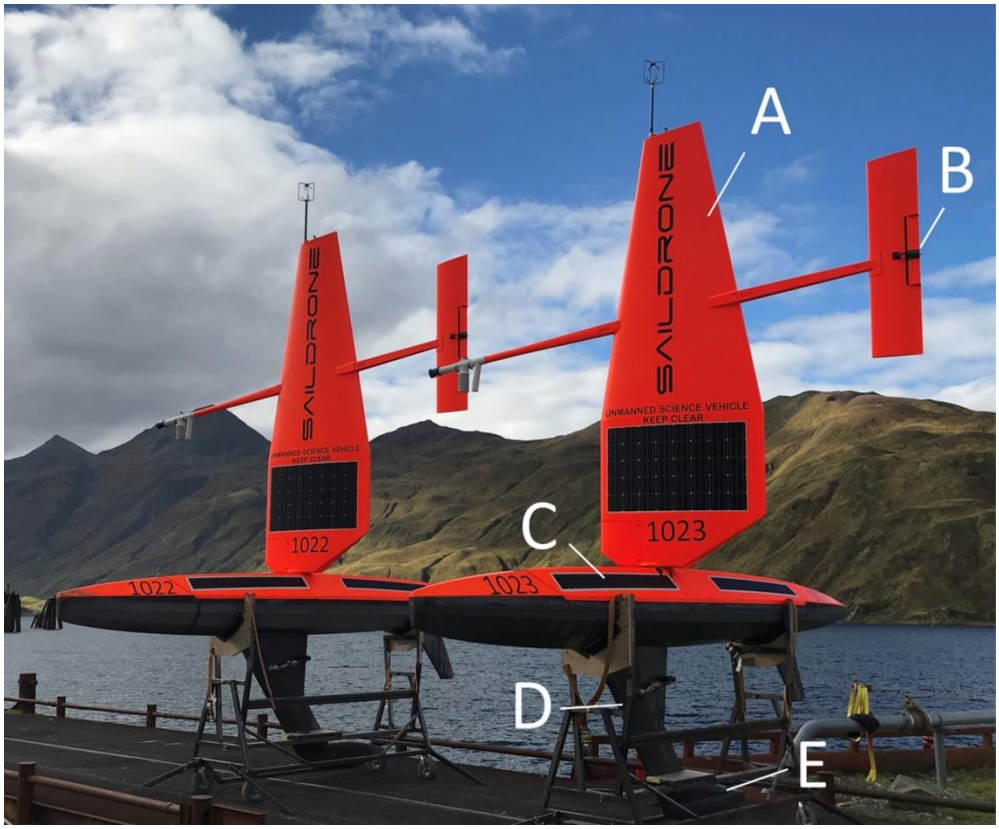

Figure 2.2 Saildrone uncrewed surface vehicles upon recovery in Dutch Harbor, Alaska. (a) Wing, (b) trim tab, (c) hull, (d) keel, and (e) transducer mount. Image courtesy of Saildrone, Inc.

Two Saildrone generation 5 USVs (SD-1022 and SD-1023, Saildrone, Inc., Figure 2.2) were used to conduct an acoustic survey of pelagic sound-scattering organisms on the Chukchi shelf. The vehicles were deployed from Dutch Harbor, Alaska, on 30 June 2018 and recovered in the same location on 06 October (98 d). The saildrone is a 7-m long wind-propelled vehicle which uses an actuator-controlled trim tab to manipulate a 5-m wing sail (Mordy et al., 2017; De Robertis et al., 2019). The vehicle autonomously navigates between operator-specified waypoints, with near real-time navigation, data reporting, and instrument control via satellite link. Onboard

instrumentation operates on battery power, which is replenished by solar panels on the hull and wing. From 14 July to 24 September 2018 (72 d) the saildrones conducted acoustic surveys of the U.S. continental shelf region of the Chukchi Sea.

To compare the distribution of backscatter during mid and late summer, two large-scale surveys were completed from 20 July to 16 August and 24 August to 11 September. The surveys were conducted between 66.5°N and 72.5°N and 168.6°W and 159.5°W (Figure 2.1, area encompassed by the dashed line) along the 0.5° latitude spaced transects as surveyed by research vessels in 2012 and 2013 (De Robertis et al., 2017). Two additional surveys were conducted on a subset of four of the transect lines between 69.5°N and 71°N from 20 July to 03 August and from 13 August to 28 August. Along with the two large-scale surveys, this resulted in four replicate small-scale surveys in a region of previously (i.e., 2012 and 2013) observed high acoustic backscatter in the northeastern Chukchi Sea (Figure 2.1, area indicated by dotted box). Both large-scale surveys and the additional two small-scale surveys were conducted from north to south along east–west acoustic transects. In total, the two saildrones traveled 7610 nautical miles (14,093 km; hereafter referred to as nmi) in the Chukchi Sea at an average speed of 1.2 m s^{-1}.

To measure backscatter from fishes, each saildrone was outfitted with a Simrad wideband autonomous transceiver (WBAT-mini) split-beam echosounder with a Simrad ES38-18/200-18C transducer (three-channel split-beam 38 kHz and single-beam 200 kHz, both with a half power beamwidth of 18°) gimbal-mounted on the keel at a depth of 1.9 m (see De Robertis et al., 2019 for details on echosounder integration). To manage power consumption, 12-min ping ensembles were transmitted between one and five times per hour (90% of data were collected with the instrument pinging continuously) defined by the operator depending on the battery state. Each ensemble consisted of simultaneous 38 and 200 kHz narrowband pings every 1.5 s using a 0.5-ms pulse

duration. Backscatter was recorded to 75 or 150 m range depending on the bottom depth. Electrical interference from the vehicle's systems precluded the use of the 200 kHz data (this issue has since been resolved by Saildrone). The echosounders were calibrated after deployment using a 60-mm copper sphere for the 38-kHz transducer following the standard sphere method (Demer et al., 2015).

Sensors aboard the saildrone monitored environmental conditions throughout the deployment at 1-min intervals (for a full suite of sensors, see Mordy et al., 2017). Water temperature and salinity at 0.5 m depth were measured using a pair of conductivity, temperature, and depth (CTD) sensors (Saildrone[3], RBR Ltd. and Sea-Bird SBE-37) on each USV. In situ comparisons between calibrated sensor pairs agreed to temperatures within ~ 0.01°C and salinities to within ~ 0.02 (PSS-78). Photosynthetically active radiation was measured at 2.5 m above the sea surface (LI-192SA, LI-COR, Inc.), and wind speed was measured using an anemometer mounted on the wing at 5.2 m (1590-PK-020, Gill Instruments Ltd.).

2.3.2 *Inferring the identity of acoustic targets*

In acoustic-trawl surveys, backscatter is attributed to species based on direct sampling (e.g., trawling) of acoustic scatterers, and by applying knowledge of the abundance and behavior (e.g., schooling characteristics and depth distributions) of the species in the study area (Horne, 2000). We were unable to conduct any trawl sampling in 2018, and thus had to rely on observations from other years to interpret the acoustic observations. Surveys in 2012 and 2013 found the age-0 Arctic cod population in the Chukchi Sea to be > 35 times larger than any other observed species (De Robertis et al., 2017). Preliminary results from pelagic trawls conducted in 2017 and 2019 also indicate that most of the acoustic scattering at 38 kHz in this area is attributable to age-0 gadids. However, walleye pollock have become more abundant in recent years. Age-0 gadids made up

> 95% of the trawl catch per unit effort in 2017 (85% Arctic cod and 10% walleye pollock by number) and > 85% of the catch per unit effort in 2019 (45% Arctic cod and 40% walleye pollock; R. M. Levine and S. Wildes unpubl.). As in previous years (De Robertis et al., 2017), other gadids such as saffron cod and Pacific cod (*Gadus macrocephalus*), and other strong sound scattering pelagic fishes such as capelin (*Mallotus villosus*) and Pacific herring (*Clupea pallasii*), were present in comparatively low abundance in 2017 and 2019 (R. M. Levine unpubl.) and occupied only a small portion of the Chukchi shelf. Although trawl sampling was not conducted during 2018, these surveys from previous and subsequent years strongly suggest that age-0 Arctic cod and walleye pollock likely dominated acoustic backscatter. Therefore, our analysis assumed that the acoustic-based measures of fish density collected by the saildrones primarily reflect the abundance and distribution of age-0 Arctic cod and walleye pollock.

2.3.3 *Acoustic data processing*

Acoustic data were processed using Echoview 10.0 (Echoview Software Pty Ltd). Mean volume backscattering strength (S_v, dB re 1 m^{-1}) at 38 kHz was used as a proxy for fish abundance. Sound speed and absorption were determined from 128 CTD casts collected during a 2017 survey of the U.S. continental shelf region of the Chukchi Sea between 67°N and 72.5°N. A mean sound speed of 1466.3 m s^{-1} was used for acoustic data post-processing, comparable to estimates of mean sound speed of the same region in other years (1470 m s^{-1} in 2013, 1472 m s^{-1} in 2019). Estimates fish backscatter were not sensitive to the sound speed used: if sound speed from any individual cast (range of 1454.6–1484.4 m s^{-1}) was used for the analysis instead of the mean value, backscatter changed by < 1%. In previous acoustic surveys, 38-kHz backscatter was dominated by backscatter with a frequency response consistent with that of fish (~ 96% in 2012 and 2013, De Robertis et al., 2017). During periods of elevated sea state, bubble entrainment caused attenuation of the

transmitted signal. These pings were removed following the methods in De Robertis et al. (2019). The nautical area scattering coefficient (s_A, $m^2\ nmi^{-2}$) was integrated from 4 m below the sea surface to 0.5 m above the sounder-detected seafloor (as determined by Echoview's "best bottom candidate" algorithm and manually corrected after visual inspection where necessary) using a −70 dB re 1 m^{-1} threshold in 0.1 nmi along-track and 5-m vertical bins. s_A is a proxy for fish abundance: it is proportional to fish density if the proportion of incident signal backscattered from the average fish in the population remains constant (MacLennan et al., 2002).

To compare backscatter between repeat surveys, the survey area was gridded into 0.5° latitude by 0.5° longitude cells. For large-scale surveys, only grid cells that contained data from both surveys were included (Figure 2.3), resulting in 75 valid grid cells encompassing 993 and 805 nmi of acoustic observations from the first and second surveys, respectively. Mean s_A was computed from acoustic measurements within each grid cell. The overall mean s_A and the standard errors for all valid grid cells were estimated for each survey by fitting a geostatistical model to the gridded data with a separate mean by survey and constant spatial autocorrelation across surveys. The model was fitted via generalized least squares (GLS) using a Gaussian spatial correlation structure with a nugget effect (Wackernagel, 2013). The same gridding and GLS model structure were applied to the four small-scale surveys to calculate mean backscatter and identify variability over time. In each of the four small-scale surveys, a subset of 42 grid cells containing 350 nmi of overlapping trackline was used for analysis (Figure 2.5). The mean location of the distribution weighted by mean s_A (center of gravity, Eq. 1 in Woillez et al., 2007), and the mean square distance between a measurement and the center of gravity (variance of spatial distribution, Eq. 3 in Woillez et al., 2007), were used to describe changes in the spatial distribution of the backscatter.

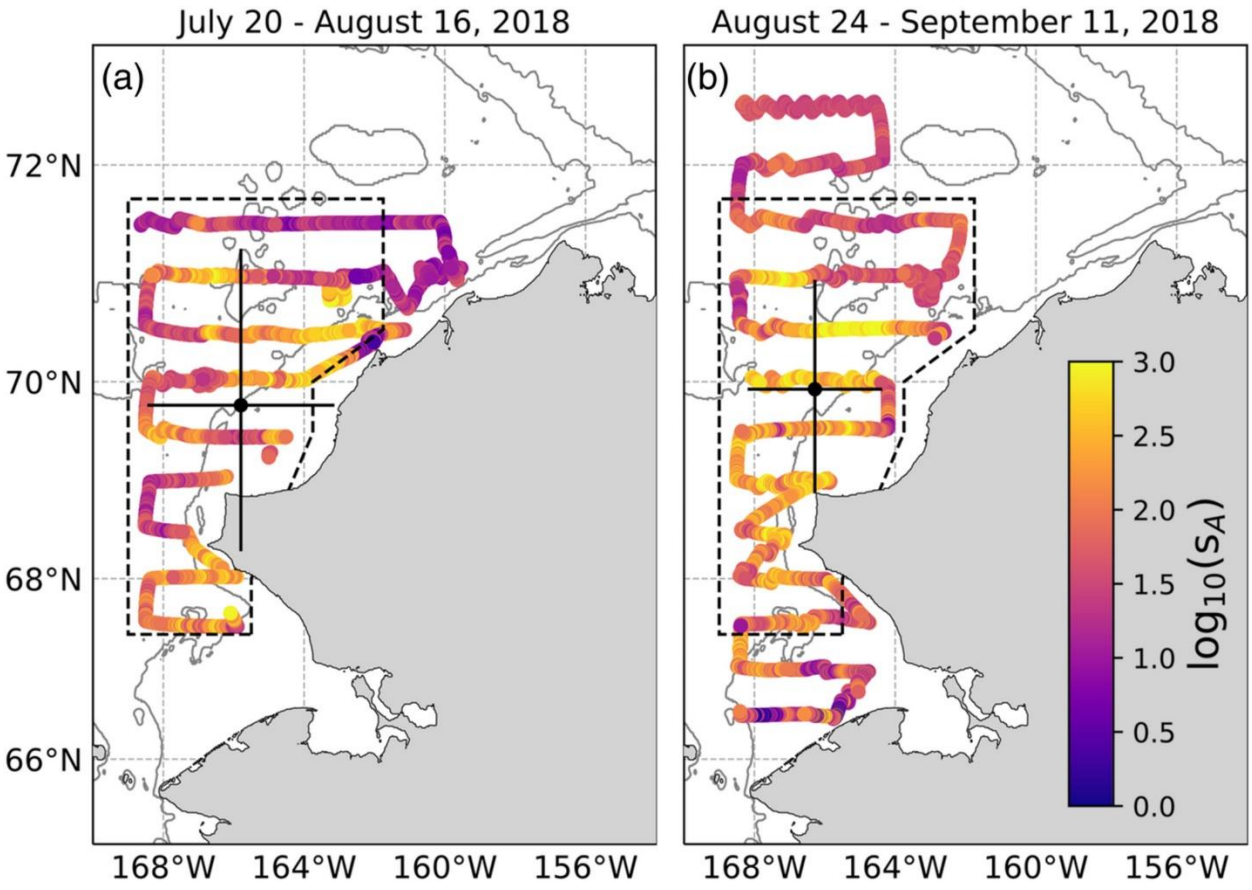

Figure 2.3 38-kHz backscatter (s_A, m^2 nmi^{-2}) along the saildrone trackline during the (a) first and (b) second large-scale surveys. Center of gravity and variance of spatial distribution computed from the gridded cells common to both surveys (region encompassed by the dashed line) are indicated by the black circles and lines, respectively. The 40-, 100-, and 1000-m depth contours are shown.

Measurements of backscattering cross-section (σ_{bs}, m^2) of individual scatterers during the four small-scale surveys were calculated from single targets identified with Echoview's split-beam single target detection (method 2) algorithm. To minimize potential biases introduced by multiple overlapping targets being interpreted as a single fish, single target detection was limited to areas where density was low. The estimated number of animals per reverberation volume (Nv, Sawada et al., 1993) was determined in 100 ping along-track and 5-m vertical bins based on a target

strength (TS, dB re 1 m^2; TS = 10 $\log_{10}(\sigma_{bs})$, where σ_{bs} is the backscattering cross-section, see MacLennan et al., 2002). Based on previous catch results indicating that Arctic cod were likely the dominant scatterer, Nv was calculated using a TS of −57.3 dB re 1 m^2 which assumes a mean Arctic cod size of 3.5 cm (De Robertis et al., 2017) and is similarly appropriate for walleye pollock of the same size class (Supplementary Table 2.1). Single targets in grid cells where Nv > 0.04 were excluded from further analyses, as recommended by Sawada et al. (1993).

To investigate changes in acoustic strength of targets during the small-scale surveys, the mean σ_{bs} of all targets during each day of each small-scale survey was calculated (79–21,542 targets per day, median of 2893 targets). The daily means were used to model the changes in σ_{bs} as a linear function of time (yearday). A TS-length relationship developed primarily from age-0 Arctic cod (Geoffroy et al., 2016) was used to infer fish length at the midpoint of each small-scale survey from σ_{bs}, defined as

$$SL = 10\left(\frac{10\log_{10}(\sigma_{bs})+65.13}{14.33}\right) \quad (2.1)$$

where SL is standard length (*see* Supplementary Table 2.1for additional details). Fish density (fish m^{-2}) at the midpoint of each small-scale survey was calculated using model-predicted σ_{bs} following MacLennan et al. (2002).

Vertical distributions of age-0 Arctic cod were quantified by calculating the weighted mean depth of the backscatter from the entire water column in 1-h intervals (Eq. 2 in Woillez et al., 2007). Hourly measurements were classified as day or night based on photosynthetically active radiation measurements from the saildrones' sensors, using a day/night threshold value of photosynthetically active radiation of 10 μmol photons s^{-1} m^{-2}, with 26% of the survey measurements occurring at night. To investigate linear trends in weighted mean depth over the duration of the surveys, an analysis of covariance was used to model the weighted mean depth of

backscatter as a linear function of time (yearday), allowing the intercept and slope to differ between day and night. The model was fit via GLS to account for possible temporal autocorrelation, assuming a continuous first-order autoregressive time series structure (corAR1, Pinheiro et al., 2019).

2.3.4 *Particle tracking simulations*

The potential for physical retention of fishes in the northeastern Chukchi Sea was examined using calculations completed using the OceanParcels python library (Lange and van Sebille, 2017) which simulates the advection of passive particles from results of a numerical ocean model. Particles were tracked using a 1/12° resolution 3D velocity field obtained from the hybrid coordinate ocean model (HYCOM) global analysis output (https://hycom.org), at 3-h time resolution from 20 July to 18 September 2018. This model has 40 depth levels, with 5-m intervals from 10 to 50 m depth. HYCOM uses the Navy Coupled Ocean Data Assimilation system which assimilates satellite altimeter and sea surface temperature data, and in situ temperature and salinity profiles from ship, drifter, and mooring instrumentation. Surface forcing for the HYCOM run is taken from the Navy Global Environmental Model (Hogan et al., 2014). The particles were seeded in areas where the first large-scale survey suggested (from observed grid cell mean s_A and survey-wide mean σ_{bs}) that fish were abundant. A single particle was seeded at the center of each model grid cell where observed fish density was ≥ 0.1 fish m^{-2} (96 of 98 model grid cells) on the start date of the first large-scale survey (20 July).

Particle positions were calculated at 3-h intervals. To evaluate the potential for depth-dependent variability in transport, four separate model runs were conducted seeding particles at fixed depths of either 10, 20, 30, or 40 m. This range of depths encompasses the portion of the water column where most of the fish were located (> 85% of backscatter was observed from 10 to

40 m). To evaluate retention in the northeastern Chukchi Sea, we identified the proportion of particles at each time step that were (1) contained within the small-scale survey region or (2) found in the Beaufort Sea or on the Chukchi Sea slope (> 100 m bottom depth).

2.4 RESULTS

2.4.1 *Repeat large-scale surveys*

The saildrones successfully completed two large-scale surveys of the U.S. continental shelf of the Chukchi Sea (Figure 2.3). Sea-ice north of 71.5°N limited the northern extent of the first survey which was completed from 20 July to 16 August 2018 by a single saildrone. The second survey was completed from 24 August to 11 September 2018 by tasking two saildrones independently with the northern and southern portions of the survey.

Although the mean backscatter in the large-scale survey area increased slightly from a mean s_A of 144 (± 37 SE) m^2 nmi^{-2} during the first survey to 188 (± 50 SE) m^2 nmi^{-2} during the second survey, the means were not significantly different (GLS, *t*-test $p = 0.37$). Fish distributions were similar in both surveys, suggesting there was no large-scale net advection of the population through the area during the survey period. The center of gravity of the backscatter shifted 18.7 km west (−165.79°W to −166.28°W) and 17.4 km north (from 69.77°N to 69.92°N), while exhibiting a slight decrease in variance of spatial distribution (−0.44° and −0.75° in latitude and longitude, respectively; Figure 2.3). During both surveys > 50% of the total backscatter occurred between 70°N and 71°N.

Temperature and salinity at 0.5 m depth ranged from −0.7°C to 11.4°C and from 26.5 to 32.8 psu during the large-scale surveys (Figure 2.4). The coldest water was encountered north of 71°N, where surface conditions suggested recent mixing with sea ice meltwater (< 7°C and salinity < 30 psu). In areas where meltwater was present at the surface, backscatter was low; 92.9% of

backscatter was observed in areas where the surface temperature was greater than 6°C and salinity was greater than 29 psu (Figure 2.4, Supplementary Figure 2.1).

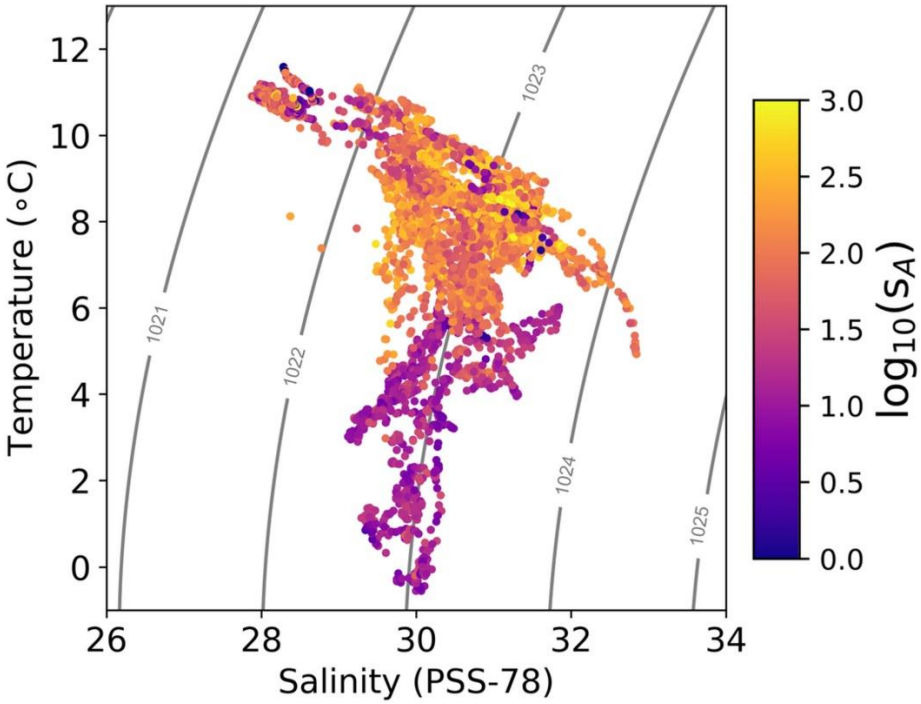

Figure 2.4 Ten-minute averaged temperature and salinity at 0.5 m depth measured by sensors on the keel of the saildrone during the large-scale surveys (Figure 2.3). Color of points indicates depth-integrated water column 38-kHz backscatter (s_A, m^2 nmi^{-2}). Contours indicate potential density.

2.4.2 *Repeat small-scale surveys*

The small-scale surveys (four-transect subarea of the large-scale survey from 69.5°N to 71°N) lasted 12–21 d: 20 July–03 August, 23 July–12 August, 13–28 August (including a 5-d gap in sampling from 17 to 21 August), and 30 August to 11 September (Figure 2.5). Mean backscatter within the 42 grid cells of the small-scale survey area varied among surveys, increasing from 197 (± 53 SE) to 369 (± 80 SE) m2 nmi−2 over the course of the summer (GLS, t-test p = 0.03, Table 1). The distribution of the population within the small-scale survey region did not shift

appreciably among surveys. The center of gravity shifted slightly to the southwest between the first and last survey (19.4 km to the south and 19.3 km to the west, from −165.56°W 70.37°N to −166.08°W 70.19°N, Figure 2.5).

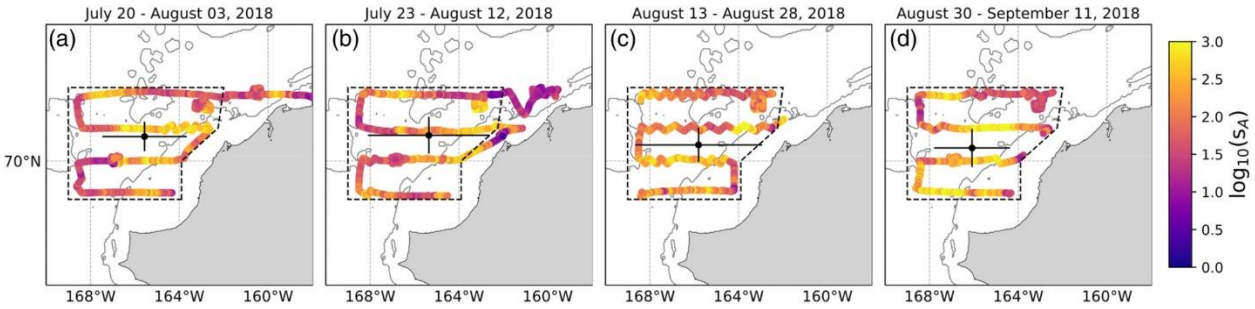

Figure 2.5 38-kHz backscatter (s_A, m^2 nmi^{-2}) along the saildrone trackline during the (a) 1st, (b) 2nd, (c) 3rd, and (d) 4th small-scale surveys. The center of gravity and variance of the spatial distribution computed from the gridded cells common to all surveys (region encompassed by the dashed line) is indicated by the black circles and lines, respectively. Note that the first two survey periods overlap in time. The 40- and 100-m depth contours are shown.

Table 2.1 Summary of small-scale survey observations. The mean s_A, model-predicted backscattering cross-section (σ_{bs}) at the midpoint of each small-scale survey, abundance from 38-kHz backscatter, and estimated standard length of gadids are given. Standard errors are given in parentheses. Lengths were calculated from the model-predicted σ_{bs} at each survey midpoint using the TS–length relationship defined for Arctic cod (Geoffroy et al., 2016, Supplementary Table 2.1).

	20 Jul–03 Aug	23 Jul–12 Aug	13–28 Aug	30 Aug–11 Sept
Mean s_A (m^2 nmi^{-2})	197 (± 53)	177 (± 76)	281 (± 79)	369 (± 80)
σ_{bs} (m^2)	1.7×10^{-6} ($\pm 1.4 \times 10^{-6}$)	2.0×10^{-6} ($\pm 1.4 \times 10^{-6}$)	2.8×10^{-6} ($\pm 1.5 \times 10^{-6}$)	3.5×10^{-6} ($\pm 1.6 \times 10^{-6}$)
Abundance index (fish m^{-2})	2.5 (± 0.6)	2.0 (± 0.8)	2.2 (± 0.6)	2.3 (± 0.5)
Estimated length (cm)	3.4 (1.1, 5.1)	3.7 (1.6, 5.4)	4.7 (2.7, 6.4)	5.5 (3.5, 7.2)

The vertical distribution of fish during the small-scale surveys was consistent with the onset of vertical migration behavior. As the summer progressed, the weighted mean depth of backscatter remained shallow at night, but daytime depth increased after the second survey (Figure 2.6a–d). Weighted mean depth during daylight hours increased from 17.7 (± 0.2 SE) to 30.0 (± 0.4 SE) m over the period of 53 d between the 1st and 4th survey (Figure 2.6a–d). In contrast, weighted mean depth at night showed less variation, ranging from 16.6 (± 0.5 SE) to 19.6 (± 0.5 SE) m during the four surveys. Daylight hours decreased from 24 h per day at the start of the 1st survey to 14 h per day at the end of the 4th survey. Weighted mean depth differed between day and night (significant interaction in GLS, *t*-test $p = 0.01$) and this difference increased as a function of yearday (significant difference in slopes, *t*-test $p = 0.005$).

Although the placement of the transducer on the saildrone is shallower than typical on most research vessels, measurements of backscatter and individual acoustic targets were restricted to > 4 m depth. We found no significant difference between day and night backscatter (*t*-test comparing day and night on all sampling days, $p = 0.27$), indicating that there were not a significant number of scatterers migrating above the sampling range during the surveys. Although it is possible that some scatterers remained shallower than the transducer at all times, it is unlikely that we missed a large portion of the fish population which would have had to remain above the insonified depth throughout the entire survey period.

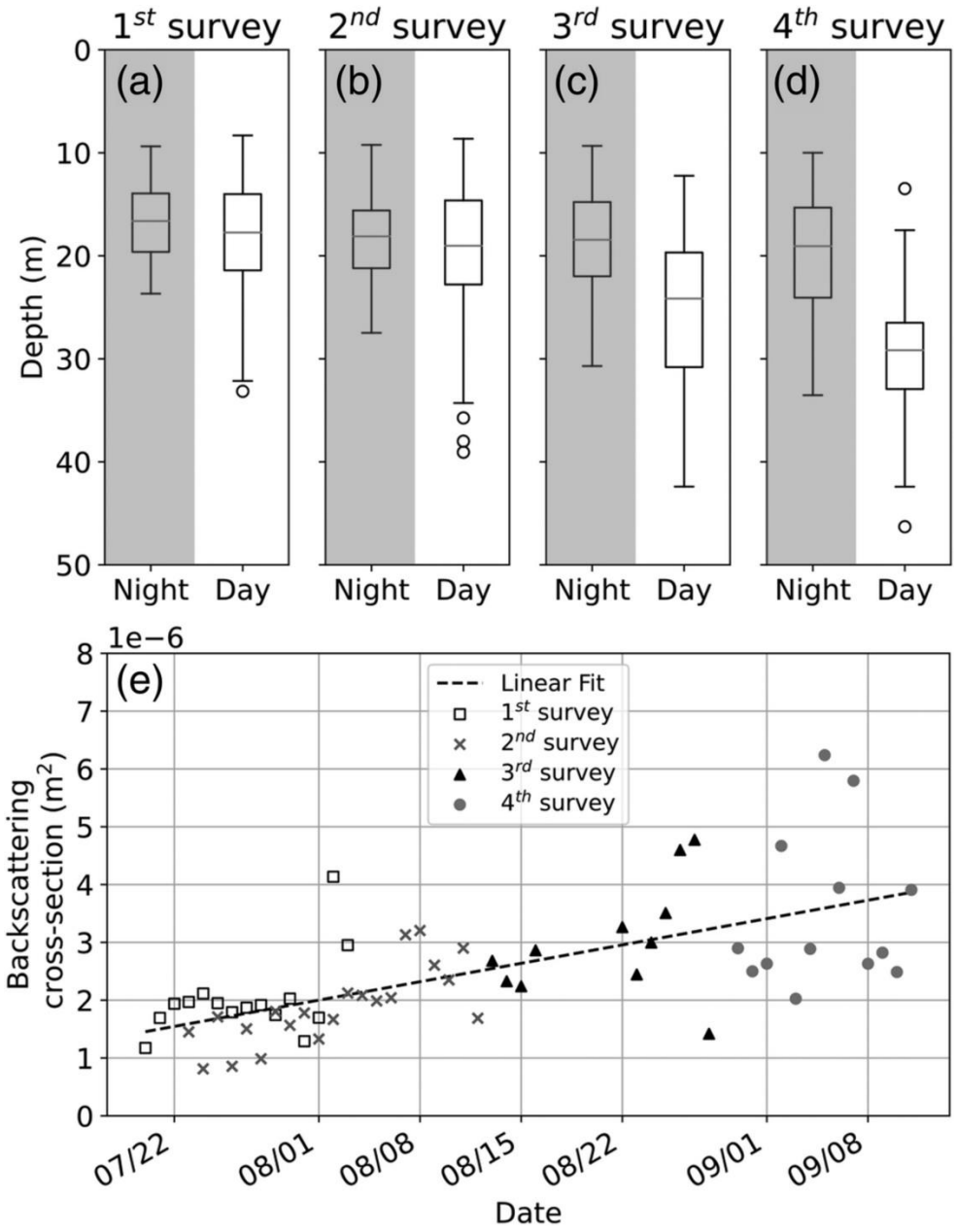

Figure 2.6 (a–d) Distributions of nighttime and daytime hourly weighted mean depth of backscatter during the small-scale surveys. Boxes indicate the interquartile range, horizontal gray lines the median, vertical lines the 5% and 95% intervals. Circles indicate observations beyond the whiskers. (e) Daily means of backscattering cross-section (σ_{bs}) of all targets observed in small-scale surveys. Linear fit for the 53-d period is indicated by the black dashed line ($\sigma_{bs} = -7.68 \times 10^{-6} + 4.54 \times 10^{-8}$(yearday), $p < 0.001$, $r^2 = 0.44$).

Backscattering cross-section (σ_{bs}) measurements were obtained from 252,949 acoustic single targets detected during the four small-scale surveys. Daily mean σ_{bs} was positively related to yearday ($\sigma_{bs} = -7.68 \times 10^{-6} + 4.54 \times 10^{-8}$(yearday), $p < 0.001$, $r^2 = 0.44$; Figure 2.6e), which results in a predicted increase in σ_{bs} from 1.7×10^{-6} ($\pm 1.4 \times 10^{-6}$ SE) to 3.5×10^{-6} ($\pm 1.6 \times 10^{-6}$ SE) between the midpoints of the first and fourth small-scale survey (Table 1). Estimates of standard length derived from σ_{bs} correspond to a change in length of 2.1 cm between the midpoints of the first and last survey (3.4–5.5 cm). Using the model-predicted values of σ_{bs} from the first day and last day of the small-scale surveys (Figure 2.6e), the change in length corresponds to a growth rate of 0.54 mm d^{-1} over the 53-d period (Supplementary Table 2.1). This estimate of growth rate is sensitive to the specific TS–length relationship used to convert scattering strength to fish length, and the use of alternative relationships results in a large range of estimates (0.24–0.89 mm d^{-1}; Supplementary Table 2.1).

2.4.3 *Particle tracking*

The passive particles in the simulation were primarily transported to the northeast (Figures 2.7a-e, Supplementary Video 2.1). By the end of the 60-d model run, the majority of particles were dispersed along the slope after being transported through Barrow Canyon (Figure 2.7e). Initial movement of particles out of the survey region (Figure 2.7a, b) was in two directions; particles in the northwest region of the survey area moved north toward Hanna Shoal, while the remainder of the particles followed the Alaska coastline to the northeast.

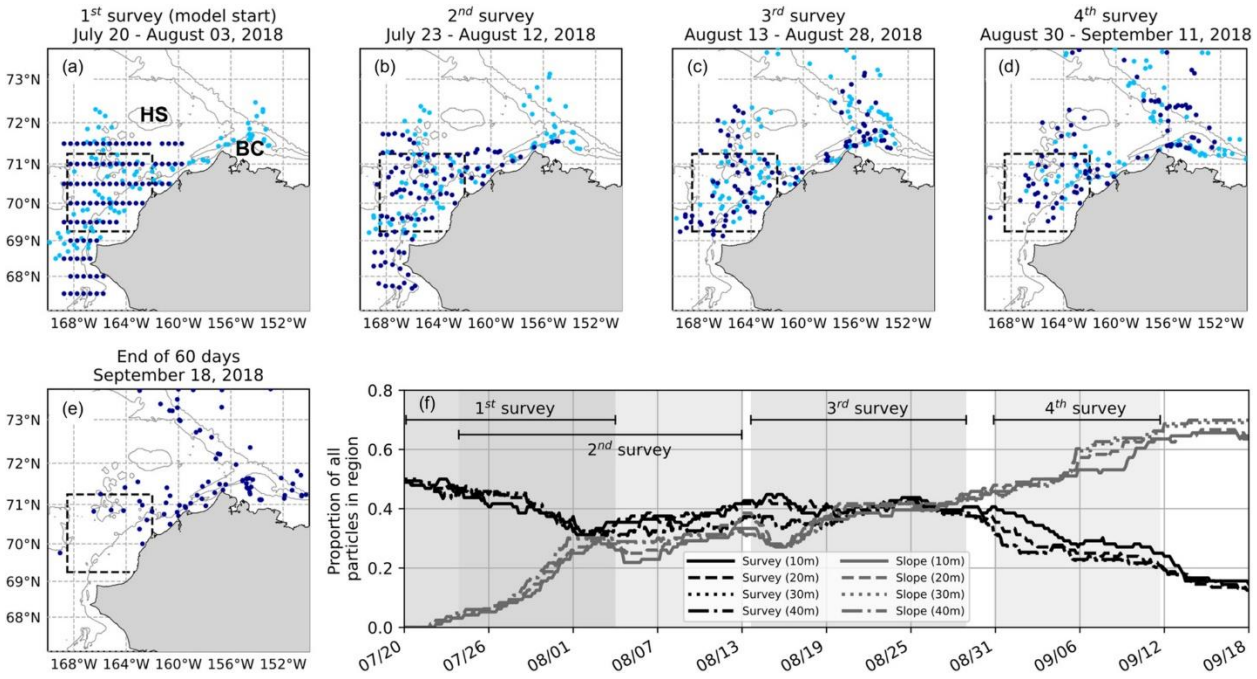

Figure 2.7 Results of particle tracking model. (a–d) Locations of particles at 20 m depth at the start (dark blue circles) and end (light blue circles) of the (a) 1st, (b) 2nd, (c) 3rd, and (d) 4th small-scale surveys. Particles were seeded on 20 July at the center of each 0.5° grid cell of the first-large-scale survey (see Supplementary Video 2.1). The locations of Hanna Shoal (HS) and Barrow Canyon (BC) are indicated in the first panel. (e) Locations of particles seeded at 20 m depth at the end of the 60-d model run. The area indicated by the dashed box represents the small-scale survey region. The 40-, 100-, and 1000-m depth contours are shown. (f) Proportion of particles remaining within the small-scale survey region (black lines), and particles transported to the Beaufort Sea and Beaufort/Chukchi slope (> 100 m bottom depth, gray lines) over a period of 2 months from the start of the 1st survey. Model results for particles seeded at fixed depths of 10–40 m are shown. The time periods of the four small-scale surveys are indicated by the gray shaded regions and lines. Note that the 1st and 2nd survey periods overlapped.

From 20 July to 02 August, particles were advected out of the small-scale survey region at a consistent rate, with the proportion remaining in the small-scale survey area decreasing from 49% to 33% (Figure 2.7f). The rate of advection out of the small-scale survey region decreased

from 02 August to 25 August, when the proportion of particles in the survey region increased to ~ 40% and there were periods where particles returned to the region from the north. Thereafter the rate of export increased, with only 11% of all particles remaining in the survey area by mid-September. Through most of the model run, the proportion of particles along the Beaufort/Chukchi slope steadily increased. By 18 September, or 60 d after the start of the first small-scale survey, 65% of particles had been advected seaward of the shelf break (> 100 m bottom depth) in the Chukchi and Beaufort Seas (Figure 2.7e). The model runs produced similar results with particles tracked across depths of 10–40 m (Figure 2.7f), indicating that (1) the system is strongly barotropic, that is, there is little vertical shear to the flow; and (2) inferences drawn from the model are not sensitive to fish depth.

2.5 DISCUSSION

2.5.1 *Acoustic surveys of age-0 gadids*

Although the timing and location of spawning events are not known, large numbers of age-0 Arctic cod have been previously observed in the Chukchi Sea in the late summer and fall (De Robertis et al., 2017). The absence of a large population of age-1+ Arctic cod suggests that age-0 fish found in the eastern Chukchi Sea likely originated elsewhere, and that either overwinter mortality is high or they do not remain in place as they grow to maturity. This mortality and/or emigration is likely also occurring for other gadids including age-0 walleye pollock, for which large spawning stocks are observed in the Bering Sea but few age-1+ fish have been reported in the eastern Chukchi Sea (Goddard et al., 2014). We analyzed repeat acoustic surveys and used particle tracking simulations to gain insights into possible directions of arrival and movement of these age-0 gadids through the eastern Chukchi Sea, and whether the absence of older individuals is most likely due to mortality or emigration of age-0 individuals.

Although we were not able to directly sample acoustic targets, acoustic scatterers throughout the areas surveyed by the saildrones have spatial distributions and scattering properties that are consistent with those expected from age-0 gadids. Backscatter was highest in the northeastern Chukchi Sea, consistent with observations from previous surveys in which trawl samples in that area were dominated by large numbers of age-0 Arctic cod (Quast, 1974; Eisner et al., 2013; De Robertis et al., 2017). The large-scale survey estimates of mean s_A (144 and 188 m^2 nm^{-2}) are similar in magnitude with estimates observed in previous acoustic surveys in the region (63.6 and 164.9 m^2 nm^{-2} observed in 2012 and 2013), in which age-0 Arctic cod < 6 cm in length were the dominant contributors to 38-kHz backscatter (De Robertis et al., 2017). More recently, preliminary data from midwater trawl surveys in 2017 and 2019 indicate that primary scatterers across the shelf are age-0 gadids < 6 cm in length, and that while Arctic cod are the historically dominant scatterers, age-0 pollock may be becoming more abundant (R. M. Levine unpubl.). The σ_{bs} measurements observed in the four small-scale surveys (1.7×10^{-6} to 3.5×10^{-6} m^2, Table 1) are consistent with observed in situ observations of both age-0 Arctic cod and walleye pollock < 6 cm (Brodeur and Wilson, 1996; Geoffroy et al., 2016) rather than the much higher σ_{bs} expected for larger individuals. For example, the σ_{bs} for a 15-cm Arctic cod is ~ 8-fold greater than for a 3.5-cm fish (Geoffroy et al., 2016), and ~ 14-fold greater for a 15-cm age-1 pollock than a 3.5-cm age-0 (Brodeur and Wilson, 1996; Traynor, 1996). Although estimates of length are sensitive to the choice of TS–length relationship (Supplementary Table 2.1), the σ_{bs}-derived lengths are consistent with the length distributions of age-0 gadids observed in previously collected trawl samples in the region (mean length of 3.5 cm, 99.7% of fish < 6.5 cm in August–September reported in De Robertis et al., 2017). These multiple lines of indirect evidence support our assumption that age-0 gadids dominated contributions to backscatter in the saildrone surveys.

The repeat acoustic surveys indicate that, while the spatial distribution of fishes in the northeastern Chukchi Sea did not change significantly from late July to early September of 2018, acoustic backscatter increased by ~87% during this period. The observed increase in acoustic backscatter could have resulted from either an increase in the abundance of scatterers, changes in the composition (i.e., size) of the scatterers, or a combination of both. During the small-scale surveys, σ_{bs} between the midpoint of the first and fourth small-scale survey increased 104%. This suggests that the size distribution of fishes in the survey region may have shifted toward larger individuals. Over the same period, estimated fish density derived from the acoustic observations remained consistent (2.0–2.5 fish m^{-2}, with overlapping standard errors, see Table 1). These estimated fish densities are similar to those observed in previous surveys (0.6 age-0 Arctic cod m^{-2} in 2012 and 2.2 Arctic cod m^{-2} in 2013, De Robertis et al., 2017).

Despite substantial variability, there is a unimodal distribution of σ_{bs} which increases over time, consistent with fish growth (Supplementary Figure 2.2). σ_{bs} is largely driven by swimbladder size, and although variability is high, average backscattering strength of individuals increases with length (Traynor, 1996; Parker-Stetter et al., 2011). The changes in σ_{bs} corresponded to an estimated growth rate of 0.54 mm d^{-1} during the small-scale survey period. This growth rate is larger than measured rates from previous field and laboratory observations of age-0 Arctic cod (0.26 mm d^{-1} at 50 mm length, Hop et al., 1997; 0.19–0.24 mm d^{-1} Bouchard and Fortier, 2011). However, growth rate is sensitive to the choice of TS–length relationship (0.24–0.89 mm d^{-1} depending on the relationship used, Supplementary Table 2.1). Furthermore, σ_{bs} is orientation dependent (Foote, 1980), and these estimates of growth assume consistent average orientation distributions over time. Although the uncertainties are large, the increase in σ_{bs} is likely related to growth, and it may ultimately be possible to estimate growth rates of Arctic gadids by measuring

target strength in some circumstances. In future work, this uncertainty can be reduced by assessing TS–length relationships directly by coupling these observations with direct sampling of fish lengths.

The observed changes in vertical distribution (change in mean nighttime depth from 17.7 to 30.0 m during small-scale surveys) provide further evidence that growing age-0 gadids may have dominated the acoustic observations. As eggs and larvae, both Arctic cod and walleye pollock are predominantly surface associated (Spencer et al., 2020), drifting until their swimming ability develops and their swimbladder fills. Individuals exhibit an ontogenetic migration, descending deeper in the water column as they age. This transition in Arctic cod and walleye pollock occurs at a length of > 30 mm, when pelagic juveniles vertically shift to deeper water during daytime, typically observed in late summer (Brodeur et al., 2000; Ponomarenko, 2000; Bouchard and Fortier, 2011). In the saildrone surveys, diel vertical migration behavior was initiated when mean TS-derived lengths were > 30 mm. This behavior also coincided with the onset of night in late-July during both the first and second small-scale surveys. This change is consistent with expected behavior for gadids as individuals increase in size over time. Together, the observed σ_{bs} and increased vertical migration suggest that increasing backscatter may be due to individual growth.

2.5.2 *Suitability of the Chukchi Sea as a nursery*

Minimal changes were observed in the spatial distribution of fish during the survey period, which is inconsistent with a single, spatially restricted pulse of fish being advected across the Chukchi shelf. If there was a continuous northward transport, a single short spawning pulse from the south would result in a northward shift in the center of gravity of the population over time, and/or large changes in abundance between surveys. We hypothesized two alternative mechanisms to account for our observations: (1) a greatly extended spawning period that continues late into summer, with

fish continuously transported north at a steady rate with balanced immigration and emigration; or, (2) retention of a population established by mid-July for most of the summer. The latter of these scenarios would be consistent with Arctic cod in other regions of the western Arctic where the majority of hatching occurs during a ~ 2-month period in late spring (Bouchard et al., 2016).

Age-0 fish populations may be enhanced by being retained on the Chukchi shelf in summer to use the region as a nursery. Predation from piscivorous fish is likely low, as large fishes are scarce in the region (Sigler et al., 2011; De Robertis et al., 2017). Piscivorous seabirds are widely distributed and abundant throughout the Bering, Chukchi, and Beaufort Seas (Kuletz et al., 2015), and thus seabird predation pressure during open-water season is relatively consistent throughout the region. In summer, seabird foraging hotspots occur on the boundaries of the Chukchi shelf near Bering Strait and to the north along Barrow Canyon, where there is also a seasonal increase marine mammal presence (Kuletz et al., 2015).

Water temperatures on the Chukchi shelf are also likely to be more conducive for growth than conditions farther north (Laurel et al., 2016). Saildrone measurements of temperature and salinity were limited to the upper 0.5 m, thus it was not possible to directly assess the conditions at the same depths as the fish. However, backscatter was lowest in the northernmost areas of the large-scale survey area (Figure 2.3), where low surface water temperatures and salinities suggested recent mixing with the meltwater which typically overlays cold winter water (Weingartner et al., 2013; Danielson et al., 2017). De Robertis et al. (2017) observed that Arctic cod on the Chukchi shelf were largely present at intermediate temperatures (3.4–6.6°C) and high salinities (> 30.4 psu) typical of Bering/Chukchi Summer Water. The Bering/Chukchi Summer Water flows north into the Chukchi Sea from the northern Bering Sea shelf (Coachman et al., 1975; Danielson et al., 2017) and gradually replaces the surface meltwater and deep winter water on the Chukchi shelf

(Weingartner et al., 2013). The warmer Bering/Chukchi Summer Water is within the temperature range (2–8°C) observed for maximum growth in Arctic cod and positive growth potential in both walleye pollock and saffron cod (Laurel et al., 2016).

2.5.3 *Advective influences on age-0 fishes*

The low backscatter in areas near meltwater indicates that these fish are unlikely to be originating from the north or areas influenced by recent ice melt and are either passively or actively remaining in warmer conditions. The Chukchi shelf is a highly advective environment, where advection is likely to dominate over the directed swimming movements of small fishes. The association of age-0 gadids with warmer water conditions supports the hypothesis that the age-0 gadids observed on the Chukchi shelf are likely advected northward from spawning areas to the south. Advective transport north across the Chukchi shelf is generally attributed to both local winds and a far field forcing relating to a sea level difference between the Pacific and the Arctic (see Woodgate et al., 2005 for discussion). Since 1990, the annual mean northward velocity of the flow through the Bering Strait has ranged from $\sim 18\ (\pm 2)$ cm s^{-1} in 2001 to $\sim 28\ (\pm 3)$ cm s^{-1} in 2014 (lowest and highest annual mean velocities of the 1991–2015 period; Woodgate, 2018). This includes periods of southward flow and thus the northward mode speed is higher (from ~ 20 to > 40 cm s^{-1}, Woodgate, 2018, their Figure 2.4). In the northeastern Chukchi Sea, the mean velocities of the upper 10 m of the water column in summer average ~ 8 cm s^{-1}, ranging from 0.5 to 22.8 cm s^{-1} from 2010 to 2015 (Stabeno et al., 2018). In respiration experiments, maximum aerobic swim speeds of Arctic cod were 3 to 3.6 body lengths s^{-1} (12–14 cm s^{-1} for a 4-cm fish) during burst swimming activity (Kunz et al., 2018). In studies of related gadid species, routine swimming speeds of juvenile fish were 0.5 to 0.6 body lengths s^{-1} (2–2.4 cm s^{-1} for a 4-cm fish, Peck et al., 2006). For age-0 gadids of 3.5 cm length, this suggests a routine swimming speed of

approximately 1.9 cm s^{-1}, which is an order of magnitude lower than typical advective currents. These estimates support the hypothesis that passive transport likely plays a dominant role determining the distribution of age-0 gadids on the Chukchi shelf, and that swimming behaviors have relatively small impacts on long-term distributions.

In late summer 2018, transport simulations suggest that age-0 gadids were advected northward, likely to the Beaufort and Chukchi slopes and Arctic basin. As expected, the model indicated that net transport was northward, with 90% of modeled particles released in the large-scale survey area dispersed along the shelf or slope to the north of the survey area at the end of the 60-d model run. However, during the month of August, only a few particles left the survey area, and during some periods transport reversed to increase particle abundance within the small-scale survey area (Figure 2.7f, Supplementary Video 2.1). The decrease in the rate of particles leaving the survey area and subsequent return of particles suggests that age-0 gadids are retained on the Chukchi shelf by episodic flow reversals. Estimates of retention based on particle transport from the survey area are consistent at 10, 20, 30, and 40 m depth (depths where the bulk of the backscatter occurred throughout the survey period). This suggests that variations in horizontal advection of fishes are likely insensitive to vertical movements or water column position.

Flow reversals similar to those occurring in the 2018 particle tracking model are commonly observed in the northeastern Chukchi Sea, and are associated with strong southward winds (Woodgate et al., 2005; Stabeno et al., 2018; Pisareva et al., 2019). De Robertis et al. (2017) speculated that difference in age-0 Arctic cod distribution between 2012 and 2013 may be linked to variability in currents and prey availability, and recent work has proposed variation in wind-driven retention as an explanation (Vestfals et al., 2019). Woodgate et al. (2005) developed a linear model for determining water velocity in the northeastern Chukchi Sea as a function of the pressure

head forcing and surface wind speed. Offshore of Cape Lisburne, assuming a baseline pressure head velocity of 9.4 cm s^{-1} (see Table 3 in Woodgate et al., 2005), surface wind speed would need to exceed 7.2 m s^{-1} to the south to balance the pressure head forcing, temporarily stopping northward transport. Wind speed measurements from the saildrones indicate that from 01 August to 30 August, the mean velocity of the north–south wind component was 2.3 m s^{-1} to the south, with 21 days having mean southward winds (Supplementary Figure 2.3). However, during 10.3% of August, wind velocity to the south was > 7.2 m s^{-1}, during which predicted net northward transport would be near zero or negative. This simplistic calculation is supported by the particle tracking model which shows this wind reversal was sufficient to account for the particle retention on the shelf. We hypothesize that wind-driven relaxation in northward transport may be responsible for, and predict, retention of age-0 gadids in the northeastern Chukchi Sea.

It also seems reasonable to hypothesize that interannual variations in circulation influence advection and subsequent retention of age-0 gadids in the Chukchi Sea. Transport through the Bering Strait (which is generally indicative of the northward flux through the Chukchi Sea, Woodgate et al., 2005) estimated from near-bottom velocity data indicates that monthly mean transport during summer 2018 (R. A. Woodgate pers. comm.) was similar to the 1990–2004 climatology (Woodgate et al., 2005), even though in the annual mean, 2018 was higher in flow than the climatology. Thus, as it is summer that most concerns us, it is likely that the observed summer residence time of age-0 gadids in the Chukchi in 2018 is fairly typical, and suggests a hypothesis that cold-adapted species such as Arctic cod may have adapted to spawn at a time and place that more or less reliably places larvae in this apparent nursery area.

The Pacific Arctic is currently undergoing rapid changes, including increased northward transport through Bering Strait in recent decades (Woodgate, 2018). These changes in advection,

temperature, and ice cover have the potential to alter Arctic gadid populations. Bouchard et al. (2017) proposed that an initial decrease in ice cover, resulting in warmer conditions, would increase survival and growth of larval Arctic cod. However, continued temperature increases beyond their preferred growth range could depress physiological condition and survival of larval Arctic cod, while enhancing conditions for larval walleye pollock (Koenker et al., 2018). Winter spawning provides a lengthy growth period for Arctic cod, during which maximizing prewinter size may be important for survival (Bouchard and Fortier, 2011). Increased northward transport in summer may more quickly transport Arctic cod off the shelf and into the Arctic basin, shortening time available for growth in this potentially favorable nursery environment.

Increased input of Pacific water onto the shelf may also increase the presence of subarctic and boreal gadids, increasing competition and predation among pelagic species (Sigler et al., 2011). This transition has already been observed in the Barents Sea, where larger boreal species have expanded their distribution, increasing predation on and competition with smaller Arctic species (Fossheim et al., 2015). Subarctic gadids of high abundance in the Bering Sea such as walleye pollock and Pacific cod may be more likely to be transported north, following the same advective pathways across the Chukchi shelf as Arctic cod. Evidence from recent midwater surveys conducted in the region (R. M. Levine unpubl.) suggest other broadly distributed fishes such as walleye pollock or saffron cod have the potential to move further north, increasing in abundance on the Chukchi shelf as conditions warm (Huntington et al., 2020). The potential for these species to survive overwinter in the Arctic, however, is still unknown.

We found that distributions of age-0 gadids in the Chukchi Sea are strongly driven by two factors: advection and retention within specific water masses. Further studies are needed to better understand specific oceanographic features (e.g., currents, fronts, ice presence, water masses) and

to investigate their demographic effects on gadids in the region. For example, in situ observations of fish movement and behavior (e.g., target tracking from moored acoustic instruments; Kaartvedt et al., 2009) paired with direct observations of currents have potential to better constrain potential pathways for transport of fishes, resolve the timing and seasonal dynamics of their development from eggs to juveniles, and predict recruitment into downstream populations along the Beaufort and Chukchi Sea slope.

2.5.4 *Insights on Arctic fishes from USV observations*

Traditionally, acoustic surveys have relied on trawl sampling of species and size composition to convert acoustic backscatter into abundance estimates (Simmonds and MacLennan, 2005). Recent advances in the integration of echosounders into autonomous platforms have increased our ability to measure acoustic backscatter remotely over long periods (Greene et al., 2014; Mordy et al., 2017; Benoit-Bird et al., 2018; Ohman et al., 2019). We used the endurance of the saildrones to collect a large number of acoustic observations over an extended period of time which would have been prohibitively expensive and logistically difficult using ships. These repeat acoustic surveys spanning large spatial and temporal scales enabled us to constrain the movement of age-0 gadid fishes on the Chukchi shelf and made it possible to determine a TS and approximate a growth rate. These insights into the transport, growth, origins, and fate of the age-0 gadid population were made possible by the high spatial and temporal coverage offered by autonomous platforms.

However, with current technology, it remains challenging, in most cases, to validate species composition, size, sex, and other organismal properties by acoustic methods alone (Bassett et al., 2018). Thus, the key challenge going forward is not how to measure acoustic scattering from autonomous vehicles, but how best to use these measurements to understand the abundance, distribution, and behavior of marine organisms (De Robertis et al., 2019). While autonomous

acoustic surveys cannot definitively identify the species and size composition of acoustic scatterers, they can be effective in regions where other data have shown that a single or distinguishable group of dominant scatterers enables interpretation of acoustic data (Mordy et al., 2017; De Robertis et al., 2019). Low-diversity, high-latitude regions may be favorable for autonomous echosounder measurements because backscatter is often dominated by a single species or group (Geoffroy et al., 2011; De Robertis et al., 2019).

With its low pelagic diversity, the Chukchi Sea provides a good ecosystem for the application of autonomous acoustic survey methods. However, Arctic ecosystems are undergoing changes that may alter species compositions (Fossheim et al., 2015; Huntington et al., 2020), and the assumptions that make these inferences possible are likely to change with time. The increased presence of species with similar acoustic properties will limit the ability to address species-specific questions without additional sampling in rapidly changing ecosystems such as the Arctic, although inference at the community level (e.g., gadids) may be feasible. Future studies of high-latitude marine environments (e.g., Arctic, Antarctic) may benefit from the use of USVs and other autonomous platforms allowing for acoustic measurement of fish and macrozooplankton populations, with the potential to expand into more complex environments and applications as the methodologies for remote species identification improve.

2.6 CONCLUSIONS

Repeat saildrone surveys indicated that advection resulted in the retention of age-0 gadids on the Chukchi Sea shelf throughout the summer where they underwent in situ growth. These fish likely originated south of the central Chukchi Sea and were advected onto the northeast shelf. In late summer, transport simulations suggest that advection played a larger role than swimming and that these fishes were passively advected further north to the Beaufort and Chukchi slopes and Arctic

basin. Variations in transport rate and trajectory may account for the interannual variability in the density and distribution of pelagic fishes on the Chukchi shelf. In a changing climate, changes in circulation and water column conditions may alter the future structure of pelagic communities in the Pacific Arctic and the suitability of the Chukchi shelf as a favorable nursery area. Although Arctic cod are currently the dominant gadid in the region, increasing temperatures and earlier transport off the Chukchi shelf could limit age-0 growth prior to their first winter, and increased subarctic pelagic fishes such as walleye pollock may lead to increased predation pressure and competition that may further limit the Arctic cod population (Fossheim et al., 2015; Huntington et al., 2020). New technologies such as autonomous vehicles are likely to provide opportunities to better quantify perturbations of this rapidly changing ecosystem.

2.7 ACKNOWLEDGEMENTS

This work was funded by the North Pacific Research Board Arctic Research Program, NOAA's Pacific Marine Environmental Laboratory's Innovative Technology for Arctic Exploration program, NOAA's Alaska Fisheries Science Center, and the Joint Institute for the Study of the Atmosphere and Ocean (JISAO) under NOAA Cooperative Agreement NA15OAR4320063. The saildrone deployments would not have been possible without the contributions of Richard Jenkins and Dave Peacock (Saildrone, Inc.), and Ivar Wagnen (Kongsberg Simrad). We would also like to thank the Alaska Waterways Safety Committee, Alaska Eskimo Whaling Commission, The North Slope Borough, and members of The Village of Wainwright, AK for their advice and assistance with saildrone operations. We thank the anonymous reviewers for their suggestions which improved this manuscript. This is contribution No. 5091 for Pacific Marine Environmental Laboratory, contribution No. 2020-1063 for JISAO, and contribution No. EcoFOCI-0947 for NOAA's Ecosystem Fisheries Oceanography Coordinated Investigations. Bering Strait mooring

observations are funded by NSF-OPP (1304052 and 1758565) with data available from http://psc.apl.washington.edu/BeringStrait.html. Any use of trade, firm, or product names is for descriptive purposes only and does not imply endorsement U.S. Government. Findings of this paper do not necessarily represent the views of the National Oceanic and Atmospheric Administration.

2.8 REFERENCES

Bassett, C., De Robertis, A., Wilson, C.D., 2018. Broadband echosounder measurements of the frequency response of fishes and euphausiids in the Gulf of Alaska. ICES J. Mar. Sci. 75, 1131–1142. https://doi.org/10.1093/icesjms/fsx204

Benoit-Bird, K.J., Patrick Welch, T., Waluk, C.M., Barth, J.A., Wangen, I., McGill, P., Okuda, C., Hollinger, G.A., Sato, M., McCammon, S., 2018. Equipping an underwater glider with a new echosounder to explore ocean ecosystems. Limnol. Oceanogr. Methods 16, 734–749. https://doi.org/10.1002/lom3.10278

Boswell, K.M., Pedersen, G., Taylor, J.C., LaBua, S., Patterson, W.F., 2020. Examining the relationship between morphological variation and modeled broadband scattering responses of reef-associated fishes from the Southeast United States. Fish. Res. 228, 105590. https://doi.org/10.1016/j.fishres.2020.105590

Bouchard, C., Fortier, L., 2011. Circum-arctic comparison of the hatching season of polar cod *Boreogadus saida*: A test of the freshwater winter refuge hypothesis. Prog. Oceanogr. 90, 105–116. https://doi.org/10.1016/j.pocean.2011.02.008

Bouchard, C., Geoffroy, M., LeBlanc, M., Majewski, A., Gauthier, S., Walkusz, W., Reist, J.D., Fortier, L., 2017. Climate warming enhances polar cod recruitment, at least transiently. Prog. Oceanogr. 156, 121–129. https://doi.org/10.1016/j.pocean.2017.06.008

Bouchard, C., Mollard, S., Suzuki, K., Robert, D., Fortier, L., 2016. Contrasting the early life histories of sympatric Arctic gadids *Boreogadus saida* and *Arctogadus glacialis* in the Canadian Beaufort Sea. Polar Biol. 39, 1005–1022. https://doi.org/10.1007/s00300-014-1617-4

Bradstreet, M.S.W., Finley, K.J., Sekerak, A.-D., Griffiths, W.B., Evans, C.R., Fabijan, M.F., Stallard, H.E., 1986. Aspects of the Biology of Arctic Cod (*Boreogadus saida*) and its Importance in Arctic Marine Food Chains, Canadian Technical Report of Fisheries and Aquatic Sciences. https://doi.org/10.1002/aic.12482

Brodeur, R.D., Wilson, M.T., 1996. Mesoscale acoustic patterns of juvenile walleye pollock (*Theragra chalcogramma*) in the western Gulf of Alaska. Can. J. Fish. Aquat. Sci. 53, 1951–1963. https://doi.org/10.1139/cjfas-53-9-1951

Brodeur, R.D., Wilson, M.T., Ciannelli, L., 2000. Spatial and temporal variability in feeding and condition of age-0 walleye pollock (*Theragra chalcogramma*) in frontal regions of the Bering Sea. ICES J. Mar. Sci. 57, 256–264. https://doi.org/10.1006/jmsc.1999.0525

Coachman, L.K., Aagaard, K., Tripp, R.B., 1975. Bering Strait: The Regional Physical Oceanography, University of Washington Press. University of Washington Press, Seattle. https://doi.org/10.1016/0146-6291(77)90492-1

Corlett, W.B., Pickart, R.S., 2017. The Chukchi slope current. Prog. Oceanogr. 153, 50–65. https://doi.org/10.1016/j.pocean.2017.04.005

Danielson, S.L., Eisner, L., Ladd, C., Mordy, C., Sousa, L., Weingartner, T.J., 2017. A comparison between late summer 2012 and 2013 water masses, macronutrients, and phytoplankton standing crops in the northern Bering and Chukchi Seas. Deep. Res. Part II Top. Stud. Oceanogr. 135, 7–26. https://doi.org/10.1016/j.dsr2.2016.05.024

De Robertis, A., Lawrence-Slavas, N., Jenkins, R., Wangen, I., Mordy, C.W., Meinig, C., Levine, M., Peacock, D., Tabisola, H., 2019. Long-term measurements of fish backscatter from Saildrone unmanned surface vehicles and comparison with observations from a noise-reduced research vessel. ICES J. Mar. Sci. 76, 2459–2470. https://doi.org/10.1093/icesjms/fsz124

De Robertis, A., Taylor, K., Wilson, C.D., Farley, E. V., 2017. Abundance and distribution of Arctic cod (*Boreogadus saida*) and other pelagic fishes over the U.S. Continental Shelf of the Northern Bering and Chukchi Seas. Deep. Res. Part II Top. Stud. Oceanogr. 135, 51–65. https://doi.org/10.1016/j.dsr2.2016.03.002

Demer, D.A., Berger, L., Bernasconi, M., Bethke, E., Boswell, K., Chu, D., Domokos, R., Dunford, A., Fassler, S., Gauthier, S., Hufnagle, L.T., Jech, J.M., Bouffant, N., Lebourges-Dhaussy, A., Lurton, X., Macaulay, G.J., Perrot, Y., Ryan, T., Parker-Stetter, S., Stienessen, S., Weber, T., Williamson, N., 2015. Calibration of acoustic instruments. ICES Cooperative Research Reports 326.

Eisner, L., Hillgruber, N., Martinson, E., Maselko, J., 2013. Pelagic fish and zooplankton species assemblages in relation to water mass characteristics in the northern Bering and southeast Chukchi seas. Polar Biol. 36, 87–113. https://doi.org/10.1007/s00300-012-1241-0

Ershova, E.A., Hopcroft, R.R., Kosobokova, K.N., 2015. Inter-annual variability of summer mesozooplankton communities of the western Chukchi Sea: 2004–2012. Polar Biol. 38, 1461–1481. https://doi.org/10.1007/s00300-015-1709-9

Foote, K.G., 1980. Effect of fish behaviour on echo energy: the need for measurements of orientation distributions. ICES J. Mar. Sci. 39, 193–201. https://doi.org/10.1093/icesjms/39.2.193

Forster, C.E., Norcross, B.L., Mueter, F.J., Logerwell, E.A., Seitz, A.C., 2020. Spatial patterns, environmental correlates, and potential seasonal migration triangle of polar cod (*Boreogadus saida*) distribution in the Chukchi and Beaufort seas. Polar Biol. 73. https://doi.org/10.1007/s00300-020-02631-4

Fossheim, M., Primicerio, R., Johannesen, E., Ingvaldsen, R.B., Aschan, M.M., Dolgov, A. V., 2015. Recent warming leads to a rapid borealization of fish communities in the Arctic. Nat. Clim. Chang. 5, 673–677. https://doi.org/10.1038/nclimate2647

Frey, K.E., Moore, G.W.K., Cooper, L.W., Grebmeier, J.M., 2015. Divergent patterns of recent sea ice cover across the Bering, Chukchi, and Beaufort seas of the Pacific Arctic Region. Prog. Oceanogr. 136, 32–49. https://doi.org/10.1016/j.pocean.2015.05.009

Geoffroy, M., Majewski, A., LeBlanc, M., Gauthier, S., Walkusz, W., Reist, J.D., Fortier, L., 2016. Vertical segregation of age-0 and age-1+ polar cod (*Boreogadus saida*) over the annual cycle in the Canadian Beaufort Sea. Polar Biol. 39, 1023–1037. https://doi.org/10.1007/s00300-015-1811-z

Geoffroy, M., Robert, D., Darnis, G., Fortier, L., 2011. The aggregation of polar cod (*Boreogadus saida*) in the deep Atlantic layer of ice-covered Amundsen Gulf (Beaufort Sea) in winter. Polar Biol. 34, 1959–1971. https://doi.org/10.1007/s00300-011-1019-9

Gjosaeter, H., 1995. Pelagic fish and the ecological impact of the modern fishing industry in the Barents Sea. Arctic 48, 267–278. https://doi.org/10.14430/arctic1248

Goddard, P., Lauth, R., Armistead, C., 2014. Results of the 2012 Chukchi Sea Bottom Trawl Survey of Bottomfishes, Crabs, and Other Demersal Macrofauna. NOAA Tech. Memo. NMFS-AFSC-, 123.

Greene, C., Meyer-Gutbrod, E., McGarry, L., Hufnagle, L., Chu, D., McClatchie, S., Packer, A., Jung, J.-B., Acker, T., Dorn, H., Pelkie, C., 2014. A Wave Glider Approach to Fisheries Acoustics: Transforming How We Monitor the Nation's Commercial Fisheries in the 21st Century. Oceanography 27, 168–174. https://doi.org/10.5670/oceanog.2014.82

Hinckley, S., 1987. The reproductive biology of walleye pollock, *Theragra chalcogramma*, in the Bering Sea, with reference to spawning stock structure. Fish. Bull. 85, 481–498.

Hogan, T.F., Liu, M., Ridout, J.A., Peng, M.S., Whitcomb, T.R., Ruston, B.C., Reynolds, C.A., Eckermann, S.D., Moskaitis, J.R., Baker, N.L., McCormack, J.P., Viner, K.C., McLay, J.G., Flatau, M.K., Xu, L., Chen, C., Chang, S.W., 2014. The navy global environmental model. Oceanography 27, 116–125. https://doi.org/10.5670/oceanog.2014.73

Hop, H., Tonn, W.M., Welch, H.E., 1997. Bioenergetics of Arctic cod (*Boreogadus saida*) at low temperatures. Can. J. Fish. Aquat. Sci. 54, 1772–1784. https://doi.org/10.1139/cjfas-54-8-1772

Horne, J.K., 2000. Acoustic approaches to remote species identification: a review. Fish. Oceanogr. 9, 356–371. https://doi.org/10.1046/j.1365-2419.2000.00143.x

Huntington, H.P., Danielson, S.L., Wiese, F.K., Baker, M., Boveng, P., Citta, J.J., De Robertis, A., Dickson, D.M.S., Farley, E., George, J.C., Iken, K., Kimmel, D.G., Kuletz, K., Ladd, C., Levine, R., Quakenbush, L., Stabeno, P., Stafford, K.M., Stockwell, D., Wilson, C., 2020. Evidence suggests potential transformation of the Pacific Arctic ecosystem is underway. Nat. Clim. Chang. https://doi.org/10.1038/s41558-020-0695-2

Kaartvedt, S., Røstad, A., Klevjer, T.A., Staby, A., 2009. Use of bottom-mounted echo sounders in exploring behavior of mesopelagic fishes. Mar. Ecol. Prog. Ser. 395, 109–118. https://doi.org/10.3354/meps08174

Koenker, B.L., Copeman, L.A., Laurel, B.J., 2018. Impacts of temperature and food availability on the condition of larval Arctic cod (*Boreogadus saida*) and walleye pollock (*Gadus chalcogrammus*). ICES J. Mar. Sci. 75, 2370–2385. https://doi.org/10.1093/icesjms/fsy052

Kono, Y., Sasaki, H., Kurihara, Y., Fujiwara, A., Yamamoto, J., Sakurai, Y., 2016. Distribution pattern of Polar cod (*Boreogadus saida*) larvae and larval fish assemblages in relation to oceanographic parameters in the northern Bering Sea and Chukchi Sea. Polar Biol. 39, 1039–1048. https://doi.org/10.1007/s00300-016-1961-7

Kuletz, K.J., Ferguson, M.C., Hurley, B., Gall, A.E., Labunski, E.A., Morgan, T.C., 2015. Seasonal spatial patterns in seabird and marine mammal distribution in the eastern Chukchi and western Beaufort seas: Identifying biologically important pelagic areas. Prog. Oceanogr. 136, 175–200. https://doi.org/10.1016/j.pocean.2015.05.012

Kunz, K.L., Claireaux, G., Pörtner, H.-O., Knust, R., Mark, F.C., 2018. Aerobic capacities and swimming performance of polar cod (*Boreogadus saida*) under ocean acidification and warming conditions. J. Exp. Biol. 221, jeb184473. https://doi.org/10.1242/jeb.184473

Lange, M., Van Sebille, E., 2017. Parcels v0.9: Prototyping a Lagrangian ocean analysis framework for the petascale age. Geosci. Model Dev. 10, 4175–4186. https://doi.org/10.5194/gmd-10-4175-2017

Laurel, B.J., Spencer, M., Iseri, P., Copeman, L.A., 2016. Temperature-dependent growth and behavior of juvenile Arctic cod (*Boreogadus saida*) and co-occurring North Pacific gadids. Polar Biol. 39, 1127–1135. https://doi.org/10.1007/s00300-015-1761-5

Laurel, B.J., Copeman, L.A., Spencer, M., Iseri, P., 2018. Comparative effects of temperature on rates of development and survival of eggs and yolk-sac larvae of Arctic cod (*Boreogadus saida*) and walleye pollock (*Gadus chalcogrammus*). ICES J. Mar. Sci. 75, 2403–2412. https://doi.org/10.1093/icesjms/fsy042

Logerwell, E., Busby, M., Carothers, C., Cotton, S., Duffy-Anderson, J., Farley, E., Goddard, P., Heintz, R., Holladay, B., Horne, J., Johnson, S., Lauth, B., Moulton, L., Neff, D., Norcross, B., Parker-Stetter, S., Seigle, J., Sformo, T., 2015. Fish communities across a spectrum of habitats in the western Beaufort Sea and Chukchi Sea. Prog. Oceanogr. 136, 115–132. https://doi.org/10.1016/j.pocean.2015.05.013

Maclennan, D.N., Fernandes, P.G., Dalen, J., 2002. A consistent approach to definitions and symbols in fisheries acoustics. ICES J. Mar. Sci. 59, 365–369. https://doi.org/10.1006/jmsc.2001.1158

Marsh, J.M., Mueter, F.J., Quinn, T.J., 2019. Environmental and biological influences on the distribution and population dynamics of polar cod (*Boreogadus saida*) in the US Chukchi Sea. Polar Biol. 1971. https://doi.org/10.1007/s00300-019-02561-w

Matley, J.K., Fisk, A.T., Dick, T.A., 2012. Seabird predation on Arctic cod during summer in the Canadian Arctic. Mar. Ecol. Prog. Ser. 450, 219–228. https://doi.org/10.3354/meps09561

Mecklenburg, C., Lynghammar, A., Johannesen, E., Byrkjedal, I., Christiansen, J.S., Karamushko, O. V, Mecklenburg, T.A., Møller, P.R., Steinke, D., Wienerroither, R.M., 2018. Marine Fishes of the Arctic Region Volume II. CAFF Monitoring Series Report 28. Akureyri, Iceland: Conservation of Arctic Flora and Fauna.

Mordy, C., Cokelet, E., De Robertis, A., Jenkins, R., Kuhn, C., Lawrence-Slavas, N., Berchok, C., Crance, J., Sterling, J., Cross, J., Stabeno, P., Meinig, C., Tabisola, H., Burgess, W., Wangen, I., 2017. Advances in Ecosystem Research: Saildrone Surveys of Oceanography, Fish, and Marine Mammals in the Bering Sea. Oceanography 30, 113–115. https://doi.org/10.5670/oceanog.2017.230

Norcross, B.L., Holladay, B.A., Busby, M.S., Mier, K.L., 2010. Demersal and larval fish assemblages in the Chukchi Sea. Deep. Res. Part II Top. Stud. Oceanogr. 57, 57–70. https://doi.org/10.1016/j.dsr2.2009.08.006

Ohman, M.D., Davis, R.E., Sherman, J.T., Grindley, K.R., Whitmore, B.M., Nickels, C.F., Ellen, J.S., 2019. Zooglider: An autonomous vehicle for optical and acoustic sensing of zooplankton. Limnol. Oceanogr. Methods 17, 69–86. https://doi.org/10.1002/lom3.10301

Parker-Stetter, S.L., Horne, J.K., Weingartner, T.J., 2011. Distribution of polar cod and age-0 fish in the U.S. Beaufort Sea. Polar Biol. 34, 1543–1557. https://doi.org/10.1007/s00300-011-1014-1

Peck, M.A., Buckley, L.J., Bengtson, D.A., 2006. Effects of temperature and body size on the swimming speed of larval and juvenile Atlantic cod (*Gadus morhua*): Implications for individual-based modelling. Environ. Biol. Fishes 75, 419–429. https://doi.org/10.1007/s10641-006-0031-3

Pinchuk, A.I., Eisner, L.B., 2017. Spatial heterogeneity in zooplankton summer distribution in the eastern Chukchi Sea in 2012–2013 as a result of large-scale interactions of water masses. Deep Sea Res. Part II Top. Stud. Oceanogr. 135, 27–39. https://doi.org/10.1016/j.dsr2.2016.11.003

Pinheiro, J., Bates, D., DebRoy, S., Sarkar, D., R Core Team, 2019. {nlme}: Linear and Nonlinear Mixed Effects Models.

Pisareva, M.N., Pickart, R.S., Lin, P., Fratantoni, P.S., Weingartner, T.J., 2019. On the nature of wind-forced upwelling in Barrow Canyon. Deep. Res. Part II Top. Stud. Oceanogr. 162, 63–78. https://doi.org/10.1016/j.dsr2.2019.02.002

Ponomarenko, V.P., 2000. Eggs, larvae, and juveniles of polar cod *Boreogadus saida* in the Barents, Kara, and White Seas. J. Ichthyol. 40, 165–173.

Ponomarenko, V.P., 1968. Some data on the distribution and migrations of polar cod in the seas of the Soviet Arctic. Rapp. Procès Verbaux Réunions CIEM 158, 131–135.

Quast, J.C., 1974. Density distribution of juvenile Arctic cod, *Boreogadus saida*, in the eastern Chukchi Sea in the fall of 1970. Fish. Bull. 72, 1094–1105.

Sawada, K., Furusawa, M., Williamson, N.J., 1993. Conditions for the precise measurement of fish target strength in situ. J. Mar. Acoust. Soc. Japan 20, 73–79. https://doi.org/10.3135/jmasj.20.73

Sigler, M.F., Mueter, F.J., Bluhm, B.A., Busby, M.S., Cokelet, E.D., Danielson, S.L., Robertis, A. De, Eisner, L.B., Farley, E. V., Iken, K., Kuletz, K.J., Lauth, R.R., Logerwell, E.A., Pinchuk, A.I., 2017. Late summer zoogeography of the northern Bering and Chukchi seas. Deep Sea Res. Part II Top. Stud. Oceanogr. 135, 168–189. https://doi.org/10.1016/j.dsr2.2016.03.005

Sigler, M., Renner, M., Danielson, S., Eisner, L., Lauth, R., Kuletz, K., Logerwell, E., Hunt, G., 2011. Fluxes, Fins, and Feathers: Relationships Among the Bering, Chukchi, and Beaufort Seas in a Time of Climate Change. Oceanography 24, 250–265. https://doi.org/10.5670/oceanog.2011.77

Simmonds, J., MacLennan, D., 2005. Fisheries Acoustics: Theory and Practice, Fish and Aquatic Resources Series.

Spear, A., Duffy-Anderson, J., Kimmel, D., Napp, J., Randall, J., Stabeno, P., 2019. Physical and biological drivers of zooplankton communities in the Chukchi Sea. Polar Biol. 42, 1107–1124. https://doi.org/10.1007/s00300-019-02498-0

Spencer, M.L., Vestfals, C.D., Mueter, F.J., Laurel, B.J., 2020. Ontogenetic changes in the buoyancy and salinity tolerance of eggs and larvae of polar cod (*Boreogadus saida*) and other gadids. Polar Biol. 43, 1141–1158. https://doi.org/10.1007/s00300-020-02620-7

Stabeno, P., Kachel, N., Ladd, C., Woodgate, R., 2018. Flow Patterns in the Eastern Chukchi Sea: 2010–2015. J. Geophys. Res. Ocean. 123, 1177–1195. https://doi.org/10.1002/2017JC013135

Steele, M., Ermold, W., Zhang, J., 2008. Arctic Ocean surface warming trends over the past 100 years. Geophys. Res. Lett. 35, 1–6. https://doi.org/10.1029/2007GL031651

Stevenson, D.E., Lauth, R.R., 2019. Bottom trawl surveys in the northern Bering Sea indicate recent shifts in the distribution of marine species. Polar Biol. 42, 407–421. https://doi.org/10.1007/s00300-018-2431-1

Traynor, J., 1996. Target-strength measurements of walleye pollock (*Theragra chalcogramma*) and Pacific whiting (*Merluccius productus*). ICES J. Mar. Sci. 53, 253–258. https://doi.org/10.1006/jmsc.1996.0031

Vestfals, C.D., Mueter, F.J., Duffy-Anderson, J.T., Busby, M.S., De Robertis, A., 2019. Spatio-temporal distribution of polar cod (*Boreogadus saida*) and saffron cod (*Eleginus gracilis*) early life stages in the Pacific Arctic. Polar Biol. 42, 969–990. https://doi.org/10.1007/s00300-019-02494-4

Wackernagel, H., 2013. Multivariate geostatistics: an introduction with applications. Springer Science & Business Media.

Whitehouse, G.A., Aydin, K.Y., 2016. Trophic Structure of the Eastern Chukchi Sea: An Updated Mass Balance Food Web Model. NOAA Tech. Memo. NMFS-AFSC-318 175 pp. https://doi.org/10.7289/V5/TM-AFSC-318

Woillez, M., Poulard, J.C., Rivoirard, J., Petitgas, P., Bez, N., 2007. Indices for capturing spatial patterns and their evolution in time, with application to European hake (*Merluccius merluccius*) in the Bay of Biscay. ICES J. Mar. Sci. 64, 537–550. https://doi.org/10.1093/icesjms/fsm025

Woodgate, R.A., 2018. Increases in the Pacific inflow to the Arctic from 1990 to 2015, and insights into seasonal trends and driving mechanisms from year-round Bering Strait mooring data. Prog. Oceanogr. 160, 124–154. https://doi.org/10.1016/j.pocean.2017.12.007

Woodgate, R.A., Aagaard, K., Weingartner, T.J., 2005. A year in the physical oceanography of the Chukchi Sea: Moored measurements from autumn 1990-1991. Deep. Res. Part II Top. Stud. Oceanogr. 52, 3116–3149. https://doi.org/10.1016/j.dsr2.2005.10.016

2.9 SUPPLEMENTARY INFORMATION

Supplementary Table 2.1 Length estimates of targets observed in each of the small-scale surveys depend on the changes in the backscatter from individual targets (Figure 2.6e) and the specific TS-length relationship used to convert scattering strength to fish length. Values reported for each survey are calculated from the backscattering cross-section (σ_{bs}) at the midpoint of each survey using the linear model presented in Figure 2.6 where

$$\sigma_{bs} = -7.68 \times 10^{-6} + 4.54 \times 10^{-8}(yearday).$$

Standard lengths (L) are calculated from $L = 10^{\left(\frac{TS+b}{a}\right)}$ where a and b are the slope and intercept of the TS-length model and $TS = 10log_{10}(\sigma_{bs})$ as defined in Maclennan et al. (2002). The lengths resulting from σ_{bs} ±1 standard error of the model are indicated in parentheses. The growth rate (r) during the 53-day period of the small-scale surveys is computed from the difference in size estimated from the predicted σ_{bs} values on 20 July and 11 September. Each row represents a different TS-length relationship for Arctic cod or walleye pollock. The predicted growth rate increases if a TS-length relationship with a smaller slope is applied.

TS-Length Model	1st Survey	2nd Survey	3rd Survey	4th Survey	r (mm d^{-1})
[1]$\boldsymbol{TS = 14.33log_{10}(L) - 65.13}$	3.4 (1.1, 5.1)	3.7 (1.6, 5.4)	4.7 (2.7, 6.4)	5.5 (3.5, 7.2)	0.54
[2]$\boldsymbol{TS = 21.8log_{10}(L) - 72.7}$	4.9 (2.4, 6.4)	5.3 (3.0, 6.7)	6.2 (4.3, 7.5)	6.8 (5.1, 8.1)	0.48
[3]$\boldsymbol{TS = 8.03log_{10}(L) - 65.13}$	2.5 (0.3, 5.2)	3.0 (0.6, 5.9)	4.6 (1.7, 8.0)	6.1 (2.8, 9.8)	0.89
[4]$\boldsymbol{TS = 12.8log_{10}(L) - 64.3}$	3.3 (1.0, 5.3)	3.7 (1.4, 5.7)	4.9 (2.6, 6.9)	5.8 (3.6, 7.9)	0.62
[5]$\boldsymbol{TS = 20log_{10}(L) - 66}$	2.6 (1.2, 3.5)	2.8 (1.5, 3.7)	3.3 (2.2, 4.2)	3.7 (2.7, 4.5)	0.28
[6]$\boldsymbol{TS = 20log_{10}(L) - 64.8}$	2.3 (1.0, 3.0)	2.4 (1.3, 3.2)	2.9 (1.9, 3.6)	3.2 (2.4, 3.9)	0.24

[1]Geoffroy, M., A. Majewski, M. LeBlanc, S. Gauthier, W. Walkusz, J. D. Reist, and L. Fortier. 2016. Vertical segregation of age-0 and age-1+ polar cod (*Boreogadus saida*) over the annual cycle in the Canadian Beaufort Sea. Polar Biol. 39: 1023–1037. doi:10.1007/s00300-015-1811-z

[2]Anonymous. 1988. Report on the joint Norwegian/USSR acoustic survey of pelagic fish in the Barents Sea, September–October 1988. Institute of Marine Research, Bergen.

[3]Parker-Stetter, S. L., J. K. Horne, and T. J. Weingartner. 2011. Distribution of polar cod and age-0 fish in the U.S. Beaufort Sea. Polar Biol. 34: 1543–1557. doi:10.1007/s00300-011-1014-1

[4]Mamylov, V. S. 1999. Some aspects of estimating the density of fish aggregations by trawl-acoustic methods. Development of technical methods for fisheries research. PINRO selected papers, Murmansk, Russia, pp. 147–163.

[5]Traynor, J. 1996. Target-strength measurements of walleye pollock (*Theragra chalcogramma*) and Pacific whiting (*Merluccius productus*). ICES J. Mar. Sci. 53: 253–258. doi:10.1006/jmsc.1996.0031

[6]McKelvey, D., and K. Williams. 2018. Abundance and distribution of age-0 walleye pollock in the eastern Bering Sea shelf during the Bering Arctic Subarctic Integrated Survey (BASIS) in 2014. U.S. Dep. Commer., NOAA Tech. Memo. NMFS-AFSC-382, 48 p.

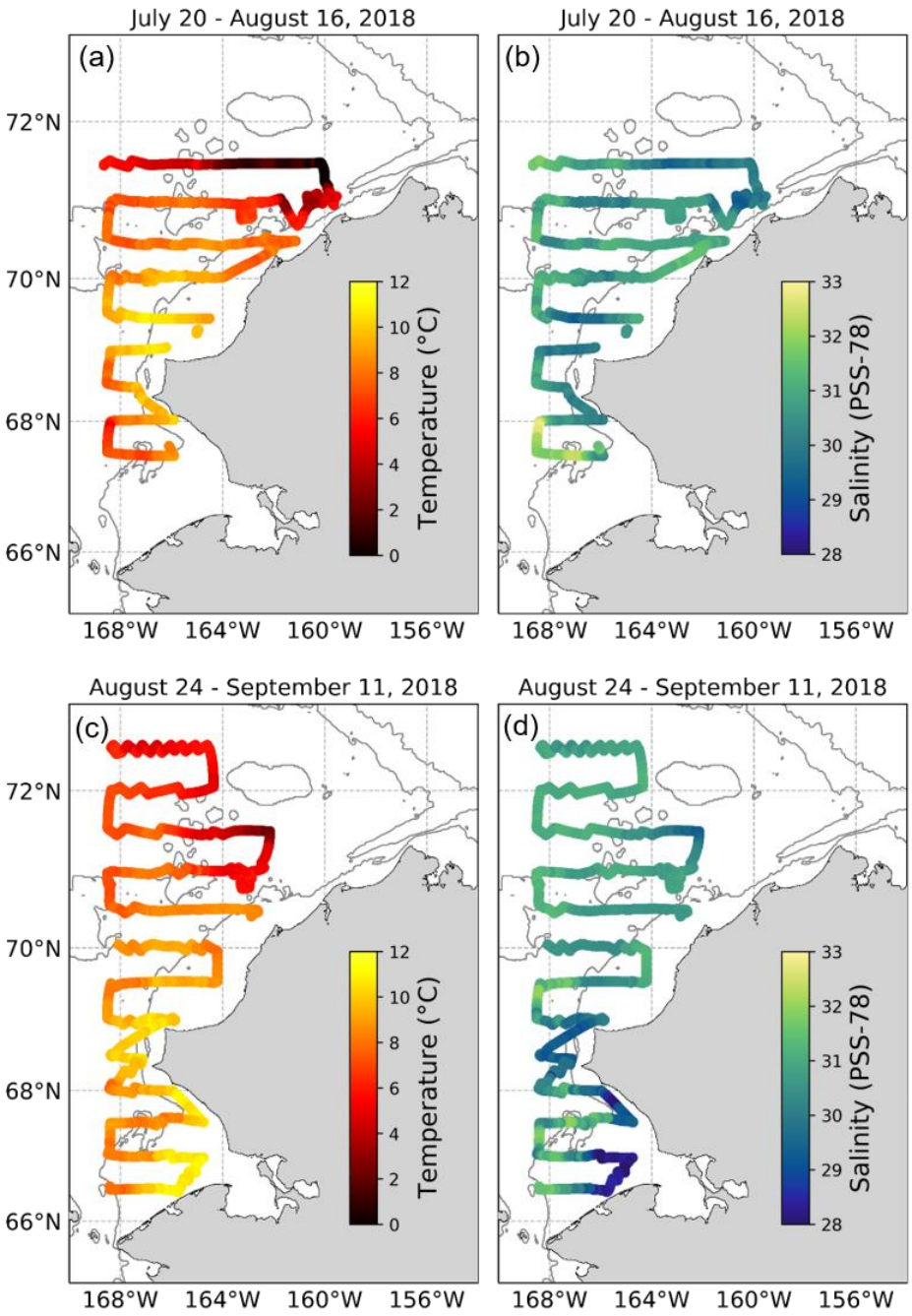

Supplementary Figure 2.1 Temperature and salinity at 0.5 m depth during the first (a,b) and second (c,d) large-scale surveys. The 40, 100, and 1000 m depth contours are shown.

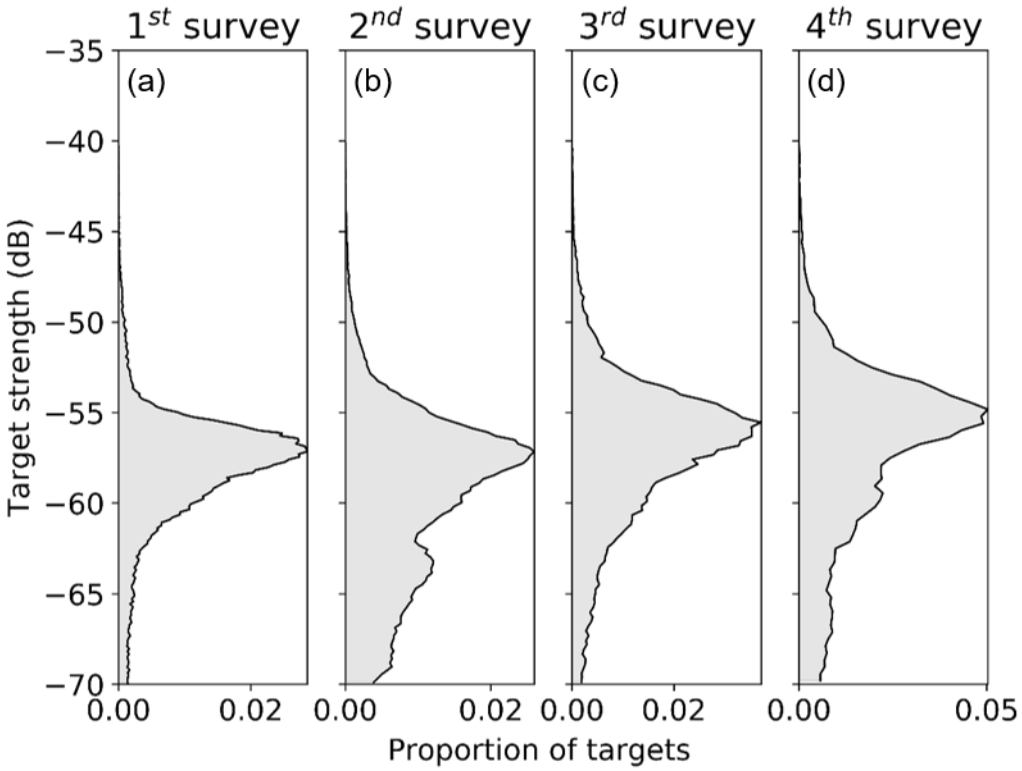

Supplementary Figure 2.2 Distribution of target strengths of single acoustic targets observed in the (a) 1st, (b) 2nd, (c) 3rd, and (d) 4th small-scale survey.

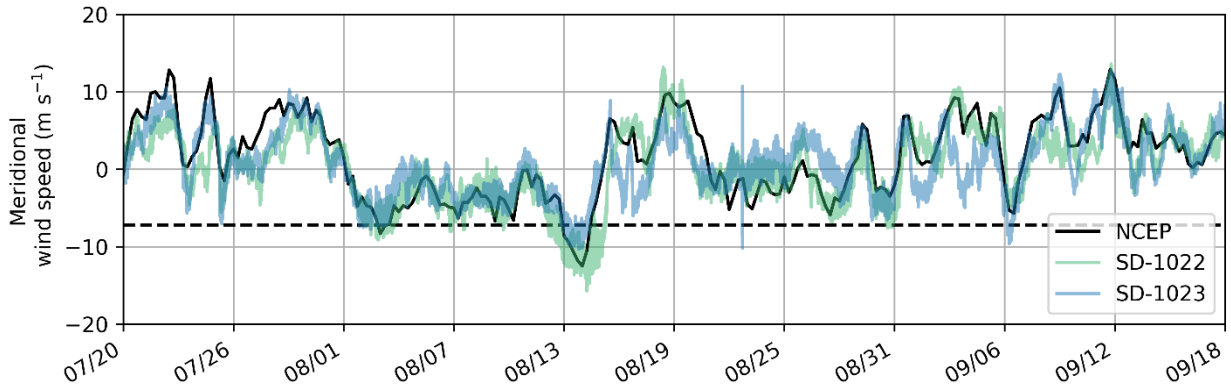

Supplementary Figure 2.3 Time series of meridional wind speed within the small-scale survey region during the survey period. NCEP/NCAR reanalysis 2.5° resolution wind speed at surface (sigma level 995) averaged over the survey region is shown in black (Kalnay et al., 1996). In situ wind speed measured by the saildrones are shown in green and blue. The dashed black line indicates a meridional wind speed of -7.2 m s^{-1}, predicted to balance the pressure head forcing (see discussion for details).

Model simulation videos available at: https://doi.org/10.1002/lno.11671

Supplementary Video 2.1 Video of particle trajectories from 20 July to 18 September 2018 indicating the position of each particle at 3-hour intervals. Particles were seeded at the center of each model grid cell where observed fish density was ≥ 0.1 fish m^{-2} on the start date of the first large-scale survey (20 July; see methods for more details). Color of particles indicates water column 38 kHz backscatter (s_A, m^2 nmi^{-2}). The 40, 100, and 1000 m depth contours are shown.

File: LNO_11671_LevineFigureS2.mp4

CHAPTER 3. CLIMATE-DRIVEN SHIFTS IN PELAGIC FISH DISTRIBUTIONS IN A RAPIDLY CHANGING PACIFIC ARCTIC

A version of this chapter has been submitted for review to Deep Sea Research Part II: Topical Studies in Oceanography as: Levine, R.M., De Robertis, A., Grünbaum, D., Wildes, S., Farley, E.V., Stabeno, P.J., Wilson, C.D. Climate-driven shifts in pelagic fish distributions in a rapidly changing Pacific Arctic.

3.1 ABSTRACT

Age-0 Arctic cod (*Boreogadus saida*) have historically dominated the pelagic fish community in the Chukchi Sea in summer, with few adults present in the region. Recent reductions in sea ice have resulted in warmer water and increased northward transport has led to an increase in Pacific-origin waters on the Chukchi shelf in summer. To examine potential effects of these environmental changes on pelagic fishes in this rapidly changing environment, we extended a time series of acoustic-trawl surveys originally conducted in 2012 and 2013 with additional surveys in 2017 and 2019. Age-0 Arctic cod were the most abundant pelagic fish in all four survey years. However, age-0 walleye pollock (*Gadus chalcogrammus*), which were scarce and confined to the southern Chukchi Sea in 2012 and 2013, were present in high abundance throughout the Chukchi shelf in 2017 and 2019. Age-0 Arctic cod were substantially more abundant in 2017, possibly due to increased survivorship of larvae under warm conditions. Arctic cod and pollock were spatially separated in 2019, with Arctic cod primarily present in the northeastern portion of the survey area, which was characterized by cool surface and bottom temperatures. The substantial increase in age-0 pollock in recent years suggests that environmental conditions now allow this species to extend

its northern range into the southern and central Chukchi Sea, at least on a seasonal basis. We hypothesize that the changes in abundance and species composition based on our 2012-2019 time series are tightly coupled to recent changes in temperature and the increasing transport of Bering Sea waters through the Bering Strait into the Chukchi Sea.

3.2 INTRODUCTION

Arctic gadids, particularly Arctic cod (*Boreogadus saida*, also referred to as polar cod), have historically dominated the pelagic fish community in the Pacific Arctic ecosystem of the northern Bering, Chukchi, East Siberian, and Beaufort Seas (Quast, 1974; Logerwell et al., 2015; De Robertis et al., 2017). Arctic cod are a circumpolar-distributed species found throughout the Central Arctic Basin and surrounding marginal seas (Mecklenburg et al., 2018). Arctic cod are abundant, lipid-rich (Copeman et al., 2017; Copeman et al., 2020) prey that serve as an energy-dense trophic link between lower trophic levels and piscivores such as seabirds and marine mammals (Bradstreet et al., 1986; Matley et al., 2012). Trophic mass balance models for the Chukchi Sea indicate that Arctic cod are central to the food web and represent a substantial portion of seabird (>20%) and piscivorous mammal (>40%) diets (Whitehouse et al., 2014). The Chukchi Sea and the entirety of the Pacific Arctic are experiencing substantial and rapid warming (Danielson et al., 2020), and the impacts of these environmental changes on pelagic fishes such as Arctic cod remain unclear.

The Chukchi Sea is warming rapidly: mean summer/fall water column temperatures in the Chukchi Sea have increased by 0.1 °C decade^{-1} over the past century (Danielson et al., 2020). This warming is likely to accelerate as air temperatures in the Arctic are anticipated to increase by >5 °C by 2100 (Overland et al., 2019). Climate predictions (Wang et al., 2018) suggest that the duration of seasonal ice cover will continue to decrease at a rate of 0.94 days year^{-1} as wind patterns

change, and transport of water, including heat, into the region continues to increase.

Increased input of warm Pacific Water into the Chukchi Sea has created a feedback loop which further increases heating in the region (Danielson et al., 2020; Huntington et al., 2020; Woodgate and Peralta-Ferriz, 2021). The Chukchi Sea is highly advective, with substantial transport of warm water from the Pacific entering through the Bering Strait in spring and summer (Woodgate et al., 2005; Stabeno et al., 2018). This transport through the Bering Strait has been increasing from its previous climatology of ~0.8 Sv at a rate of ~0.01 Sv $year^{-1}$ in recent decades (Woodgate, 2018; Woodgate and Peralta-Ferriz, 2021). The associated northward heat flux helps to initiate the seasonal retreat of the Chukchi shelf sea ice (Woodgate et al., 2010). Shorter periods of ice cover further reduce the albedo of the sea surface in spring and summer with increasing solar warming further accelerating ice melt in spring and delaying ice formation in fall (Danielson et al., 2020).

The physiology and recruitment success of Arctic gadids is highly temperature- dependent and species-specific (Mueter et al., 2011; Laurel et al., 2016; Koenker et al., 2018). Changes in habitat suitability that result from changes in Bering Strait transports are particularly important for early life stages, for which survival is largely dependent on the ability to maximize growth prior to winter (Bouchard et al., 2017). Thus, changes in transport of heat, reduction in ice, and increased solar warming in the Chukchi Sea are likely to affect the abundance and role of fishes in energy transfer within Arctic food webs. Increased warming may affect the relative abundance and distributions of different species (Laurel et al., 2016; Baker, 2021). For example, boreal (subarctic) species such as walleye pollock (*Gadus chalcogrammus*, hereafter pollock) and Pacific cod (*Gadus macrocephalus*) may benefit from warming (Marsh and Mueter, 2020), while Arctic species may

be negatively impacted by reduced habitat (Baker, 2021) and increased competition (Bouchard et al., 2017).

Globally, boreal species have expanded their distributions northwards into the Arctic as high-latitude regions have warmed (Wassman et al., 2011). The Barents Sea, for example, is a shallow marginal sea of the Arctic Ocean which shares some commonalities with the Chukchi Sea (Hunt et al., 2013). Rapid warming in the Barents Sea has changed the spatial distribution of fish communities as subarctic species expand northward (Fossheim et al., 2015). These spatial shifts in pelagic community structure can alter ecosystem function due to changes in food web structure (Kortsch et al., 2015). Evidence for this is seen in the distribution of adult fishes in the Bering Sea, where boreal species such as pollock and Pacific cod have expanded their range northwards (Stevenson and Lauth, 2019; Eisner et al., 2020; Spies et al., 2020). Similarly, the southern limits of Arctic species such as Arctic cod have shifted further north, with boreal species taking their place (Marsh and Mueter, 2020; Baker, 2021).

Northward advection from the Bering Sea structures the species composition of pelagic communities in the Chukchi Sea. Transport from the south brings planktonic organisms of Pacific-origin onto the Chukchi shelf (Eisner et al., 2013; Sigler et al., 2017). Northward advection across the Chukchi shelf is also hypothesized to structure the spatial distributions of age-0 fishes, as the current speeds surpass their swimming abilities (Levine et al., 2020; Vestfals et al., 2021). Age 1+ gadids are scarce in the Chukchi Sea (De Robertis et al., 2017), likely because they are transported northward off the shelf as juveniles by the prevailing currents (Levine et al., 2020; Vestfals et al., 2021). Increased transport may further reduce the residence time for growth in high productivity regions on the Chukchi shelf (Levine et al., 2020).

Acoustic-trawl (AT) surveys were conducted in 2012 and 2013 by De Robertis et al. (2017) to establish a baseline of the distribution of pelagic fishes in the northern Bering and Chukchi Seas. Similar to previous observations in the region (Norcross et al., 2013; Logerwell et al., 2015), large numbers of Arctic cod were observed, with the greatest abundances in the northern Chukchi Sea. However, these were primarily age-0 fish with an average length of 3.5 cm, with <0.3% longer than 6.5 cm (De Robertis et al., 2017). Given the relatively high abundances of age-0 fish at a critical life stage, the Chukchi shelf may serve as an important nursery area (De Robertis et al., 2017; Levine et al., 2020). If so, continued warming of the Chukchi Sea has the potential to negatively impact the growth and survival of this population. Further investigations of environmental factors influencing Arctic cod abundance and distribution are needed to better understand how changing climate may alter this ecosystem.

To examine longer-term trends in pelagic fishes in this rapidly changing environment, we extended the time series of observations collected in 2012 and 2013 with additional AT surveys in 2017 and 2019. The AT methodology provided extensive spatial coverage and comparable measurements to previous surveys. This enabled us to assess the impacts of temperature and transport on the distribution of the abundant pelagic fish population in this highly dynamic region. The primary objectives of this study were to characterize the abundance and distribution of the major pelagic fishes in the Chukchi Sea, and to identify environmental drivers that influence the Chukchi Sea pelagic fish community. Future changes in sea ice, temperature, and transport that result from a changing climate on the Chukchi shelf are likely to be dramatic and the consequences for the age-0 Arctic cod population are unclear. Our goal was to better understand the mechanisms structuring the pelagic fish community in the Chukchi Sea to improve predictions of how future environmental changes will affect these populations.

3.3 METHODS

Acoustic-trawl surveys were conducted in the U.S. continental shelf region of the Chukchi Sea and coastal regions of the western Beaufort Sea (Figure 3.1). The surveys occurred from 1 August to 27 September 2017, and 27 August to 26 September 2019 on the R/V *Ocean Starr*. Bottom depths were <60 m in 93% of the survey area in 2017 and 91% of the survey area in 2019. Stations were arranged on a 1° longitude and 0.5° latitude grid in 2017. Transect spacing was increased to a 0.75° latitude grid in 2019. Sampling stations were occupied as the vessel reached these locations along the transects. In both years, the survey began in the northern Chukchi Sea and progressed south. Acoustic data were collected during daylight hours as the ship transited at ~3.3 m s^{-1} along survey transects oriented in an east/west direction. Observations collected during daylight while transiting between transects were included in the analysis.

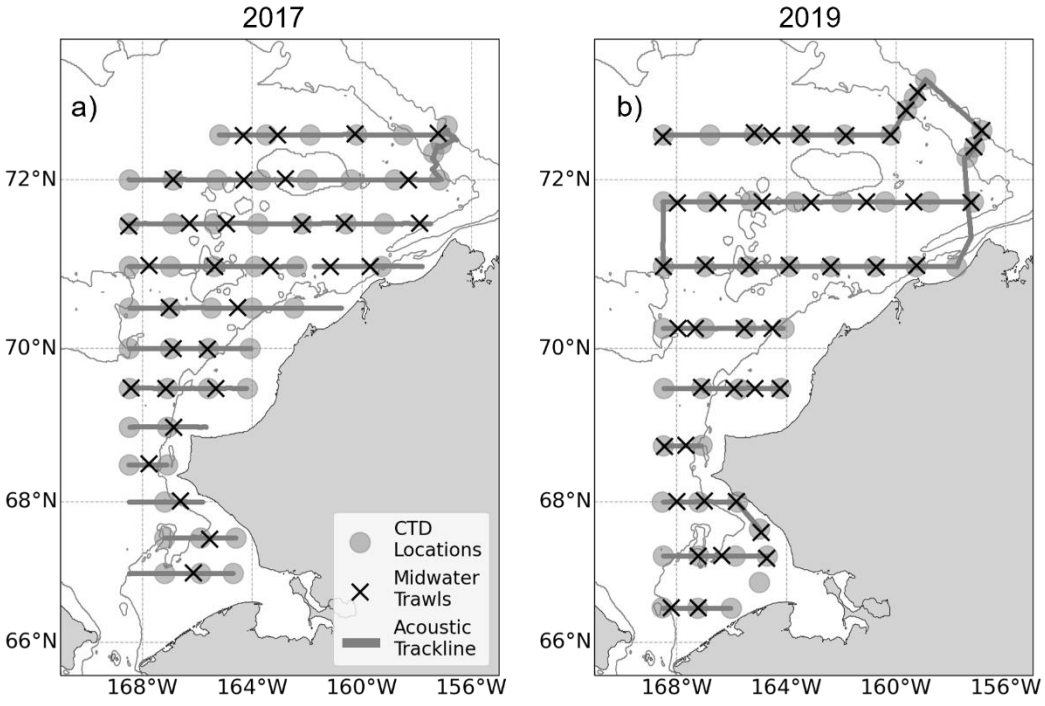

Figure 3.1 Study area in (a) 2017 and (b) 2019. The 40-, 100-, and 1000-m depth contours are shown.

Survey methods were consistent with previous work conducted in 2012 and 2013 (De Robertis et al., 2017). The 2012 and 2013 surveys of the Chukchi Sea both took place from 7 August to 8 September. This was approximately 3 weeks earlier than the surveys in 2017 and 2019. These earlier surveys transited from south to north along the same transects indicated in Figure 3.1a, with the same station spacing as the 2017 survey.

3.3.1 *Acoustic data collection*

Acoustic backscatter at 38 and 120 kHz was measured using a split-beam Simrad EK60 echosounder operating ES38B and ES120-7C transducers mounted at 3.7 m depth on the vessel's hull. Data were collected using a pulse length of 0.5 ms at a ping rate of 2 Hz. In deep water (>250 m depth), longer pulse lengths (1 ms at 120 kHz, 4 ms at 38 kHz) were used to increase signal-to-noise ratios, and the ping rate was slowed to ~0.3-0.5 Hz. The echosounders were calibrated at the beginning and end of each survey using the standard sphere technique (Demer et al., 2015). Results from the two calibrations were averaged before being applied in post-processing. Calibration results were consistent among surveys. Gains from the averaged pre- and post-survey calibrations for the 0.5 ms pulse length differed by 0.09 dB (2.2%) at 38 kHz and 0.17 dB (4.0%) at 120 kHz. Gains at the longer pulse lengths used in deeper waters differed between years by 0.04 dB (0.2%) at 38 kHz and 0.4 dB (8.9%) at 120 kHz.

3.3.2 *Midwater trawl sampling*

The species and size composition of pelagic acoustic scatterers was determined from targeted midwater trawls in areas of high backscatter. Backscatter was generally evenly distributed throughout the survey area. Many trawl hauls were conducted at the survey sampling stations for logistical convenience, but hauls were targeted to the depth of greatest backscatter. Acoustically

observed fish aggregations were sampled using a modified Marinovich herring trawl equipped with a fine-mesh 2 by 3 mm codend liner used in previous surveys (De Robertis et al., 2017). Prior to the 2017 survey, this trawl was modified with a redesigned aft section that resulted in lower selectivity and better retention of small fishes (De Robertis et al., in prep). Midwater trawls were conducted at 33 sites in 2017 and 43 sites in 2019 (Figure 3.1), with an average ship speed of 1-1.5 m s^{-1} during trawling. Net openings and depths were monitored with either a Simrad FS70 or Marport Trawl Explorer net sounder attached to the headrope. The trawl opening was approximately 8 m horizontal by 7.5 m vertical, with a mean headrope depth of 27.1 m (range 11.4-46.7 m) in 2017 and 34.9 m (range 13.2-227.9 m) in 2019.

Trawl catches were weighed, sorted, and identified to species. Fish lengths (3392 in 2017, 9124 in 2019) and jellyfish bell diameters (1211 in 2017, 751 in 2019) were measured on a subsample of individuals (up to 60 gadids, 10 of all other species) to the nearest 1.0 mm using an electronic measuring board (Towler and Williams, 2010). Length measurement methodology varied among years for the key gadid species. Age-0 gadids length was measured as fork length in 2012 and 2013, total length in 2017, and standard length in 2019. To account for these differences, we conducted repeat measurements of fork, total and standard length on the same individuals and calculated linear models to convert among length types (Supplementary Table 3.1). Tissue samples from a subsample of measured gadid fishes (894 in 2017, 3155 in 2019) were collected and used to confirm field identifications based on genetic markers. Genetic analyses indicated that field identifications of juvenile gadids were unreliable, particularly when distinguishing between age-0 Arctic cod and pollock (see Wildes et al., in prep for details). For gadids with a tissue sample (40% and 56% of gadids specimens in 2017 and 2019, respectively), the species identifications were updated based on the genetic identifications. For the remaining gadid specimens with no genetic

sampling, species was assigned probabilistically based on the length-dependent species composition of the genetically identified individuals in that haul (see supplementary material 3.8.2).

A subsample of gadid specimens collected in 2012 and 2013 (De Robertis et al., 2017) were validated using the same genetic analyses. Genetics indicated that few pollock were present in the survey region during this period (Wildes et al., in prep). This provided confidence for further comparison of the 2017/2019 surveys with the historical 2012/2013 data despite the lack of a genetic-based species assignment in the 2012/2013 surveys.

3.3.3 *Data processing and abundance estimation*

Fish abundances were estimated by combining backscatter measurements and size and species composition information from genetically corrected trawl samples following the methods in De Robertis et al. (2017). 38 kHz acoustic backscatter was integrated in 0.5 nmi along-transect intervals with a minimum Sv threshold of -70 dB re 1 m^{-1}, excluding data shallower than 6.5 m and deeper than 0.5 m above the seafloor. Trawl catches were corrected for size- and species-dependent net selectivity based on fine-mesh recapture nets mounted to the trawl to account for the size- and species-specific likelihood of capture (De Robertis et al., in prep). Pacific cod had too few specimens to estimate net selectivity for the species, so pollock net selectivity was applied as the fish are of similar origin and morphology. There are no estimates of selectivity for invertebrates and these species could not be corrected for selectivity; however, these species are very weak contributors to scattering relative to fish with swimbladders, and the lack of selectivity corrections for these taxa is unlikely to affect the abundance estimates of other species (De Robertis et al., 2017). The selectivity-corrected size and species composition estimates were combined with size- and species-specific scattering properties to allocate observed acoustic

backscatter to each species in the catch. Target strength relationships from the literature were used to estimate acoustic scattering for each species in the trawl catch (see De Robertis et al., 2017, their Table 1). The proportion of total areal backscatter attributable to each species was then calculated along acoustic transects using species and size compositions from the nearest trawl (De Robertis et al., 2017, their equations 1-7). The AT method is best-suited for abundant, strongly-scattering species (Simmonds and MacLennan, 2005). The analysis thus was limited to Arctic cod, pollock, Pacific cod, saffron cod (*Eleginus gracilis*), Pacific herring (*Clupea pallasii*), and capelin (*Mallotus catervarius*). These species accounted for 96.2% and 63.7% of fish by number in the trawl catch in 2017 and 2019, respectively. Abundances of these same species from surveys conducted in 2012 and 2013 were used in our analyses (De Robertis, 2021). The contribution of other less abundant or weakly scattering species to backscatter was estimated, but abundance estimates were not made. For example, as in previous surveys, we were unable to estimate Arctic sand lance (*Ammodytes hexapterus*) abundance using AT methods with confidence. This is because they are weak acoustic scatterers due to their lack of a swimbladder, which results in high uncertainty if stronger scatterers are misclassified as sand lance (Yasuma et al., 2009; De Robertis et al., 2017).

3.3.4 *Environmental data collection and processing*

Water column properties were measured using a conductivity, temperature, and depth (CTD, Sea-Bird Electronics 911*plus*) sensor. At all stations, a CTD sensor was deployed from surface to ~5 m above seafloor. Mean water column temperature and salinity in 2017 and 2019 were calculated at each station for the upper 10 m (hereafter referred to as surface temperature/salinity), and the deepest 5 m of the cast (hereafter referred to as bottom temperature/salinity) of each cast. Equivalent measures were available for the CTD casts from the 2012 and 2013 surveys (Danielson

et al., 2017). Measurements were available from 68 stations in 2012, 55 stations in 2013, 39 stations in 2017, and 46 stations in 2019. To associate fish with environmental conditions, each 0.5 nmi interval of transect was assigned to the nearest CTD station, and the average fish abundances (fish m^{-2}) for each grouping of intervals were calculated. Water mass classifications from Danielson et al. (2017) were used to describe station conditions based on temperature; 2 °C and 7 °C were used to represent the boundaries between Alaskan Coastal Water (>7 °C), Bering/Chukchi Summer Water (2-7 °C), and Bering Chukchi Winter Water (<2 °C).

3.4 RESULTS

3.4.1 *Trawl catches*

Catch rates were >6-fold higher in 2017 (mean catch per unit effort for all fishes of 0.248 fish m^{-3} in 2017 and 0.034 fish m^{-3} in 2019) primarily due to high abundances of Arctic cod (0.189 fish m^{-3} in 2017 and 0.017 fish m^{-3} in 2019). Trawl catches were dominated by small fishes (80% <7.3 cm in 2017 and <8.0 cm in 2019). Gadids (Arctic cod, pollock, saffron cod, Pacific cod), Arctic sand lance, pricklebacks (Stichaeidae), Pacific herring, and capelin accounted for 98.6% of catch by number (16.0% by weight) in 2017, and 93.4% of catch by number (6.7% by weight) in 2019 (Figure 3.2a, b). The same species accounted for 95.2% and 87.3% of the catch by number in 2012 and 2013, respectively (De Robertis et al., 2017). Jellyfish made up a small portion of the catch by number (0.7% in 2017, 5.5% in 2019), but a large portion of the catch by weight (83.8% of the biomass in 2017, 93.1% in 2019). *Chrysaora melanaster* was prevalent throughout the survey area in both years, accounting for 60.8% of all jellyfish by weight in 2017 and 58.3% in 2019.

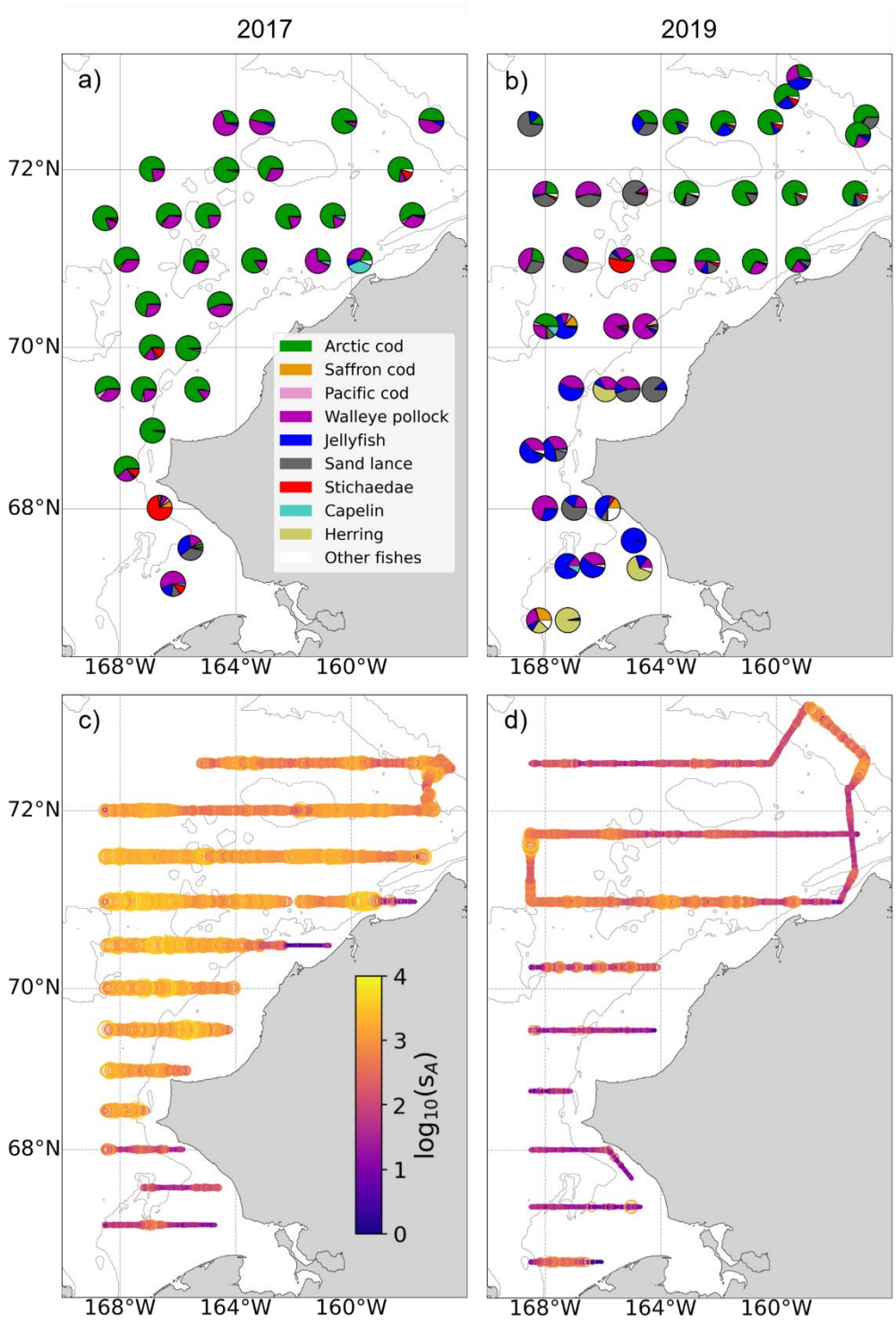

Figure 3.2 Catch composition as proportion of individuals captured in each midwater trawl in (a) 2017 and (b) 2019. 38 kHz backscatter from fishes (s_A, m^2 nmi^{-2}) along the survey transects during the c) 2017 and d) 2019 surveys. The 40-, 100-, and 1000-m depth contours are shown.

Age-0 Arctic cod dominated the catch throughout the survey region in 2017, except in the southern Chukchi (south of 68.5 °N) where the catch composition was highly variable (Figure 3.2a). Age-0 pollock were widely distributed and captured at lower abundance throughout the survey area (Figure 3.2a). The catch composition was much more spatially stratified in 2019, with Arctic cod primarily restricted to the northeastern part of the survey area (Figure 3.2b). The northwestern portion of the survey area was dominated by pollock and Arctic sand lance. South of 71 °N, pollock were the most abundant fishes in the trawl catches, with capelin and Pacific herring occurring at some nearshore locations (Figure 3.2b).

3.4.2 *Acoustic backscatter*

In the region north of the Bering Strait (>66 °N), mean backscatter in 2017 was 4.5-fold higher than in 2019 (Table 3.1), 4.9-fold higher than 2013, and 15.5-fold higher than 2012. Acoustic backscatter in 2017 was high throughout the survey region north of 68 °N, which coincided with the areas where age-0 Arctic cod were numerically abundant in trawl catches (Figure 3.2c). The greatest backscatter levels in 2019 were found between 70 and 72 °N, where both age-0 Arctic cod and pollock were the dominant species in the catch (Figure 3.2b, d). Patchy high-backscatter schools in the southern Chukchi Sea in 2019 were attributed to Pacific herring (Figure 3.2d, Supplementary Figure 3.3). Arctic cod, pollock, saffron cod, and Pacific cod were the dominant acoustic scatterers. These species accounted for 94.3% of the backscatter in 2017 and 88.3% in 2019. Capelin and Pacific herring were the next most abundant sound scattering pelagic species in the catch. Together, they accounted for 1.9% of the backscatter in 2017 and 5.5% in 2019. Although jellyfish dominated the biomass, they have a much lower mass-specific target strength than fishes with swimbladders (De Robertis and Taylor, 2014) and were not major contributors to

the observed backscatter (<1.3% in both years). Thus, the primary contributors to 38 kHz backscatter were age-0 gadids.

Table 3.1 Mean fish backscatter and total number of fish for abundant pelagic sound scattering species, estimated with acoustic-trawl methods in 2017 and 2019. The total area of the survey region was 1.48 x 10^5 km^2 in 2017 and 1.53 x 10^5 km^2 in 2019, with ~92% of the survey area overlapping between both years. Low abundance fishes, e.g. Pacific cod, make up a low proportion of the backscatter and thus their abundance estimates are more uncertain. However, these estimates are included here to provide a baseline for future assessments in the region.

	2017	2019
Mean fish backscatter (s_A, m^2 nmi^{-2})	1094.8	239.6
Arctic cod	5.6 x 10^{11}	9.8 x 10^{10}
Walleye pollock	1.5 x 10^{11}	3.8 x 10^{10}
Capelin	1.3 x 10^{10}	2.3 x 10^9
Saffron cod	1.5 x 10^9	1.2 x 10^9
Pacific cod	2.7 x 10^9	9.3 x 10^8
Pacific herring	Not present	2.0 x 10^9

3.4.3 *Fish abundance and distribution*

Gadids dominated the acoustic-trawl abundance estimates in 2017 and 2019. They composed 98% of fishes in 2017 and 96% in 2019. Arctic cod were particularly abundant and composed 76.3% of fish abundance in 2017 and 68.6% in 2019. Arctic cod also dominated AT abundance estimates in the 2012 and 2013 surveys. High abundances of small pollock were observed in 2017 and 2019. Pollock made up 21.1% of fishes in 2017 and 26.6% in 2019. This was not the case in earlier surveys – pollock accounted for only 0.1% of fishes in 2012 and <0.001% of fishes in 2013 in trawl catches north of 66 °N. Abundances of Arctic cod and pollock in 2017 were 5.7- and 4.0-

fold greater than in 2019, respectively (Table 3.1). Arctic cod and pollock densities in 2017 were greater in the central and northern Chukchi Sea compared to other survey years (Figure 3.3). Furthermore, the relatively high densities of Arctic cod in 2017 were widespread and extended throughout much of the shelf. Pollock were also distributed throughout the survey region at much greater densities than previously observed (Figure 3.3e, f).

The lengths of Arctic cod and pollock were consistent with age-0 fish for these species (Figure 3.4, Brodeur et al., 2002; Helser et al., 2017). The mean length of Arctic cod was 4.4 cm (±0.5 cm SD) in 2017, and 4.7 (±0.5 cm SD) cm in 2019 (Figure 3.4a). The Arctic cod in 2017 and 2019 were on average ~1 cm larger than those observed north of the Bering Strait in 2012 and 2013 (3.5 cm in both years, Figure 3.4a). Pollock mean length was 4.9 cm (±0.6 cm SD) in 2017 and 5.2 cm (±0.4 cm SD) in 2019 (Figure 3.4b).

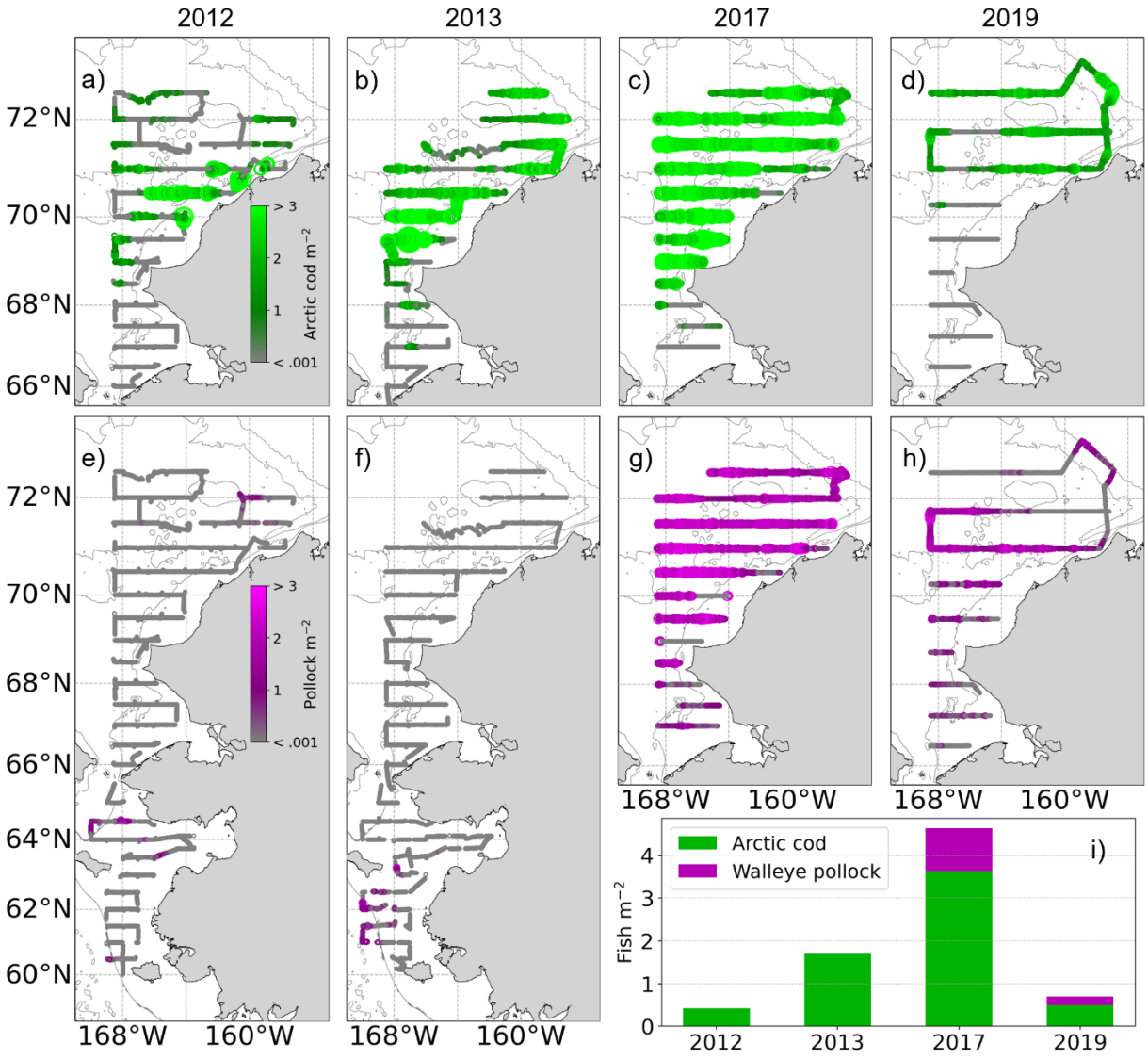

Figure 3.3 Density of Arctic cod as estimated by acoustic-trawl methods in 0.5 nmi along-transect intervals in (a) 2012, (b) 2013, (c) 2017, and (d) 2019. Density of walleye pollock in (e) 2012, (f) 2013, (g) 2017, and (h) 2019. The 40-, 100-, and 1000-m depth contours are shown. In 2017 and 2019, the entire survey extent is shown. In 2012 and 2013, plots for Arctic cod (a, b) show only the region north of the Bering Strait (66 °N). This encompasses all Arctic cod except for an aggregation of large (age 1+) individuals captured in one trawl in 2012 at 65 N (not shown; see De Robertis et al. [2017], their Figure 2). (i) Mean areal density (fish m^{-2}) of Arctic cod and pollock north of 66 °N. Pollock were present in 2012, but their density was too low to be visible on the chart.

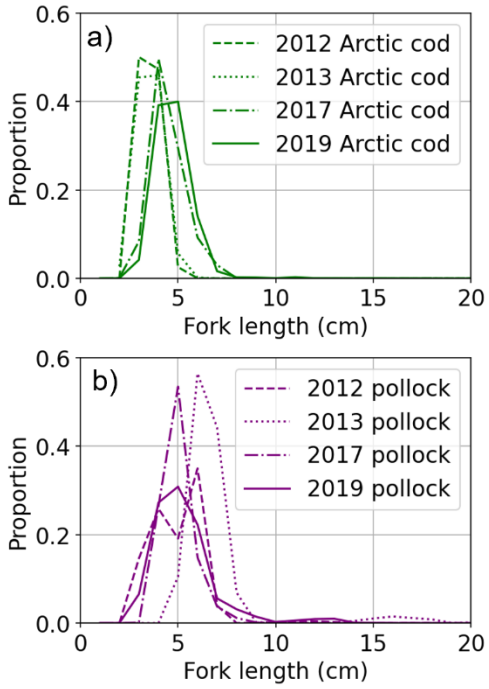

Figure 3.4 Size distributions estimated by acoustic-trawl methods of (a) Arctic cod and (b) pollock in each survey year.

3.4.4 *Environmental conditions and associations*

Arctic cod and pollock exhibited associations with temperature and salinity but these were not consistent among surveys (Figure 3.5). Surface temperature and salinity at sampling stations ranged from 2.5 to 7.5 °C and 25.4 to 32.3 in 2017 (Figure 3.5g), and 3.2 to 10.6 °C and 27.1 to 32.1 in 2019 (Figure 3.5h). Relative to other years, surface temperatures in 2017 fell within a relatively narrow band of intermediate temperatures. Bottom temperature and salinity ranged from -0.7 to 6.5 °C and 31.0 to 34.7 in 2017 (Figure 3.5g), and -1.4 to 10.6 °C and 29.1 to 34.7 in 2019 (Figure 3.5h). The coldest surface and bottom waters were encountered in the northeastern portion of the survey area in both years (Supplementary Figure 3.1).

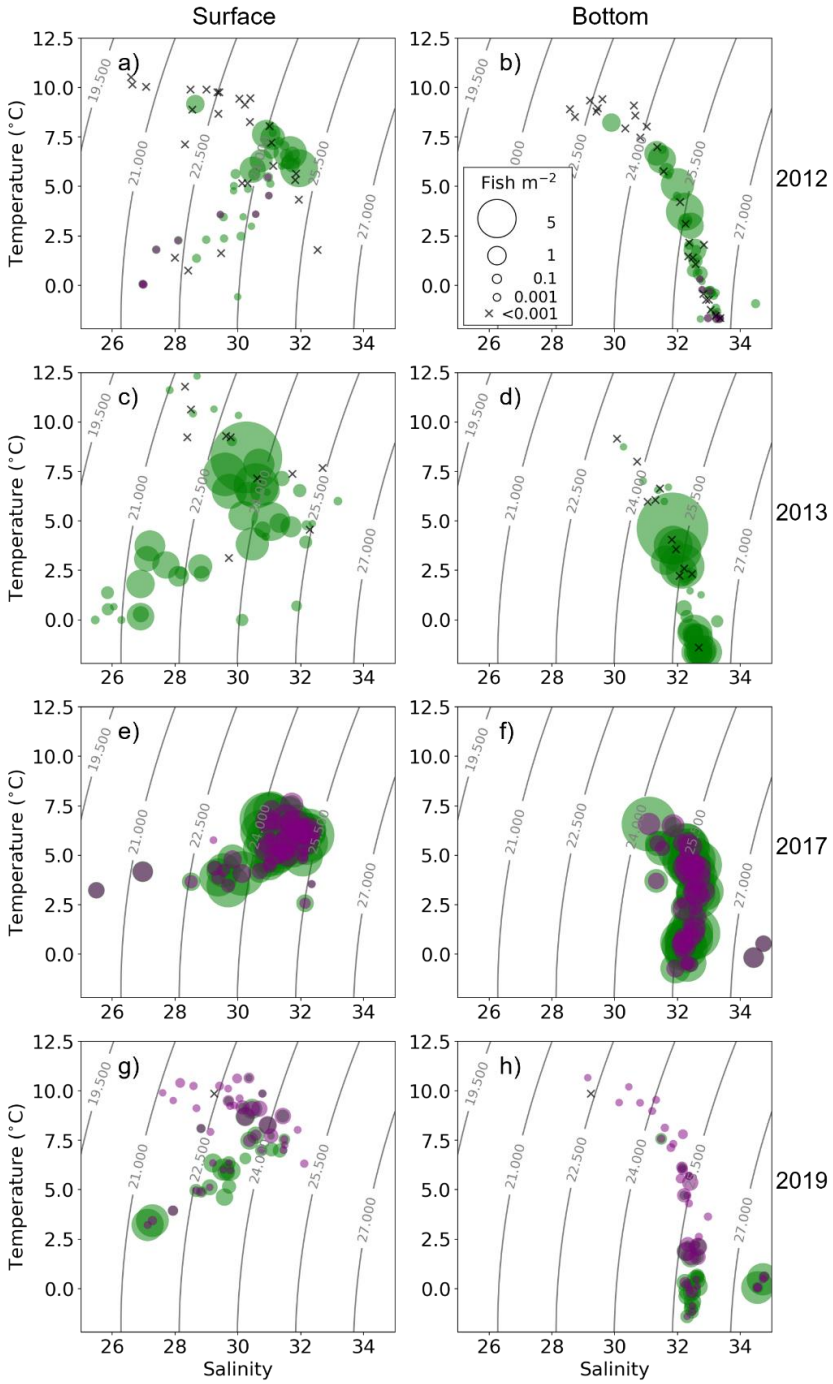

Figure 3.5 Surface and bottom temperature and salinity at CTD stations in (a, b) 2012, (c, d) 2013, (e, f) 2017, and (g, h) 2019, where the size of each point indicates the abundance of Arctic cod (green) and walleye pollock (purple) in the transect intervals associated with the station (see methods for details). CTD stations where fish density in the associated transect intervals was < 0.001 fish m^{-2} are indicated by a black x.

Arctic cod and pollock distributions overlapped broadly and inhabited similar water masses in 2017 (Figures 3.3d, g, 3.5e, f). In contrast, the two species were spatially separated, present largely in different thermal environments, in 2019 (Figures 3.3d, h, 3.5g, h). Pollock were the primary gadids in the southern and western portion of the survey area in 2019 (Figure 3.3h), which exhibited warm (>7 °C) surface temperatures that typify Alaskan Coastal Water and warm (>2 °C) bottom waters typical of Bering/Chukchi Summer Water (Figure 3.5g, h, Supplementary Figure 3.1). Conversely, Arctic cod were largely restricted to the northeastern region of the survey area in 2019 (Figure 3.3d), where surface temperatures were <7 °C (Figure 3.5g, Supplementary Figure 3.1d) and bottom temperatures were <2 °C, typical of Bering/Chukchi Winter Water (Figure 3.5h, Supplementary Figure 3.1h). Arctic cod were observed in 2012 and 2013 in similar surface water conditions but in the full range of observed bottom temperatures (Figure 3.5).

Arctic cod and pollock were distributed closer to the surface in regions with cold bottom water (Figure 3.6). Fish were relatively evenly distributed throughout the water column in 2017 (Figure 3.6a, b) when water across the shelf was well mixed (Figure 3.5e, f, Supplementary Figure 3.1c, g), and >65% of the total survey abundance was in areas with bottom water >2 °C. Only 25% of abundance was in areas with bottom water >2 °C in 2019; fish in these locations were more evenly distributed throughout the water column (Figure 3.6c, d), with only 28% of the abundance shallower than 25 m. Arctic cod were largely restricted to areas with bottom waters <2 °C in 2019, which was not the case in previous years (Figure 3.5h). In the colder regions of the survey area (bottom temperature <2 °C), >55% of the fish were shallower than 25 m in 2019, driven by the relatively large abundance of Arctic cod high in the water column (Figure 3.6c).

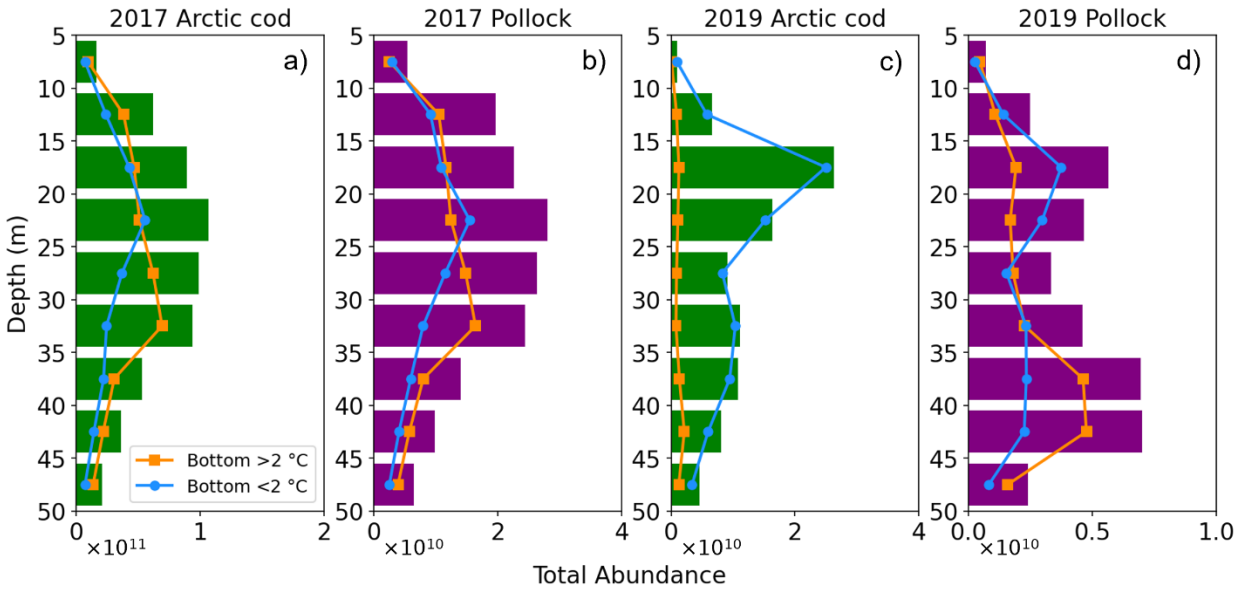

Figure 3.6 Total abundance of Arctic cod (green) and walleye pollock (purple) by depth in the water column in (a, b) 2017 and (c, d) 2019. The lines in each panel partition the total abundance into regions where bottom temperatures were >2 °C (orange) <2 °C (blue).

3.5 DISCUSSION

3.5.1 *Abundance and distribution of fishes*

Observations from four surveys spanning a seven-year period suggest that the pelagic fish community in the Chukchi Sea is changing. We observed that age-0 gadids continue to dominate the pelagic fishes on the Chukchi shelf (Quast 1974; Logerwell et al., 2015; De Robertis et al., 2017). However, their abundance and species composition were highly variable. Age-0 gadids were substantially more abundant in 2017 relative to the other years, which was apparent in both the AT abundance estimates and the trawl catch rates. This was due to both a large increase in Arctic cod and an influx of pollock, which were sparse in previous years. While age-0 Arctic cod continue to be the dominant pelagic fish in much of the Chukchi Sea, age-0 pollock, which were previously near-absent in the region, were present in substantial numbers in 2017 and 2019.

Arctic cod, pollock, saffron cod, Pacific cod, and capelin were the most abundant species in 2017 and 2019. Pacific herring were also present in the southern portion of the survey area within Kotzebue Sound in 2019 (Table 3.1, Supplementary Figure 3.3). With the exception of pollock, these same species groups were dominant in the 2012 and 2013 AT survey observations (De Robertis et al., 2017) and in previous surveys of the Pacific Arctic (Eisner et al., 2013; Goddard et al., 2014; Logerwell et al., 2015). Although we were unable to confidently estimate the abundance of Arctic sand lance abundance using acoustic-trawl methods due to their weak acoustic scattering, they were abundant in trawl catches in the central and northwestern portion of the survey region in 2019 (Figure 3.2b).

Few age-1+ gadids were present in the region, consistent with previous surveys of the eastern Chukchi Sea (Goddard et al., 2014; Logerwell et al., 2015; De Robertis et al., 2017) which we believe to accurately represent the community composition rather than be the result of gear selectivity. Gadid lengths from both surveys support the acoustic observations made with a USV in 2018 which concluded that pelagic fishes were primarily age-0 gadids based on the strength of echoes from individuals (target strength) and found little evidence for scattering from adult-sized gadids (Levine et al., 2020). In addition, no large gadids were caught in surface trawls conducted using a large Nordic rope trawl (184 m long, ~315 m^2 net opening) during the 2017 and 2019 surveys (Farley and Levine, 2021a; Farley and Levine, 2021b). The absence of large gadids in 2017 and 2019 was not likely due to gear selectivity, as the Marinovich herring trawl used in this study has retained larger individuals when used in other regions. For example, pollock up to 61 cm were captured in several Marinovich herring trawl hauls in the Bering Sea (Honkalehto and McCarthy, 2015). A bottom trawl (3 m vertical and 12 m horizontal trawl opening) similar in size to the Marinovich has also been effective at capturing adult pollock when fished in midwater

(Kotwicki et al., 2017). Thus, we are confident that our trawl sampling establishes that relatively few pelagic adult gadids were present within the survey area.

We hypothesize that the dramatic increase in age-0 pollock in the Chukchi Sea is a recent occurrence. Small pollock and Arctic cod are difficult to distinguish based solely on external morphological characteristics in field collections, due to the unavailability of suitable field identification characteristics to differentiate pollock from Arctic cod (Mecklenburg et al., 2018). Without genetic analyses, we would have failed to identify the unexpected presence of pollock within the survey area in 2017 (Wildes et al., in prep). Post-survey genetic identification was necessary to accurately estimate abundances and distributions of each species (see supplementary material 3.8.2 for details). Although the spatial coverage of specimens from previous surveys is limited, the same genetic analyses conducted on specimens from 2012 and 2013 suggests that pollock were not abundant in the survey region (Wildes et al., in prep), thus these observations are not the result of previous errors in species identification.

3.5.2 *Temperature impacts on Arctic cod populations*

The spatial distribution of Arctic cod and pollock closely resembles the distribution of warm and cold waters across the Chukchi shelf. The distributions of Arctic cod and pollock overlapped broadly in 2017 (Figure 3.3c, g), with both species co-occurring in the relatively narrow range of surface and bottom temperatures found in the survey area compared to other years (Figure 3.5e, f). In contrast, in 2019, Arctic cod and pollock were spatially distinct (Figure 3.3d, h) and were associated with different water masses (Figure 3.5g, h). Minimum temperatures observed in 2019 were colder than in 2017, and cold water (<2 °C) was more widespread (Supplementary Figure 3.1). In 2019, Arctic cod were found primarily on the northeast Chukchi shelf where bottom temperatures were <2 °C. This is typical of the colder water that forms in winter on the Bering and

Chukchi shelves (Coachman et al., 1975; Woodgate et al., 2005). These Arctic cod were shallow (Figure 3.6b), likely remaining in the intermediate temperatures >2 °C in the upper water column. One possibility is that this shallow distribution is due to limited vertical migration resulting from reduced swimming ability. However, this is unlikely because the size of Arctic cod in 2019 was similar to that in 2017 when fish were relatively evenly distributed throughout the water column (Figure 3.6a). This change in vertical distribution more likely reflects a behavioral choice. That is, Arctic cod may be avoiding colder deep waters or concentrating at depths where food availability is high.

Arctic cod in 2017 and 2019 were on average ~1 cm larger than those observed north of the Bering Strait in 2012 and 2013, which we attribute partially to differences in survey timing but mostly to the effect of increasing temperatures on age-0 growth and survival in the region. The summer is a period of rapid growth for age-0 gadids on the Chukchi shelf (Levine et al., 2020; Deary et al., 2021), and the recent surveys in 2017 and 2019 occurred approximately 3 weeks later than those in 2012 and 2013. For a 3.5 cm Arctic cod at 9 °C, the temperature of maximum growth (Laurel et al., 2017), an additional 21 days reflecting later surveys in 2017 and 2019 could explain approximately 0.5 cm of increased length (based on Laurel et al., 2017, their Table 2 model B_0). However, even at this maximum growth rate, this would only account for approximately half of the increased size observed in 2017 and 2019.

Warmer water temperatures are also likely to have contributed to recent increases in gadid body size and higher gadid abundance. Mean water temperatures between the approximate timing of Arctic cod spawning and the survey dates (January to August, Figure 3.7; Bouchard and Fortier 2011) in the Bering Strait (A3 mooring site, 66.29 °N, 168.96 °W, Woodgate, 2018; Woodgate and Peralta-Ferriz, 2021) in 2017 and 2019 were 0.5-1.5 °C warmer than in 2012 and 2013. This

was driven principally by warmer conditions in spring and summer (Supplementary Figure 3.4). Exceptionally warm temperatures in spring 2017 were observed in the Bering Strait (Supplementary Figure 3.4a), when water was 0.5 °C warmer than the same period in 2019 and >1 °C warmer than in 2012 and 2013 (Figure 3.7). Increased growth rates resulting from warmer temperatures may have led to larger individuals in 2017 and 2019 (Laurel et al., 2017). Based on the growth rates of age-0 Arctic cod laboratory specimens reported in Laurel et al., (2017), the ~1 °C difference in temperature between the spawning period and survey (Figure 3.7) could account for a ~0.5 cm increase in length by the time of the survey in September.

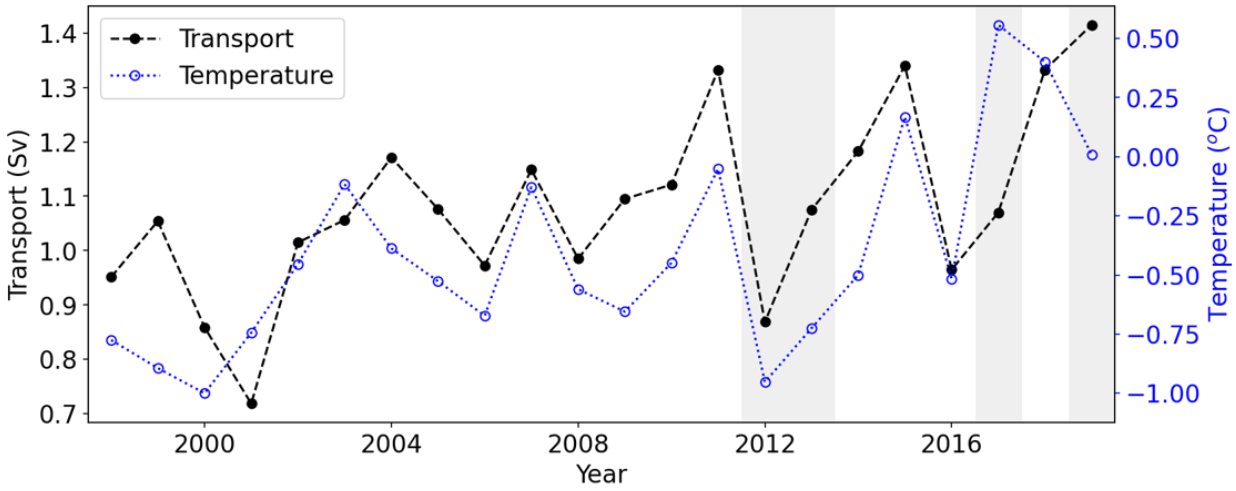

Figure 3.7 Mean transport (black dashed line) and bottom temperatures (blue dotted line) measured at Bering Strait (A3 mooring, Woodgate, 2018; Woodgate and Peralta-Ferriz, 2021) from January to August of each year (1998 - 2019). The years of the acoustic-trawl surveys (2012, 2013, 2017, 2019) are indicated by the grey-shaded regions.

Increased survival of early-hatched Arctic cod larvae may have also contributed to increased mean size in 2017 and 2019. Observations of Arctic cod in the Canadian Arctic suggest that higher temperatures reduce time-to-hatch and improve the survival of early hatching larvae

(Bouchard and Fortier 2011; Bouchard et al., 2017). Dupont et al. (2020) proposed that increased early-season survival rates would lead to an increase in mean age and length during surveys. As length is strongly associated with hatch date (Bouchard et al., 2017), a greater proportion of older individuals leads to an increase in the mean length in the population. Improved early larval survival may also lead to increased size and lower mortality of age-0 fishes (Dupont et al., 2020), which may have contributed to the high abundances of age-0 Arctic cod observed in 2017.

3.5.3 *Drivers of age-0 pollock appearance in the Chukchi Sea*

The high abundances of age-0 pollock in the Chukchi Sea in recent years may also be indirectly driven by increased temperatures in the northern Bering Sea, which resulted from decreased ice extent and earlier ice retreat. Few pollock of any age class have been observed north of the Bering Strait in previous surveys (Quast, 1974; Norcross et al., 2013; Logerwell et al., 2015; De Robertis et al., 2017). Ice cover in the Bering Sea has historically supported the formation of an extensive "cold pool" on the eastern Bering Sea shelf; a region where cold (<2 °C) bottom waters persist summer and early fall (Wyllie-Echeverria and Wooster, 1998; Stabeno and Bell, 2019). Adult pollock typically avoid the cold pool and move to the outer shelf region of the Bering Sea when the cold pool is extensive (Kotwicki et al., 2005; Stevenson and Lauth, 2019). Reduced ice formation and duration results in a diminished cold pool, which reduces the barrier for adult pollock to remain on the inner and northern shelf throughout the year.

The Bering Sea has experienced extreme warming in recent years, which reduced the size of the cold pool in both 2017 and 2019 (Stabeno and Bell, 2019). Pollock distributions shifted northward during this period, resulting in high densities of adult pollock in the northern Bering Sea (Stevenson and Lauth, 2019; Eisner et al., 2020). High abundances of juvenile and adult pollock were also observed in the Russian sector of the southern Chukchi Sea in 2019 (Orlov et

al., 2020). This northern pollock population was likely absent during the 2012 and 2013 surveys due to the presence of an extensive cold pool (O'Leary et al., 2020). We hypothesize that the recent northward movement of pollock resulted in increased production of pollock larvae in the northern Bering Sea, which were then transported into the Chukchi Sea by the prevailing northward transport (Vestfals et al., 2021).

Cold Winter Water (<2 °C) which forms during ice formation is gradually displaced to the north after seasonal ice melt by water entering the shelf from the Bering Sea (Lowry et al., 2015; Woodgate, 2018; Danielson et al., 2020). The intermediate temperatures of 2 to 7 °C and relatively high salinities (>30.4) observed in surface waters are typical of Bering/Chukchi Summer Water. Bering/Chukchi Summer Water originates in the Chukchi and northern Bering Seas (Danielson et al., 2017) and replaces the Winter Water and meltwater on the Chukchi shelf in summer (Weingartner et al., 2013). The temperature range of the Bering/Chukchi Summer Water is favorable for growth of both Arctic cod and pollock (Laurel et al., 2016).

We hypothesize that the spatial separation between pollock and Arctic cod distributions in the Chukchi observed in 2019 was driven by the association of each species with distinct water masses, which remained separate while undergoing increased transport from the Bering Sea. Bering Strait transport during the period between the approximate time of first spawning of Arctic cod and the survey (January to August) was substantially higher in 2019 relative to previous years (Figure 3.7). Surface temperatures at the time of the 2019 survey exceeded 8 °C in the central and southern half of the survey area where pollock were abundant (Figures 3.3, 3.5). These temperatures are similar to those typical of Alaskan Coastal Water, which primarily originates on the inner Bering Sea shelf, driven by river input in spring and summer (Coachman et al., 1975; Woodgate et al., 2005). In previous surveys, this water was restricted to the nearshore regions of

the eastern Chukchi. However, in 2019, the Alaskan Coastal Water was found as far north as 72 °N in the central Chukchi, extending well offshore (Supplementary Figures 3.1, 3.2), likely due to southwestward winds forcing the current away from the coast (Woodgate et al., 2015; Morris, 2019). Age-0 pollock were likely advected within this Bering-origin water mass potentially explaining their widespread distribution in the Chukchi Sea. Similarly, the increased transport likely displaced age-0 Arctic cod northwards. Arctic cod were present largely in areas where bottom waters still reflected characteristics of Winter Water (Figure 3.5f), which was present over the shelf prior to the input of warm water in spring. While age-0 pollock were found in high abundance in summer, it remains unclear if these fish are able to establish permanent populations given the persistent near-freezing temperatures they would experience on the shelf in winter (Woodgate et al., 2005; Stabeno et al., 2018).

3.5.4 *The future of the Chukchi shelf pelagic community*

If lower energy content subarctic species such as pollock continue to displace age-0 Arctic cod, the transition in gadid community structure could reduce the availability of high-quality prey to higher trophic levels in the Chukchi Sea (Copeman et al., 2017). Our analysis suggests that the anticipated continued warming of the Chukchi shelf (Danielson et al., 2020) will substantially alter ecosystem function. We propose that the observations of gadids in this short survey time series can be described by a conceptual model encompassing three environmental regimes. Under "historical" conditions (Figure 3.8a), ice in the northern Bering Sea retreats in May and June (Frey et al., 2015), the Chukchi Sea remains relatively cool and surface waters reflect a mix of melt water, Bering/Chukchi Summer Water, and Alaskan Coastal Water (Danielson et al., 2017). In this regime, age-0 Arctic cod, that are likely to have spawned to the south (Vestfals et al., 2021), are the dominant gadids on the Chukchi shelf in late summer. They are primarily present in the

northeastern Chukchi Sea, where they experience intermediate temperatures as Winter Water warms. These fish are then advected northwards during the fall towards the Chukchi and Beaufort shelf breaks and the central basin (Levine et al., 2020).

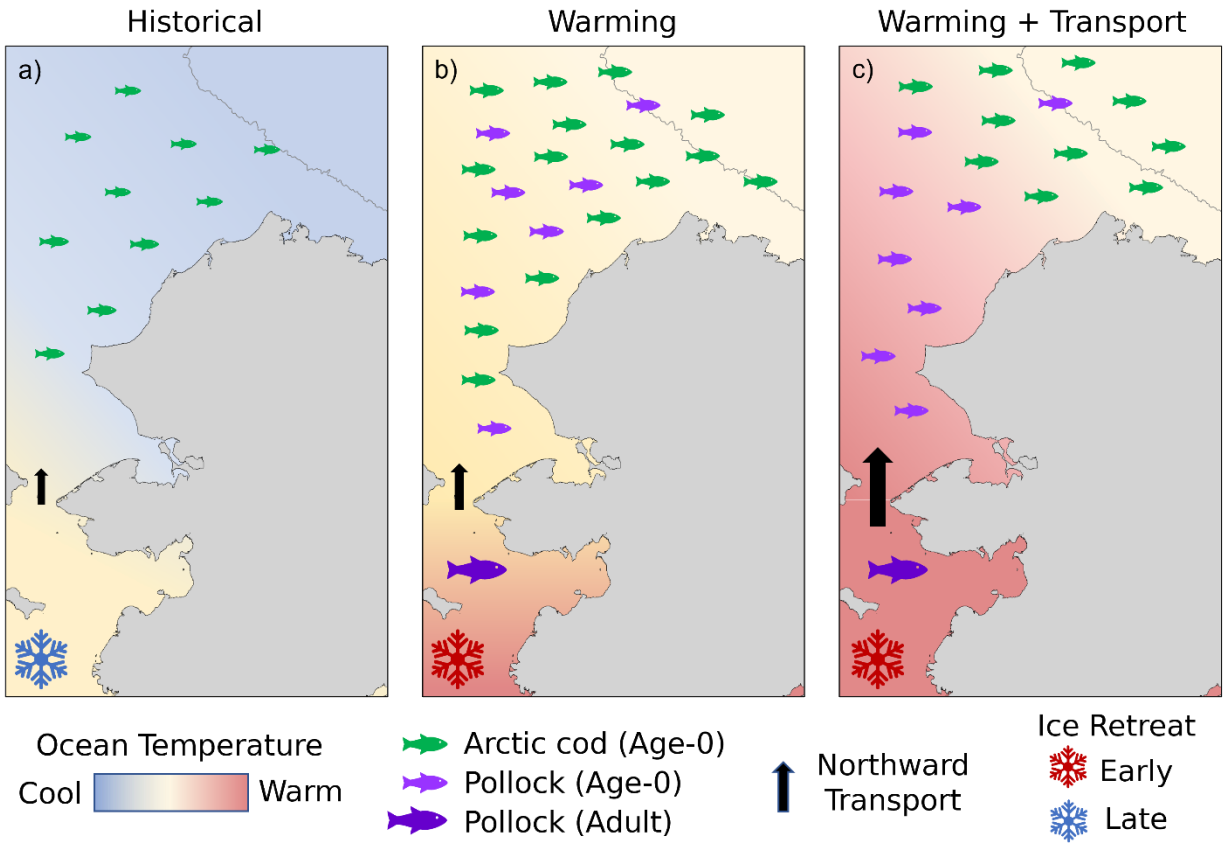

Figure 3.8 Hypothesized climate-driven shifts of the Chukchi Sea gadids. (a) Under historical conditions of later ice retreat, Arctic cod are present in intermediate and cool waters across the Chukchi Shelf. (b) With increased warming and early ice retreat, age-0 Arctic cod increase in abundance and size as a result of increasing temperatures. Increased presence of adult walleye pollock in the northern Bering Sea results in the transport of age-0 pollock into the Chukchi, where conditions are favorable for both gadid species. (c) With increased transport of warmer waters from the Bering Sea, Arctic cod are displaced further north, along with the intermediate temperature waters. Age-0 pollock from the northern Bering Sea are transported with the warmer waters and become the dominant gadid in the southern portion of the shelf. The 1000-m depth contour is shown to indicate the Chukchi shelf break.

Under warming ocean conditions (Figure 3.8b), when ice retreats from the northern Bering Sea earlier in spring (Wang et al., 2018), we propose a "warming" regime where temperatures are warmer across the shelf as a result of decreased sea ice extent and earlier ice retreat. With a reduced cold pool in the Bering Sea, the density of adult pollock near the Bering Strait increases. This leads to an increased supply of age-0 pollock in the Northern Bering Sea which are advected onto the Chukchi shelf (Eisner et al., 2020; Baker, 2021). Hatch success of all gadids also increases as a result of warmer conditions on the Chukchi shelf, resulting in larger age-0 individuals in fall (Bouchard et al., 2017) that are subsequently advected farther north.

Under a third, "warming and increased transport" regime, northward transport increases as well as temperature (Figure 3.8c; Woodgate, 2018). Pelagic age-0 pollock and Arctic cod continue to be present on the Chukchi shelf in summer. As a result of increased transport, the residence time of age-0 gadids on the Chukchi shelf decreases. Under this regime, Arctic cod, which are known to spawn under sea ice (Ponomorenko, 2000), originate further north than pollock. Adult pollock increasingly overwinter and spawn in the ice-free central and northern Bering Sea. The population of age-0 Arctic cod is displaced to the Chukchi shelf break and Beaufort Sea earlier in the summer season, as the water present on the Chukchi shelf is transported north more rapidly. The consequences of this displacement are unknown for Arctic cod. For example, the displacement may result in a potential timing mismatch of their ontogenetic migration to take advantage of warmer Atlantic water along the Chukchi and Beaufort shelf breaks during transport off the Chukchi shelf in fall (Geoffroy et al., 2016). Age-0 pollock that may originate further south in the northern Bering Sea would be transported into the Chukchi along with the warmer water masses and will dominate the gadid distribution on the central and southern shelf in late summer. Although adult pollock do not appear to be present in appreciable densities, under continued warming they

may eventually colonize the Chukchi as they have the northern Bering (Eisner et al., 2020). While our time series of survey observations is limited, we interpret the 2012 and 2013 surveys as representative of the cooler historical regime (Figure 3.8a), 2017 representative of the warming regime (Figure 3.8b), and 2019 representative of the warming and increased transport regime (Figures 3.7, 3.8c).

The spawning population that produces the age-0 Arctic cod observed in the northern Chukchi Sea remains unknown. A migration path between spawning and feeding grounds for Arctic cod has been proposed (Forster et al., 2020) where fish spawn under sea ice in the northern Bering Sea, follow the ice retreat north to seasonal feeding areas, and return to the spawning grounds in late fall. This proposed migration may be altered by continued warming, as the reduction in suitable habitat (bottom temperatures <2 °C) for Arctic cod in the northern Bering Sea has led to decreases in Arctic cod in the summer (Baker, 2021). Particle tracking models suggest that the age-0 Arctic cod population observed on the Chukchi shelf were likely spawned in the northern Bering Sea and/or along the Chukotka Peninsula, and subsequently advected north (Levine et al., 2020; Vestfals et al., 2021). However, this is difficult to confirm as spawning Arctic cod are difficult to sample due to seasonal ice cover. Without direct observations and tracking of spawning populations, we have only limited understanding of the spatio-temporal distribution patterns exhibited by age-0 gadids as they develop and return as adults, and the key environmental drivers that determine juvenile and adult survival and reproductive success. Year-round in situ observations of Arctic cod migration and transport, for example through remote sampling of environmental DNA (Wietz et al., 2021), passive acoustic monitoring (Riera et al., 2018), or target tracking from moored echosounders (Kaartvedt et al., 2009), are needed to further confirm and quantify the roles of transport in the distribution and movement of these fish (Levine et al., 2020).

If, as we hypothesize, the ongoing changes observed in the physical oceanography of the Chukchi Sea influence growth and transport of age-0 gadids, indirect environmental measurements could provide a basis for predicting future summer-time distributions of pelagic fishes in this region. Mooring-, satellite-, and shore-based observations as well as model-based predictions of ice, temperature, and transport are well established in the region (Frey et al., 2015; Woodgate, 2018; Janzen et al., 2019; Wang et al., 2018). These data sources are the basis for the predictions of continued warming and higher transport into the Chukchi Sea. Northward shifts in the distribution of other marine animals have been associated with these changes in the physical environment. For example, changes in water mass transport have strongly influenced shifts in zooplankton distributions (Spear et al., 2020) which, in turn, have influenced distribution shifts of their mobile predators (e.g., seabirds, Kuletz et al., 2020). These shifts in populations, which are now also documented in the pelagic fish community, provide insight into potential future states of the Chukchi ecosystem. Developing a mechanistic understanding of how the anticipated rapid increases in warming and transport in the Pacific Arctic will affect fishes is key to understanding future impacts on pelagic fish communities, their role in the ecosystem, and effective management of the ecosystem.

3.6 ACKNOWLEDGEMENTS

This research was conducted under the Arctic Integrated Ecosystem Research Program (http://www.nprb.org/arctic-program). Funding for the program was provided by North Pacific Research Board, the Bureau of Ocean Energy Management, the Collaborative Alaskan Arctic Studies Program, and the Office of Naval Research. In-kind support was contributed by the National Oceanic and Atmospheric Administration's (NOAA) Alaska Fisheries Science Center

and Pacific Marine Environmental Laboratory, the University of Alaska Fairbanks, the U.S. Fish & Wildlife Service, and the National Science Foundation. Bering Strait mooring observations are funded by NSF-OPP (1304052 and 1758565) with data available at http://psc.apl.washington.edu/BeringStrait.html and NCEI. We would like to thank the captain, crew, and science party of the RV *Ocean Starr* for their assistance at sea. Any use of trade, firm, or product names is does not imply endorsement by the U.S. Government. The findings of this paper do not necessarily represent the views of the National Oceanic and Atmospheric Administration.

3.7 REFERENCES

Baker, M.R., 2021. Contrast of warm and cold phases in the Bering Sea to understand spatial distributions of Arctic and sub-Arctic gadids. Polar Biol. https://doi.org/10.1007/s00300-021-02856-x

Bouchard, C., Fortier, L., 2011. Circum-arctic comparison of the hatching season of polar cod *Boreogadus saida*: A test of the freshwater winter refuge hypothesis. Prog. Oceanogr. 90, 105–116. https://doi.org/10.1016/j.pocean.2011.02.008

Bouchard, C., Geoffroy, M., LeBlanc, M., Majewski, A., Gauthier, S., Walkusz, W., Reist, J.D., Fortier, L., 2017. Climate warming enhances polar cod recruitment, at least transiently. Prog. Oceanogr. 156, 121–129. https://doi.org/10.1016/j.pocean.2017.06.008

Bradstreet, M.S.W., Finley, K.J., Sekerak, A.-D., Griffiths, W.B., Evans, C.R., Fabijan, M.F., Stallard, H.E., 1986. Aspects of the Biology of Arctic Cod (*Boreogadus saida*) and its Importance in Arctic Marine Food Chains, Canadian Technical Report of Fisheries and Aquatic Sciences. https://doi.org/10.1002/aic.12482

Brodeur, R.D., Wilson, M.T., Ciannelli, L., Doyle, M., Napp, J.M., 2002. Interannual and regional variability in distribution and ecology of juvenile pollock and their prey in frontal structures of the Bering Sea. Deep Sea Res. Part II Top. Stud. Oceanogr. 49, 6051–6067. https://doi.org/10.1016/S0967-0645(02)00333-8

Coachman, L.K., Aagaard, K., Tripp, R.B., 1975. Bering Strait: The Regional Physical Oceanography, University of Washington Press. University of Washington Press, Seattle. https://doi.org/10.1016/0146-6291(77)90492-1

Copeman, L.A., Laurel, B.J., Spencer, M., Sremba, A., 2017. Temperature impacts on lipid allocation among juvenile gadid species at the Pacific Arctic-Boreal interface: An

experimental laboratory approach. Mar. Ecol. Prog. Ser. 566, 183–198. https://doi.org/10.3354/meps12040

Copeman, L., Spencer, M., Heintz, R., Vollenweider, J., Sremba, A., Helser, T., Logerwell, L., Sousa, L., Danielson, S., Pinchuk, A.I., Laurel, B., 2020. Ontogenetic patterns in lipid and fatty acid biomarkers of juvenile polar cod (*Boreogadus saida*) and saffron cod (*Eleginus gracilis*) from across the Alaska Arctic. Polar Biol. https://doi.org/10.1007/s00300-020-02648-9

Danielson, S.L., Eisner, L., Ladd, C., Mordy, C., Sousa, L., Weingartner, T.J., 2017. A comparison between late summer 2012 and 2013 water masses, macronutrients, and phytoplankton standing crops in the northern Bering and Chukchi Seas. Deep Sea Res. Part II Top. Stud. Oceanogr. 135, 7–26. https://doi.org/10.1016/j.dsr2.2016.05.024

Danielson, S.L., Ahkinga, O., Ashjian, C., Basyuk, E., Cooper, L.W., Eisner, L., Farley, E., Iken, K.B., Grebmeier, J.M., Juranek, L., Khen, G., Jayne, S.R., Kikuchi, T., Ladd, C., Lu, K., McCabe, R.M., Moore, G.W.K., Nishino, S., Ozenna, F., Pickart, R.S., Polyakov, I., Stabeno, P.J., Thoman, R., Williams, W.J., Wood, K., Weingartner, T.J., 2020. Manifestation and consequences of warming and altered heat fluxes over the Bering and Chukchi Sea continental shelves. Deep Sea Res. Part II Top. Stud. Oceanogr. 177. https://doi.org/10.1016/j.dsr2.2020.104781

[Dataset] De Robertis, A., 2021. De Robertis et al., 2017 – Chukchi shelf acoustic-trawl survey (corrected). Mendeley Data, v1. https://doi.org/10.17632/py3859yhnf.1

De Robertis, A., Taylor, K., 2014. In situ target strength measurements of the scyphomedusa *Chrysaora melanaster*. Fish. Res. 153, 18–23. https://doi.org/10.1016/j.fishres.2014.01.002

De Robertis, A., Taylor, K., Wilson, C.D., Farley, E. V., 2017. Abundance and distribution of Arctic cod (*Boreogadus saida*) and other pelagic fishes over the U.S. Continental Shelf of the Northern Bering and Chukchi Seas. Deep Sea Res. Part II Top. Stud. Oceanogr. 135, 51–65. https://doi.org/10.1016/j.dsr2.2016.03.002

Deary, A.L., Vestfals, C.D., Mueter, F.J., Logerwell, E.A., Goldstein, E.D., Stabeno, P.J., Danielson, S.L., Hopcroft, R.R., 2021. Seasonal abundance, distribution, and growth of the early life stages of polar cod (*Boreogadus saida*) and saffron cod (*Eleginus gracilis*) in the US Arctic. Polar Biol. https://doi.org/10.1007/s00300-021-02940-2

Demer, D.A., Berger, L., Bernasconi, M., Bethke, E., Boswell, K., Chu, D., Domokos, R., Dunford, A., Fassler, S., Gauthier, S., Hufnagle, L.T., Jech, J.M., Bouffant, N., Lebourges-Dhaussy, A., Lurton, X., Macaulay, G.J., Perrot, Y., Ryan, T., Parker-Stetter, S., Stienessen, S., Weber, T., Williamson, N., 2015. Calibration of acoustic instruments. ICES Coop. Res. Rep. 326.

Dupont, N., Durant, J.M., Langangen, Ø., Gjøsæter, H., Stige, L.C., 2020. Sea ice, temperature, and prey effects on annual variations in mean lengths of a key Arctic fish, *Boreogadus saida*, in the Barents Sea. ICES J. Mar. Sci. https://doi.org/10.1093/icesjms/fsaa040

Eisner, L., Hillgruber, N., Martinson, E., Maselko, J., 2013. Pelagic fish and zooplankton species assemblages in relation to water mass characteristics in the northern Bering and southeast Chukchi seas. Polar Biol. 36, 87–113. https://doi.org/10.1007/s00300-012-1241-0

Eisner, L.B., Zuenko, Y.I., Basyuk, E.O., Britt, L.L., Duffy-Anderson, J.T., Kotwicki, S., Ladd, C., Cheng, W., 2020. Environmental impacts on walleye pollock (*Gadus chalcogrammus*) distribution across the Bering Sea shelf. Deep Sea Res. Part II Top. Stud. Oceanogr. 181–182, 104881. https://doi.org/10.1016/j.dsr2.2020.104881

[Dataset] Farley, E., Levine, R., 2021a. Surface Trawl Dataset, Arctic Integrated Ecosystem Research Program, August - September 2017. Research Workspace, v10.24431_rw1k58b_20210608T181300Z. https://doi.org/10.24431/rw1k58b

[Dataset] Farley, E., Levine, R., 2021b. Surface Trawl Dataset, Arctic Integrated Ecosystem Research Program, August - September 2019. Research Workspace, v10.24431_rw1k58a_20210608T172806Z. https://doi.org/10.24431/rw1k58ba

Forster, C.E., Norcross, B.L., Mueter, F.J., Logerwell, E.A., Seitz, A.C., 2020. Spatial patterns, environmental correlates, and potential seasonal migration triangle of polar cod (*Boreogadus saida*) distribution in the Chukchi and Beaufort seas. Polar Biol. 73. https://doi.org/10.1007/s00300-020-02631-4

Fossheim, M., Primicerio, R., Johannesen, E., Ingvaldsen, R.B., Aschan, M.M., Dolgov, A. V., 2015. Recent warming leads to a rapid borealization of fish communities in the Arctic. Nat. Clim. Chang. 5, 673–677. https://doi.org/10.1038/nclimate2647

Frey, K.E., Moore, G.W.K., Cooper, L.W., Grebmeier, J.M., 2015. Divergent patterns of recent sea ice cover across the Bering, Chukchi, and Beaufort seas of the Pacific Arctic Region. Prog. Oceanogr. 136, 32–49. https://doi.org/10.1016/j.pocean.2015.05.009

Geoffroy, M., Majewski, A., LeBlanc, M., Gauthier, S., Walkusz, W., Reist, J.D., Fortier, L., 2016. Vertical segregation of age-0 and age-1+ polar cod (*Boreogadus saida*) over the annual cycle in the Canadian Beaufort Sea. Polar Biol. 39, 1023–1037. https://doi.org/10.1007/s00300-015-1811-z

Goddard, P., Lauth, R., Armistead, C., 2014. Results of the 2012 Chukchi Sea bottom trawl survey of bottomfishes, crabs, and other demersal macrofauna. U.S. Dep. Commer., NOAA Tech. Memo. NMFS-AFSC-278, 110 p.

Helser, T.E., Colman, J.R., Anderl, D.M., Kastelle, C.R., 2017. Growth dynamics of saffron cod (*Eleginus gracilis*) and Arctic cod (*Boreogadus saida*) in the Northern Bering and Chukchi Seas. Deep Sea Res. Part II Top. Stud. Oceanogr. 135, 66–77. https://doi.org/10.1016/j.dsr2.2015.12.009

Honkalehto, T., McCarthy, A., 2015. Results of the acoustic-trawl survey of walleye pollock (*Gadus chalcogrammus*) on the U.S. and Russian Bering Sea Shelf in June - August 2014 (DY1407). AFSC Processed Rep. 2015-07, 63 p. Alaska Fish. Sci. Cent., NOAA, Natl. Mar. Fish. Serv., 7600 Sand Point Way NE, Seattle WA 98115.

Hunt, G.L., Blanchard, A.L., Boveng, P., Dalpadado, P., Drinkwater, K.F., Eisner, L., Hopcroft, R.R., Kovacs, K.M., Norcross, B.L., Renaud, P., Reigstad, M., Renner, M., Skjoldal, H.R., Whitehouse, A., Woodgate, R.A., 2013. The Barents and Chukchi seas: Comparison of two Arctic shelf ecosystems. J. Mar. Syst. 109–110, 43–68. https://doi.org/10.1016/j.jmarsys.2012.08.003

Huntington, H.P., Danielson, S.L., Wiese, F.K., Baker, M., Boveng, P., Citta, J.J., De Robertis, A., Dickson, D.M.S., Farley, E., George, J.C., Iken, K., Kimmel, D.G., Kuletz, K., Ladd, C., Levine, R., Quakenbush, L., Stabeno, P., Stafford, K.M., Stockwell, D., Wilson, C., 2020. Evidence suggests potential transformation of the Pacific Arctic ecosystem is underway. Nat. Clim. Change 10, 342–348. https://doi.org/10.1038/s41558-020-0695-2

Janzen, C.D., McCammon, M., Danielson, S.S.L., Weingartner, T., Statscewich, H., Page, E., Heim, B., 2019. Innovative real-time observing capabilities for remote coastal regions. Front. Mar. Sci. 6, 1–8. https://doi.org/10.3389/fmars.2019.00176

Kaartvedt, S., Røstad, A., Klevjer, T.A., Staby, A., 2009. Use of bottom-mounted echo sounders in exploring behavior of mesopelagic fishes. Mar. Ecol. Prog. Ser. 395, 109–118. https://doi.org/10.3354/meps08174

Koenker, B.L., Copeman, L.A., Laurel, B.J., 2018. Impacts of temperature and food availability on the condition of larval Arctic cod (*Boreogadus saida*) and walleye pollock (*Gadus chalcogrammus*). ICES J. Mar. Sci. 75, 2370–2385. https://doi.org/10.1093/icesjms/fsy052

Kortsch, S., Primicerio, R., Fossheim, M., Dolgov, A. V., Aschan, M., 2015. Climate change alters the structure of arctic marine food webs due to poleward shifts of boreal generalists. Proc. R. Soc. B Biol. Sci. 282. https://doi.org/10.1098/rspb.2015.1546

Kotwicki, S., Buckley, T.W., Honkalehto, T., Walters, G., 2005. Variation in the distribution of walleye pollock (*Theragra chalcogramma*) with temperature and implications for seasonal migration. Fish. Bull., U.S. 103, 574–587.

Kotwicki, S., Lauth, R.R., Williams, K., Goodman, S.E., 2017. Selectivity ratio: A useful tool for comparing size selectivity of multiple survey gears. Fish. Res. 191, 76–86. https://doi.org/10.1016/j.fishres.2017.02.012

Kuletz, K., Cushing, D., Labunski, E., 2020. Distributional shifts among seabird communities of the northern Bering and Chukchi seas in response to ocean warming during 2017–2019. Deep Sea Res. Part II Top. Stud. Oceanogr. 181–182, 104913. https://doi.org/10.1016/j.dsr2.2020.104913

Laurel, B.J., Copeman, L.A., Spencer, M., Iseri, P., 2017. Temperature-dependent growth as a function of size and age in juvenile Arctic cod (*Boreogadus saida*). ICES J. Mar. Sci. 74, 1614–1621. https://doi.org/10.1093/icesjms/fsx028

Laurel, B.J., Spencer, M., Iseri, P., Copeman, L.A., 2016. Temperature-dependent growth and behavior of juvenile Arctic cod (*Boreogadus saida*) and co-occurring North Pacific gadids. Polar Biol. 39, 1127–1135. https://doi.org/10.1007/s00300-015-1761-5

Levine, R.M., De Robertis, A., Grünbaum, D., Woodgate, R., Mordy, C.W., Mueter, F., Cokelet, E., Lawrence-Slavas, N., Tabisola, H., 2020. Autonomous vehicle surveys indicate that flow reversals retain juvenile fishes in a highly advective high-latitude ecosystem. Limnol. Oceanogr. 9999, lno.11671. https://doi.org/10.1002/lno.11671

Logerwell, E., Busby, M., Carothers, C., Cotton, S., Duffy-Anderson, J., Farley, E., Goddard, P., Heintz, R., Holladay, B., Horne, J., Johnson, S., Lauth, B., Moulton, L., Neff, D., Norcross, B., Parker-Stetter, S., Seigle, J., Sformo, T., 2015. Fish communities across a spectrum of habitats in the western Beaufort Sea and Chukchi Sea. Prog. Oceanogr. 136, 115–132. https://doi.org/10.1016/j.pocean.2015.05.013

Lowry, K.E., Pickart, R.S., Mills, M.M., Brown, Z.W., van Dijken, G.L., Bates, N.R., Arrigo, K.R., 2015. The influence of winter water on phytoplankton blooms in the Chukchi Sea. Deep Sea Res. Part II Top. Stud. Oceanogr. 118, 53–72. https://doi.org/10.1016/j.dsr2.2015.06.006

Marsh, J.M., Mueter, F.J., 2020. Influences of temperature, predators, and competitors on polar cod (*Boreogadus saida*) at the southern margin of their distribution. Polar Biol. 43, 995–1014. https://doi.org/10.1007/s00300-019-02575-4

Matley, J.K., Fisk, A.T., Dick, T.A., 2012. Seabird predation on Arctic cod during summer in the Canadian Arctic. Mar. Ecol. Prog. Ser. 450, 219–228. https://doi.org/10.3354/meps09561

Mecklenburg, C., Lynghammar, A., Johannesen, E., Byrkjedal, I., Christiansen, J.S., Karamushko, O. V, Mecklenburg, T.A., Møller, P.R., Steinke, D., Wienerroither, R.M., 2018. Marine Fishes of the Arctic Region Volume II. CAFF Monitoring Series Report 20. Akureyri, Iceland: Conservation of Arctic Flora and Fauna.

Morris, B.A., 2019. Seasonality and forcing factors of the Alaskan Coastal Current in the Bering Strait from July 2011 to July 2012. M.S. thesis. University of Washington, Seattle WA. 82 p.

Mueter, F.J., Bond, N.A., Ianelli, J.N., Hollowed, A.B., 2011. Expected declines in recruitment of walleye pollock (*Theragra chalcogramma*) in the eastern Bering Sea under future climate change. ICES J. Mar. Sci. 68, 1284–1296. https://doi.org/10.1093/icesjms/fsr022

Norcross, B.L., Raborn, S.W., Holladay, B.A., Gallaway, B.J., Crawford, S.T., Priest, J.T., Edenfield, L.E., Meyer, R., 2013. Northeastern Chukchi Sea demersal fishes and associated environmental characteristics, 2009-2010. Cont. Shelf Res. 67, 77–95. https://doi.org/10.1016/j.csr.2013.05.010

O'Leary, C.A., Thorson, J.T., Ianelli, J.N., Kotwicki, S., 2020. Adapting to climate-driven distribution shifts using model-based indices and age composition from multiple surveys in the walleye pollock (*Gadus chalcogrammus*) stock assessment. Fish. Oceanogr. 29, 541–557. https://doi.org/10.1111/fog.12494

Orlov, A.M., Benzik, A.N., Vedishcheva, E.V., Gafitsky, S.V., Gorbatenko, K.M., Goryanina, S.V., Zubarevich, V.L., Kodryan, K.V., Nosov, M.A., Orlova, S.Y., Pedchenko, A.P., Rybakov, M.O., Sokolov, A.M., Somov, A.A., Subbotin, S.N., Taptygin, M.Y., Firsov, Y.L., Khleborodov, A.S., Chikilev, V.G., 2019. Fisheries research in the Chukchi Sea at the RV *Professor Levanidov* in August 2019: some preliminary results. Tr. VNIRO 178, 206–220. https://doi.org/10.36038/2307-3497-2019-178-206-220

Overland, J., Dunlea, E., Box, J.E., Corell, R., Forsius, M., Kattsov, V., Olsen, M.S., Pawlak, J., Reiersen, L.O., Wang, M., 2019. The urgency of Arctic change. Polar Sci. 21, 6–13. https://doi.org/10.1016/j.polar.2018.11.008

Ponomarenko, V.P., 2000. Eggs, larvae, and juveniles of polar cod *Boreogadus saida* in the Barents, Kara, and White seas. J. Ichthyol. 40, 165–173.

Quast, J.C., 1974. Density distribution of juvenile Arctic cod, *Boreogadus saida*, in the eastern Chukchi Sea in the fall of 1970. Fish. Bull., U.S. 72, 1094–1105.

Riera, A., Rountree, R.A., Pine, M.K., Juanes, F., 2018. Sounds of Arctic cod (*Boreogadus saida*) in captivity: A preliminary description. J. Acoust. Soc. Am. 143, EL317–EL321. https://doi.org/10.1121/1.5035162

Sigler, M.F., Mueter, F.J., Bluhm, B.A., Busby, M.S., Cokelet, E.D., Danielson, S.L., Robertis, A. De, Eisner, L.B., Farley, E. V., Iken, K., Kuletz, K.J., Lauth, R.R., Logerwell, E.A., Pinchuk, A.I., 2017. Late summer zoogeography of the northern Bering and Chukchi seas. Deep Sea Res. Part II Top. Stud. Oceanogr. 135, 168–189. https://doi.org/10.1016/j.dsr2.2016.03.005

Simmonds, J., MacLennan, D., 2005. Fisheries Acoustics: Theory and Practice, 2nd ed. Blackwell.

Spear, A., Napp, J., Ferm, N., Kimmel, D., 2020. Advection and in situ processes as drivers of change for the abundance of large zooplankton taxa in the Chukchi Sea. Deep Sea Res. Part II Top. Stud. Oceanogr. 177, 104814. https://doi.org/10.1016/j.dsr2.2020.104814

Spies, I., Gruenthal, K.M., Drinan, D.P., Hollowed, A.B., Stevenson, D.E., Tarpey, C.M., Hauser, L., 2020. Genetic evidence of a northward range expansion in the eastern Bering Sea stock of Pacific cod. Evol. Appl. 13, 362–375. https://doi.org/10.1111/eva.12874

Stabeno, P.J., Bell, S.W., 2019. Extreme conditions in the Bering Sea (2017–2018): Record-breaking low sea-ice extent. Geophys. Res. Lett. 46, 8952–8959. https://doi.org/10.1029/2019GL083816

Stabeno, P., Kachel, N., Ladd, C., Woodgate, R., 2018. Flow patterns in the eastern Chukchi Sea: 2010–2015. J. Geophys. Res. Ocean. 123, 1177–1195. https://doi.org/10.1002/2017JC013135

Stevenson, D.E., Lauth, R.R., 2019. Bottom trawl surveys in the northern Bering Sea indicate recent shifts in the distribution of marine species. Polar Biol. 42, 407–421. https://doi.org/10.1007/s00300-018-2431-1

Towler, R., Williams Kresimir, K., 2010. An inexpensive millimeter-accuracy electronic length measuring board. Fish. Res. 106, 107–111. https://doi.org/10.1016/j.fishres.2010.06.012

Vestfals, C.D.C.D., Mueter, F.J.F.J., Hedstrom, K.S.K.S., Laurel, B.J.B.J., Petrik, C.M.C.M., Duffy-Anderson, J.T.J.T., Danielson, S.L.S.L., 2021. Modeling the dispersal of polar cod (*Boreogadus saida*) and saffron cod (*Eleginus gracilis*) early life stages in the Pacific Arctic using a biophysical transport model. Prog. Oceanogr. 196, 102571. https://doi.org/10.1016/j.pocean.2021.102571

Wang, M., Yang, Q., Overland, J.E., Stabeno, P., 2018. Sea-ice cover timing in the Pacific Arctic: the present and projections to mid-century by selected CMIP5 models. Deep Sea Res. Part II Top. Stud. Oceanogr. 152, 22–34. https://doi.org/10.1016/j.dsr2.2017.11.017

Wassmann, P., Duarte, C.M., Agustí, S., Sejr, M.K., 2011. Footprints of climate change in the Arctic marine ecosystem. Glob. Change Biol. 17, 1235–1249. https://doi.org/10.1111/j.1365-2486.2010.02311.x

Weingartner, T., Dobbins, E., Danielson, S., Winsor, P., Potter, R., Statscewich, H., 2013. Hydrographic variability over the northeastern Chukchi Sea shelf in summer-fall 2008-2010. Cont. Shelf Res. 67, 5–22. https://doi.org/10.1016/j.csr.2013.03.012

Whitehouse, G.A., Aydin, K., Essington, T.E., Hunt, G.L., 2014. A trophic mass balance model of the eastern Chukchi Sea with comparisons to other high-latitude systems. Polar Biol. 37, 911–939. https://doi.org/10.1007/s00300-014-1490-1

Wietz, M., Bienhold, C., Metfies, K., Torres-Valdés, S., von Appen, W.-J., Salter, I., Boetius, A., 2021. The Polar Night Shift: Annual Dynamics and Drivers of Microbial Community Structure in the Arctic Ocean. bioRxiv 2021.04.08.436999. https://doi.org/10.1101/2021.04.08.436999

Woodgate, R.A., Peralta-Ferriz, C., 2021. Warming and freshening of the Pacific inflow to the Arctic from 1990-2019 implying dramatic shoaling in Pacific winter water ventilation of the Arctic water column. Geophys. Res. Lett. https://doi.org/10.1029/2021GL092528

Woodgate, R.A., Aagaard, K., Weingartner, T.J., 2005. A year in the physical oceanography of the Chukchi Sea: Moored measurements from autumn 1990-1991. Deep Sea Res. Part II Top. Stud. Oceanogr. 52, 3116–3149. https://doi.org/10.1016/j.dsr2.2005.10.016

Woodgate, R.A., Weingartner, T., Lindsay, R., 2010. The 2007 Bering Strait oceanic heat flux and anomalous Arctic sea-ice retreat. Geophys. Res. Lett. 37, 1–5. https://doi.org/10.1029/2009GL041621

Woodgate, R.A., 2018. Increases in the Pacific inflow to the Arctic from 1990 to 2015, and insights into seasonal trends and driving mechanisms from year-round Bering Strait mooring data. Prog. Oceanogr. 160, 124–154. https://doi.org/10.1016/j.pocean.2017.12.007

Wyllie-Echeverria, T., Wooster, W.S., 1998. Year-to-year variations in Bering Sea ice cover and some consequences for fish distributions. Fish. Oceanogr. 7, 159–170. https://doi.org/10.1046/j.1365-2419.1998.00058.x

Yasuma, H., Nakagawa, R., Yamakawa, T., Miyashita, K., Aoki, I., 2009. Density and sound-speed contrasts, and target strength of Japanese sandeel *Ammodytes personatus*. Fish. Sci. 75, 545–552. https://doi.org/10.1007/s12562-009-0091-3

3.8 SUPPLEMENTARY INFORMATION

3.8.1 *Supplementary figures and tables*

Supplementary Table 3.1 Linear models used to convert total length (TL) to standard length (SL), total length to fork length (FL), and standard length to fork length based on the different length measurements taken on the same fish specimen. Number of observations (n) and the range of lengths used to fit each model are included. All models were significant ($p<0.001$).

Species	X	Y	N	Length range in model (mm)	Intercept	Slope	R^2
Arctic cod	TL	SL	1055	18-189	0.364	0.909	0.999
	TL	FL	192	28-189	-0.137	0.967	0.999
	FL	SL	190	27-230	0.496	0.936	0.998
	SL	FL	190	28-230	-0.39	1.066	0.998
Pollock	TL	SL	103	41-108	1.135	0.902	0.996
	TL	FL	38	71-108	-0.636	0.991	0.997
	FL	SL	77	37-106	-1.711	0.948	0.997
	SL	FL	77	42-106	2.031	1.051	0.997
Saffron cod	TL	SL	195	17-268	-0.177	0.92	1
	TL	FL	18	106-222	-0.681	0.991	0.999
	FL	SL	42	54-260	-9.703	0.972	0.996
	SL	FL	42	68-260	10.755	1.025	0.996
Pacific cod	TL	SL	120	47-110	1.284	0.902	0.987
	TL	FL	0	N/A	N/A	N/A	N/A
	FL	SL	11	51-78	-0.663	0.952	0.97
	SL	FL	11	55-78	2.701	1.019	0.97

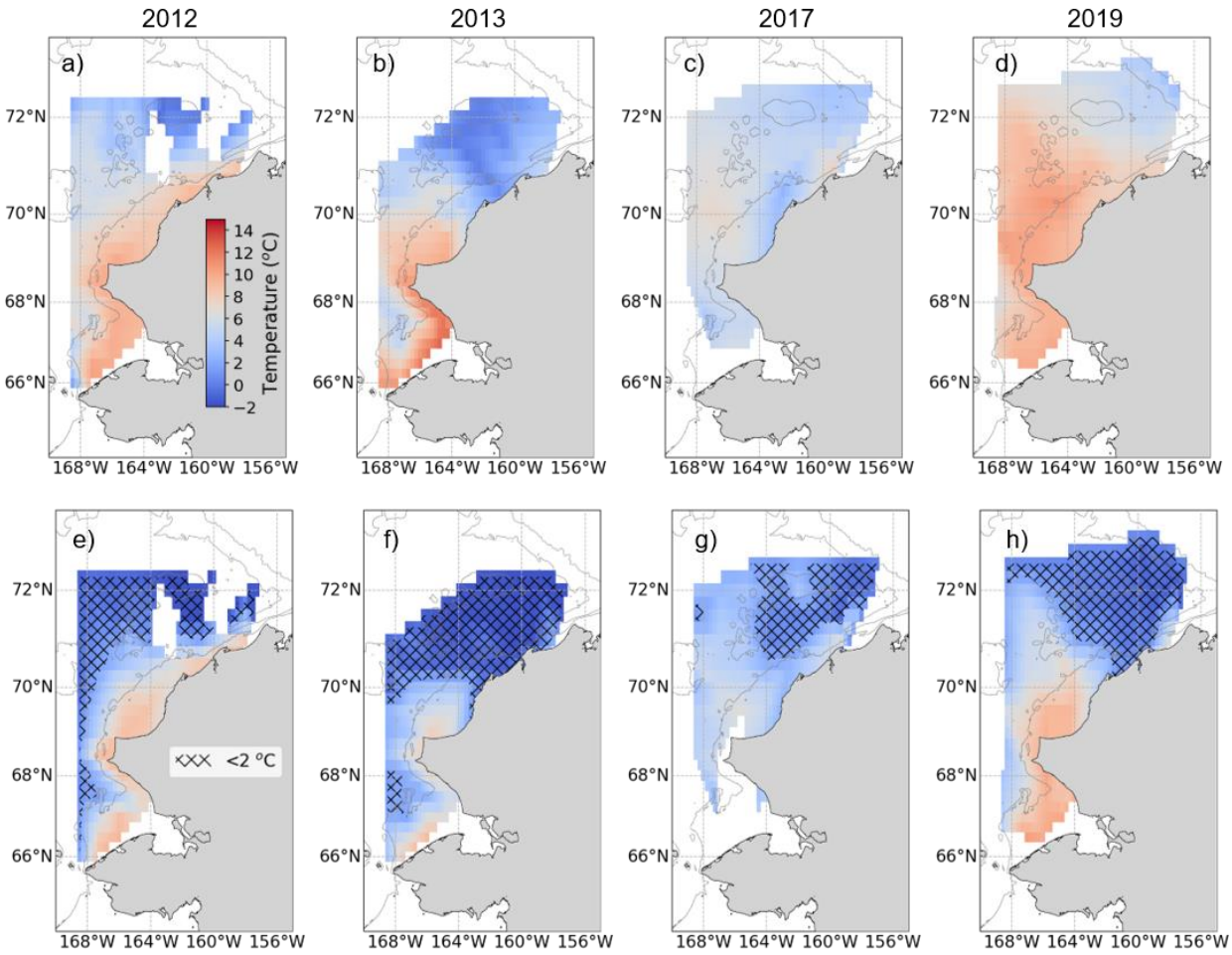

Supplementary Figure 3.1 Linearly interpolated mean surface (top row) and bottom (bottom row, see methods for details) temperatures observed in CTD casts in (a, e) 2012, (b, f) 2013, (c, g) 2017, and (d, h) 2019. Regions where bottom temperatures were <2 °C indicated by hatching.

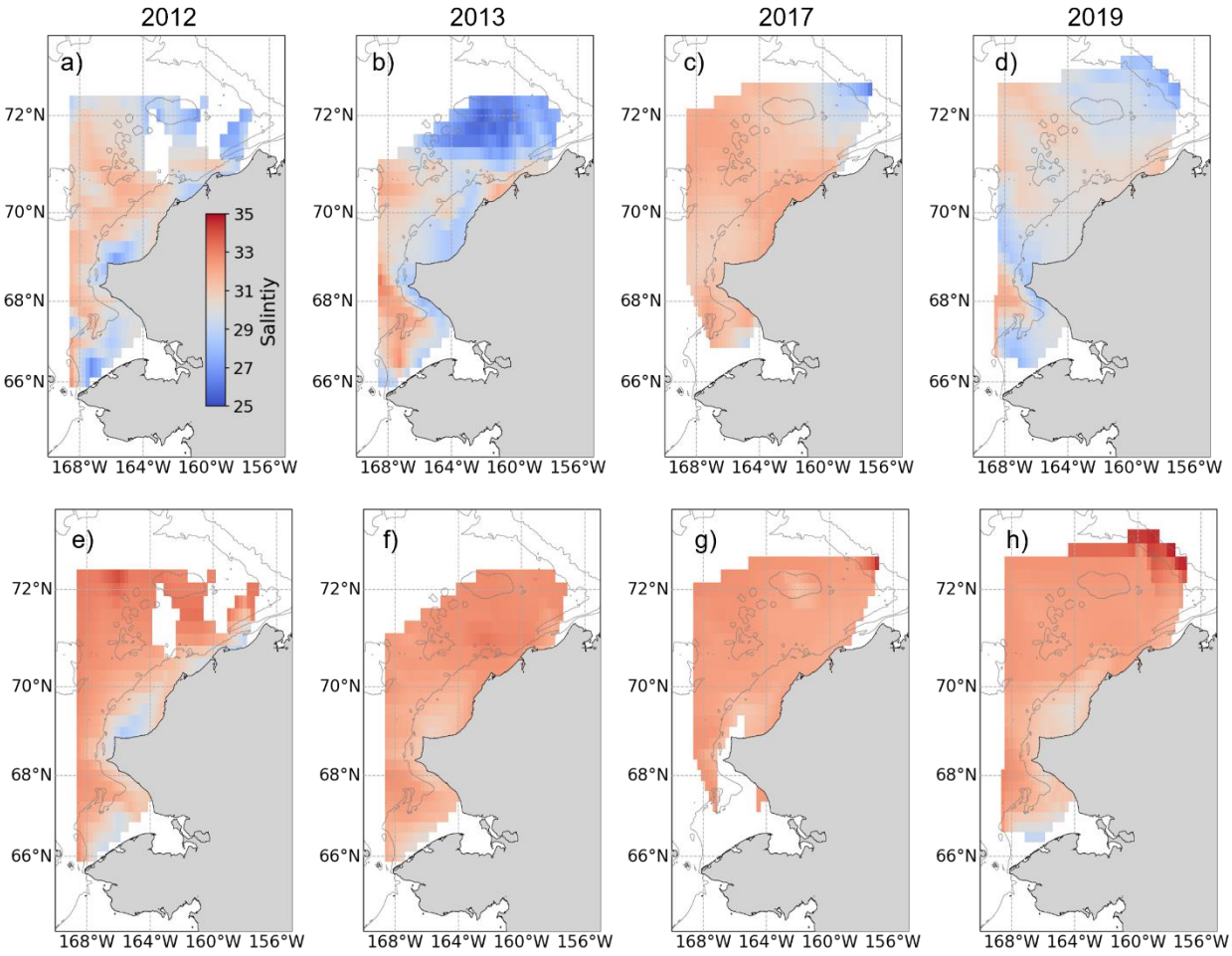

Supplementary Figure 3.2 Linearly interpolated mean surface (top row) and bottom (bottom row, see methods for details) salinities observed in CTD casts in (a, e) 2012, (b, f) 2013, (c, g) 2017, and (d, h) 2019.

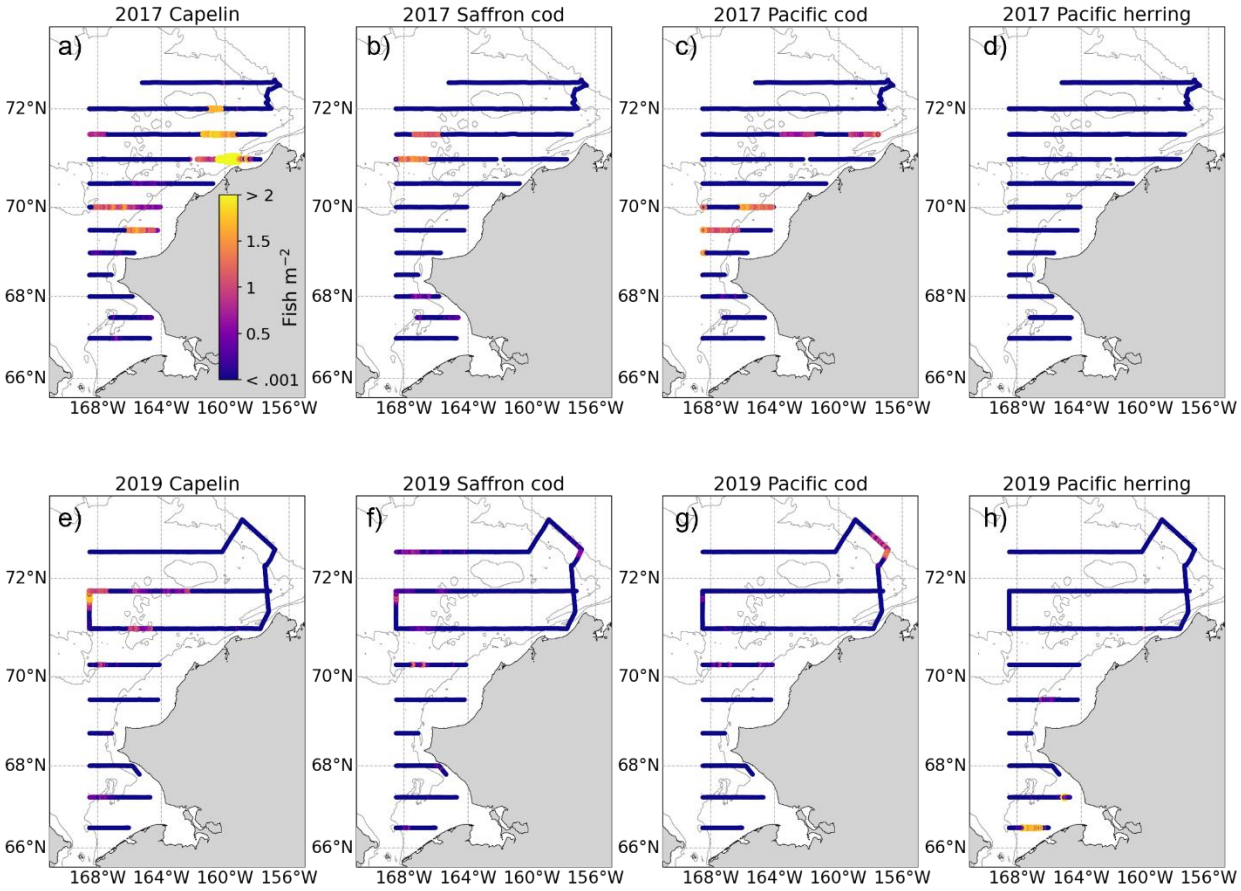

Supplementary Figure 3.3 Density (fish m^{-2}) of (a, e) capelin, (b, f) saffron cod, (c, g) Pacific cod, and (d, h) Pacific herring estimated by acoustic-trawl methods in 0.5 nmi along-track intervals in 2017 (top row) and 2019 (bottom row). The 40-, 100-, and 1000-m depth contours are shown.

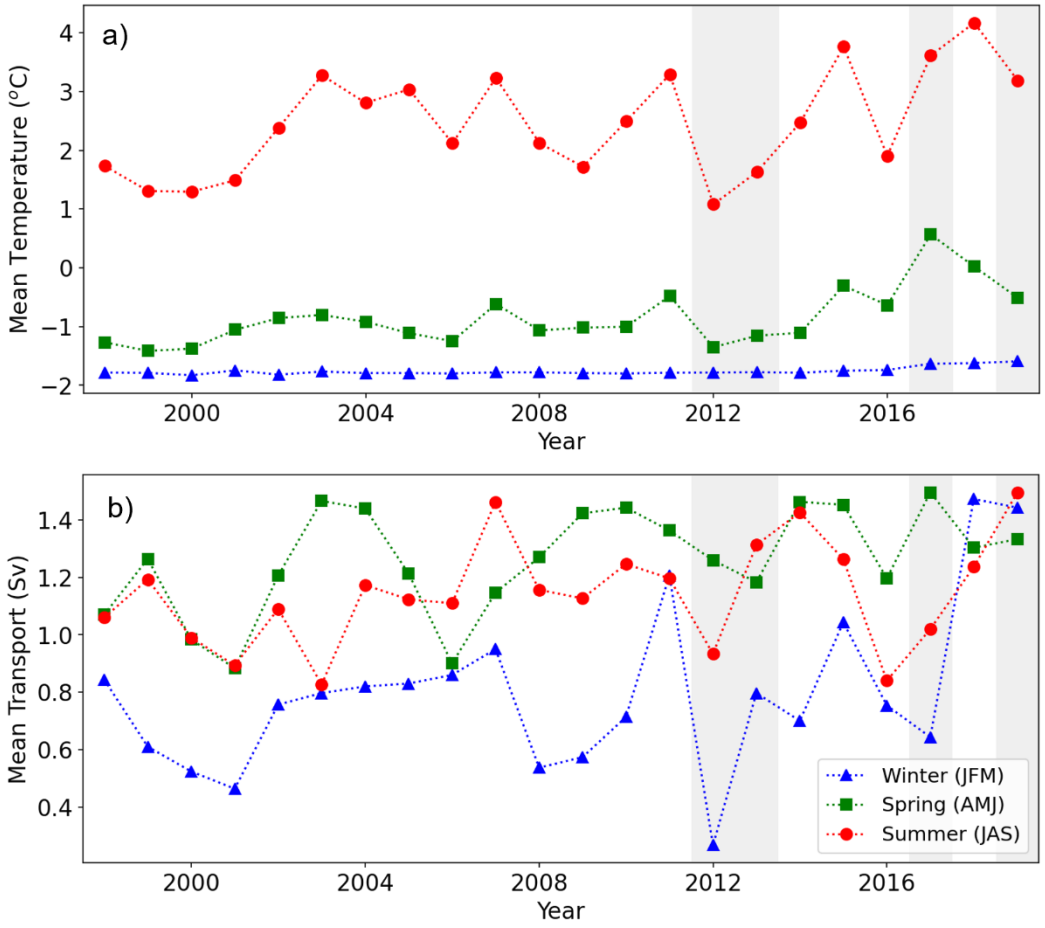

Supplementary Figure 3.4 Mean winter (January, February, March), spring (April, May, June) and summer (July, August, September) a) bottom temperature and b) transport observed at Bering Strait A3 mooring. The years of the acoustic-trawl surveys (2012, 2013, 2017, 2019) are indicated by the grey-shaded regions.

References

Woodgate, R.A., 2018. Increases in the Pacific inflow to the Arctic from 1990 to 2015, and insights into seasonal trends and driving mechanisms from year-round Bering Strait mooring data. Progress in Oceanography 160: 124-154, doi:10.1016/j.pocean.2017.12.007.

Woodgate, R.A., and C. Peralta-Ferriz, 2021. Warming and Freshening of the Pacific Inflow to the Arctic from 1990-2019 implying dramatic shoaling in Pacific Winter Water ventilation of the Arctic water column. Geophysical Research Letters, doi:10.1029/2021GL092528.

3.8.2 *Genetic correction of gadid species assignment*

Species identifications made during field sampling were modified based on the genetic verification of species identity described in Wildes et al. (in prep). In the midwater trawls, 40% of all gadid specimens (n = 2244) in 2017 and 56% of all fish specimens in 2019 (n = 5676) were genetically confirmed. Unverified specimens <24 cm in length were assigned to a species as a function of the gadid species proportion-at-length in each trawl as described below. In practice, only 59 specimens >10 cm in length were modified as a result of the model reassignment, which constitutes 0.3 % of all measured specimens. All fish >= 24 cm retained their species identification as determined in the field.

For a given trawl, the proportions of each of the five gadid species (*B. saida*, *G. chalcogrammus*, *E. gracilis*, *G. macrocephalus*, and *A. glacialis*) were determined from the genetically confirmed specimens. Proportions of each species were calculated for specimen grouped into the following length classes: 2 cm <= standard length (SL) < 4 cm, 4 <= SL < 6 cm, and 6 cm <= SL < 30 cm. The proportion (P) of a species s of length class l in trawl t was calculated from the number of genetically confirmed individuals (N) of species s of length class l from trawl t,

$$P_{s,t,l} = \frac{N_{s,t,l}}{\sum_s N_{s,t,l}}$$

For each specimen that was not genetically analyzed, a species was assigned based on the determined genetically identified proportions. For example, trawl t contains the following probabilities P for length class l: $P_{s_1,t,l} = 0.55$, $P_{s_2,t,l} = 0.25$, $P_{s_3,t,l} = 0.2$, $P_{s_4,t,l} = 0$, and $P_{s_5,t,l} = 0$. A value x is randomly generated where $0 < x \leq 1$. The specimen is assigned to species s based on the following conditions:

$$s = \begin{cases} s_1, & x \leq P_{s_1,t,l} \\ s_2, & P_{s_1,t,l} < x \leq P_{s_1,t,l} + P_{s_2,t,l} \\ & \dots \\ s_n, & P_{s_1,t,l} + P_{s_2,t,l} \dots P_{s_{n-1},t,l} < x \leq P_{s_1,t,l} + P_{2,t,l} \dots P_{s_n,t,l} \end{cases}$$

To evaluate the performance of the genetic reassignment model, the identity of all genetically identified specimens were predicted using a leave-one-out method. The identity of each individual was predicted based on the other genetically identified gadid specimens from the same trawl haul. The model-predicted species matched the genetic identification for >80% for individuals in both years. The allocation of acoustic backscatter from trawl data is based on the length distribution and the proportion of each species in the catch, thus the model was also evaluated based on the ability to predict the proportions of each gadid species in each trawl and the impact of reassignment on the length distributions of each species.

The model reassignment introduces a random element due to the probabilistic species assignment of the specimens which were not genetically identified. However, the average species compositions of gadids in a given haul after reassignment exhibited very little difference to those derived from the genetically identified specimens (Supplementary Figure 3.5). The mean of the absolute difference between the proportions of Arctic cod and pollock from only genetic specimens and all specimens for each haul was <5% in 2017 and <3% in 2019. The higher variability in 2017 is likely due to both a greater spatial overlap between species, and greater overlap in their size composition (Supplementary Figure 3.6) and a higher proportion of unconfirmed identifications than in 2019.

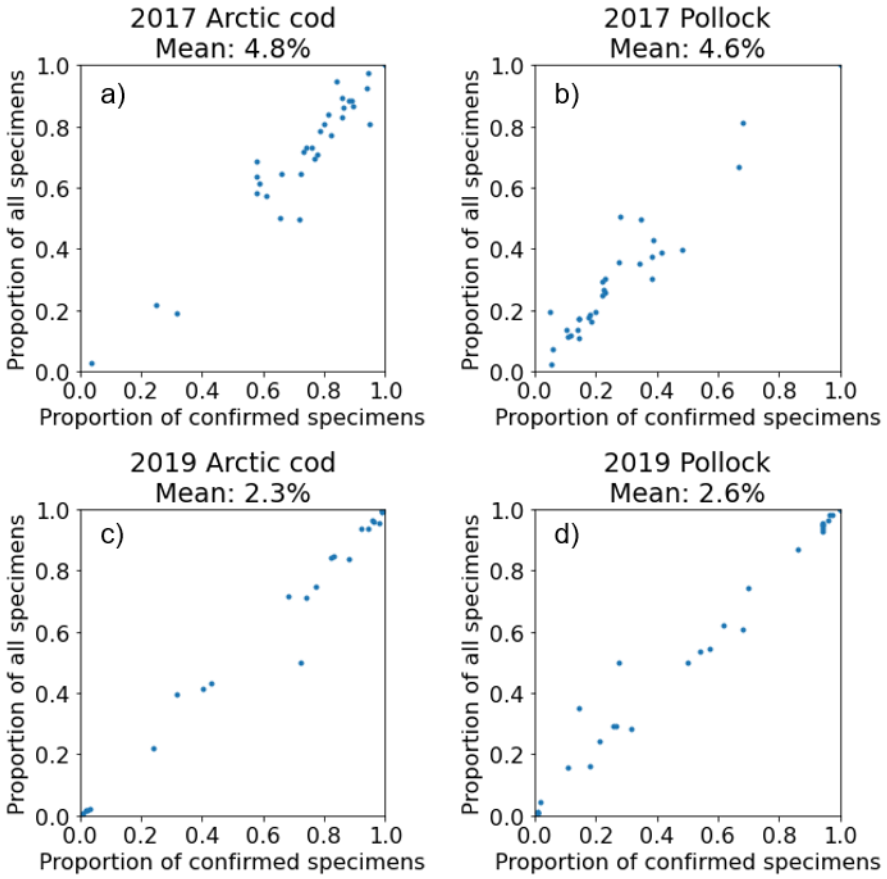

Supplementary Figure 3.5 Comparison of the proportion of (a, c) Arctic cod and (b, d) walleye pollock in each trawl determined from only the genetically confirmed specimens, and from all specimens after model reassignment. Mean absolute difference between the proportions from only genetic specimens and all specimens for each haul is indicated for each set of measurements.

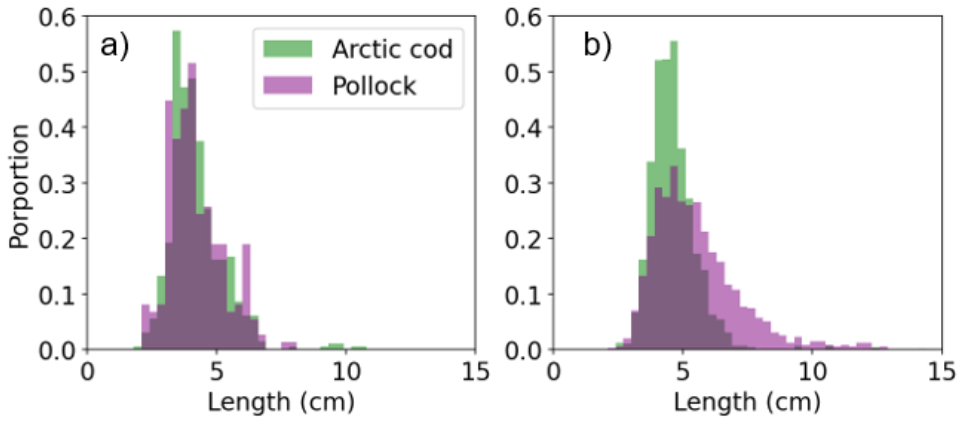

Supplementary Figure 3.6 Proportion at length of genetically identified Arctic cod and pollock in (a) 2017 and (b) 2019.

To quantify agreements in length between genetically identified versus all specimens, we calculated the two-sample Kolmogorov-Smirnov (KS) test between the known and model-assigned lengths for each gadid species in each trawl. The KS statistic was not significant in any trawls, indicating no significant differences between the length-frequency distributions between the genetically confirmed specimens and all specimens after model reassignment. Mean absolute differences between known and reassigned mean species length in each trawl haul were < 0.5 cm for both Arctic cod and pollock in both years (pollock: 0.43 in 2017 and 0.23 in 2019, Arctic cod: 0.07 in 2017 and 0.09 in 2019).

When catches were subsampled, total catch weights and abundances were modified based on the updated identifications of specimens to accurately reflect the final species composition in each trawl catch. This can introduce changes in the weight and number of individuals of a given species in a trawl haul due to the extrapolation from the measured subsamples to the total catch (Supplementary Figures 3.7 and 3.8). To evaluate the potential changes to the total catch resulting from species reassignments, total weight, total number, sampled weight, and sampled number of each gadid species in each trawl in both years were calculated from the original field assignments

and the genetically reassigned data. Changes to these measures as a result of reassignment were typically <0.5% (sum of the total number of gadid species present in each trawl in each year; n = 106 in 2017, n = 92 in 2019), with only 5 samples across both years showing changes in any of the metrics by >1% (Supplementary Figures 3.7 and 3.8). These errors were identified as a result of rounding errors for the mean weight of individuals (i.e., mean individual weights were assigned as 0.002 kg rather than 0.001 kg) introduced by the 0.001 kg precision used in the field collection database.

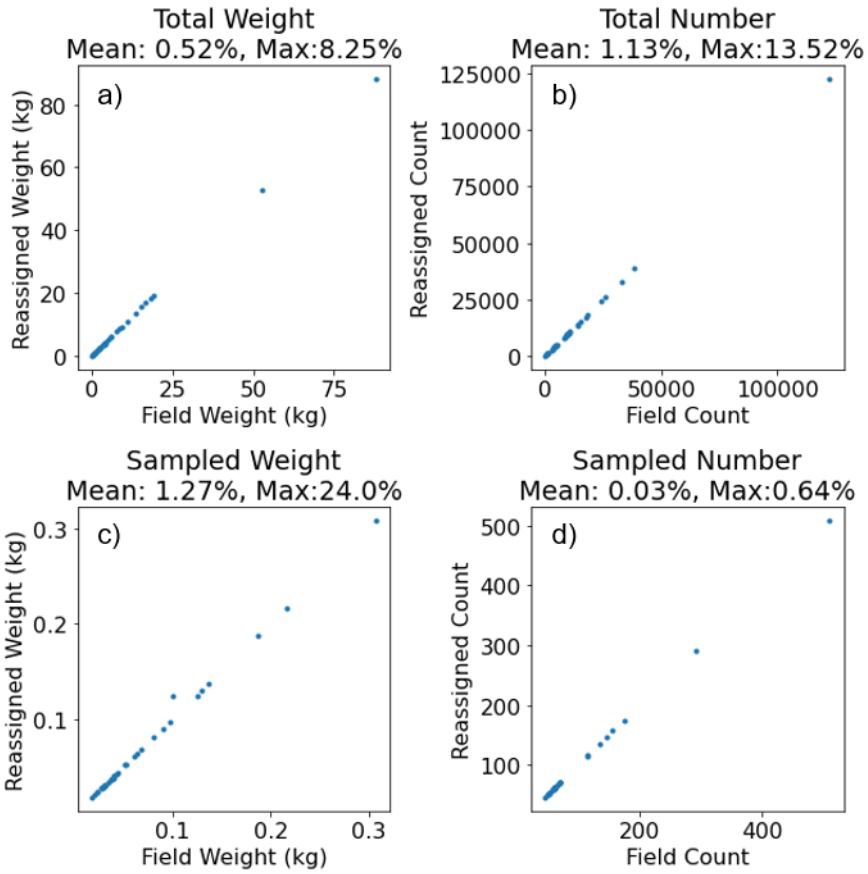

Supplementary Figure 3.7 Comparison of field and reassigned (a) total weight, (b) total number, (c) sampled weight, and (c) sampled number of gadids for all 2017 trawls. Each point represents the total for a single gadid species in a trawl. Mean and maximum values of the absolute difference between the field and reassigned values for each haul are indicated for each set of measurements.

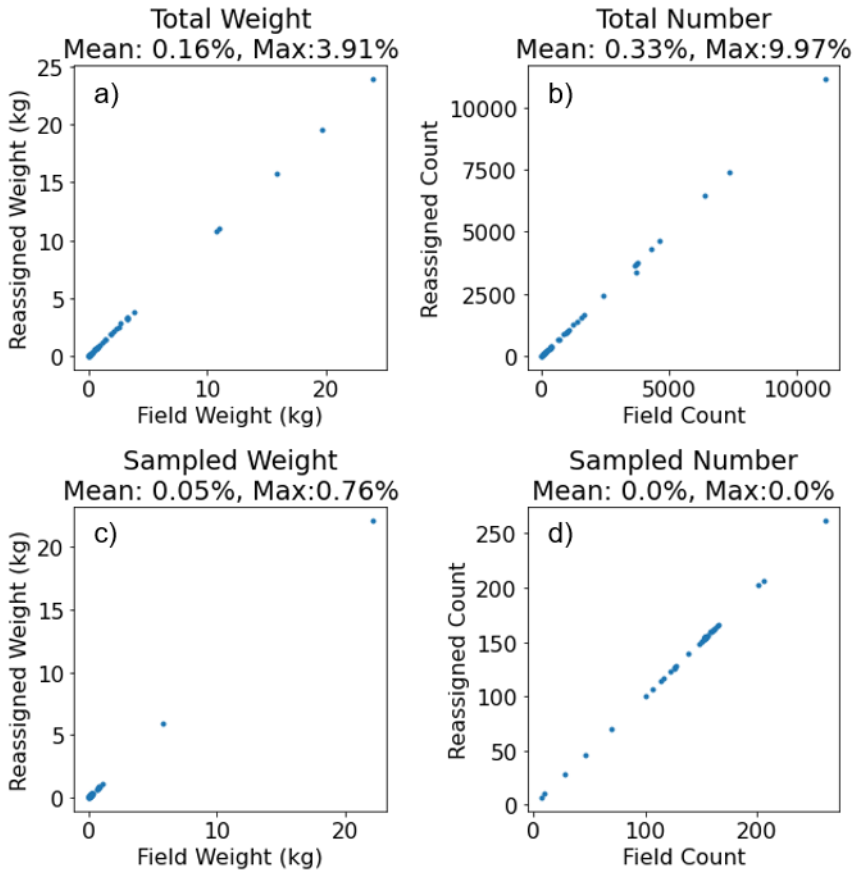

Supplementary Figure 3.8 Comparison of field and reassigned (a) total weight, (b) total number, (c) sampled weight, and (c) sampled number of gadids 2019 for all trawls. Each point represents the total for a single gadid species in a trawl. Mean and maximum values of the absolute difference between the field and reassigned values for each haul are indicated for each set of measurements.

CHAPTER 4. MULTI-YEAR AUTONOMOUS OBSERVATIONS OF SEASONALITY IN MOVEMENT, BEHAVIOR, AND GROWTH OF PELAGIC FISHES IN THE CHUKCHI SEA

4.1 ABSTRACT

Recent summer surveys of the Chukchi Sea determined that pelagic fishes were dominated by large numbers of age-0 Arctic cod and walleye pollock, while adult fishes were comparatively scarce. Particle tracking from a regional current model indicates that these age-0 fishes are likely advected to the north in fall. However, the source and fate of these fishes remains unclear, as sampling in this region is impeded by seasonal ice cover during much of the year. To determine the movement and seasonal variability of this age-0 gadid population, seafloor-moored echosounders were deployed at three locations in the northeastern Chukchi Sea from summer 2017 to summer 2019. These year-round observations indicate that the abundance and composition of the pelagic fish community on the Chukchi Sea shelf is highly variable on seasonal time scales. Fish abundance was very low in winter, increased in May, and reached peak abundance in late summer in both years. Fish tracking indicated that fish velocities and headings were strongly correlated with local currents. Two modes of fish (and current) direction were apparent; movement was primarily to the northeast with periodic reversals towards the southwest driven by changes in regional wind. The displacement of age-0 gadids to the northeast is consistent with the dominant patterns of advection on the shelf, and the flux of fishes indicates that a large portion of the pelagic fishes present on the Chukchi shelf in summer are transported to the northeast by fall. This strong advection likely explains the low abundances of age-1+ fishes in this environment.

4.1 INTRODUCTION

The Chukchi Sea is a highly seasonally dynamic region. This shallow continental shelf sea is covered by sea ice in late winter and spring before warm water from the south initiates the retreat of ice in spring (Woodgate et al., 2010) leading to a largely ice-free summer. Seasonal sea ice extent in the Chukchi has declined over recent decades (Frey et al., 2015) and is predicted to continue to decrease at a rate of 0.94 days $year^{-1}$ (0.11 – 1.55, Wang et al., 2018) as temperatures in the region continue to increase (Danielson et al., 2020). These changes are expected to alter the ecology of endemic Arctic fishes and enable further intrusion of boreal species, moving the southern boundary of Arctic species northward and altering composition of the local ecosystem (Mueter et al., 2021).

Age-0 gadids, particularly Arctic cod (*Boreogadus saida*), dominate the pelagic fish community on the Chukchi shelf in summer (De Robertis et al., 2017). Arctic cod is a circumpolar distributed species found throughout the Arctic basin and surrounding shelves (Mecklenburg et al., 2018). Arctic cod are common throughout the region (Lowry and Frost 1981; Rand and Logerwell 2011; De Robertis et al., 2017), where they are a key pelagic component of energy transfer between lower and upper trophic levels (Whitehouse et al., 2014). However, while large numbers of age-0 Arctic cod have been observed in the Chukchi in summer, adult fishes are comparatively scarce (De Robertis et al., 2017; Levine et al., in review). The observed density of adult Arctic cod does not have the reproductive potential to produce the population of age-0 fishes observed on the shelf in summer and thus these age-0 fishes likely originated elsewhere (Marsh et al., 2019). Arctic cod are known to spawn under sea ice (Ponomorenko et al., 2000). Although the source of these age-0 Arctic cod has not been confirmed, modeling studies of regional advection

indicate that these age-0 Arctic cod may originate in the southern Chukchi or northern Bering Seas in winter and early spring (Deary et al., 2021; Vestfals et al., 2021).

The composition of pelagic fishes is changing under present warming conditions. Boreal species such as walleye pollock (*Gadus chalcogrammus*) make up an increasing portion of the age-0 gadid community (Levine et al., in review; Wildes et al., in review). As a result of recent warming, the distribution of adult pollock in the Bering Sea has shifted, with high densities of mature adults in the northern Bering Sea (Stevensen and Lauth, 2019; Eisner et al., 202 Eggs and larvae from this northern Bering population are likely to be transported north along with the movement of water through Bering Strait (Woodgate et al., 2005). Thus, the age-0 pollock in the Chukchi Sea are hypothesized to originate from this large population of adult fishes south of Bering Strait (Levine et al., in review).

The Chukchi shelf is hypothesized to be an important nursery area for these age-0 fishes in summer (De Robertis et al., 2017; Levine et al., 2021), when relatively warm temperatures support high growth rates for both Arctic cod and pollock (Laurel et al., 2018). Such conditions are necessary to maximize growth prior to experiencing winter conditions. However, it remains unclear whether the abundant age-0 fishes observed in summer provide recruits to other areas or act as an ecological sink with fish not surviving through the winter (De Robertis et al., 2017). As development of age-0 gadids is largely temperature-dependent (Laurel et al., 2018), the potential fates of populations observed on the Chukchi shelf may depend on their movement into environments conducive to survival during winter. Identifying the mechanisms and pathways by which these fish are distributed across the Chukchi shelf will help to constrain the fate of this age-0 population and help predict how ongoing environmental changes may further alter their abundance and distribution in the region.

The Chukchi Sea serves as the pathway for Pacific water into the Arctic basin. Advection from the south structures the distribution of the planktonic communities in the Chukchi in summer (Eisner et al., 2013; Danielson et al., 2017; Pinchuk and Eisner, 2017; Spear et al., 2020). Northward currents are also hypothesized to exert a strong influence on the gadid populations, as larvae are likely passively transported (Vestfals et al., 2019; Vestfals et al., 2021). Repeat surveys in 2018 indicated that advection played a key role in the distribution of age-0 gadids on the Chukchi shelf in summer (Levine et al., 2021). Periods of on-shelf retention of the population were likely important for growth for these small fishes, prior to their being transported off the shelf towards the Beaufort Sea and Central Arctic Basin in fall (Levine et al., 2021). While modeling studies based on summer distributions have hypothesized the passive northward movement of fishes (Deary et al., 2021; Vestfals et al., 2021), there are no direct observations to validate whether the large age-0 population observed in summer is transported to other areas or if this region serves as a sink with fishes failing to survive through winter conditions. If advection is the primary mechanism of, measurements or model predictions of currents provide opportunities to predict changes in distribution of these age-0 fishes on the Chukchi shelf.

Historically, direct observations of fishes in ice covered areas have been rare. Because access to ice-covered areas is limited and traditional trawling gear cannot be used, sampling has been restricted in spatial and temporal extent (Lønne and Gulliksen, 1989; Gradinger and Bluhm, 2004; Melnikov and Chernova, 2013). To monitor fishes during periods of ice cover, acoustic observations of pelagic fishes have been collected from ships (Benoit et al., 2008) and autonomous underwater vehicles operating under sea ice (Fernandes et al., 2003). Net systems designed to sample in ice have made it easier to collect specimens under sea ice over a greater area (Flores et al., 2012; David et al., 2016). However, these methods are logistically difficult and expensive.

Winter surveys rely on ships with ice-strengthened hulls to provide access to areas that are seasonally inaccessible, and the deployment of autonomous platforms or net systems in ice-covered areas is typically limited to a few discrete locations and relatively short periods of time.

In contrast, in seasonally ice-covered regions, moored instrumentation can be deployed during the ice-free period and left to collect data year-round. In these seasonal ice zones, acoustic doppler current profilers (Wallace et al., 2010) and echosounders (Miksis-Olds et al., 2013; Darnis et al., 2017; Kitamura et al., 2017; Gonzalez et al., 2021) have used acoustic observations to study zooplankton and fish presence during extended periods of ice cover. However, moorings have not been previously used to collect long-term observations of fish movements through ice-covered regions. Moored echosounders can be used to collect continuous data to study fish abundance and swimming behavior (Trevorrow, 2005; Kaartvedt et al., 2009; Urmy et al., 2012; Ross et al., 2013; De Robertis et al., 2018). Detection of individual scatterers from split-beam observations can also be used to infer the size composition, transport, and behavior of fishes from moored platforms. While acoustic observations offer limited capacity to identify sound-scattering organisms, in low-diversity regions where backscatter is dominated by a single species or group, moorings can be used to infer information about the population as the primary sound scatterers known and interpretation of the acoustic signal is less dependent on the collection of biological samples. For example, if the species of the primary scatterers is known, length can be inferred from acoustic target size using established target strength to length regressions (Traynor, 1996; Geoffroy et al., 2016). The positions of fish tracked over successive pings can be used to infer swimming speed and direction (Ehrenberg and Torkelson, 1996).

This study presents two years of near-continuous observations of age-0 gadids collected by seafloor-mounted echosounders at three sites in the northeastern Chukchi Sea. The primary

objectives of this study were to characterize the seasonal patterns in pelagic fish abundance in the Chukchi Sea, and to determine the role of advective transport and fish behavior in the movement of age-0 gadids. Year-round observations enabled us to resolve the timing and seasonal dynamics of the pelagic ecosystem, helping to constrain the potential spawning region and determine the fate of the large juvenile population of fishes present during the summer months.

4.2 METHODS

4.2.1 *Mooring deployments*

Three moorings were deployed in the northeastern Chukchi Sea in locations where fish densities had previously been observed to be high in summer (De Robertis et al., 2017). The moorings were deployed for two years at 71.03N 160.50W (49 m depth, hereafter referred to as northern), 70.83N 163.11W (44 m depth, hereafter referred to as central), and 70.01N 166.85W (47 m depth, hereafter referred to as southern) (Figure 4.1). The moorings were initially deployed between 08-15 August 2017, recovered and redeployed between 12-15 August 2018 after data recovery and maintenance, then finally recovered between 26 August and 05 September 2019.

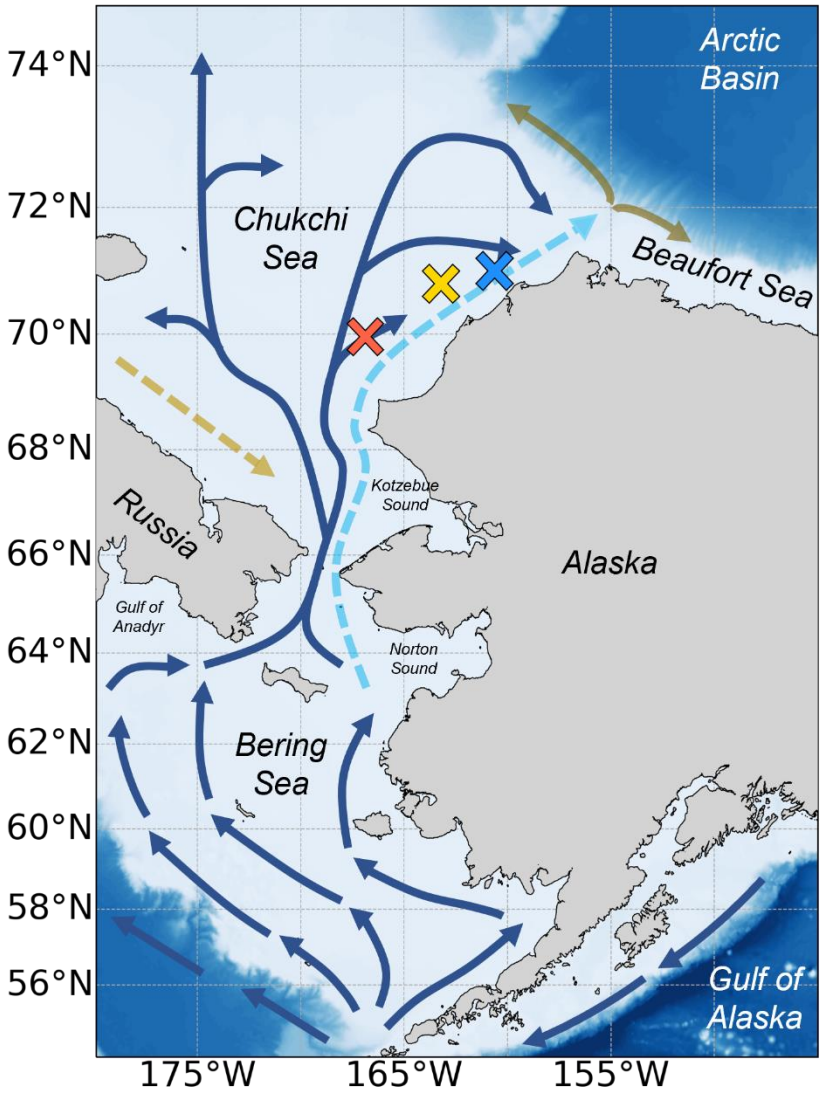

Figure 4.1 Map of the study region. The locations of the southern (red), central (yellow), and northern (blue) mooring sites are indicated by an x. The primary annual mean transport pathways through the Bering and Chukchi Seas identified in Weingartner et al. (2005) and Corlett and Pickart (2017) are shown: Alaskan Coastal Current (light blue), Bering Sea water (dark blue), Siberian Coastal Current (yellow), slope current (brown, westward) and shelf break jet (brown, eastward). Dashed lines indicate seasonal currents.

4.2.2 *Composition of acoustic scatterers*

The Chukchi Sea is well-suited for the use of autonomous acoustics. The low diversity pelagic community of the Chukchi shelf simplifies the process of making biological inferences from backscatter measurements. Acoustic-trawl surveys in the northeastern Chukchi Sea in 2012 and 2013 identified age-0 Arctic cod as the primary sound scatterers (De Robertis et al., 2017). Recent surveys during the mooring deployment period in summer 2017 and 2019 similarly found that age-0 gadids, particularly Arctic cod and walleye pollock, were the dominant pelagic scatters, accounting for 94.3% and 88.3% of the 38 kHz backscatter in 2017 and 2019, respectively (Levine et al., in review). Genetic analyses have confirmed that the increase in the proportion of pollock within the gadid community appears to have occurred during the period of these surveys (Wildes et al., in review). Thus, walleye pollock were likely present throughout our 2017-2019 deployment period. Other strong sound scattering pelagic fishes such as capelin (*Mallotus villosus*) and Pacific herring (*Clupea pallasii*) were present in trawls only in comparatively low abundances and accounted for < 6% of backscatter during summer surveys in both 2017 and 2019 (Levine et al., in review). Therefore, we assume that the primary contributors to backscatter were age-0 gadids, and that acoustic-based measures of fish density reflect the abundance and distribution of age-0 Arctic cod and walleye pollock combined.

4.2.3 *Mooring Instrumentation*

The mooring platforms were designed to be low profile to maximize the range of water column sampled by the echosounder, and to minimize the likelihood of damage due to sea ice. Each mooring was composed of two stacked 1.2 by 1.8 m fiberglass grates, separated with 0.2 m spacers (Supplementary Figure 4.1). The moorings were anchored to the seafloor by four 23 kg lead feet, one positioned on each corner. The feet were replaced with 18 kg steel discs during the second

year of deployment to reduce the mooring weight in order to increase the safety margin during recovery. Each mooring contained two acoustic release pop-up recovery packages (EdgeTech PORT-MFE) with 100 m of recovery line connecting a hoist point on the mooring to a 15 cm diameter syntactic foam-filled float. All scientific instrumentation was mounted to the upper grate (Supplementary Figure 4.1).

The moorings were instrumented with battery-powered scientific echosounders (wideband autonomous transceiver, Simrad AS). Each echosounder operated an upwards-facing 70 kHz 18° split-beam transducer (ES70-18CD), positioned upward in a two-axis gimbal equipped with a 0.7 kg counterweight. Each echosounder also operated a combined 38 kHz 18° split-beam and 200 kHz 18° single-beam transducer (ES38-18/200-18C) mounted to the grating without a gimbal. Both transducer faces were positioned at a height of 0.8 m above the seafloor. During the deployment, the echosounders transmitted an ensemble of 300 pings (200 pings at 70 kHz, 100 pings at 38 and 200 kHz) at a ping rate of 0.4 s every two hours. Data were recorded to a range of 60 m. The echosounders were calibrated at the surface using a 38.1-mm tungsten carbide sphere, following the standard sphere method (Demer et al., 2015; Renfree et al., 2019). Echosounders used in 2017-2018 were calibrated prior to deployment. The echosounders used in 2018-2019 were calibrated following their final recovery, because the transducers recovered in summer 2018 were immediately redeployed. Due to a post-recovery instrument failure, the echosounder and transducer deployed at the southern mooring site could not be calibrated. The average gains of the five other instrument calibrations were used for data processing along with the factory-specified beamwidth. The average gains for each frequency were 19.12 (±0.80 SD) dB at 38 kHz, 19.98 (±0.86 SD) dB at 70 kHz, and 17.98 (±0.55 SD) dB at 200 kHz. These calibrations did not account for potential pressure effects; however preliminary field experiments using the ES70-18CD

transducer indicate that targets strength observations vary by <1.2 dB at depths of up to 100 m transducer depth (De Robertis, unpublished).

To determine the heading of the transducers when settled on the seafloor, each mooring was deployed with a calibrated compass mounted at a fixed position aligned with the forward direction of the transducers. Deployments used either a custom underwater magnetometer produced by the Engineering Development division of the NOAA Pacific Marine Environmental Lab or an Aaronia GPS Logger (Aaronia AG) sealed in a custom waterproof PVC pressure housing. Measurements were recorded for 0.3 - 385 days of each deployment due to variability in the battery life of each compass. Compasses in four deployments recorded for > 295 d, during which the hourly mean headings varied by < 5° (Supplementary Figure 4.2). These long-duration compass recordings confirmed that mooring orientations were stable throughout the deployment. The mode of all observations collected after deployment, corrected for magnetic declination at each site, was used to represent the mooring orientation (Table S4.1).

4.2.4 *Acoustic data processing*

Acoustic data were recorded from 8 August 2017 to 26 August 2019 at the southern site, 9 August 2017 to 4 September 2019 at the central site, and 15 August 2018 to 5 September 2019 at the northern site. Data were not available for the northern mooring site for the 2017-2018 deployment as a result of instrument failure. In addition, the 38 kHz channel at the central mooring site failed during the 2018-2019 deployment. Thus, only the 70 and 200 kHz data were included in analyses. Due to interference (likely from side-lobe reverberation) appearing at 16-20 and 27-30 m depth at 200 kHz at the central mooring site during the 2018-2019 deployment, only data within those ranges where the signal was 10 dB higher than the observed noise level were included.

Acoustic data were processed using Echoview 12.0 (Echoview Software Pty Ltd). The 70 kHz backscatter was used as a proxy for fish abundance. The depth of the sea surface/ice echo was determined by Echoview's threshold offset operator with a minimum detection threshold of -50 dB re 1 m^{-1} below the surface/ice, and manually corrected after visual inspection. The nautical area backscattering coefficient (s_A, m^2 nmi^{-2}; MacLennan et al., 2002) for all frequencies were integrated in 1-m bins from 2 m above the transducer to 2 m below the sea surface/ice echo for every 2-h ensemble. The weighted mean depth ("centre of mass" in Urmy et al., 2012, their Table 1) of s_A was calculated for each ensemble. To investigate seasonality of diel vertical migration, the difference between the weighted mean depth of fishes at maximum and minimum solar altitude was calculated, determined as a function of datetime and location using the Pysolar library for Python (http://pysolar.org/).

The strength of backscatter across frequencies varies as a function of animal scattering properties (reviewed in Benoit-Bird and Lawson, 2016) and can be used to differentiate among key groups of scatterers (Jech and Michaels, 2006; De Robertis et al., 2010). Higher backscatter at 200 kHz than at 70 kHz is indicative of scattering from zooplankton, while gadids exhibit higher scattering at 70 kHz than at 200 kHz (De Robertis et al., 2010). To investigate potential changes in the composition of acoustic scatterers over the length of the deployment, the difference between the mean 70 kHz and 200 kHz S_v ($\Delta S_{v,70\text{-}200}$, dB) for each ensemble was calculated to infer dominant scatterer type.

4.2.5 *Fish tracking and flux estimates*

Echoes from individual fishes were identified with Echoview's split-beam single target detection (method 2), using a detection threshold of -70 dB re 1 m^2. To minimize the potential bias due to overlapping targets being interpreted as a single fish, single target detection was limited to portions

of the water column where density was low. The average number of animals per reverberation volume (Nv, Sawada et al., 1993) was calculated in 5-m vertical bins for each ensemble using a target strength of -55.5 dB re 1 m^2 (Geoffroy et al., 2016), which assumes a mean Arctic cod size of approximately 4.5 cm consistent with the size of fishes observed in surveys in 2017 and 2019 (Levine et al., in review). Single targets in grid cells where Nv > 0.04 were excluded as recommended by Sawada et al. (1993). Single targets were joined into individual fish trajectories using Echoview's 4D alpha-beta tracker (Blackman, 1986; see Table S4.2 for parameters used in this study). A minimum of 5 single targets from a single individual was required to classify a track, with a maximum gap of 5 pings (2 s). The mean target strength (TS, dB re 1 m^2) of each tracked fish was calculated as the mean TS of the single targets contained in each track, calculated from the mean of the linear TS values (σ_{bs}, m^2). Fish headings were calculated by fitting a linear model with respect to time for the x, y, and z positions of the single target detections assigned to each fish track. The model positions at the first and last time point of each track were used to calculate speed and heading. Headings were converted from a coordinate system relative to the transducer into a geographic reference frame based on the compass orientation.

Speed was calculated by dividing the total distance along the model-fit linear track by the duration of the track. In addition to representing the net displacement of tracks through the acoustic beam, the use of the linear model also reduced range-dependent errors associated with the angular resolution of split-beam transducers. As range increases, angular errors as a result of the discrete resolution in the acoustic data correspond to greater increases in the calculated physical distance between targets, resulting in a range-dependent increase in track speed (Klevjar and Kaartvedt, 2003). This bias was reduced by using a linear model compared with a B-spline or similar curve

fitting representations, for tracks in which the distance between control points is likely to be affected by such angular errors (Supplementary Figure 4.3).

Fish density (fish m^{-2}) was calculated at each ensemble using the mean of the observed linear target strengths (σ_{bs}, m^2) and s_A following MacLennan et al. (2002). The flux of fish (Q, fish m^{-1} s^{-1}) was estimated using the fish density (A) and mean speed and direction of tracks during each ensemble, such that:

$$Q = AV \tag{4.1}$$

Velocity (V) was calculated along the dominant direction of movement, defined as the mode of track headings (in 5° bins) for all tracks observed at each site (hereafter referred to as the reference heading). Thus, flux represents the number of fishes per second in the entire water column crossing underneath a 1 m line of the sea surface perpendicular to the reference heading.

4.2.6 *Environmental data*

Bottom temperature and salinity were measured using a conductivity, temperature, and depth (CTD, Sea-Bird SBE-37) sensor mounted on each mooring. Hourly current measurements were derived from acoustic doppler current profilers (ADCP, Teledyne RD Instruments WorkHorse operating at either 300 or 600 kHz varying by site and year) deployed <500 m away from the echosounder moorings (see Stabeno et al., 2018 for a description of ADCP data processing). To investigate the relationship between currents and fish tracks along a uniform direction, current velocities relative to the reference heading were calculated from the zonal (east-west) and meridional (north-south) components of each depth bin. Fish tracks were matched with the closest ADCP measurement in time and depth.

Sea ice concentrations were obtained from the NOAA/NSIDC Climate Data Record of Passive Microwave Sea Ice Concentration, Version 3 (Peng et al., 2013; Meier et al., 2017). Daily

measurements were extracted from the 25 by 25 km grid cell that contained each mooring site. The NCEP/NCAR reanalysis (Kalnay et al., 1996) wind forecasts were used to estimate the wind speed and direction. Near-surface (0.995 sigma level) values of zonal and meridional wind, available in 6-h intervals, were obtained from the 2.5° grid cell nearest to each mooring. Wind velocities were calculated along the mode of wind direction over the course of the deployment (65°).

4.3 RESULTS

4.3.1 *Seasonal characteristics of acoustic scatterers*

Backscatter was highest during the late-summer and early fall, decreasing in winter and then increasing the following June/July across all sites during both years of deployment (Figure 4.2). Backscatter was lowest in early spring in all deployments. In early summer of 2018 and 2019, high backscatter first developed in the upper water column, deepening over the course of the summer (Figure 4.2a-c), indicating that the fish increased their depth distribution in summer.

Strong seasonal variability in pelagic community composition is demonstrated by the difference in volume backscatter observed at 70 and 200 kHz ($\Delta S_{v,70\text{-}200}$, Figure 4.3). In late winter and spring, $\Delta S_{v,70\text{-}200}$ is consistent with zooplankton-like scatterers at all three sites (blue regions, Figure 4.3). Fish-like scatterers (red regions, Figure 4.3) appear concurrently with the increase in backscatter in early summer (Figure 4.2). The highest backscatter occurs during periods when $\Delta S_{v,70\text{-}200}$ indicates that the backscatter is dominated by fish-like scatterers ($\Delta S_{v,70\text{-}200}$ > -5 dB, Figure 4.4), consistent with previous survey observations of small fishes dominating pelagic backscatter in summer (De Robertis et al., 2017; Levine et al., in review). Thus analyses presented below interpreted s_A as a proxy for the abundance of pelagic fishes (as described in the methods above).

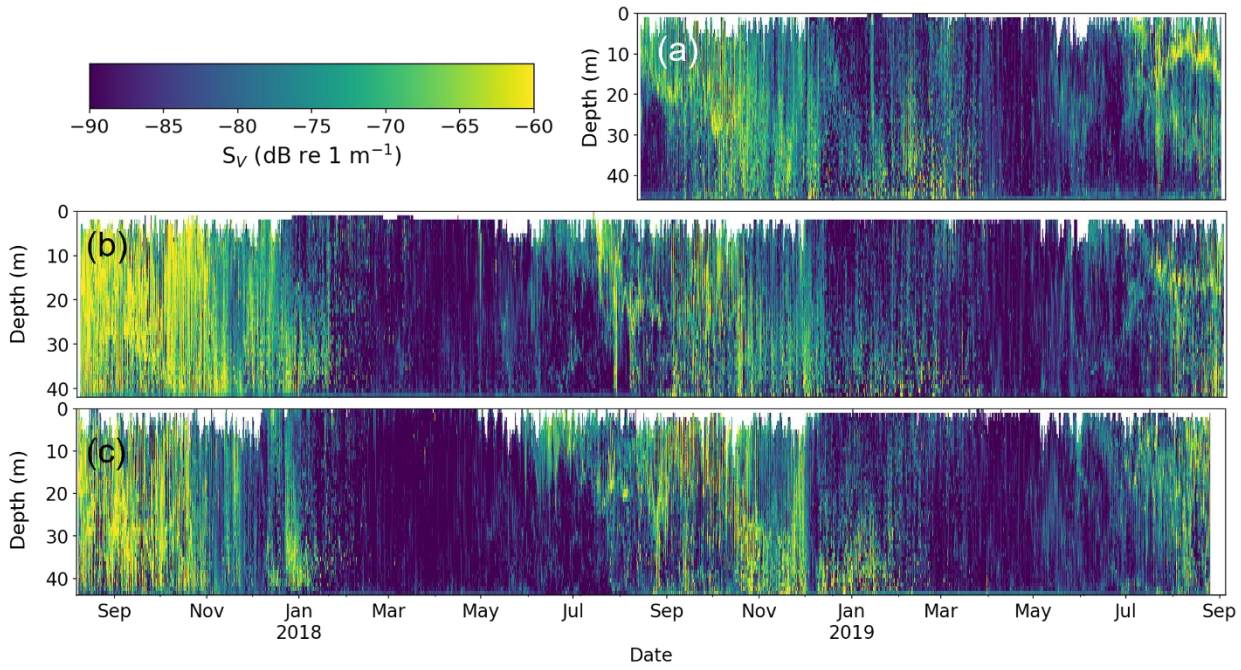

Figure 4.2 Echogram of 70 kHz backscatter (S_v, dB re 1 m^{-1}) recorded during each 2-h ensemble from 7 August 2017 to 06 September 2019 at the (a) northern, (b) central, and (c) southern mooring. Each point represents the mean of all observations in a 1 m depth bin of the water column recorded every 2 hours. White portions of the echogram indicate areas where backscatter from the sea surface and/or sea ice have been removed.

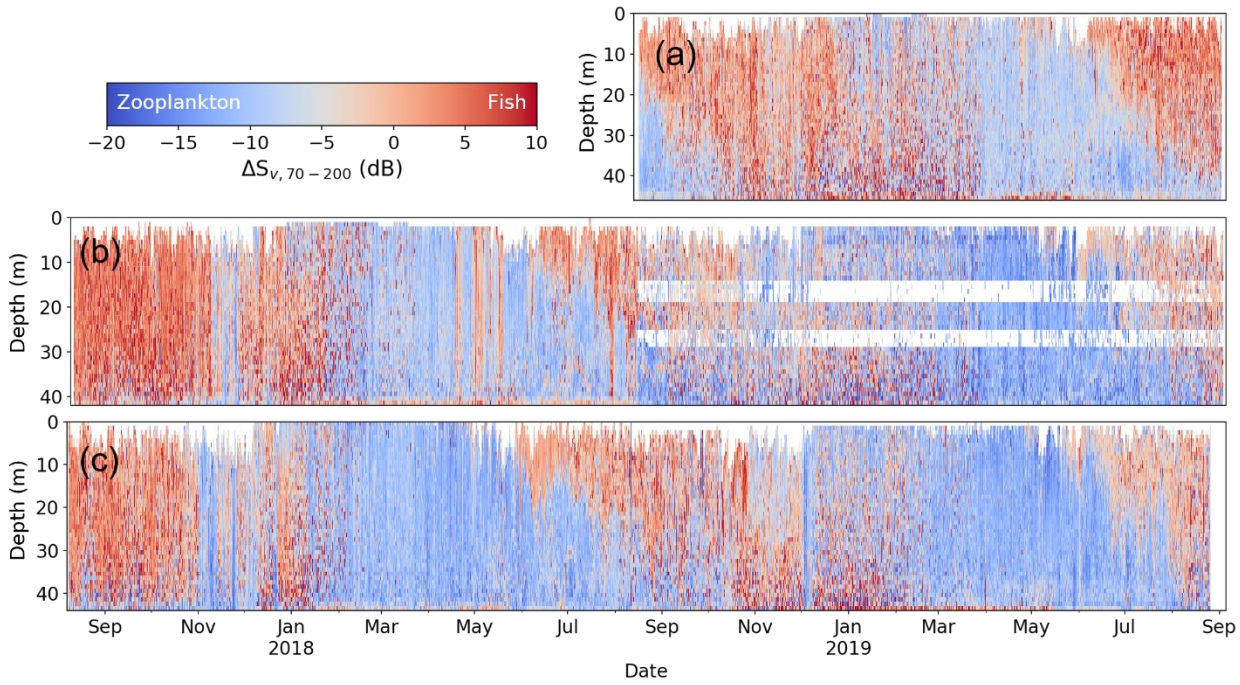

Figure 4.3 Echogram of difference between 70 kHz and 200 kHz volume backscatter ($\Delta Sv_{,70-200}$, dB) for the complete time series at the (a) northern, (b) central, and (c) southern mooring. Red indicates bins where Sv is greater at 70 kHz (fish-like scatterers) and blue indicates bins where sA is greater at 200 kHz (zooplankton-like scatterers). Each point represents the mean of all observations in a 1 m depth bin of the water column recorded every 2 hours. White portions of the echogram indicate areas of no data due to the removal of backscatter from the sea surface and ice. Due to interference between 16-20 and 27-30 m depth at 200 kHz at the central site during the 2018-2019 deployment, data where the signal was <10 dB higher than the noise level were removed (see methods).

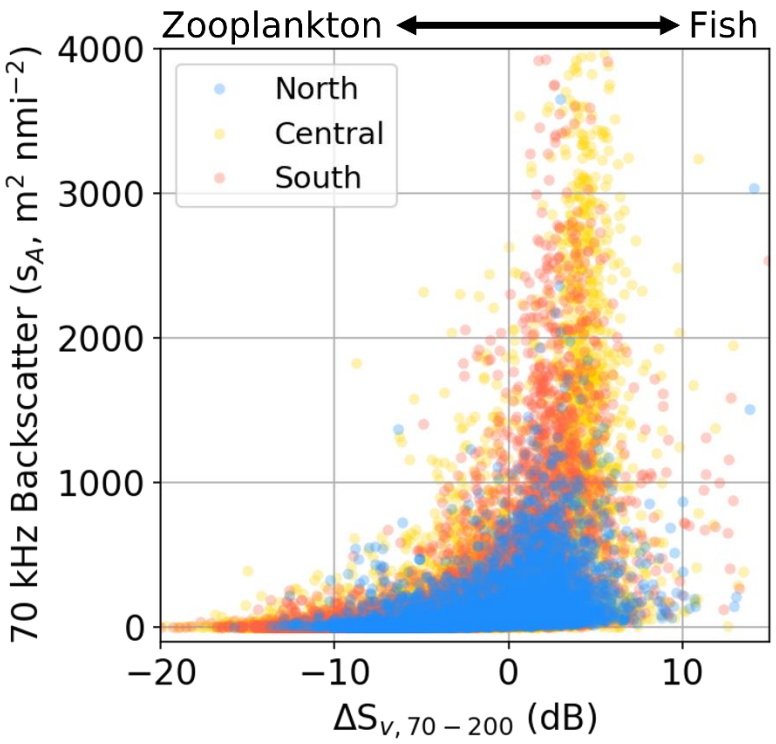

Figure 4.4 Daily mean 70 kHz backscatter (s_A, m^2 nmi^{-2}) as a function of the mean difference between 70 kHz and 200 kHz volume backscatter ($\Delta S_{v,70\text{-}200}$, dB) for each ensemble at the northern (blue), central (yellow), and southern (red) mooring sites. Higher ΔS_v values are consistent with backscatter dominated by fishes.

4.3.2 *Seasonal changes in fish size, abundance, and vertical distribution*

Acoustic backscatter indicates that there was strong seasonality in the abundance, size, and vertical distribution of pelagic fishes at all three mooring sites (Figures 4.2, 4.5b, 4.6b, 4.7b). Fish abundance began to increase in July in both 2018 and 2019, peaking in fall. During this period, target strengths were high (Figures 4.5c, 4.6c, 4.7c), consistent with the $\Delta S_{v,70\text{-}200}$ indicating the presence of fishes. Target strengths in summer were consistent with previous observations of scattering from age-0 gadids (average TS of ~-55 dB re 1 m^2 at 5 cm length, Geoffroy et al., 2016). Given the limited observations of target strengths consistent with large scatterers (e.g., TS ~-35 for a 35 cm adult pollock; Traynor, 1996), there was little evidence of a significant number of

larger fishes throughout the deployments (Supplementary Figure 4.4a). Abundance was highest when bottom temperatures were > 1 °C (Figure 4.8a). This result was observed at all sites in late summer and fall (Figures 4.5ab, 4.6ab 4.7ab).

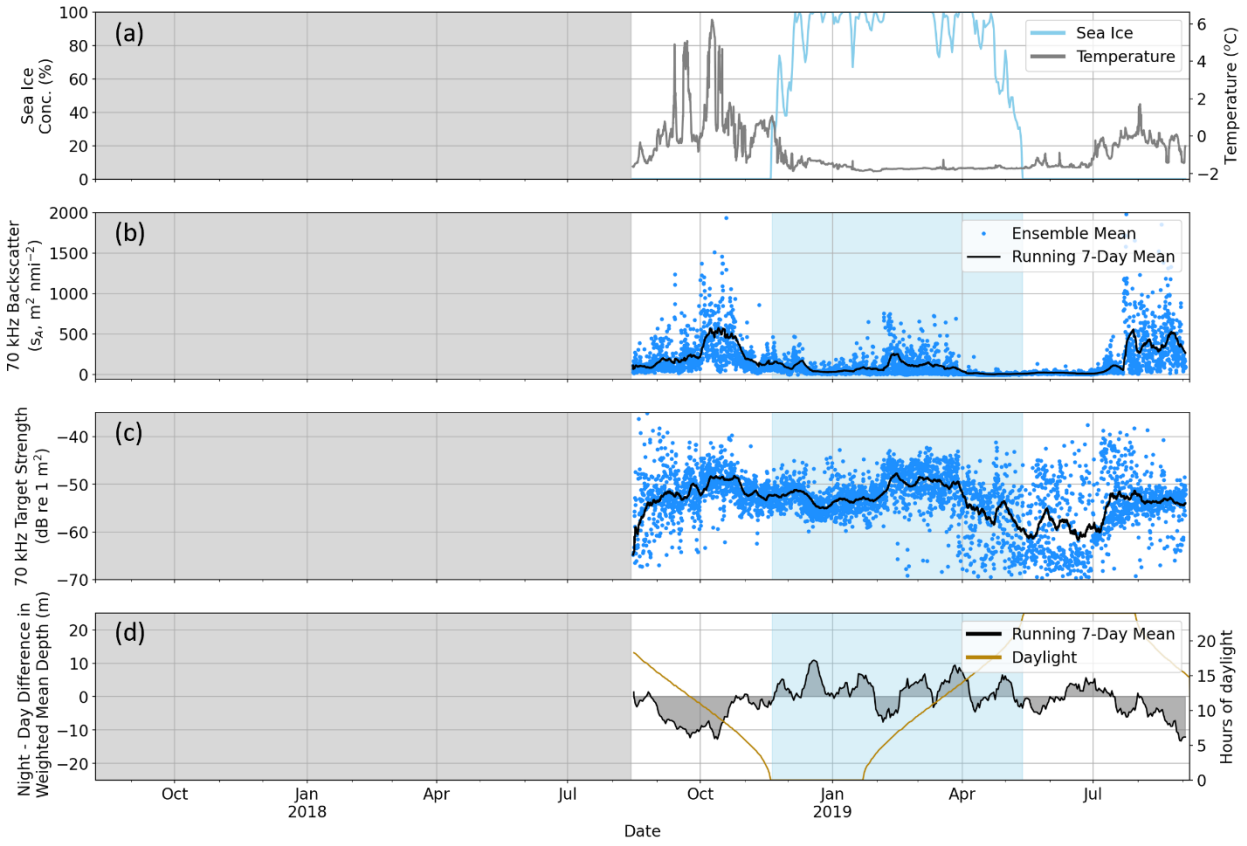

Figure 4.5 Time series of the northern mooring site. (a) Sea ice concentration of the nearest 25 km^2 grid cell of satellite observations (blue line) and bottom temperature recorded by the conductivity, temperature, and depth sensor mounted on the mooring platform (grey line). Mean of each 2-hour ensemble (blue points) and running 7-day mean (black line) of (b) water column 70 kHz backscatter (s_A) and (c) 70 kHz target strength. (d) Running 7-day mean difference in weighted mean depth of 70 kHz backscatter between minimum (night) and maximum (day) solar altitude. Negative values correspond to a shallower distribution at night. The gold line indicates the number of hours of daylight. Blue shading (panels b, c, and d) indicates periods when sea ice concentration was > 20%. Due to instrument failure, data are not available for the northern mooring site from the 2017-2018 deployment (grey region).

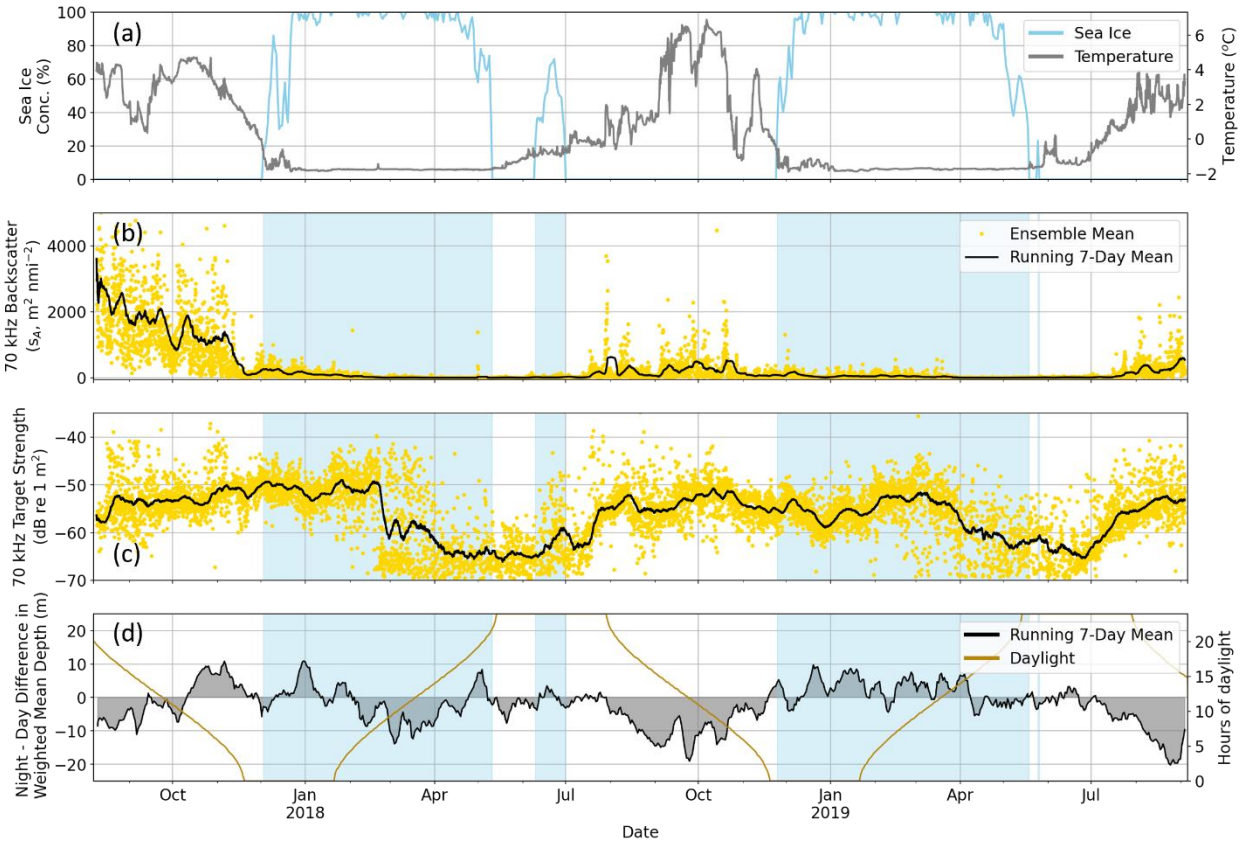

Figure 4.6 Time series of the central mooring site. (a) Sea ice concentration of the nearest 25 km^2 grid cell of satellite observations (blue line) and bottom temperature recorded by the conductivity, temperature, and depth sensor mounted on the mooring platform (grey line). Mean of each 2-hour ensemble (yellow points) and running 7-day mean (black line) of (b) water column 70 kHz backscatter (s_A) and (c) 70 kHz target strength. (d) Running 7-day mean difference in weighted mean depth of 70 kHz backscatter between minimum (night) and maximum (day) solar altitude. Negative values correspond to a shallower distribution at night. The gold line indicates the number of hours of daylight. Positive and negative values are shown in blue and red, respectively. Blue shading (panels b, c, and d) indicates periods when sea ice concentration was > 20%.

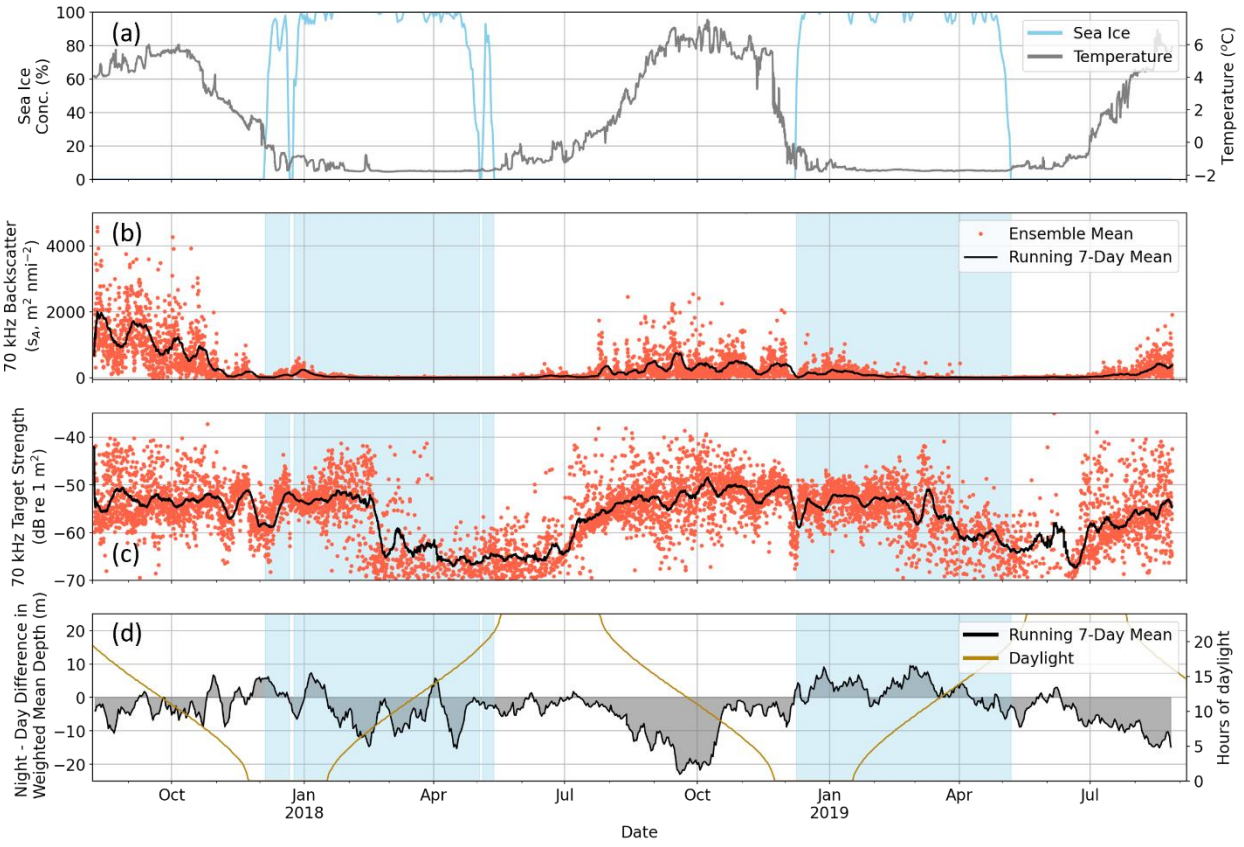

Figure 4.7 Time series of the southern mooring site. (a) Sea ice concentration of the nearest 25 km^2 grid cell of satellite observations (blue line) and bottom temperature recorded by the conductivity, temperature, and depth sensor mounted on the mooring platform (grey line). Mean of each 2-hour ensemble (red points) and running 7-day mean (black line) of (b) water column 70 kHz backscatter (s_A) and (c) 70 kHz target strength. (d) Running 7-day mean difference in weighted mean depth of 70 kHz backscatter between minimum (night) and maximum (day) solar altitude. Negative values correspond to a shallower distribution at night. The gold line indicates the number of hours of daylight. Positive and negative values are shown in blue and red, respectively. Blue shading (panels b, c, and d) indicates periods when sea ice concentration was > 20%.

Between August and October, night-day differences in weighted mean depth of fish increased (Figures 4.5d, 4.6d, 4.7d), with the greatest difference occurring during periods of 14-20 hours of daylight (Figure 4.9). Night-day depth differences peaked in fall when the length of

daylight and darkness are approximately equal (Figure 4.9). This night-day difference then decreased later into fall as day length shortened (Figures 4.5d, 4.6d, 4.7d, 4.9).

As sea ice concentration over the moorings increased in November and December, fish abundance decreased (Figures 4.5ab, 4.6ab, 4.7ab). The onset of sea ice was associated with decreased fish abundance: mean backscatter was ~3-8 times lower at all three mooring sites when sea ice concentration was > 20% (t-test on log-transformed 70 kHz s_A, $p<0.001$ at all sites, Figure 4.8b). However, target strengths remained consistent, indicating that fish of similar size were still present, though in reduced numbers (Figures 4.5bc, 4.6bc, 4.7bc).

In winter, the backscatter observations indicated that fish densities were very low at all three sites, with the lowest abundances occurring between March and May. Target strength decreased substantially during this period, reflecting a transition in scatterer type, likely from small swim-bladdered gadids to a zooplankton-dominated pelagic community with lower target strengths (Figures 4.5c, 4.6c, 4.7c). The change in the frequency response also supports this inference - unlike in summer, where $\Delta S_{v,70\text{-}200}$ was high, higher backscatter was observed at 200 kHz than 70 kHz throughout the water column from approximately March to May of both years (lower values of $\Delta S_{v,70\text{-}200}$, blue regions, Figure 4.3). Among the few periods where fish-like scatterers (TS > -60 dB re 1 m^2) dominated the water column during early winter, vertical distribution remained deep throughout day and night with little evidence of migration (Figure 4.9).

After sea ice retreated in May, bottom temperatures and fish abundance increased. Changes in the $\Delta S_{v,70\text{-}200}$ indicated a transition to fish-like scatterers in June and July beginning near the surface (Figure 4.3). Fishes appeared to grow during this period, as evidenced by increases in target strength (Figures 4.5c, 4.6c, 4.7c). As TS increased, the night-day depth differences also increased

(Figures 4.5d, 4.6d, 4.7d), consistent with the onset of vertical migration behavior expected for age-0 gadids (Brodeur et al., 2000; Ponomarenko, 2000).

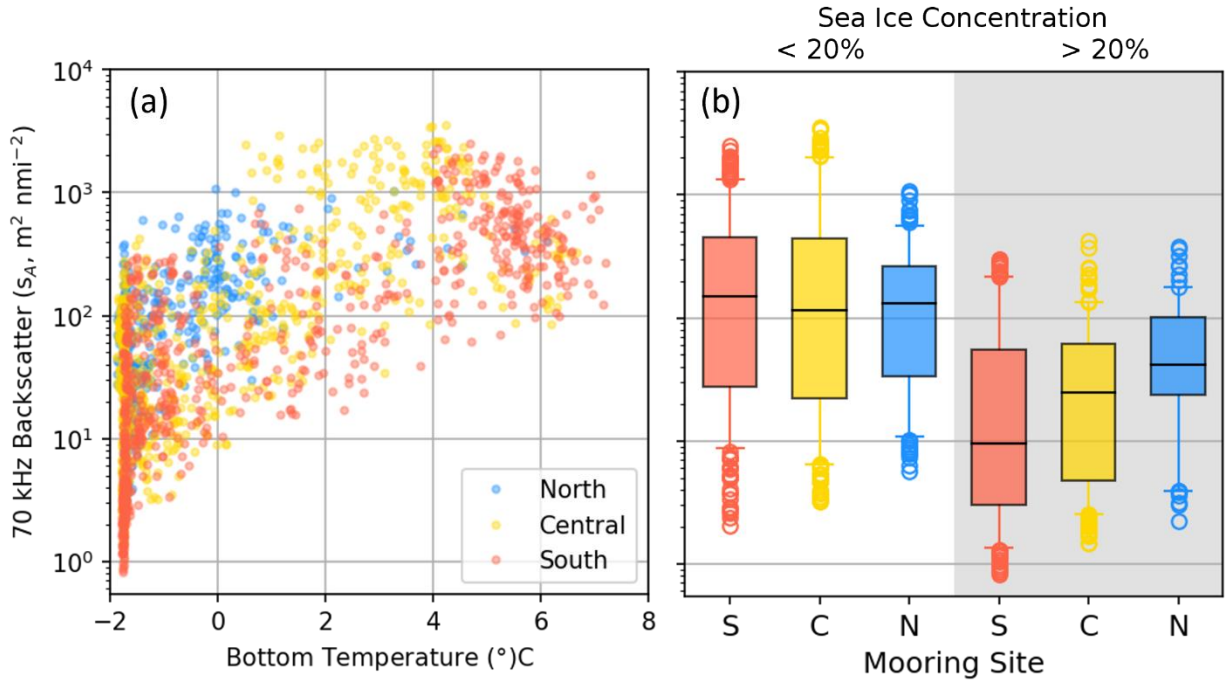

Figure 4.8 (a) Mean daily 70 kHz backscatter (s_A, m^2 nmi^{-2}) as a function of temperature at the northern (blue), central (yellow), and southern (red) mooring sites. (b) Distributions of mean daily 70 kHz backscatter when sea ice concentrations were < 20% (white background) and > 20% (grey background). Boxes indicate the interquartile range, horizontal black lines the median, vertical lines the 5% and 95% intervals. Circles indicate observations beyond the 5% and 95% intervals.

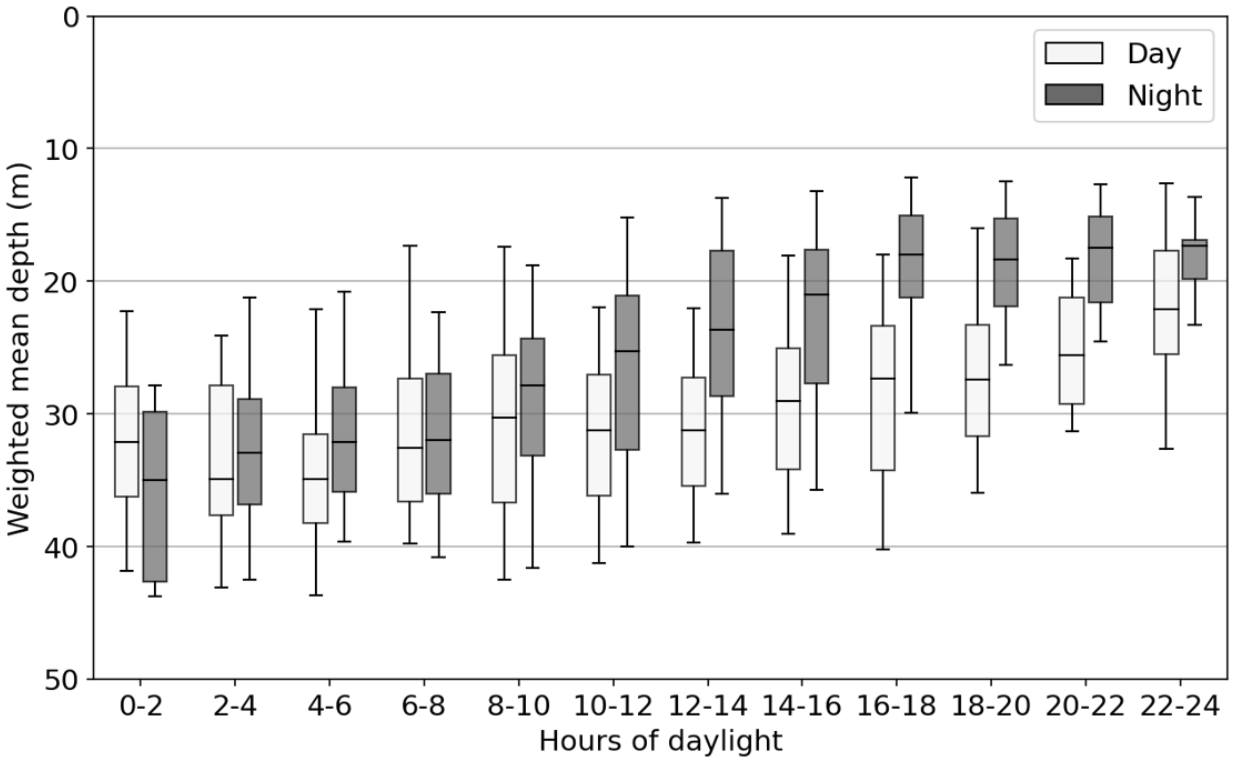

Figure 4.9 Night (minimum solar altitude, grey boxes) and day (maximum solar altitude, white boxes) distributions of weighted mean depth in 2-hour bins of length of daylight. Only ensembles where mean target strength indicates that scattering was likely from fishes (TS > -60 dB re 1 m^2) are included.

4.3.3 *Drivers of fish movement*

Fish tracks and ACDP measurements of currents indicate that fishes were moving largely as passively advected particles. A total of 40317, 83024, and 63674 fish tracks were reconstructed from single target measurements at the northern, central, and southern moorings, respectively, during the two years of deployments. The mean track depth was 27 (±10 SD) m (Supplementary Figure 4.4b). Over the observation period, the majority of track headings were towards the northeast, with the mode of heading distributions ("reference headings") for each mooring at 45° (southern), 75° (central), and 65° (northern). The daily mean track heading was correlated with current direction measured independently from the nearby (< 500 m) ADCP (R^2=0.58, $p<0.001$,

Figure 4.10a). Two modes were apparent in the current and fish headings corresponding to movement to the northeast and southwest (Figure 4.10a). The mean speed of all individual tracks was 23 (±14 SD) cm s-1. Daily mean fish track velocities and current velocities calculated along the reference heading for each site were strongly correlated (R2=0.81, p<0.001, Figure 4.10b), and the mean difference between fish track and current velocities was not significantly different from zero, suggesting fish were passively moving with the current. Record mean of all track velocities along the reference headings were 8.2 (±23.3 SD) cm s^{-1}, indicating net movement to the northeast.

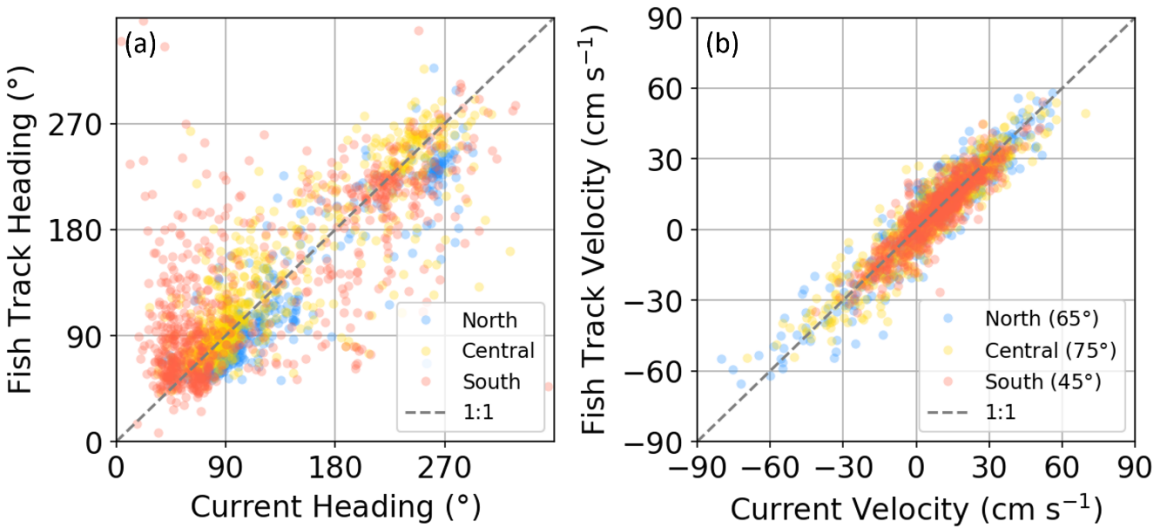

Figure 4.10 (a) Mean daily heading of currents measured from the acoustic doppler current profilers (ADCP) and fish tracks using the nearest depth bin of current observations for each track. (b) Mean daily current and fish track velocities along the reference heading (the mode of track headings observed at each site) indicated in the legend for each site. The 1:1 line on each plot is shown as a reference (grey dashed line).

Table 4.1 Mean flux (Fish m^{-1} s^{-1}) and total cumulative flux over the course of each deployment (Fish m^{-1}) calculated along the reference heading for each mooring.

Deployment	Site	Reference Heading	Mean Flux (Fish m^{-1} s^{-1})	Cumulative Flux (Fish m^{-1})
2017 - 2018	Southern	45°	0.07	1.8×10^6
	Central	80°	0.23	6.8×10^6
2018 - 2019	Southern	45°	0.08	2.8×10^6
	Central	80°	0.09	3.0×10^6
	Northern	75°	0.13	4.4×10^6

The flux of fishes was primarily to the northeast at all three sites (Figure 4.11, Table 4.1). Mean flux was highest at the central site in 2017-2018 and the northern site in 2018-2019, with the lowest estimates of flux at the southern site in both years (Table 4.1). Fluxes were highest during the summer and fall when fish were abundant (Figure 4.11). The highest mean flux over a 7-day period, 2.6 fish m^{-1} s^{-1}, was observed in September 2017 at the central mooring site (Figure 4.11b). This corresponds with the highest fish abundances observed throughout the deployments (Figure 4.6b). The magnitude of the flux was primarily driven by the abundance (Supplementary Figure 4.5), with fish fluxes being lowest during ice-covered periods when fish were scarce (Figure 4.11). Although mean current velocities to the northeast were also 1.8-6.8 times slower when ice was present at the northern (t-test, $p<0.05$) and central sites ($p<0.1$), velocities did not vary significantly at the southern site ($p=0.8$).

Cumulative fluxes indicate that over longer timescales, the net movement of fishes was consistently to the northeast (Table 4.1). However, short episodes of fish movement to the southwest occurred throughout the year (blue bars, Figure 4.11). These reversals in flux were associated with shifts in current and wind speed and direction (Figures 4.12, 4.13). Daily mean estimated northeastward wind speeds during the deployment period ranged from -13.5 to 19.9 m s^{-1} (mean of 0.04 m s^{-1} ±5.5 SD). When wind speeds to the northeast were high, fish primarily

moved to the northeast/east (Figure 4.12). Fish headings became more variable as northeastward winds weakened and transitioned to the southwest when winds were strong towards the southwest (Figure 4.12).

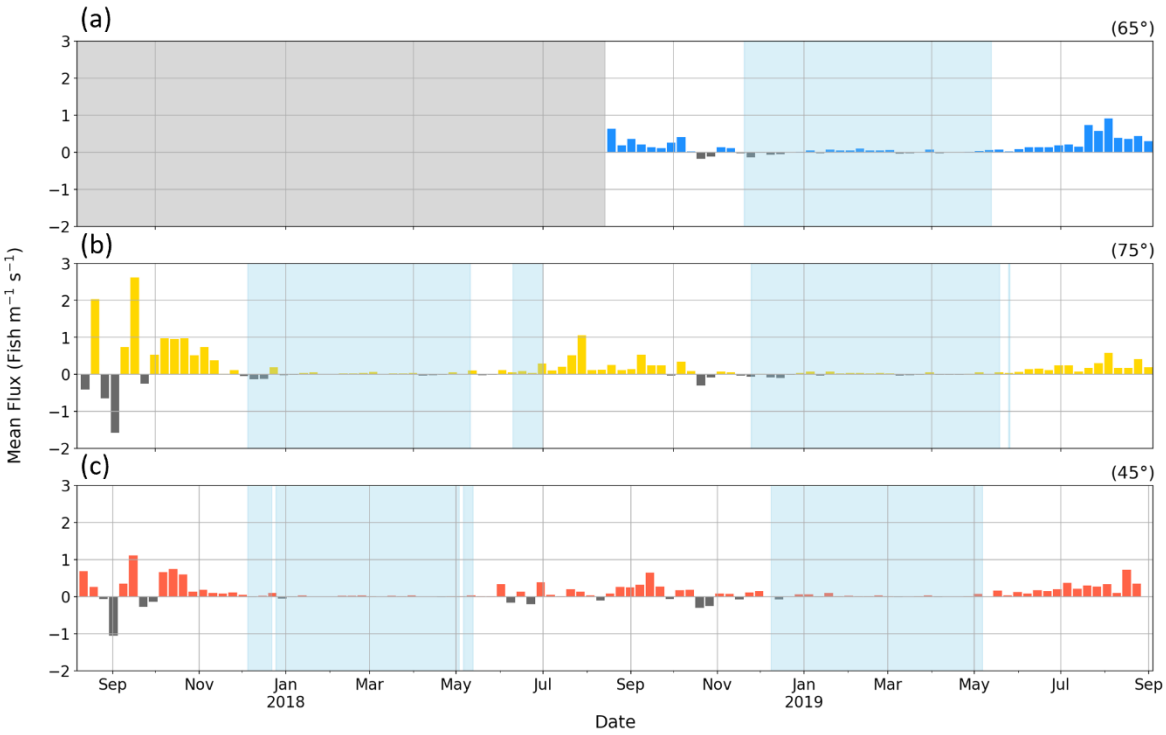

Figure 4.11 Mean flux of fishes (fish m^{-1} s^{-1}) at the (a) northern, (b) central, (d) and southern mooring sites. Each bar represents the mean flux during a single week of deployment. Values represent the number of fish passing through a 1-m wide water column perpendicular to the reference heading (the mode of track headings observed at each site) indicated in the top right of each panel. Positive (within 90° of the refence heading) and negative (within 90° of 180° from the reference heading) values are shown in red and blue, respectively.

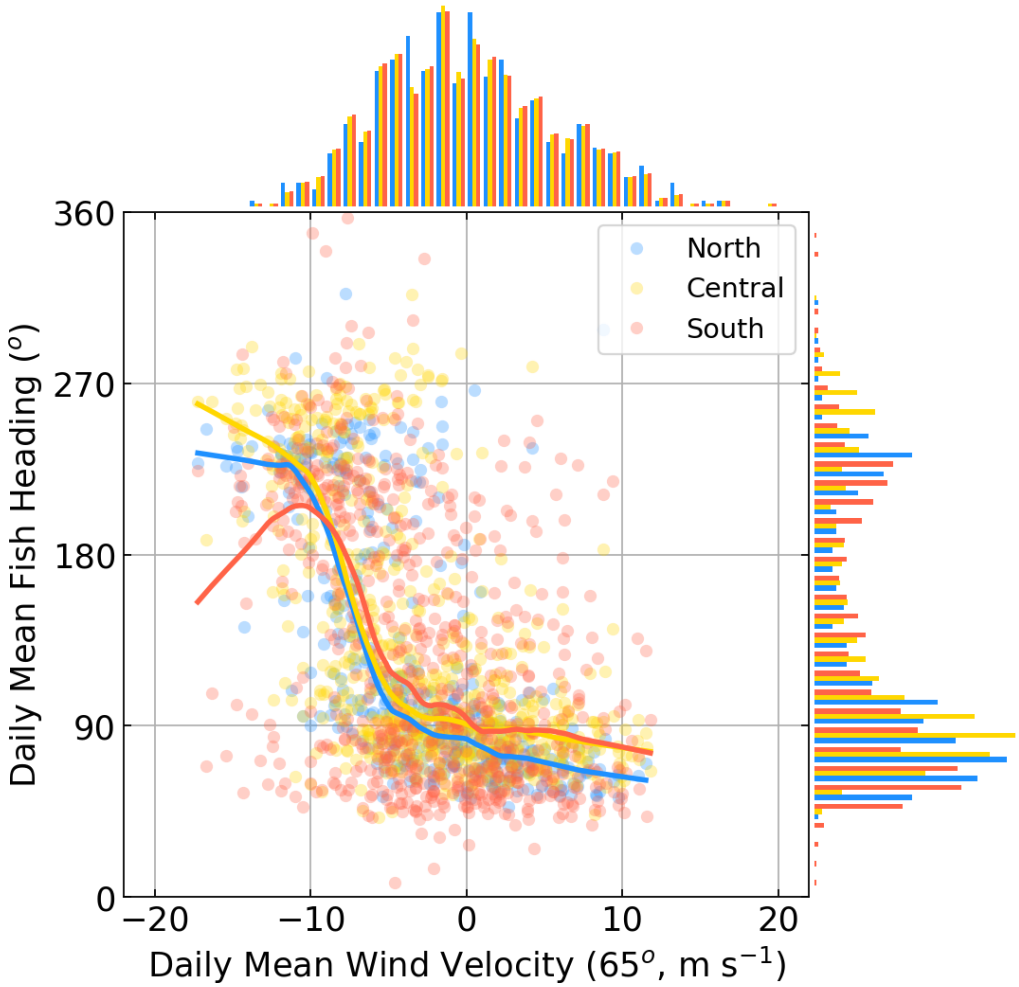

Figure 4.12 Daily mean fish heading as a function of mean wind velocity at the northern (blue), central (yellow), and southern (red) mooring site. Histograms represent the distribution of wind speeds (top) and fish headings (right) for both years of deployments at each moorings site. Wind velocity was calculated along the mode direction of surface winds over the deployment periods (65°). The solid lines represent a locally estimated scatterplot smoothing curve (Cleveland, 1979) of the daily means for each mooring to indicate the trend.

4.4 DISCUSSION

4.4.1 *Seasonality of fishes*

The mooring observations provide further evidence of strong seasonality in the abundance of the pelagic fish community on the Chukchi shelf. Large numbers of age-0 gadids have been observed in summer (De Robertis et al., 2017; Levine et al., in review). However, few age-1+ individuals were observed in these surveys, indicating that either mortality in this region is high or that these fish emigrate to other regions. Using two years of year-round observations from moored echosounders in the northeastern Chukchi Sea, we found that the age-0 gadids appear in the region in late summer and disappear in early winter. Tracking of fish targets revealed that fish movements correlated with local currents, and estimates of fish flux indicate that the majority of the age-0 population in summer is likely transported to the north and east off towards the Beaufort Sea and Arctic Basin each fall and winter. These findings suggest that these small fishes are transported much like passive particles, which supports the inferences drawn from passive particle tracking simulations which predict the displacement of the summer age-0 population to the northeast off the Chukchi shelf in fall (Levine et al., 2021).

The presence of fish appears to be strongly associated with seasonal warm waters entering the region. Temperature is a key driver of both Arctic cod and pollock distribution (Sigler et al., 2017; Eisner et al., 2020; Baker, 2021; Levine et al., in review) and growth (Laurel et al., 2018). The northward transport of warm Bering Sea water in spring and summer into the northeastern Chukchi Sea (Danielson et al., 2017) has been associated with increases in abundance of zooplankton (Eisner et al., 2013; Ashjian et al., 2017; Spear et al., 2020) and fishes (Logerwell et al., 2020; Levine et al., in review). Increases in abundance of fishes in the northeastern Chukchi Sea in summer appear to coincide with the arrival of southern-origin water masses. These flow north into the Chukchi Sea from the Bering Sea shelf (Coachman et al., 1975; Danielson et

al., 2017), replacing the colder winter water on the Chukchi shelf (Weingartner et al., 2013). The age-0 gadids observed in the northeastern Chukchi in summer are primarily associated with the warmer (2-8 °C) conditions of these seasonal water masses (De Robertis et al., 2017; Marsh et al., 2019; Levine et al., in review). The observations in this study further indicate that the seasonality of age-0 gadids in the northeastern Chukchi Sea is driven by the advective movement of the fish population within this warm water.

Abundance was much higher in the summer and fall of 2017 than in the following two years at the central and southern sites. This high interannual variability is consistent with survey observations of substantially higher age-0 gadid abundances in 2017 than 2019 (Levine et al., in review). Levine et al., (in review) hypothesized that this increase in gadids was attributed to anomalously warm conditions in spring, resulting in earlier hatch and favorable growth conditions that led to increased length-at-age and thus increased age-0 fish survival. The lower fish abundance in 2018-2019 is consistent with acoustic observations from conducted in 2018 (Levine et al., 2021) and 2019 (Levine et al., in review).

While it was not possible to directly assess the size of fishes, the moorings confirm previous observations that the pelagic community in summer is dominated by small fishes. Mean target strengths during periods dominated by fish-like scattering were consistent with the target strength expected from small (<6 cm) age-0 fishes (Traynor, 1996; Geoffroy et al., 2016; Levine et al., 2021). However, while these reported target strength-length relationships for age-0 gadids are based on ship-based (dorsal) observations at 38 kHz (Traynor, 1996; Geoffroy et al., 2016), our inferred length from mooring observations are ventral measurements collected at 70 kHz. While target strength of individuals is orientation- and frequency-dependent (Foote 1980; Francis and Foote 2003), the difference in volume backscattering strength at 38 kHz and 70 kHz is small for

walleye pollock (De Robertis et al., 2010); we therefore applied the target strength-length relationships estimated at 38 kHz to our observations at 70 kHz with the expectation that the associated error as a result of frequency was minimal.

The impact of the use of ventral observations from the moorings is also likely to be low. Most of the variability in target strength of an individual as a result of behavior is due to the change in tilt angle of the fish (Horne, 2003) and model predictions estimate that the variability between dorsal and ventral measurements of the same orientation is low relative to changes in tilt angle (Francis and Foote 2003). Even with these potential sources of variability in the target- strength-length relationship (e.g. high variability in TS from a single individual, Dawson and Karp, 1990), the scarce observations of high (>-35 dB re 1 m^2) target strengths (Supplementary Figure 4.4a) indicate that larger fishes such as adult pollock were likely not present in significant abundance.

The increase in target strength from July to October, along with the increase in diel vertical migration indicated by increasing difference between day and night weighted mean depth, is potential evidence of growth in the age-0 population during the late summer (July - October) as observed in summer surveys (Deary et al., 2021; Levine et al., 2021). Arctic cod and pollock are typically surface-associated as eggs and larvae (Spencer et al., 2020). As they increase in size and swimming ability, juveniles begin to move deeper into the water column during the day, a behavioral shift typically occurring at a length of ~ 30 mm in both species (Brodeur et al., 2000; Ponomorenko 2000). The increase in night-day depth difference beginning in July of each year at all three sites (Figures 4.5d, 4.6d, 4.7d) is consistent with the onset of diel vertical migration (DVM). We found little evidence of diel vertical migration occurring during polar night and the adjacent periods of minimal daylight, though young Arctic cod have been observed to undergo migration during polar winter in response to small changes in twilight (Benoit et al., 2010). Thus,

the lack of vertical migration in winter is consistent with our other observations suggesting that age-0 fishes are virtually absent during March to June.

4.4.2 *Fate of age-0 gadids*

Our results show that advection appears to be the primary mechanism of movement in fishes on the northeastern Chukchi shelf. Fish headings and velocities were consistent with those of the currents, with little evidence of significant horizontal fish displacement as a result of swimming or other behavior. While age-0 gadids are capable of fast swimming speeds (aerobic threshold of 2-3 body lengths s^{-1}, Hurst, 2007; Kunz et al., 2018), routine speeds are much slower (0.25 – 1 body lengths s^{-1}, Rose et al., 1995; Hurst, 2007). In the fast current velocities observed on the Chukchi shelf (mean speed of 19.9 [range of 0.2-105.2] cm s^{-1} across all sites), routine swimming behavior is likely to have minimal impact on fish displacement relative to advection (<5% of current observations across all sites were < 4.5 cm s^{-1}). These in situ observations support the assumptions commonly used in modelling studies using passive drift to determine horizontal distributions of age-0 gadids in summer (Deary et al., 2021; Vestfals et al., 2021). This work is further evidence that future studies can use direct observations (e.g., ADCPs) or model predictions of regional transport to assess historic and future trends in the source and fate of this age-0 population observed in summer.

We found substantial variability in the flux of age-0 fishes across seasons and among mooring locations. The magnitude of flux was primarily driven by seasonal changes in abundance. Our data show that the fish flux variability between sites was due to variability in local currents. During 2018-2019, the mean flux was highest at the northern site, although fish abundance was lower than the other sites. Current velocities are typically faster at this mooring site than the central and southern sites (Weingartner et al., 2005; Woodgate et al., 2005; Stabeno et al., 2018),

particularly in summer (Stabeno et al., 2018) when we observed the highest fish abundances. Although fish density was comparable between the southern and central sites, (Figures 4.6, 4.7), fluxes were lowest in both years at the southern site. This variability in flux is likely due to the relatively slower velocities typically observed in this portion of the shelf compared to velocities closer in proximity to Barrow Canyon (Woodgate et al., 2005; Stabeno et al., 2018).

The flux of fishes to the northeast may provide evidence that the age-0 fishes present in summer are transported out of the northeastern Chukchi shelf by their first winter. Our results are consistent with particle tracking simulations based on modeled regional advection which predicted that fishes observed in the central portion of the eastern shelf in summer would be transported beyond the shelf break in fall (Levine et al., 2021). If the northern site is representative of the surrounding area of the shelf, we hypothesize that the flux at the northern mooring site may account for a significant portion of the export of age-0 fishes off the shelf. Using the estimate of 4.4×10^6 fish m^{-1} (Table 4.1) observed at the northern mooring site, flux would need to be consistent across only ~35 km of the eastern Chukchi shelf in order to represent the export of the approximately 1.5×10^{11} fishes reported in the 2019 survey (Levine et al., in review). At 71 °N, this represents approximately one-tenth of the eastern (US) portion of the Chukchi shelf. The ability to extrapolate mooring observations over a wider area is a function many things, including flow consistency and the behavior of the species being observed relative to their environment. When abundances are high, fishes on the Chukchi shelf are relatively evenly distributed over large portions of the shelf (De Robertis et al., 2017; Levine et al., in review), and, when placed in a region of relatively uniform distribution (i.e., large-scale scattering layers rather than discrete schools), moorings are likely to represent abundance over a much broader spatial area than the small area directly observed in the acoustic beam (Brierly et al., 2006; De Robertis et al., 2018). Abundance and

distribution of fishes can also be depth-dependent and vary as a function of local topography due to changes in either behavior or advection, therefore extrapolation of mooring observations may only apply within appropriate depth ranges (De Robertis et al., 2018). However, the eastern Chukchi shelf has a relatively consistent depth, thus the moorings may be representative of a larger area.

Age-1+ Arctic cod have been found in low abundance during demersal surveys of the Chukchi shelf in summer (Norcross et al., 2013; Goddard et a., 2014; Logerwell et al., 2017). While the demersal abundances of Arctic cod are significantly lower than pelagic estimates (De Robertis et al., 2017), the presence of these age-1+ fish along the seafloor indicates that Arctic cod likely transition to spend more time at depth as they age. Following this transition, these fish would likely not be observable in our mooring data if they are below the transducers and are inaccessible to pelagic trawls. More work is needed to identify the potential shift of this pelagic age-0 population to demersal habitat on the Chukchi shelf. However, the low abundance of adults in previous surveys and lack evidence of fish transitioning to the bottom in the mooring observations leads us to hypothesize that advection out of the region is the most likely explanation for the limited presence of adult fishes.

Thus, the low densities of age-1+ gadids in the region are likely the result of this continued northward transport of the age-0 population observed in summer. The very low densities of age-1+ gadids during summer surveys (De Robertis et al., 2017; Levine et al., in review) suggests that the age-0 fishes found in the eastern Chukchi Sea likely originated in other areas. Previous studies using models have hypothesized that the distribution of age-0 fishes observed in summer and fall reflects the northward advection of fishes from southern spawning areas (Deary et al., 2021., Vestfals et al., 2021). Our observations are consistent with these hypotheses: While our study did

not identify the spawning location, we infer from the strong correlation between fish displacement and currents that age-0 gadids in the Chukchi during summer are likely of southern origin (Levine et al., in review). Larger fish, however, are likely not allowing themselves to be passively transported with their drifting eggs and are more likely to maintain their position in their preferred habitat. Age-1+ fishes have also likely developed the swimming ability required to return to spawning grounds. While we did not identify any evidence for high target strength fishes migrating south indicating the return of large fishes to spawning grounds in our observations, some portion of the age-0 population is likely returning as mature adults in order to maintain the spawning population, possibly in areas farther offshore (Forster et al., 2020).

While Arctic cod are adapted to tolerate near-freezing conditions, pollock are not (Laurel et al., 2018; Koenker et al., 2018), thus the potential of the age-0 fishes we observed in the Chukchi to survive over winter after being advected into the Arctic remains unclear. Growth and lipid accumulation are species-specific and temperature-dependent in age-0 gadids. Based on their body condition, age-0 pollock captured during recent surveys of the Chukchi Sea in summer are unlikely to have sufficient lipid reserves to survive overwinter under Arctic conditions (Copeman, pers. comm.). Thus, while the flux of fishes supports the hypothesis of emigration of the population to other areas as they age, quantifying the mortality of these age-0 pollock in their new environment is still required to address the long-term survival of the population and the ability of boreal species observed seasonally on the shelf to establish permanent populations in the region. In contrast, Arctic cod are widely present throughout the Arctic basin and are capable of surviving Arctic winter conditions. Large aggregations of age-1+ Arctic cod have been observed at depth in Barrow Canyon (De Robertis et al., 2017) and the Beaufort Sea shelf break (Parker-Stetter et al., 2011; Rand and Logerwell, 2011), and genetic studies have not identified any significant population

stratification between Arctic cod observed on the Chukchi shelf and those in the western Beaufort Sea (Wilson et al., 2019; Nelson et al., 2020). These populations may recruit from the age-0 Arctic cod being transported off of the Chukchi shelf, and further work is necessary to identify whether the Chukchi shelf slope and western Beaufort are the wintering grounds for the majority of these age-0 fish.

4.4.3 *Influence of regional winds*

The direction of fish movements appears to be driven primarily by changes in current speed and direction. On the Chukchi shelf, advective transport that moves water of Bering Sea origin north is believed to be driven by the pressure head created by differences in sea surface height between the Pacific and Arctic Oceans (Woodgate et al., 2005; Danielson et al., 2014, Peralta-Ferriz and Woodgate, 2017). This northward flow is restrained by winds to the southwest and variations in the current are primarily wind-driven (Weingartner et al., 2005; Woodgate, et al., 2005). Increases in winds to the southwest can slow this northward flow and when strong enough, lead to episodic flow reversals (Woodgate et al., 2005; Stabeno et al., 2018; Pisareva et al., 2019). Conversely, during periods of strong winds to the northeast, the northward flow across the shelf increases. Particle tracking simulations have suggested that this variability in wind and the resulting shift in currents is a major source of interannual variability observed in late-summer distribution of age-0 fishes in the Chukchi Sea (Levine et al., 2021; Vestfals et al., 2021).

We observed two modes in fish displacement, which varied with changes in wind speed on the northeastern shelf. During periods of strong northward wind, current and fish speeds increased, and the movement of both currents and fish was to the north/east (yellow box, Figure 4.13). When winds were > ~6 m s^{-1} to the southwest, a reversal was seen in both the currents and fish tracks, with a higher proportion of fish moving to the south/west (purple box, Figure 4.13). During periods

of weak and variable winds, fish tracks remained towards the northeast (Figures 4.12, 4.13), consistent with the expected flow on the northeastern shelf (Stabeno et al., 2018). These wind-driven modes of water movement in the northeastern Chukchi have previously been documented and a threshold of 6 m s^{-1} winds towards the southwest (Fang et al., 2017) has been reported as the requirement for transition between states.

In recent years, the frequency of northward wind events in the region has increased, (Stabeno and Bell, 2019). As the region continues to warm, the input of water through the Bering Strait is also predicted to increase (Danielson et al., 2020), which would increase northward transport across the Chukchi shelf. Transport has already been increasing over recent decades, considerably reducing the amount of time needed to flush and renew the water on the Chukchi shelf (Woodgate et al., 2018). Based on the mean fish track velocity of 8.2 cm s^{-1}, the residence time of fish on the Chukchi shelf is ~85 days (based on ~600 km of transit from Bering Strait to Barrow Canyon). Our study occurred during a period of high transport relative to previous decades (Woodgate and Peralta-Ferriz, 2021; Levine et al., in review). This enhanced transport may be more nearly the norm in future decades, and future changes in transport are likely to further decrease the residence time of age-0 gadids on the Chukchi shelf. The time spent on the Chukchi shelf by age-0 fishes in summer is likely important for maximizing growth (Levine et al., 2021). A decrease in the amount of time spent in the Chukchi Sea in summer where conditions are conducive to growth may have negative consequences for the overwinter survival of these fishes. Thus, further research is needed to identify the consequences of decreased residence time.

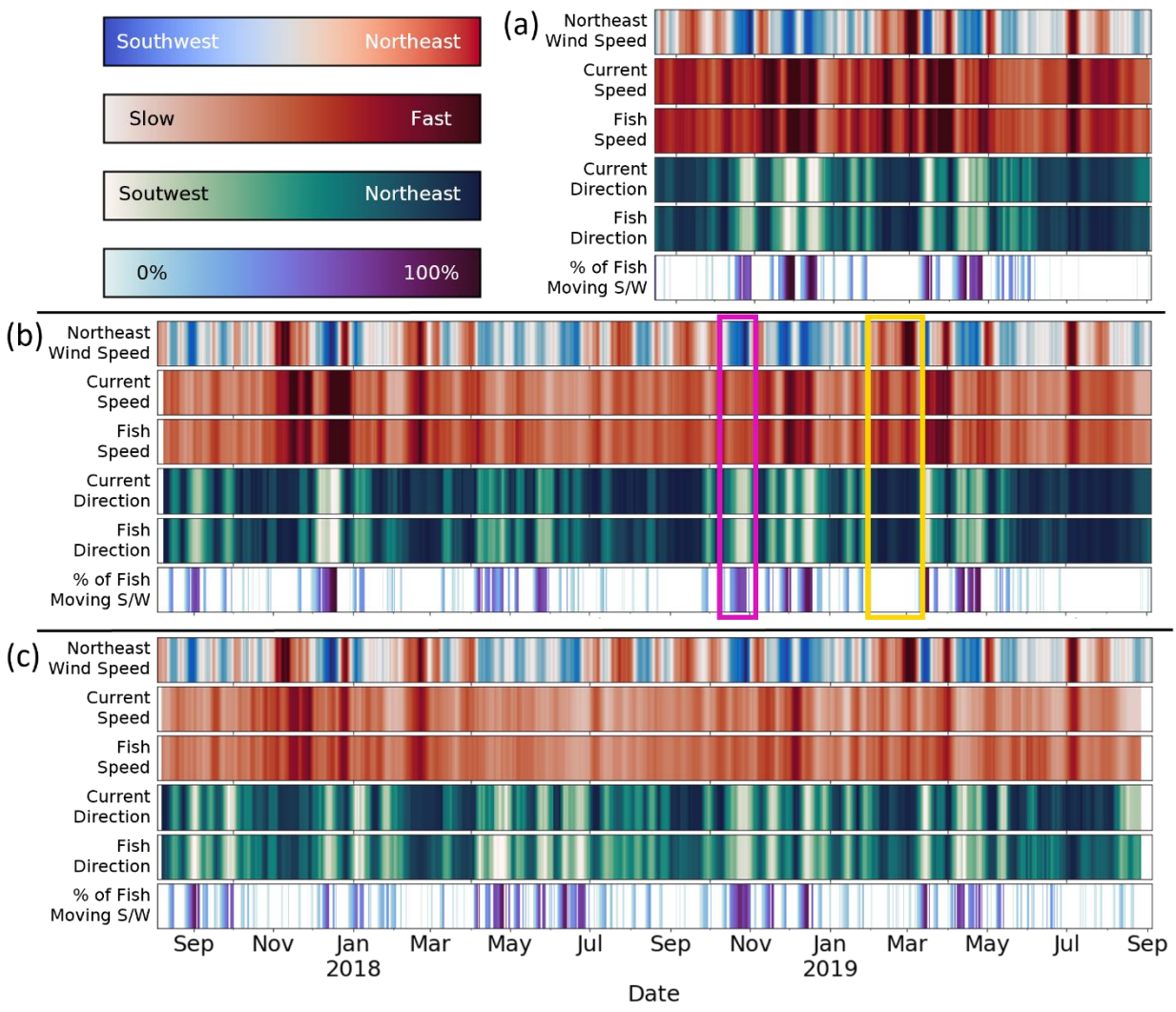

Figure 4.13 Time series of 7-day rolling means of north-south winds, current and fish speeds, and current and fish directions at the (a) northern, (b) central, and (c) southern mooring sites. Within each panel, the top heatmap indicates the northward (meridional component) wind speed, calculated along the mode direction of surface winds over the deployment periods (65°). Red indicates strong northeastward winds and blue indicates strong southwestward winds. The second and third heatmaps indicate the speed of both the current and fishes, where darker colors indicate faster speeds. The fourth and fifth heatmaps indicate the direction of the current and fishes, where darker colors indicate coherence with the reference heading (towards the northeast, see methods, Figure 4.9). The bottom heatmap shows the % of fish tracks moving opposed to the reference heading (to the southwest). As examples, the purple box and yellow box highlight a period of strong southward and northward winds, respectively (see results).

4.5 CONCLUSIONS

The abundance and composition of the pelagic fish community on the Chukchi shelf is highly seasonal. This study provides evidence that the abundant age-0 gadids observed on the Chukchi shelf in summer are likely temporary residents of the region. Our data suggest that their distribution and movement across the shelf are primarily driven by advection, providing additional evidence that these fish are likely originating from the south. However, transport in the region is changing, with potential consequences for the future of this ecosystem and the structure of the summer pelagic fish community. Enhanced transport from the south is hypothesized to be driving the recent increased presence of boreal species such as pollock in the eastern Chukchi Sea (Levine et al., in review). While these southern-origin species likely cannot survive overwinter in Arctic conditions (Koenker et al., 2018), their increased presence during summer may increase competition with and predation on endemic species, further altering the structure of the summer community. The role of advection in structuring this seasonal population allows us to use observations and predictions of the physical environment to understand how this ecosystem will be structured under future change.

4.6 ACKNOWLEDGEMENTS

This research was conducted under the Arctic Integrated Ecosystem Research Program (http://www.nprb.org/arctic-program). Funding for the program was provided by North Pacific Research Board, the Bureau of Ocean Energy Management, the Collaborative Alaskan Arctic Studies Program, and the Office of Naval Research. In-kind support was contributed by the National Oceanic and Atmospheric Administration's (NOAA) Alaska Fisheries Science Center and Pacific Marine Environmental Laboratory, the University of Alaska Fairbanks, the U.S. Fish & Wildlife Service, and the National Science Foundation. We would like to thank Phyllis Stabeno

for providing us with the ADCP data presented here. We would also like to thank Christian Meinig and Steven Anderson for their work in the design and construction of the mooring platform, and Matthew Casari for development of the underwater compasses. The mooring deployments and recoveries would not have been possible without the captains, crews, and science parties of the RV *Ocean Starr* and USCGC *Healy*.

4.7 REFERENCES

Ashjian, C.J., Campbell, R.G., Gelfman, C., Alatalo, P., Elliott, S.M., 2017. Mesozooplankton abundance and distribution in association with hydrography on Hanna Shoal, NE Chukchi Sea, during August 2012 and 2013. Deep. Res. Part II Top. Stud. Oceanogr. 144, 21–36. https://doi.org/10.1016/j.dsr2.2017.08.012

Baker, M.R., 2021. Contrast of warm and cold phases in the Bering Sea to understand spatial distributions of Arctic and sub-Arctic gadids. Polar Biol. 44, 1083–1105. https://doi.org/10.1007/s00300-021-02856-x

Benoit, D., Simard, Y., Fortier, L., 2008. Hydroacoustic detection of large winter aggregations of Arctic cod (*Boreogadus saida*) at depth in ice-covered Franklin Bay (Beaufort Sea). J. Geophys. Res. Ocean. 113, 1–9. https://doi.org/10.1029/2007JC004276

Benoit, D., Simard, Y., Gagné, J., Geoffroy, M., Fortier, L., 2010. From polar night to midnight sun: Photoperiod, seal predation, and the diel vertical migrations of polar cod (*Boreogadus saida*) under landfast ice in the Arctic Ocean. Polar Biol. 33, 1505–1520. https://doi.org/10.1007/s00300-010-0840-x

Benoit-Bird, K.J., Lawson, G.L., 2016. Ecological Insights from Pelagic Habitats Acquired Using Active Acoustic Techniques. Ann. Rev. Mar. Sci. 8, 463–490. https://doi.org/10.1146/annurev-marine-122414-034001

Blackman, S.S., 1986. Multiple-target tracking with radar applications. Artech House, Inc., Dedham, MA.

Brierley, A.S., Saunders, R.A., Bone, D.G., Murphy, E.J., Enderlein, P., Conti, S.G., Demer, D.A., 2006. Use of moored acoustic instruments to measure short-term variability in abundance of Antarctic krill. Limnol. Oceanogr. Methods 4, 18–29. https://doi.org/10.4319/lom.2006.4.18

Brodeur, R.D., Wilson, M.T., Ciannelli, L., 2000. Spatial and temporal variability in feeding and condition of age-0 walleye pollock (*Theragra chalcogramma*) in frontal regions of the Bering Sea. ICES J. Mar. Sci. 57, 256–264. https://doi.org/10.1006/jmsc.1999.0525

Cleveland, W.S., 1979. Robust locally weighted regression and smoothing scatterplots. J. Am. Stat. Assoc. 74, 829–836. https://doi.org/10.1080/01621459.1979.10481038

Coachman, L.K., Aagaard, K., Tripp, R.B., 1975. Bering Strait: The Regional Physical Oceanography, University of Washington Press. University of Washington Press, Seattle. https://doi.org/10.1016/0146-6291(77)90492-1

Copeman, L., Spencer, M., Heintz, R., Vollenweider, J., Sremba, A., Helser, T., Logerwell, L., Sousa, L., Danielson, S., Pinchuk, A.I., Laurel, B., 2020. Ontogenetic patterns in lipid and fatty acid biomarkers of juvenile polar cod (*Boreogadus saida*) and saffron cod (*Eleginus gracilis*) from across the Alaska Arctic. Polar Biol. https://doi.org/10.1007/s00300-020-02648-9

Danielson, S.L., Ahkinga, O., Ashjian, C., Basyuk, E., Cooper, L.W., Eisner, L., Farley, E., Iken, K.B., Grebmeier, J.M., Juranek, L., Khen, G., Jayne, S.R., Kikuchi, T., Ladd, C., Lu, K., McCabe, R.M., Moore, G.W.K., Nishino, S., Ozenna, F., Pickart, R.S., Polyakov, I., Stabeno, P.J., Thoman, R., Williams, W.J., Wood, K., Weingartner, T.J., 2020. Manifestation and consequences of warming and altered heat fluxes over the Bering and Chukchi Sea continental shelves. Deep. Res. Part II Top. Stud. Oceanogr. 177. https://doi.org/10.1016/j.dsr2.2020.104781

Danielson, S.L., Eisner, L., Ladd, C., Mordy, C., Sousa, L., Weingartner, T.J., 2017. A comparison between late summer 2012 and 2013 water masses, macronutrients, and phytoplankton standing crops in the northern Bering and Chukchi Seas. Deep. Res. Part II Top. Stud. Oceanogr. 135, 7–26. https://doi.org/10.1016/j.dsr2.2016.05.024

Darnis, G., Hobbs, L., Geoffroy, M., Grenvald, J.C., Renaud, P.E., Berge, J., Cottier, F., Kristiansen, S., Daase, M., E. Søreide, J., Wold, A., Morata, N., Gabrielsen, T., 2017. From polar night to midnight sun: Diel vertical migration, metabolism and biogeochemical role of zooplankton in a high Arctic fjord (Kongsfjorden, Svalbard). Limnol. Oceanogr. 62, 1586–1605. https://doi.org/10.1002/lno.10519

David, C., Lange, B., Krumpen, T., Schaafsma, F., van Franeker, J.A., Flores, H., 2016. Under-ice distribution of polar cod Boreogadus saida in the central Arctic Ocean and their association with sea-ice habitat properties. Polar Biol. 39, 981–994. https://doi.org/10.1007/s00300-015-1774-0

De Robertis, A., Levine, R., Wilson, C.D., 2018. Can a bottom-moored echo sounder array provide a survey-comparable index of abundance? Can. J. Fish. Aquat. Sci. 75, 629–640. https://doi.org/10.1139/cjfas-2017-0013

De Robertis, A., McKelvey, D.R., Ressler, P.H., 2010. Development and application of an empirical multifrequency method for backscatter classification. Can. J. Fish. Aquat. Sci. 67, 1459–1474. https://doi.org/10.1139/F10-075

De Robertis, A., Taylor, K., Wilson, C.D., Farley, E. V., 2017. Abundance and distribution of Arctic cod (Boreogadus saida) and other pelagic fishes over the U.S. Continental Shelf of

the Northern Bering and Chukchi Seas. Deep. Res. Part II Top. Stud. Oceanogr. 135, 51–65. https://doi.org/10.1016/j.dsr2.2016.03.002

Deary, A.L., Vestfals, C.D., Mueter, F.J., Logerwell, E.A., Goldstein, E.D., Stabeno, P.J., Danielson, S.L., Hopcroft, R.R., 2021. Seasonal abundance , distribution , and growth of the early life stages of polar cod (*Boreogadus saida*) and saffron cod (*Eleginus gracilis*) in the US Arctic. Polar Biol. https://doi.org/10.1007/s00300-021-02940-2

Ehrenberg, J., Torkelson, T.C., 1996. Application of dual-beam and split-beam target tracking in fisheries acoustics. ICES J. Mar. Sci. 53, 329–334. https://doi.org/10.1006/jmsc.1996.0044

Eisner, L.B., Zuenko, Y.I., Basyuk, E.O., Britt, L.L., Duffy-Anderson, J.T., Kotwicki, S., Ladd, C., Cheng, W., 2020. Environmental impacts on walleye pollock (*Gadus chalcogrammus*) distribution across the Bering Sea shelf. Deep. Res. Part II Top. Stud. Oceanogr. 181–182, 104881. https://doi.org/10.1016/j.dsr2.2020.104881

Eisner, L., Hillgruber, N., Martinson, E., Maselko, J., 2013. Pelagic fish and zooplankton species assemblages in relation to water mass characteristics in the northern Bering and southeast Chukchi seas. Polar Biol. 36, 87–113. https://doi.org/10.1007/s00300-012-1241-0

Fang, Y.C., Potter, R.A., Statscewich, H., Weingartner, T.J., Winsor, P., Irving, B.K., 2017. Surface Current Patterns in the Northeastern Chukchi Sea and Their Response to Wind Forcing. J. Geophys. Res. Ocean. 122, 9530–9547. https://doi.org/10.1002/2017JC013121

Fernandes, P.G., Stevenson, P., Brierley, A.S., Armstrong, F., Simmonds, E.J., 2003. Autonomous underwater vehicles: Future platforms for fisheries acoustics. ICES J. Mar. Sci. 60, 684–691. https://doi.org/10.1016/S1054-3139(03)00038-9

Flores, H., van Franeker, J.A., Siegel, V., Haraldsson, M., Strass, V., Meesters, E.H., Bathmann, U., Wolff, W.J., 2012. The association of Antarctic krill *Euphausia superba* with the under-ice habitat. PLoS One 7. https://doi.org/10.1371/journal.pone.0031775

Foote, K.G., 1980. Effect of fish behaviour on echo energy: the need for measurements of orientation distributions. ICES J. Mar. Sci. 39, 193–201. https://doi.org/10.1093/icesjms/39.2.193

Forster, C.E., Norcross, B.L., Mueter, F.J., Logerwell, E.A., Seitz, A.C., 2020. Spatial patterns, environmental correlates, and potential seasonal migration triangle of polar cod (*Boreogadus saida*) distribution in the Chukchi and Beaufort seas. Polar Biol. 73. https://doi.org/10.1007/s00300-020-02631-4

Francis, D.T.I., Foote, K.G., 2003. Depth-dependent target strengths of gadoids by the boundary-element method. J. Acoust. Soc. Am. 114, 3136–3146. https://doi.org/10.1121/1.1619982

Frey, K.E., Moore, G.W.K., Cooper, L.W., Grebmeier, J.M., 2015. Divergent patterns of recent sea ice cover across the Bering, Chukchi, and Beaufort seas of the Pacific Arctic Region. Prog. Oceanogr. 136, 32–49. https://doi.org/10.1016/j.pocean.2015.05.009

Geoffroy, M., Majewski, A., LeBlanc, M., Gauthier, S., Walkusz, W., Reist, J.D., Fortier, L., 2016. Vertical segregation of age-0 and age-1+ polar cod (*Boreogadus saida*) over the annual cycle in the Canadian Beaufort Sea. Polar Biol. 39, 1023–1037. https://doi.org/10.1007/s00300-015-1811-z

Goddard, P., Lauth, R., Armistead, C., 2014. Results of the 2012 Chukchi Sea Bottom Trawl Survey of Bottomfishes, Crabs, and Other Demersal Macrofauna. U.S Dep. Commer. NOAA Tech. Memorandum, 110.

Gonzalez, S., Horne, J.K., Danielson, S.L., 2021. Multi-scale temporal variability in biological-physical associations in the NE Chukchi Sea. Polar Biol. 44, 837–855. https://doi.org/10.1007/s00300-021-02844-1

Gradinger, R.R., Bluhm, B.A., 2004. In-situ observations on the distribution and behavior of amphipods and Arctic cod (*Boreogadus saida*) under the sea ice of the High Arctic Canada Basin. Polar Biol. 27, 595–603. https://doi.org/10.1007/s00300-004-0630-4

Horne, J.K., 2003. The influence of ontogeny, physiology, and behaviour on the target strength of walleye pollock (*Theragra chalcogramma*). ICES J. Mar. Sci. 60, 1063–1074. https://doi.org/10.1016/S1054-3139(03)00114-0

Hurst, T.P., 2007. Thermal effects on behavior of juvenile walleye pollock (*Theragra chalcogramma*): Implications for energetics and food web models. Can. J. Fish. Aquat. Sci. 64, 449–457. https://doi.org/10.1139/F07-025

Jech, J.M., Michaels, W.L., 2006. A multifrequency method to classify and evaluate fisheries acoustics data. Can. J. Fish. Aquat. Sci. 63, 2225–2235. https://doi.org/10.1139/F06-126

Kaartvedt, S., Røstad, A., Klevjer, T.A., Staby, A., 2009. Use of bottom-mounted echo sounders in exploring behavior of mesopelagic fishes. Mar. Ecol. Prog. Ser. 395, 109–118. https://doi.org/10.3354/meps08174

Kalnay, E., Kanamitsu, M., Kistler, R., Collins, W., Deaven, D., Gandin, L., Iredell, M., Saha, S., White, G., Woollen, J., Zhu, Y., Chelliah, M., Ebisuzaki, W., Higgins, W., Janowiak, J., Mo, K.C., Ropelewski, C., Wang, J., Leetmaa, A., Reynolds, R., Jenne, R., Joseph, D., 1996. The NCEP/NCAR 40-year reanalysis project. Bull. Am. Meteorol. Soc. https://doi.org/10.1175/1520-0477(1996)077<0437:TNYRP>2.0.CO;2

Kitamura, M., Amakasu, K., Kikuchi, T., Nishino, S., 2017. Seasonal dynamics of zooplankton in the southern Chukchi Sea revealed from acoustic backscattering strength. Cont. Shelf Res. 133, 47–58. https://doi.org/10.1016/j.csr.2016.12.009

Koenker, B.L., Copeman, L.A., Laurel, B.J., 2018. Impacts of temperature and food availability on the condition of larval Arctic cod (*Boreogadus saida*) and walleye pollock (Gadus chalcogrammus). ICES J. Mar. Sci. 75, 2370–2385. https://doi.org/10.1093/icesjms/fsy052

Kunz, K.L., Claireaux, G., Pö Rtner, H.-O., Knust, R., Mark, F.C., Pörtner, H.-O., Knust, R., Mark, F.C., 2018. Aerobic capacities and swimming performance of polar cod (*Boreogadus saida*) under ocean acidification and warming conditions. J. Exp. Biol. 221, jeb184473. https://doi.org/10.1242/jeb.184473

Laurel, B.J., Copeman, L.A., Spencer, M., Iseri, P., 2018. Comparative effects of temperature on rates of development and survival of eggs and yolk-sac larvae of Arctic cod (*Boreogadus saida*) and walleye pollock (*Gadus chalcogrammus*). ICES J. Mar. Sci. 75, 2403–2412. https://doi.org/10.1093/icesjms/fsy042

Levine, R.M., De Robertis, A., Grünbaum, D., Woodgate, R., Mordy, C.W., Mueter, F., Cokelet, E., Lawrence-Slavas, N., Tabisola, H., 2021. Autonomous vehicle surveys indicate that flow reversals retain juvenile fishes in a highly advective high-latitude ecosystem. Limnol. Oceanogr. 66, 1139–1154. https://doi.org/10.1002/lno.11671

Logerwell, E.A., Busby, M., Mier, K.L., Tabisola, H., Duffy-Anderson, J., 2020. The effect of oceanographic variability on the distribution of larval fishes of the northern Bering and Chukchi seas. Deep. Res. Part II Top. Stud. Oceanogr. 177, 104784. https://doi.org/10.1016/j.dsr2.2020.104784

Logerwell, E., Rand, K., Danielson, S., Sousa, L., 2017. Environmental drivers of benthic fish distribution in and around Barrow Canyon in the northeastern Chukchi Sea and western Beaufort Sea. Deep Sea Res. Part II Top. Stud. Oceanogr. https://doi.org/10.1016/j.dsr2.2017.04.012

Lønne, O.J., Gulliksen, B., 1989. Size, age and diet of polar cod, *Boreogadus saida* (Lepechin 1773), in ice covered waters. Polar Biol. 9, 187–191. https://doi.org/10.1007/BF00297174

Lowry, L.F., Frost, K.J., 1981. Distribution, growth, and foods of Arctic cod (*Boreogadus saida*) in the Bering, Chukchi and Beaufort Seas. Can. Field-Naturalist 95, 186–191. https://doi.org/10.1017/CBO9781107415324.004

Maclennan, D.N., Fernandes, P.G., Dalen, J., 2002. A consistent approach to definitions and symbols in fisheries acoustics. ICES J. Mar. Sci. 59, 365–369. https://doi.org/10.1006/jmsc.2001.1158

Marsh, J.M., Mueter, F.J., Quinn, T.J., 2019. Environmental and biological influences on the distribution and population dynamics of polar cod (*Boreogadus saida*) in the US Chukchi Sea. Polar Biol. 1971. https://doi.org/10.1007/s00300-019-02561-w

Mecklenburg, C., Lynghammar, A., Johannesen, E., Byrkjedal, I., Christiansen, J.S., Karamushko, O. V, Mecklenburg, T.A., Møller, P.R., Steinke, D., Wienerroither, R.M., 2018. Marine Fishes of the Arctic Region Volume II, in: CAFF Monitoring Series Report 28. Akureyri, Iceland: Conservation of Arctic Flora and Fauna. Akureyri, Iceland.

Meier, W.N., Fetterer, F., Savoie, M., Mallory, S., Duerr, R., Stroeve, J., 2017. NOAA/NSIDC Climate Data Record of Passive Microwave Sea Ice Concentration, Version 3. Boulder, Colorado, USA. NSIDC National Snow Ice Data Center. https://doi.org/https://doi.org/10.7265/N59P2ZTG

Melnikov, I.A., Chernova, N. V., 2013. Characteristics of under-ice swarming of polar cod *Boreogadus saida* (Gadidae) in the Central Arctic Ocean. J. Ichthyol. https://doi.org/10.1134/S0032945213010086

Miksis-Olds, J.L., Stabeno, P.J., Napp, J.M., Pinchuk, A.I., Nystuen, J.A., Warren, J.D., Denes, S.L., 2013. Ecosystem response to a temporary sea ice retreat in the Bering Sea: Winter 2009. Prog. Oceanogr. 111, 38–51. https://doi.org/10.1016/j.pocean.2012.10.010

Mueter, F.J., Planque, B., Hunt Jr, G.L., Alabia, I.D., Hirawake, T., Eisner, L., Dalpadado, P., Drinkwater, K.F., Harada, N., Arneberg, P., Saitoh, S.-I., 2021. Possible future scenarios in the Gateways to the Arctic for Subarctic and Arctic marine systems: Prey resources, food webs, fish, and fisheries. ICES J. Mar. Sci.

Nelson, R.J., Bouchard, C., Fortier, L., Majewski, A.R., Reist, J.D., Præbel, K., Madsen, M.L., Rose, G.A., Kessel, S.T., Divoky, G.J., 2020. Circumpolar genetic population structure of polar cod, *Boreogadus saida*. Polar Biol. 43, 951–961. https://doi.org/10.1007/s00300-020-02660-z

Norcross, B.L., Raborn, S.W., Holladay, B.A., Gallaway, B.J., Crawford, S.T., Priest, J.T., Edenfield, L.E., Meyer, R., 2013. Northeastern Chukchi Sea demersal fishes and associated environmental characteristics, 2009-2010. Cont. Shelf Res. 67, 77–95. https://doi.org/10.1016/j.csr.2013.05.010

Parker-Stetter, S.L., Horne, J.K., Weingartner, T.J., 2011. Distribution of polar cod and age-0 fish in the U.S. Beaufort Sea. Polar Biol. 34, 1543–1557. https://doi.org/10.1007/s00300-011-1014-1

Peng, G., Meier, W.N., Scott, D.J., Savoie, M.H., 2013. A long-term and reproducible passive microwave sea ice concentration data record for climate studies and monitoring. Earth Syst. Sci. Data 5, 311–318. https://doi.org/10.5194/essd-5-311-2013

Pinchuk, A.I., Eisner, L.B., 2017. Spatial heterogeneity in zooplankton summer distribution in the eastern Chukchi Sea in 2012–2013 as a result of large-scale interactions of water masses. Deep Sea Res. Part II Top. Stud. Oceanogr. 135, 27–39. https://doi.org/10.1016/j.dsr2.2016.11.003

Pisareva, M.N., Pickart, R.S., Lin, P., Fratantoni, P.S., Weingartner, T.J., 2019. On the nature of wind-forced upwelling in Barrow Canyon. Deep. Res. Part II Top. Stud. Oceanogr. 162, 63–78. https://doi.org/10.1016/j.dsr2.2019.02.002

Ponomarenko, V.P., 2000. Eggs, larvae, and juveniles of polar cod *Boreogadus saida* in the Barents, Kara, and White Seas. J. Ichthyol. 40, 165–173.

Rand, K.M., Logerwell, E.A., 2011. The first demersal trawl survey of benthic fish and invertebrates in the Beaufort Sea since the late 1970s. Polar Biol. 34, 475–488. https://doi.org/10.1007/s00300-010-0900-2

Rose, G.A., DeYoung, B., Colbourne, E.B., 1995. Cod (Gadus morhua L.) migration speeds and transport relative to currents on the north-east Newfoundland Shelf. ICES J. Mar. Sci. 52, 903–913. https://doi.org/10.1006/jmsc.1995.0087

Ross, T., Keister, J.E., Lara-Lopez, A., 2013. On the use of high-frequency broadband sonar to classify biological scattering layers from a cabled observatory in Saanich Inlet, British Columbia. Methods Oceanogr. 5, 19–38. https://doi.org/10.1016/j.mio.2013.05.001

Sawada, K., Furusawa, M., Williamson, N.J., 1993. Conditions for the precise measurement of fish target strength in situ. J. Mar. Acoust. Soc. Japan 20, 73–79. https://doi.org/10.3135/jmasj.20.73

Sigler, M.F., Mueter, F.J., Bluhm, B.A., Busby, M.S., Cokelet, E.D., Danielson, S.L., Robertis, A. De, Eisner, L.B., Farley, E. V., Iken, K., Kuletz, K.J., Lauth, R.R., Logerwell, E.A., Pinchuk, A.I., 2017. Late summer zoogeography of the northern Bering and Chukchi seas. Deep Sea Res. Part II Top. Stud. Oceanogr. 135, 168–189. https://doi.org/10.1016/j.dsr2.2016.03.005

Spear, A., Napp, J., Ferm, N., Kimmel, D., 2020. Advection and in situ processes as drivers of change for the abundance of large zooplankton taxa in the Chukchi Sea. Deep. Res. Part II Top. Stud. Oceanogr. 177, 104814. https://doi.org/10.1016/j.dsr2.2020.104814

Spencer, M.L., Vestfals, C.D., Mueter, F.J., Laurel, B.J., 2020. Ontogenetic changes in the buoyancy and salinity tolerance of eggs and larvae of polar cod (*Boreogadus saida*) and other gadids. Polar Biol. 43, 1141–1158. https://doi.org/10.1007/s00300-020-02620-7

Stabeno, P.J., Bell, S.W., 2019. Extreme Conditions in the Bering Sea (2017–2018): Record-Breaking Low Sea-Ice Extent. Geophys. Res. Lett. 46, 8952–8959. https://doi.org/10.1029/2019GL083816

Stabeno, P., Kachel, N., Ladd, C., Woodgate, R., 2018. Flow Patterns in the Eastern Chukchi Sea: 2010–2015. J. Geophys. Res. Ocean. 123, 1177–1195. https://doi.org/10.1002/2017JC013135

Stevenson, D.E., Lauth, R.R., 2019. Bottom trawl surveys in the northern Bering Sea indicate recent shifts in the distribution of marine species. Polar Biol. 42, 407–421. https://doi.org/10.1007/s00300-018-2431-1

Traynor, J., 1996. Target-strength measurements of walleye pollock (*Theragra chalcogramma*) and Pacific whiting (*Merluccius productus*). ICES J. Mar. Sci. 53, 253–258. https://doi.org/10.1006/jmsc.1996.0031

Trevorrow, M. V., 2005. The use of moored inverted echo sounders for monitoring meso-zooplankton and fish near the ocean surface. Can. J. Fish. Aquat. Sci. 62, 1004–1018. https://doi.org/10.1139/f05-013

Urmy, S.S., Horne, J.K., Barbee, D.H., 2012. Measuring the vertical distributional variability of pelagic fauna in Monterey Bay. ICES J. Mar. Sci. 69, 184–196. https://doi.org/10.1093/icesjms/fsr205

Vestfals, C.D.C.D., Mueter, F.J.F.J., Hedstrom, K.S.K.S., Laurel, B.J.B.J., Petrik, C.M.C.M., Duffy-Anderson, J.T.J.T., Danielson, S.L.S.L., 2021. Modeling the dispersal of polar cod (*Boreogadus saida*) and saffron cod (*Eleginus gracilis*) early life stages in the Pacific Arctic using a biophysical transport model. Prog. Oceanogr. 196, 102571. https://doi.org/10.1016/j.pocean.2021.102571

Vestfals, C.D., Mueter, F.J., Duffy-Anderson, J.T., Busby, M.S., De Robertis, A., 2019. Spatio-temporal distribution of polar cod (Boreogadus saida) and saffron cod (*Eleginus gracilis*) early life stages in the Pacific Arctic. Polar Biol. 42, 969–990. https://doi.org/10.1007/s00300-019-02494-4

Wang, M., Yang, Q., Overland, J.E., Stabeno, P., 2018. Sea-ice cover timing in the Pacific Arctic: The present and projections to mid-century by selected CMIP5 models. Deep. Res. Part II Top. Stud. Oceanogr. 152, 22–34. https://doi.org/10.1016/j.dsr2.2017.11.017

Weingartner, T., Aagaard, K., Woodgate, R., Danielson, S., Sasaki, Y., Cavalieri, D., 2005. Circulation on the north central Chukchi Sea shelf. Deep Sea Res. Part II Top. Stud. Oceanogr. 52, 3150–3174. https://doi.org/10.1016/j.dsr2.2005.10.015

Weingartner, T., Dobbins, E., Danielson, S., Winsor, P., Potter, R., Statscewich, H., 2013. Hydrographic variability over the northeastern Chukchi Sea shelf in summer-fall 2008-2010. Cont. Shelf Res. 67, 5–22. https://doi.org/10.1016/j.csr.2013.03.012

Wilson, R.E., Sage, G.K., Wedemeyer, K., Sonsthagen, S.A., Menning, D.M., Gravley, M.C., Sexson, M.G., Nelson, R.J., Talbot, S.L., 2019. Micro-geographic population genetic structure within Arctic cod (*Boreogadus saida*) in Beaufort Sea of Alaska. ICES J. Mar. Sci. 76, 1713–1721. https://doi.org/10.1093/icesjms/fsz041

Woodgate, R.A., Peralta-Ferriz, C., 2021. Warming and Freshening of the Pacific Inflow to the Arctic from 1990-2019 implying dramatic shoaling in Pacific Winter Water ventilation of the Arctic water column. Geophys. Res. Lett. https://doi.org/10.1029/2021GL092528

Woodgate, R.A., 2018. Increases in the Pacific inflow to the Arctic from 1990 to 2015, and insights into seasonal trends and driving mechanisms from year-round Bering Strait

mooring data. Prog. Oceanogr. 160, 124–154. https://doi.org/10.1016/j.pocean.2017.12.007

Woodgate, R.A., Weingartner, T., Lindsay, R., 2010. The 2007 Bering Strait oceanic heat flux and anomalous Arctic sea-ice retreat. Geophys. Res. Lett. 37, 1–5. https://doi.org/10.1029/2009GL041621

Woodgate, R.A., Aagaard, K., Weingartner, T.J., 2005. A year in the physical oceanography of the Chukchi Sea: Moored measurements from autumn 1990-1991. Deep. Res. Part II Top. Stud. Oceanogr. 52, 3116–3149. https://doi.org/10.1016/j.dsr2.2005.10.016

4.8 SUPPLEMENTARY INFORMATION

Supplementary Table 4.1 Compass heading and magnetic declination at each mooring deployment site.

Deployment	Site	Compass Heading (°)	Magnetic Declination (°)
2017 - 2018	Southern	335	9.6
	Central	208	11.6
2018 - 2019	Southern	172	10.3
	Central	198	12.2
	Northern	293	13.4

Supplementary Table 4.2 Parameter values used in Echoview's fish four-dimensional alpha-beta fish tracking module (Echoview Software Pty Ltd; Blackman, 1986).

Parameter	Major axis	Minor Axis	Range	Target Strength	Ping Gap
Alpha	0.6	0.6	0.6		
Beta	0.0	0.0	0.0		
Exclusion Distance (m)	0.7	0.7	0.3		
Missed Ping Expansion (%)	10	10	10		
Parameter Weighting	30	30	30	30	10

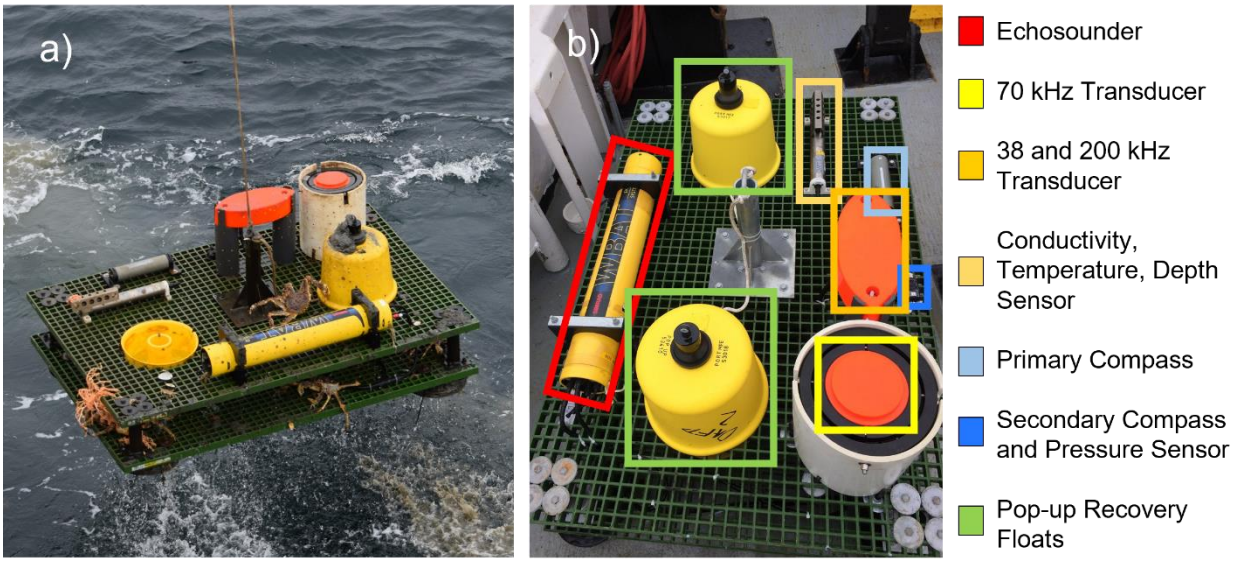

Supplementary Figure 4.1 Photographs of (a) mooring upon recovery and (b) mooring instrumentation.

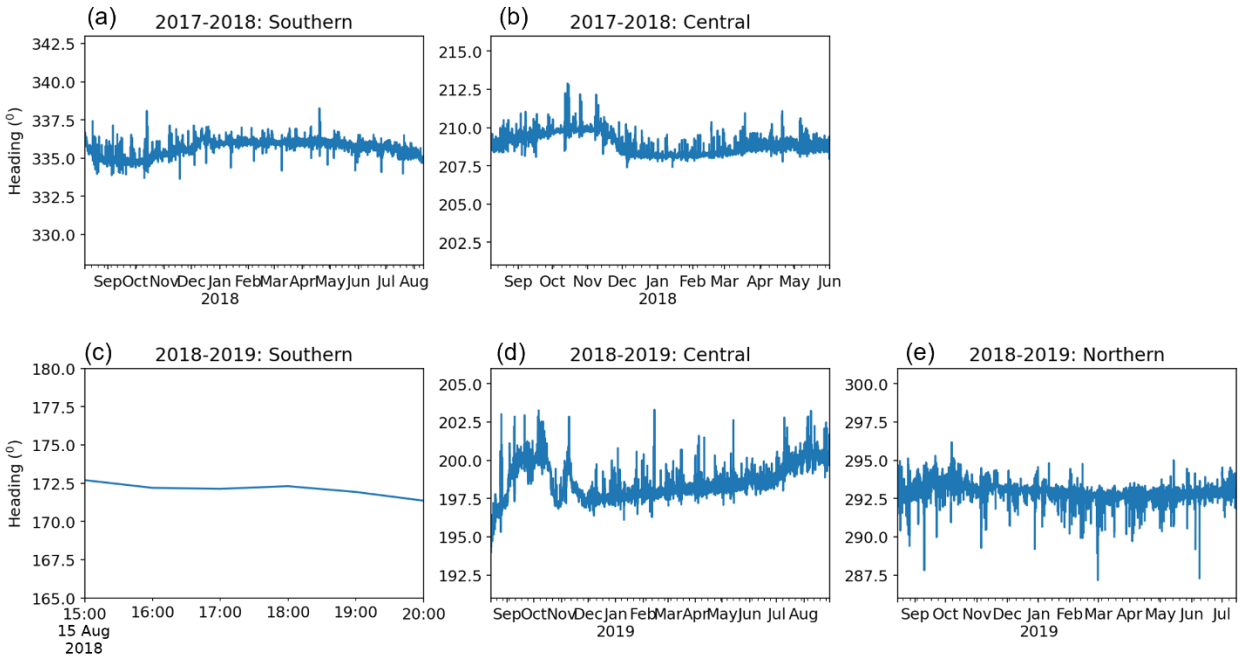

Supplementary Figure 4.2 Heading direction recorded by primary compass during 2017-2018 deployments at the (a) southern and (b) central mooring sites, and during 2018-2019 deployments at the (c) southern, (d) central, and (e) northern mooring sites. Five deployments (a, b, d, and e) were collected by a custom underwater magnetometer produced by the Engineering Development division of the NOAA Pacific Marine Environmental Lab. The short duration of the recording at the southern site in 2018-2019 (c) is due to battery limitations of the Aaronia GPS Logger (Aaronia AG) used on this mooring.

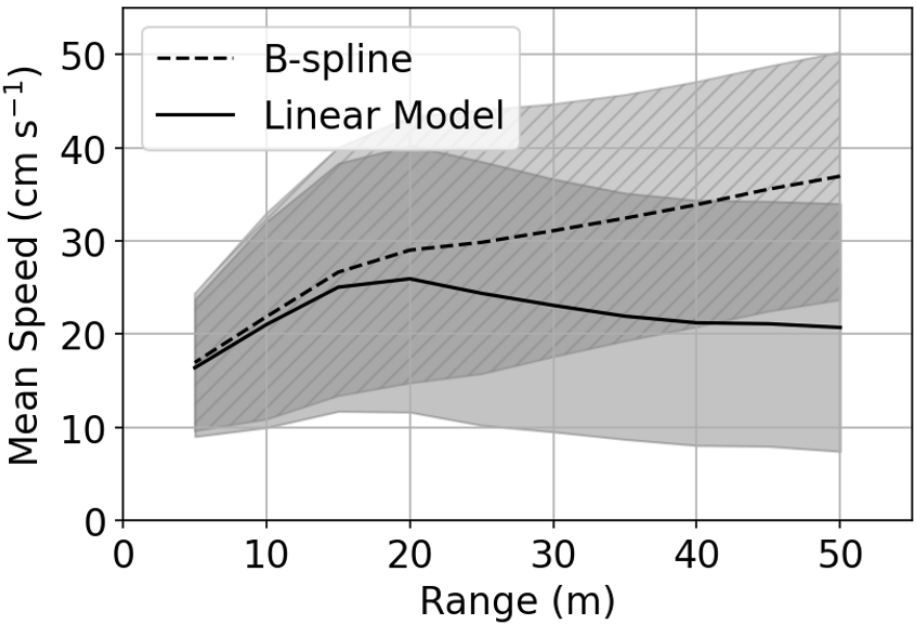

Supplementary Figure 4.3 Mean speed of fish tracks (cm s^{-1}) as a function of range (5-m bins) calculated from the B-spline range (solid line) and linear model (dashed line) representations of all fish tracks. ±1 SD is shown for the linear (solid grey) and B-spline (hatched grey) speeds.

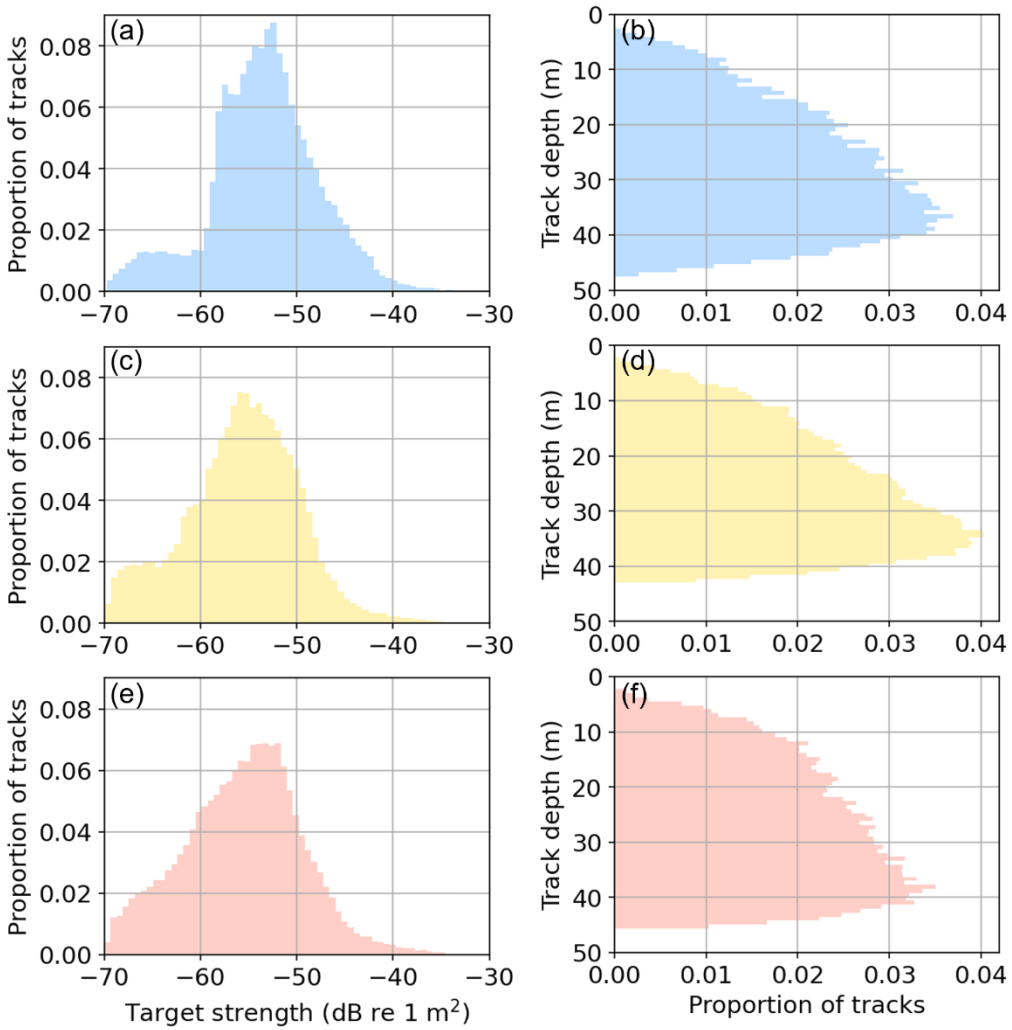

Supplementary Figure 4.4 Distribution of mean target strength (dB re 1 m^2) of all fish tracks at the (a) northern, (c) central, and (e) southern sites. A threshold of -70 dB re 1 m^2 was used for target detection. Depth distribution of fish tracks at (b) northern, (d) central, and (f) southern sites.

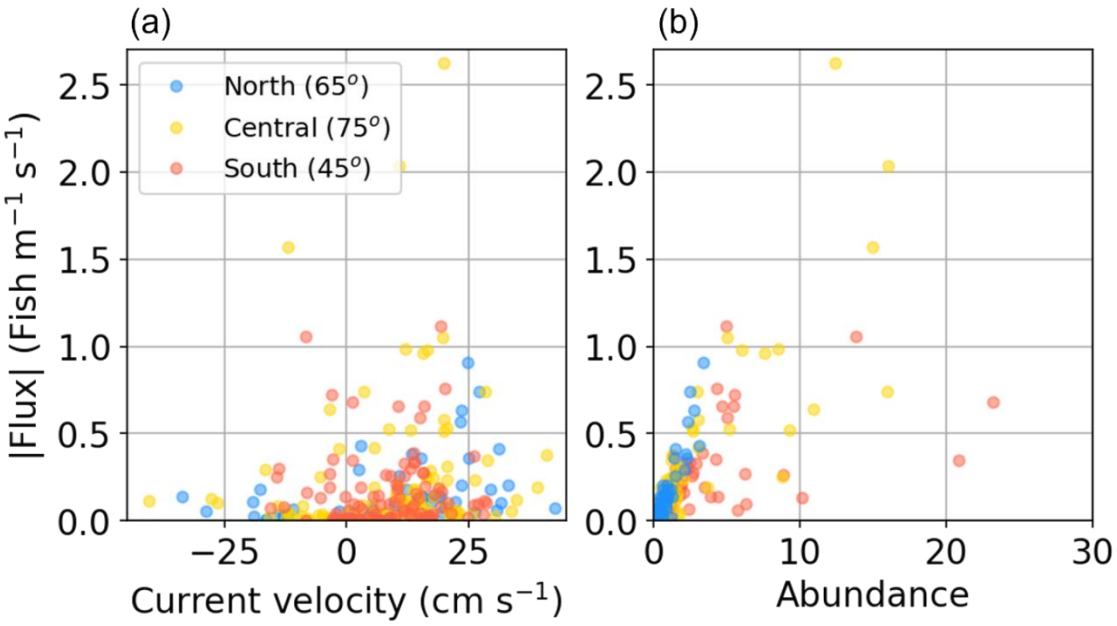

Supplementary Figure 4.5 Absolute value of mean weekly fish fluxes calculated along the reference heading along the reference heading (the mode of track headings observed at each site) indicated in the legend for each site relative to (a) the mean weekly current velocity and (b) mean weekly fish abundance at the northern (blue), central (yellow), and southern (red) sites.

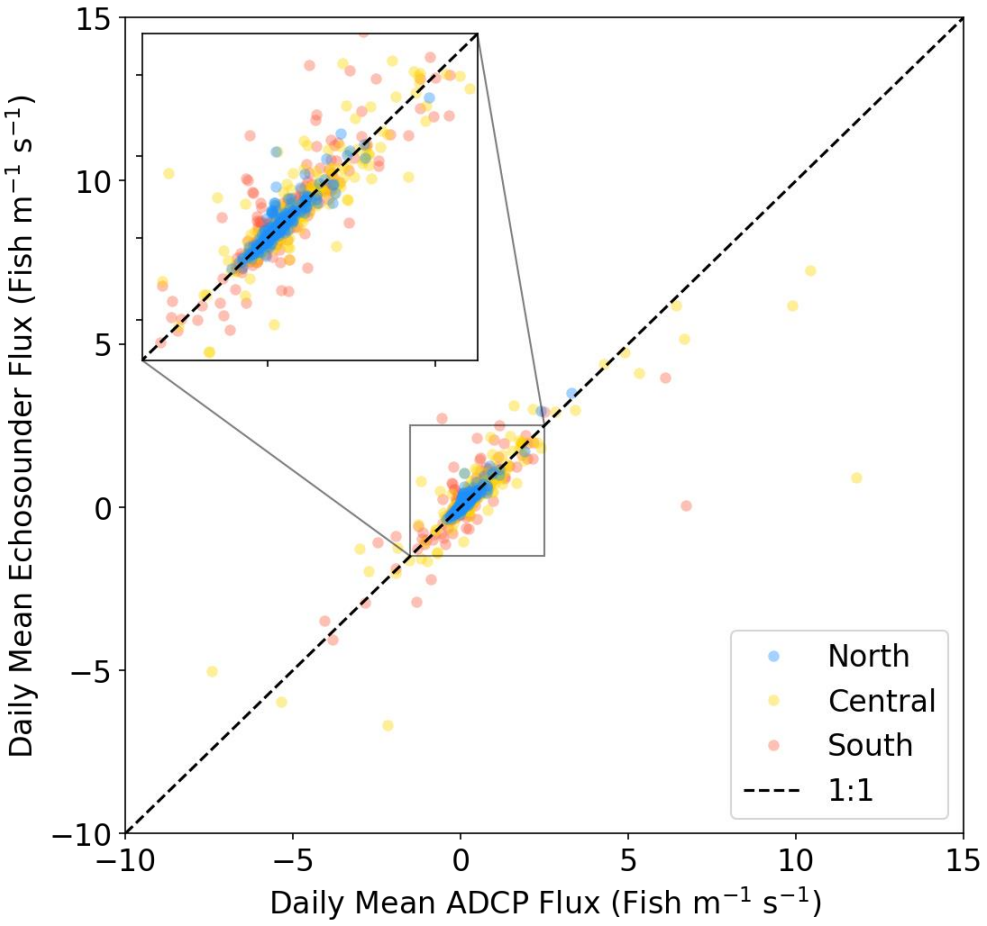

Supplementary Figure 4.6 Comparison of daily fish flux at the northern (blue), central (yellow), and southern (red) mooring sites calculated using velocity and heading from the acoustic doppler current profiler (ADCP) and fish tracks measured by the echosounder. The 1:1 line is shown as a reference (black dashed line).

CHAPTER 5. SOUND AND THE SEAFLOOR: DETERMINING BATHYMETRY USING STUDENT-BUILT ACOUSTIC SENSORS

A version of this manuscript has been previously published as:

Levine, R.M., Seroy, S. K, Grünbaum, D. (2020). Sound and the Seafloor: Determining bathymetry using student-built acoustic sensors. Oceanography, 33(3): 71-77. https://doi.org/10.5670/oceanog.2020.305

5.1 PURPOSE

Many undergraduate oceanography students have few opportunities to use ocean technologies on seagoing research vessels. For those who do, understanding sensor function and principles governing instruments like the echosounder systems used to detect the seafloor can be complex and inaccessible. This activity's goal is to introduce students to the concept and function of underwater acoustics using inexpensive and commercially available sensor building materials. The activity gives students experience with ocean sensors through (1) hands-on engagement with electronics and building of circuits, (2) construction and use of their own simplified echosounder, (3) application of acoustics in ocean bathymetry and seafloor mapping by producing a map of acoustic soundings along a transect, and (4) use of their own data to explore implications of sampling resolution. This activity also serves as an introduction to microcontrollers and

environmental sensing, providing students with a foundation for working with additional applications and sensors, and for further exploration.

5.2 Audience

The activity was designed for an intermediate-level undergraduate oceanography course in ocean technology and engineering. With minimal modifications, this activity is appropriate for introductory through advanced undergraduate-level oceanography courses across a variety of disciplines, as well as for high school marine science, technology, or physics students. Variations of this activity are provided in the supplementary material.

5.3 Time Required

Prior to conducting this activity, we recommend instructors familiarize themselves with the Sensor Assembly Guide provided in the online supplementary material. Instructors should identify the components of assembly the students will be responsible for and give themselves sufficient time to acquire the necessary materials. We suggest conducting this activity over the course of two lab periods of one to two hours each. During the first session, students review the background information, assemble their sensors, and test the sensors in air. In the second session, students collect and analyze the data. We suggest that students work in small groups of two to four, depending on sensor availability and class size, though this activity can also be done individually.

5.4 BACKGROUND

5.4.1 *Bathymetry*

Bathymetry is the measurement of the depth of a body of water, and bathymetric surveys in which the seafloor is mapped serve many purposes across industries and research fields. For example, depth observations are used to create navigational charts, identify obstructions on the seafloor that could damage fishing gear, investigate underwater archaeological sites, and explore marine geologic phenomena such as underwater ridges and hydrothermal vents. Improving the coverage and resolution of these surveys is critical for maritime industries and for advancing our scientific understanding of many Earth processes.

Bathymetric measurements from ships are made using depth soundings. Historically, measurements were made using a weighted rope or wire, referred to as a sounding line, lowered to the seafloor over the side of a ship to measure water depth. The line was marked to indicate standard length intervals and deployed by hand or reel. Once the weight reached the seafloor, the length of line between the mark at the surface and the weight indicated the depth. These measurements were particularly hard to collect in deep water where, even using motorized reels, the process was time-consuming and inefficient for taking multiple measurements. Nonetheless, in the nineteenth and twentieth centuries, sounding machines deploying line or wire via a reel were commonly used for ocean exploration and led to major discoveries of seafloor features such as the Mid-Atlantic Ridge and the Mariana Trench (Dierssen and Theberge 2014; Figure 5.1).

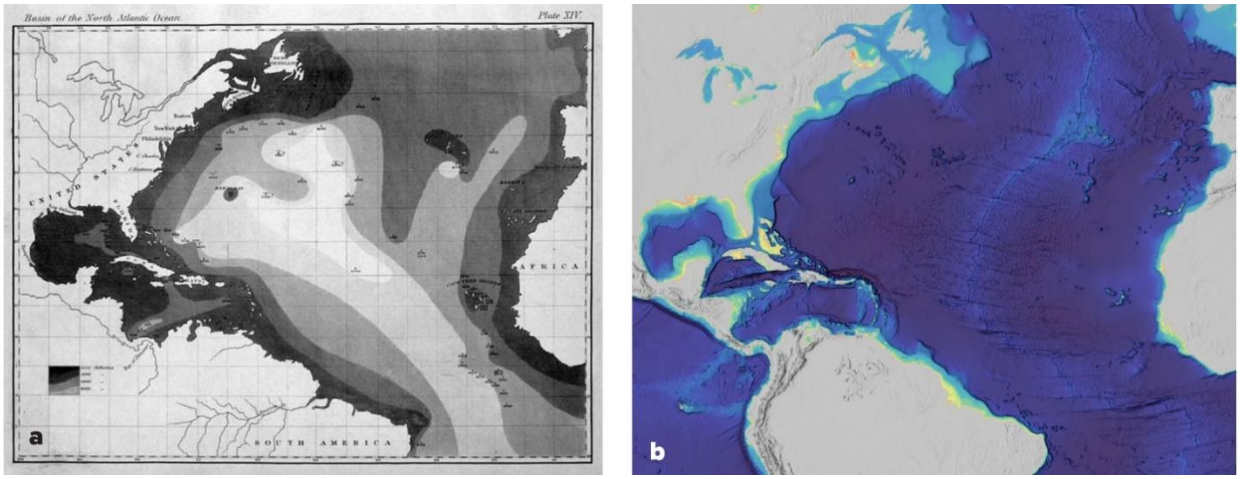

Figure 5.1 (a) First recorded bathymetric map of North Atlantic produced by Matthew Fontaine Maury in 1853 showing an indication of the Mid-Atlantic Ridge (courtesy of NOAA Photo Library). (b) Modern digital elevation model of the North Atlantic produced using a combination of echosounder and satellite measurements (NOAA National Centers for Environmental Information)

The invention of the piezoelectric transducer in 1917 made it possible for ships to collect echo soundings, depth measurements calculated by transmitting a pulse of sound through the water column and recording the echo that is reflected from the seafloor (Katzir 2012). In 1922, the US Navy conducted the first seafloor survey using an echosounder and compared depths measured via echo to those measured via sounding line (Anonymous 1923). The first commercial echosounder systems were produced in 1925 and quickly became the standard depth measurement instrument for hydrographic surveys. With the integration of echosounders into naval and research fleets, our understanding of the seafloor (particularly of deep regions of ocean basins) expanded quickly

during the mid-twentieth century. Further technological developments, including multibeam echosounders that image large swaths of the seafloor and satellite-based ranging, have continued to improve mapping capabilities (Figure 5.1).

5.4.2 *Sound in water*

Sound is a pressure wave, and thus needs a medium to propagate through—a gas, a liquid, or a solid. The speed of sound in water was first measured in 1827 by Colladon and Sturm at Lake Geneva. In their experiment, they simultaneously created a flash of light and rang a bell underwater and measured the timing of the arrival of those signals 16 km across the lake (Colladon 1893). By measuring the delay between the two signals, they could measure the speed of travel. The speed at which sound travels (c) is a function of compressibility, or its inverse the bulk modulus (B), and density (ρ):

$$c = \sqrt{\frac{B}{\rho}} \tag{5.1}$$

A sound wave is a propagation of a local compression. Mediums with lower compressibility push back with more force for a given decrease in volume when compressed. For example, water has much lower compressibility than air. We can represent a parcel of water as a strong spring and a parcel of air as a weak spring. To compress both springs to the same size, the strong spring (water) requires more force than the weak spring (air). This additional force means that the strong spring will bounce back faster and with greater force to return to its original state. This is the equivalent of a parcel of water exerting the force of a compression wave onto a

neighboring parcel. Due to this enhanced transfer of the compressional wave, sound both travels faster and propagates farther in water than in air. Though water is also denser, the difference in density is too small to compensate for the difference in compressibility. Because the speed of sound in any medium is a function of compressibility and density, the speed varies throughout the ocean due to changes in temperature, salinity, and pressure (Wong and Zhu 1995). On average, the speed of sound in the ocean is approximately 1,480 m s^{-1}, more than fourfold the average speed of sound in air (344 m s^{-1} at sea level and 21°C).

The ability to use sound to detect the seafloor is a function of the intensity of the transmitted signal (I_0), the energy lost during travel, and the reflectivity of the seafloor:

$$I_{rec} = I_0 \frac{e^{-4\alpha r}}{r^4} \sigma A \quad (5.2)$$

where I_{rec} is the intensity of the echo received at the transducer, r is the distance between the transducer and the seafloor, α is the absorption coefficient, A is the area of the seafloor the sound reflects off of, and σ is the scattering cross section. The scattering cross section is a function of the acoustic properties of the target (i.e., changes in the sound speed and the density relative to the water) that determines how much energy is reflected (Jackson and Richardson 2007). Energy lost as the pressure wave moves through the water, represented by $\frac{e^{-4\alpha r}}{r^4}$ in Equation 5.2, is a function of both geometric spreading and absorption. Geometric spreading is a decrease in the intensity of the signal per unit area as the signal travels away from the source and the energy spreads out over a larger area. Absorption is the loss of acoustic energy due to the conversion of the signal's energy to heat.

Once an echo from the seafloor is received, the time between when the signal was transmitted from the surface and when the echo was received is used to calculate the distance traveled, and thus the range to the seafloor (Figure 5.2):

$$d = ct \tag{5.3}$$

Here, distance (d) is the product of the speed of sound (c) and the time it takes the signal to travel (t). For example, given an echo with a delay of 0.5 s from the transmitted signal and the speed of sound in water (c = 1,480 m s^{-1}), Equation 5.3 tells us that d = (1,480 m s^{-1})(0.5 s) = 740 m. The estimated range to the seafloor is 370 m, half of the total distance traveled to and from the seafloor by the transmitted signal.

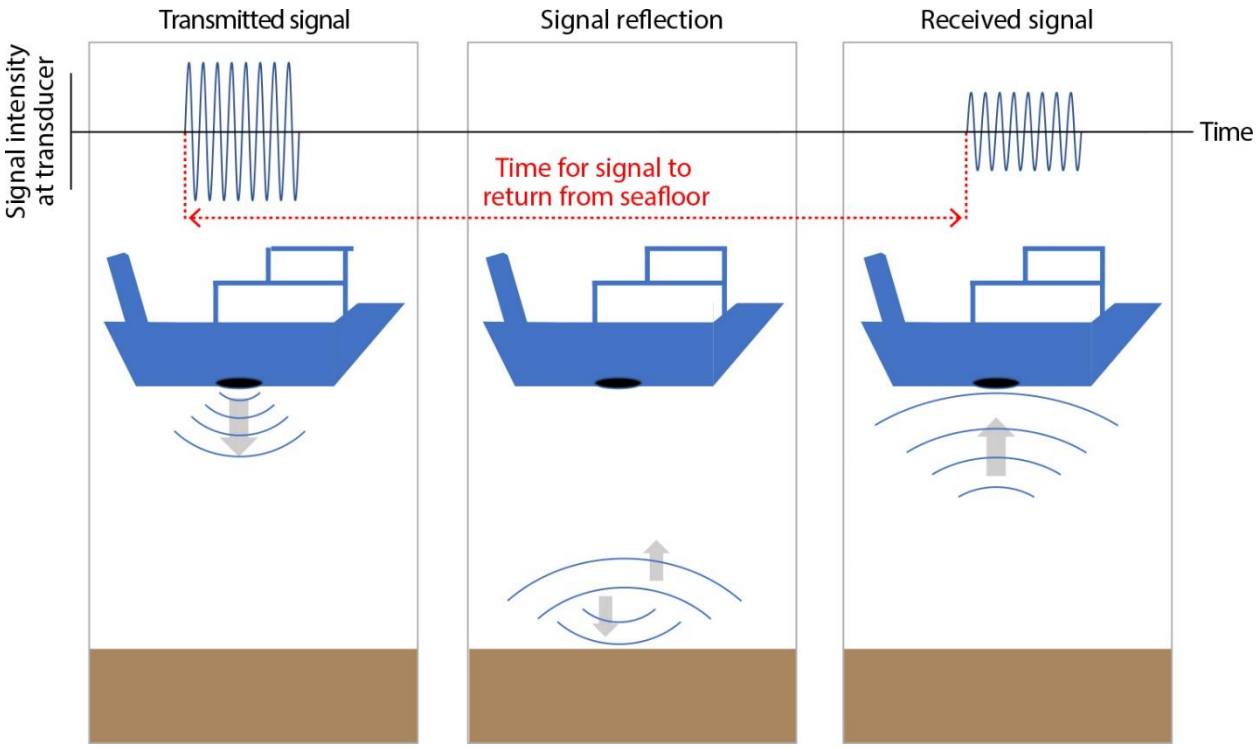

Figure 5.2 Steps of echosounder detection of seabed, with direction of sound wave (blue lines) indicated by grey arrows. A signal is transmitted by the transducer at the surface (left box). Upon reaching the seafloor, the signal is reflected to the surface (middle box). The return signal is received by the transducer (right box). The signal intensity is lower upon return due to transmission loss.

5.4.3 *Sampling resolution*

These calculations to (1) detect the seafloor, and (2) calculate the depth based on the distance traveled are the foundations of acoustic bathymetry. The ability to detect, resolve, and map features on the seafloor depends on the sampling resolution and coverage. On many modern vessels, echosounder systems use a single-beam transducer mounted to the hull. For single-beam systems,

increasing the horizontal resolution of the bathymetry measurements requires increasing the number of observations of the seafloor collected over a given distance. The distance between measurements is dictated by both the speed at which the ship is moving and the ping rate (number of sound waves transmitted per unit time). In practice, the horizontal resolution is also limited by the angle at which the acoustic beam expands as it moves away from the transducer. The width of the acoustic beam at a given depth is referred to as the beamwidth. The narrower the beamwidth, the smaller the area of the seafloor reflecting the signal. Narrow beamwidths enable collection of more closely spaced measurements. A higher number of independent observations can then be made over a given distance to construct a higher resolution map. More advanced technologies, such as multibeam systems that sample a swath of the seafloor, are elaborations of these same acoustic principles; they increase the sampling resolution by increasing the number and density of seafloor observations that can be measured from a ship's position.

5.4.4 *Active learning through sensor building*

In our activity, students use basic acoustic principles and Equation 5.3, the distance equation, to repurpose an inexpensive ultrasonic distance sensor as a single-beam echosounder to conduct a bathymetric survey. A key component of this activity is the construction and use of low-cost microcontroller-based sensors that operate using the same principles as commercial instrumentation. Hands-on sensor activities can help students understand the design and use of ocean technology in oceanographic industry and research (Kelley and Grünbaum 2018). Sensor

building exposes students to principles of electronics and engineering, while facilitating an understanding of oceanography and physics concepts through hands-on applications. Through sensor building, students can more effectively learn and apply field-specific concepts (Seroy et al., 2019). Across STEM disciplines, active learning experiences like these have been shown to increase working knowledge of scientific concepts (Freeman et al., 2014) and provide exposure to engineering principles and skills that may benefit students beyond their educational endeavors (Boss and Loftin 2012).

5.5 ACTIVITY

During this activity, students assemble waterproof ultrasonic distance sensors, and use them to take echo soundings in a local body of water to map bathymetry. These sensors utilize the sonar equation to detect the distance of an object located in the path of the acoustic signal. The associated open-source materials provide an opportunity for a range of engagements with concepts in both oceanography and physics.

5.5.1 *Research question*

Students are directed to answer the question: What is the slope and structure of the bottom of a body of water? In the process of collecting data, they will also identify sources of error and assess the precision of their sensors. By collaborating with other students to increase the resolution of their data set, they will also explore the role of sampling frequency in their ability to resolve bottom features.

5.5.2 *Materials*

To gain experience with sensor technology and demystify sensor function, students should construct their own sensors during an initial class period. Details on microcontrollers, components, and sensor assembly can be found in the Sensor Assembly Guide in the supplementary material and at PublicSensors (https://www.publicsensors.org/). Sensor components include:

- A MicroPython-based microcontroller. Examples are shown using Adafruit's Feather HUZZAH with ESP8266 ($17), a MicroPython-based microcontroller (Figures 5.3 and 5.4b). Up-to-date firmware and required Python scripts are available on the PublicSensors GitHub repository (https://github.com/publicsensors). Other microcontrollers (e.g., Arduino-based) are compatible, but resources are not provided.
- An ultrasonic distance sensor (hereafter referred to as an acoustic sensor) with a waterproof transducer (JSN-SR04T, $11). This acoustic sensor operates using the same principles as a scientific echosounder. When the sensor receives a trigger signal, it transmits a set of 8 pulses at 40 kHz into the water. The sensor then waits 38 milliseconds for an echo to be received. In water with no obstructions, this timeout corresponds to a theoretical maximum detection distance of ~28 m (~6 m in air). However, loss of signal energy as described in the background can further limit this distance. Due to transducer construction, frequency, and length of transmit signal, the minimum distance an object can be detected in water is ~0.8 m (~0.2 m in air).

Students will also need a laptop for communication with the microcontroller and for data plotting/analysis.

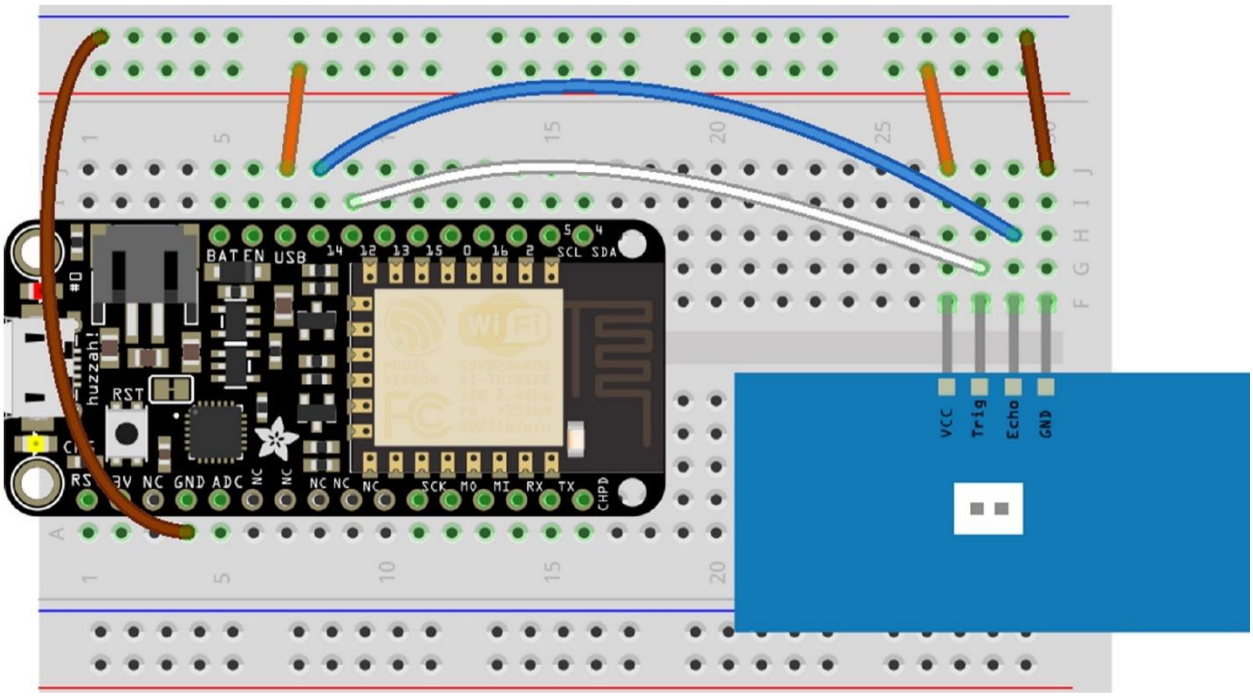

Figure 5.3 Fritzing (www.fritzing.org) diagram showing the wiring required for the JSN-SR04T using a breadboard. The *Trig* and *Echo* pins on the JSN-SR04T should be connected to GPIO 12 and 14, respectively, on the ESP8266 Feather. The *GND* pin on the JSN-SR04T should be connected to the GND pin on the ESP8266 Feather and the *VCC* pin on the JSN-SR04T to the SB pin on the ESP8266 Feather. Both the *GND* and *VCC* pins can be connected to the microcontroller via the breadboard rails.

Figure 5.4 Acoustic measurements being taken along a dock. (b) Assembled microcontroller using breadboard connections for acoustic sensor and Feather HUZZAH with ESP8266 microcontroller. (c) The transducer lowered so that the 10 cm tape mark is located at the waterline for consistent sampling.

5.5.3 *Sensor assembly and initial exploration*

We recommend providing students with microcontrollers already containing the firmware and necessary files installed, although we encourage instructors to have students conduct as much of the construction and assembly as possible, depending on the time and resources available (see

Sensor Assembly Guide sections 3–5 in the supplementary material for detailed step-by-step instructions).

Using a breadboard and male/male jumper wires, connect the acoustic sensor to the microcontroller as shown in Figure 5.3. The transducer cable should be marked with a piece of colored electrical tape or another easily identifiable marker at 10 cm distance from the face of the transducer.

- Connect the microcontroller to a computer with the USB cable. Using a serial terminal (e.g., Beagle Term), connect to the microcontroller. To initialize the sensor, import the *hcsr04* library: `import hcsr04`
- Set pin designations and speed of sound: `sensor = hcsr04.HCSR04(trigger_pin = 12, echo_pin = 14, c = 344)`
- Use the distance function to collect a measurement (reported in centimeters): `sensor.distance()`

Students can complete an initial exploration using their sensors in air (c = 344 m s^{-1}) to assess sensor accuracy and precision, while informing their understanding of potential sources of variability when collecting measurements in water. See Alternative Approaches and Extensions below for optional activities to first determine the speed of sound. Students should collect replicate measurements from a fixed, known distance such as from a tabletop to the floor, wall, or other stationary object. They should consider measurement consistency and possible sources of variability. How are precision and accuracy affected by directly introducing known variability

(e.g., measuring the distance from an angled surface or moving a hand between the sensor and the target object)?

Students can assess the role of sampling resolution in resolving features by profiling a feature in air (e.g., a book on the floor) and taking measurements at different spatial intervals relative to feature size. This exploration, analogous to the in-water component of the activity, will help troubleshoot and provide background for understanding how to interpret underwater measurements. Using items on the floor or furniture against a wall, students can take measurements along a continuous transect and consider the necessary number of samples or the interval between measurements that would be required to resolve (1) that a feature is present, and (2) the relief of said feature.

5.5.4 *Data collection*

Before students collect their measurements in water, the sampling transect should be defined and students assigned to their sampling positions. We recommend providing students opportunities to test and explore their sensors in water.

- Mark sampling positions at fixed intervals along an accessible shallow body of water (i.e., dock, pool). We recommend approximately 20 sampling locations at one-meter intervals to provide space for groups of students sampling at adjacent positions. However, this is flexible depending on the size and accessibility of the sampling site.

- Assign each group of students a starting point and sampling interval (e.g., Group 1 begins at the zero-meter position and samples every two meters, and Group 2 begins at the one-meter position and samples every two meters).

Students should collect replicate measurements at each assigned sampling position using c = 1,480 m s^{-1}. See Alternative Approaches and Extensions below for an optional component to determine the speed of sound in situ. When working in proximity to water, students should take extra caution and be provided with proper safety equipment (e.g., life vests), if necessary.

- At each sampling position, lower the sensor so that the transducer is completely submerged, and the marked 10 cm line is at the water's surface (Figure 5.4c).
- Collect a measurement of depth and record the value (Table 5.1). Be sure to include the offset of the distance of the transducer below the water's surface (e.g., if the sensor reports a distance of 525 cm and the tape mark is at 10 cm, add the additional 10 cm to the distance and record 535 cm).
- Take an additional two measurements at the same position, waiting a minimum of 10 seconds between each measurement.
- Repeat at each subsequent sampling position.

Table 5.1 Example of a sample recording table. Students record location as a measure of distance (e.g., “4 m”) and values for three measurements collected at that location in units of meters. Additional examples of data recording are included in the supplementary material.

Sampling Position (m)	Measurement 1 (m)	Measurement 2 (m)	Measurement 3 (m)
0	4.53	4.62	4.61
2	5.02	4.90	5.02
…	…	…	…
20	7.80	7.80	7.74

5.5.5 *Data analysis*

Students should create a bathymetry plot from their own data, where the x-axis is distance along the dock and the y-axis is depth (Figure 5.5).

- Include all three distances measured at each location to indicate the precision of the depth estimate.
- Groups with alternating starting locations should share their data with each other, to compare the combined data set with their own.

Examples of plotting methods using both Microsoft Excel and Python Jupyter Notebooks are included in the supplementary material. After plotting the data, students should calculate estimates of seafloor depth and slope along the dock, including derived measurements such as height and maximum/minimum relief (angle) of features.

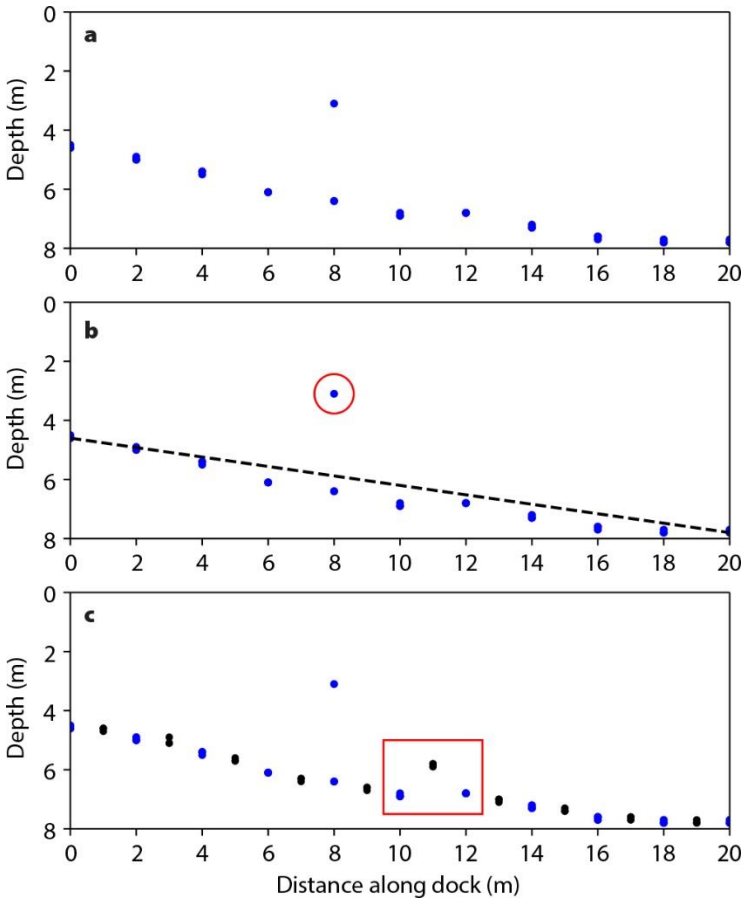

Figure 5.5 Example data analysis figures showing (a) data collected by a single group; (b) the identification of an outlier and slope of seafloor shown as the dashed line; and (c) combined datasets of two groups, indicating the presence of a feature previously unidentified in the original dataset (red box).

5.5.6 *Reflection*

Once students have plotted their data, they should consider what their observations imply and the sources of variability. Questions might include the following:

- What features could you identify from your own data?

- Were there features that were possible to discern only in the combined, higher-resolution data set? What were the apparent size and shape of these features?
- How precise was your sensor (how variable were replicate measurements taken at a single location)? What are the possible causes of that variability?
- Identify and remove apparent outliers (https://en.wikipedia.org/wiki/Outlier) from your data set and replot the measurements. Justify your decision for removing these points in the context of the rest of your data. What could have caused measurement outliers? How might this affect the bathymetric profile and statistics?

5.6 ALTERNATIVE APPROACHES AND EXTENSIONS

Students can use the sensor to quantify the speed of sound in air or water by calibrating the sensor using an object positioned at a fixed known distance. This can also be accomplished by using a sounding line to ground truth depths at a subset of locations in the same body of water as the bathymetry activity. This is most effective when completed prior to the profiling activity, as an opportunity for students to calculate the speed of sound in one or both mediums themselves. It can be further expanded by conducting the same calibration activity in a variety of mediums with varying densities, such as fresh vs. salt water. Details are outlined in the Activity Extensions supplementary material.

In addition to taking vertical profiles along a transect, the sensor can be used to take measurements at multiple fixed angles along the original transect. These observations can be used

to create a contour plot of bathymetry. Measurements taken at an angle along the transect demonstrate the function of side-scan and multibeam echosounder systems and can be used to investigate more advanced data processing and visualization methods. Students could consider:

- How does the apparent depth/distance vary as a function of angle?
- What is the maximum angle at which a return echo is received?

Additional extensions and materials for the approaches described above can be found at PublicSensors (https://www.publicsensors.org/).

5.7 Acknowledgements

We would like to thank the students of OCEAN 351 at the University of Washington who participated in the original iterations of this lab module. We also thank Emmanuel Boss, Tom Weber, and two anonymous reviewers for helpful comments that improved this lab exercise.

5.8 References

Anonymous, 1923. Echo sounding. Int. Hydrogr. Rev. 1.

Boss, E., Loftin, J., 2012. Engineering literacy for undergraduates in marine science a case for hands on. Oceanography 25, 220–222. https://doi.org/10.5670/oceanog.2012.61

Colladon, J.D., 1893. Souvenirs et mémoires: Autobiographie de J. Daniel Colladon. Albert-Schuchardt, Geneva.

Dierssen, H.M., Theberge, A.E., 2014. Bathymetry: Seafloor mapping history, in: Yeqiao Wang (Ed.), Encyclopedia of Natural Resources - Water and Air - Vol II. CRC Press, Boca Raton, FL, pp. 644–648.

Freeman, S., Eddy, S.L., McDonough, M., Smith, M.K., Okoroafor, N., Jordt, H., Wenderoth, M.P., 2014. Active learning increases student performance in science, engineering, and mathematics. Proc. Natl. Acad. Sci. U. S. A. 111, 8410–8415. https://doi.org/10.1073/pnas.1319030111

Jackson, D.R., Richardseon, M.D., 2007. High-Frequency Seafloor Acoustics. Springer Science & Business Media, New York, NY.

Katzir, S., 2012. Who knew piezoelectricity? Rutherford and Langevin on submarine detection and the invention of sonar. Notes Rec. R. Soc. https://doi.org/10.1098/rsnr.2011.0049

Kelley, D., Grünbaum, D., 2018. Seastate: Experiential C-STEM Learning Through Environmental Sensor Building. Oceanography 31, 147–147. https://doi.org/10.5670/oceanog.2018.123

Seroy, S.K., Zulmuthi, H., Grünbaum, D., 2020. Connecting chemistry concepts with environmental context using student-built pH sensors. J. Geosci. Educ. 68, 334–344. https://doi.org/10.1080/10899995.2019.1702868

Wong, G.S.K., Zhu, S. ming, 1995. Speed of sound in seawater as a function of salinity, temperature, and pressure. J. Acoust. Soc. Am. 97, 1732–1736. https://doi.org/10.1121/1.413048

5.9 SUPPLEMENTARY INFORMATION

5.9.1 *Sensor assembly guide*

The following instructions provide instructors and students with the necessary steps to assemble and operate the acoustic sensor used in the activity. Instructions in the *Sensor Assembly and Initial Exploration* section of the activity are summarized from sections 3, 4, and 5 and assume students have microcontrollers that have been set up according to the instructions provided in sections 1 and 2 below. Instructors are encouraged to have students conduct as much of the sensor construction and assembly as possible given the time and resources available.

5.9.1.1 Materials list

Suggested materials are detailed in Supplementary Table 5.1, including cost estimates. While we recommend the Feather Huzzah with ESP8266, the activity and materials provided are meant for use with any MicroPython-based microcontroller. Support for additional sensors and alternative microcontrollers is provided on the PublicSensors Microcontroller Kit GitHub repository. Other microcontrollers or programming languages (i.e., CircuitPython, Arduino) can be used, though instructions are not provided. We recommend the use of a breadboard and Male/Male jumper wires to connect the ultrasonic module to the microcontroller, though Male/Female pins directly connecting the module and microcontroller can be used in place of a breadboard.

Supplementary Table 5.1 Required materials for the assembly of the sensors, with cost per unit and total pricing for 12 kits (10 students groups + 2 spare). Additional materials for conducting the activity are included. Many of the Adafruit products listed are also available via Digi-Key (www.digikey.com) and other online retailers.

Sensor Materials		
Components	Cost Per Unit	Cost Per 12 kits
Feather Huzzah with ESP8266	$16.95 (www.adafruit.com)	$203.40 (12)
Male/Male Jumper Wires	$1.95 (www.adafruit.com)	$7.80 (4)
JSN-SR04T (or JSN-SR04T2.0/AJ-SR04M) waterproof ultrasonic module	$10.95 (www.jameco.com)	$131.40 (12)
MicroUSB cable	$2.95 (www.adafruit.com)	$35.40 (12)
Half-size breadboard	$5.00 (www.adafruit.com)	$60.00 (12)
	Total Cost	$438.00
Additional Materials		
Laptop	1 per group to communicate with sensors	
Color Coding Electrical Tape	1 roll to label transducer cable	
Tape Measure	1 to measure and mark sampling positions	

5.9.1.2 ESP8266 setup

The following are instructions for getting started with an ESP8266-based microcontroller. Additional information and instructions can be found in the open-access textbook Foundations of

Environmental Sensing, available via PublicSensors. The textbook and website also include additional activities and applications for MicroPython-based microcontrollers using other sensor modules.

Soldering

Microcontrollers can be purchased pre-soldered or with loose pin headers (Figure S1). Headers are required for use with both a breadboard and Female jumper wires. Pin headers come in strips and can be cut to size using a sharp edge (wire cutters, knife, etc.). The pins can then be soldered in place. Using a breadboard to hold the pins and microcontroller will help stabilize the materials while soldering. Once soldered, the microcontroller should look like the photo below (Supplementary Figure 5.1).

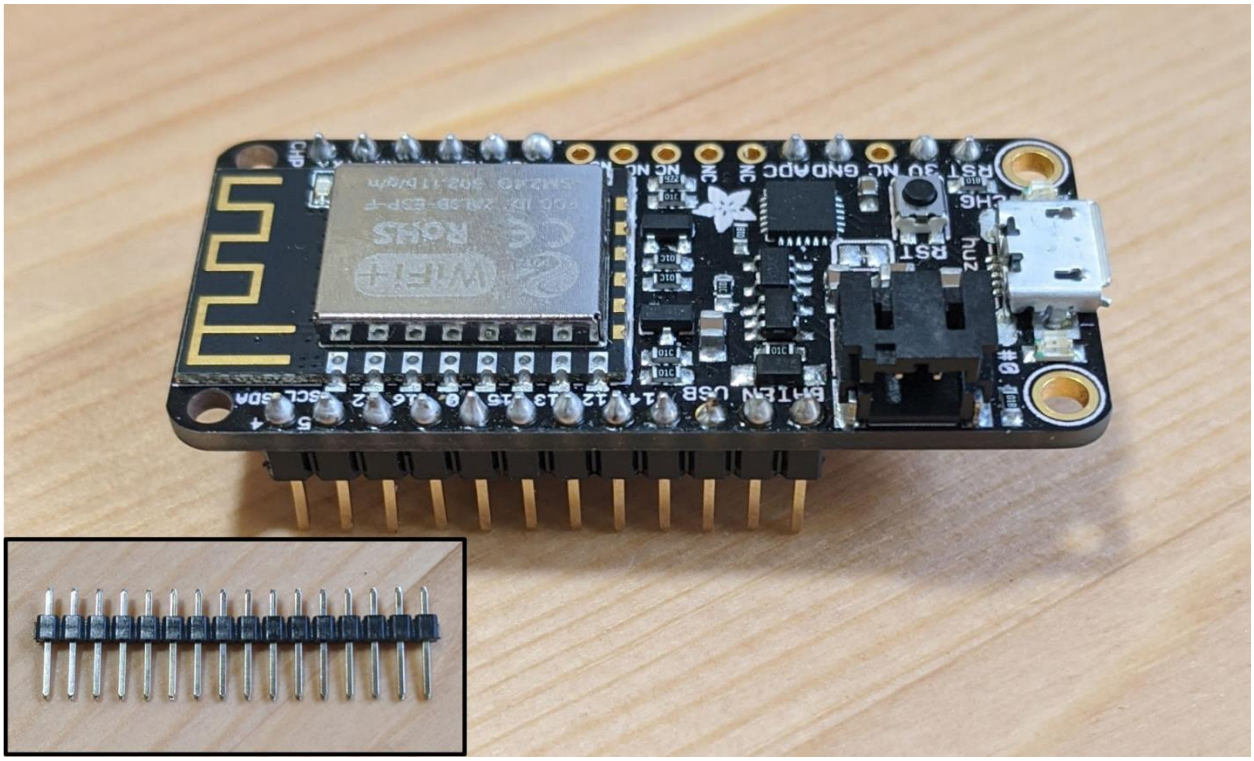

Supplementary Figure 5.1 Feather Huzzah with ESP8266, with pin headers (shown prior to soldering in the inset, lower left) soldered for use in a breadboard.

Micropython firmware

MicroPython is a Python programming language interpreter for use on microcontrollers. This allows students to use Python, a common programming language used in geosciences, to interact with their sensors. New microcontrollers will require MicroPython firmware be installed. The most recent firmware available, as well as instructions for loading the firmware onto the microcontroller, can be found in the MicroPython documentation available on their website, as well as in the activity GitHub repository. To install the firmware:

1. Download the ESP8266 Micropython firmware from MicroPython.org or the GitHub repository as linked above.
2. Install esptool (https://github.com/espressif/esptool/).
3. Connect the microcontroller to a computer using the USB cable, and using esptool, erase the flash by running esptool from the command line or terminal:

```
(base) C:\>esptool --port COM38 erase_flash
esptool.py v2.8
Serial port COM38
Connecting....
Detecting chip type... ESP8266
Chip is ESP8266EX
Features: WiFi
Crystal is 26MHz
MAC: bc:dd:c2:14:74:c0
Uploading stub...
Running stub...
Stub running...
Erasing flash (this may take a while)...
Chip erase completed successfully in 6.9s
Hard resetting via RTS pin...

(base) C:\>
```

‘COM38’ is the device address of the microcontroller and will likely be different based on the computer and microcontroller. You can determine the device name using the Windows device manager or using the ‘ls /dev/tty.*’ command on Mac OS or Linux.

4. Navigate to the directory of the firmware file downloaded in step 1 and deploy the new firmware:

```
(base) C:\firmware_folder>esptool --port COM38 --baud 460800 write_flash --flash_size=detect 0 firmware.bin
esptool.py v2.8
Serial port COM38
Connecting....
Detecting chip type... ESP8266
Chip is ESP8266EX
Features: WiFi
Crystal is 26MHz
MAC: bc:dd:c2:14:74:c0
Uploading stub...
Running stub...
Stub running...
Changing baud rate to 460800
Changed.
Configuring flash size...
Auto-detected Flash size: 4MB
Flash params set to 0x0040
Compressed 601860 bytes to 393107...
Wrote 601860 bytes (393107 compressed) at 0x00000000 in 9.2 seconds (effective 520.6 kbit/s)...
Hash of data verified.

Leaving...
Hard resetting via RTS pin...

(base) C:\firmware_folder>
```

Transferring files to the microcontroller

The ESP8266 Feather can be communicated with via USB or WiFi. For simplicity, we recommend having students start using the USB connection. WiFi connectivity can be useful when working with more advanced environmental sensors which are likely to be deployed in waterproof or cable-

less housings. To communicate with ESP8266 microcontrollers running MicroPython via USB, we suggest using one of the following tools, both of which are available for all operating systems:

- mpfshell: a python-based command line utility
- Beagle Term: an extension for Google Chrome

They key difference is that mpfshell allows for file transfer while Beagle Term does not. The following instructions are for transferring the necessary python files to the microcontrollers for the activity using mpfshell:

1. Install mpfshell by downloading the necessary files and following the instructions on the mpfshell GitHub repository.
2. Download ‘boot.py’, ‘hcsr04.py’, and ‘print_distance.py’ from the activity GitHub repository.
3. With the microcontroller connected to the computer, run mpfshell in a command window or terminal by typing ‘mpfshell’:

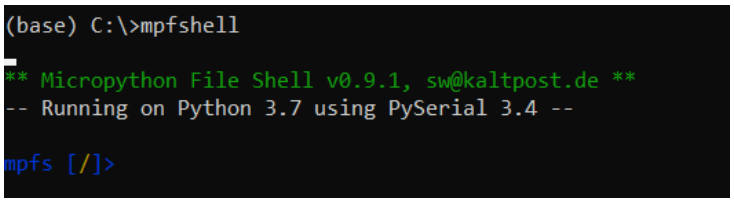

4. To connect to the microcontroller, type ‘open *SERIAL_DEVICE_ID*’, where *SERIAL_DEVICE_ID* is the device label or com port of the microcontroller, as described in section 2.2 above:

```
mpfs [/]> open com38
Connected to esp8266
mpfs [/]>
```

5. To add files to the microcontroller, use ‘put *FILENAME*.py’, where *FILENAME*.py is the target file:

```
mpfs [/]> open com38
Connected to esp8266
mpfs [/]> put hcsr04.py
mpfs [/]>
```

We recommend instructors conduct this portion of the setup themselves and provide students with microcontrollers that have already had MicroPython firmware and necessary files installed. Students can then use Beagle Term, which allows for serial communication within a Google Chrome browser window, to run commands and collect measurements. The instructions for conducting the activity using Beagle Term are presented in section 4 below. Foundations of Environmental Sensing provides additional instructions for using mpfshell (Chapter 1.2) or the ESP8266 WiFi connection (Chapter 1.3) for communication and file transfer using MicroPython’s WebREPL client.

5.9.1.3 Sensor assembly

The following instructions are included in the Sensor Assembly and Initial Exploration section of the activity and are also contained in the student handouts in the associated GitHub repository.

The USB cable provides 5V to the board, which means we can use the USB pin on the ESP8266 to give 5V to the JSN-SR04T. Newer versions of the sensor (JSN-SR04T-2.0) can operate at lower voltage, but still perform optimally at 5 volts. The JSN-SR04T sensor has 4 pins, GND,

VCC, Trig, and Echo.

1. Connect the *Trig* pin on the JSN-SR04T to GPIO 12 on the ESP8266 Feather.
2. Connect the *Echo* pin on the JSN-SR04T to GPIO 14 on the ESP8266 Feather.
3. Connect the *GND* pin on the JSN-SR04T to the GND pin on the ESP8266 Feather.
4. Connect the *VCC* pin on the JSN-SR04T to the USB pin on the ESP8266 Feather.
5. Using the breadboard, both the *GND* and *VCC* pins can be connected to the microcontroller via the breadboard rails (Supplementary Figure 5.2).
6. If not already connected, connect the transducer to the JSN-SR04T module.

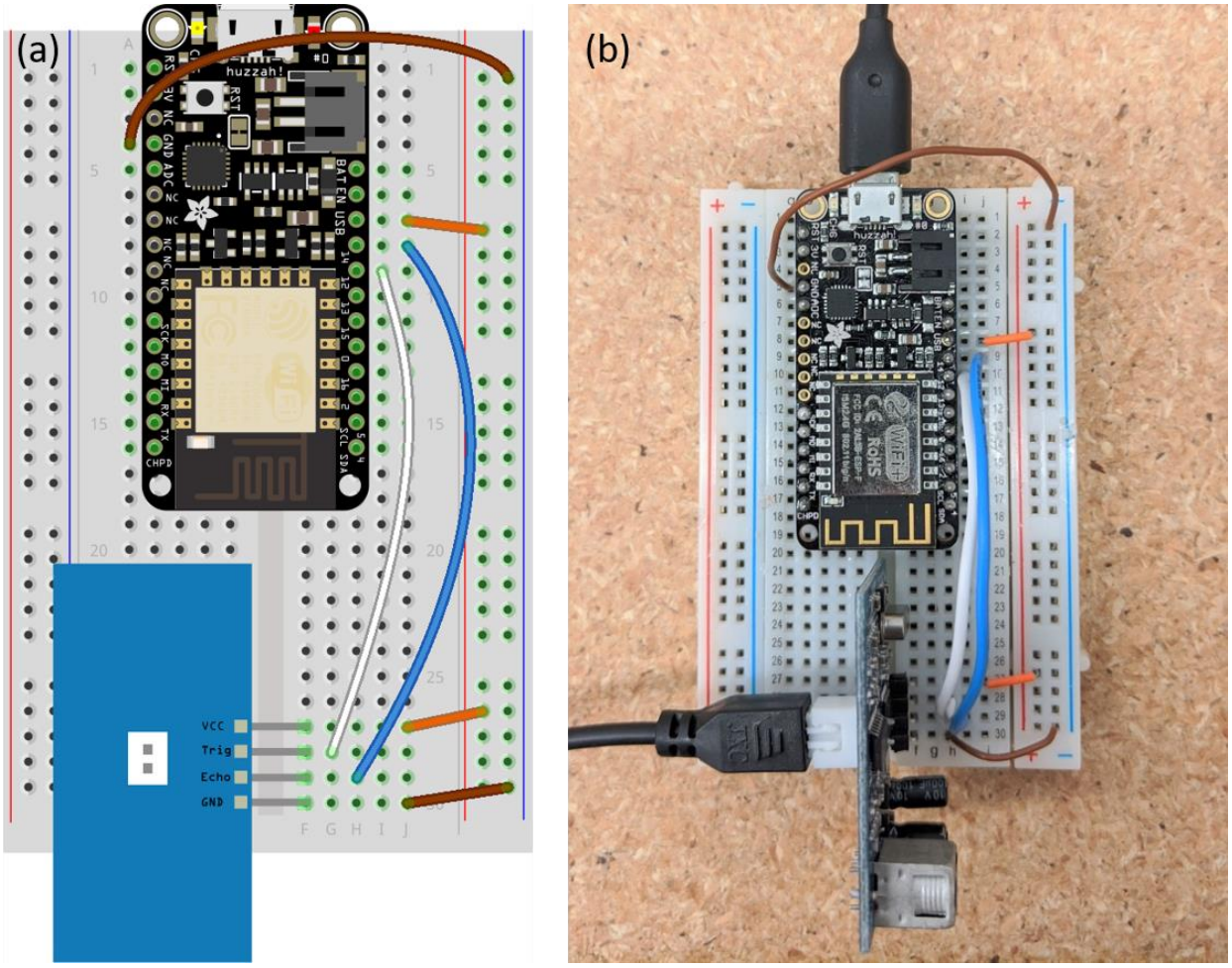

Supplementary Figure 5.2 (a) Fritzing (Fritzing.org) diagram showing the wiring required for the JSN-SR04T using a breadboard. (b) Photo of assembled sensor.

5.9.1.4 Connecting to the microcontroller

The instructions below should be provided to students for communication via Beagle Term. Additional materials and troubleshooting are available on the PublicSensors resources page.

1. Install the Google Chrome app, Beagle Term, which emulates a serial terminal inside of a browser window. From the Chrome Web Store add the Beagle Term app to the browser. If

you have difficulty finding it, searching ‘Beagle Term’ on Google will direct you to the app page in the Chrome Web Store.

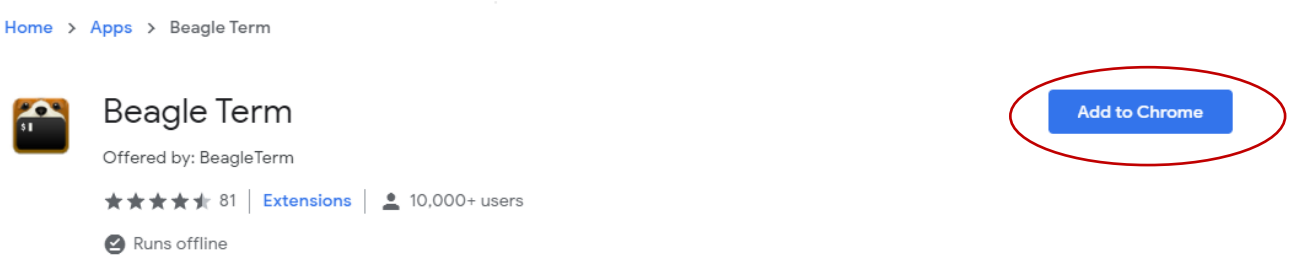

2. Once you add the app, you will be able to launch it from the same page:

Or access it via the Chrome Apps page :

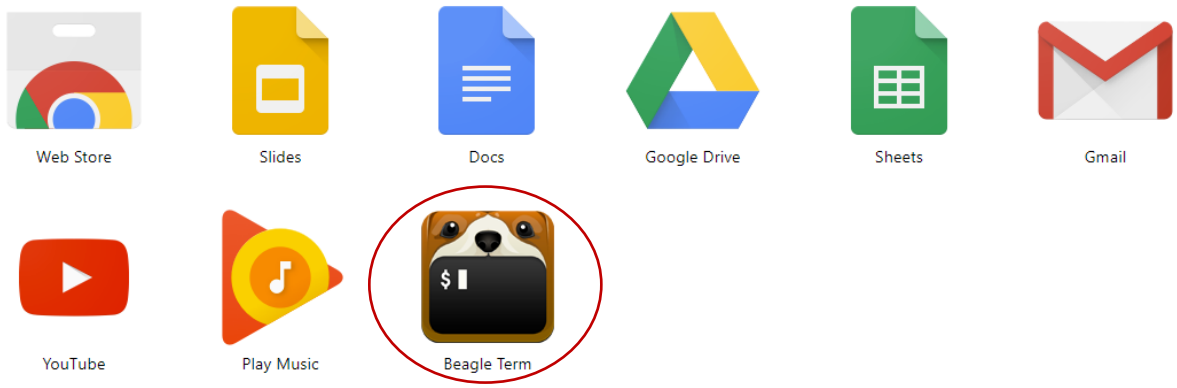

3. Plug in the ESP8266 Feather using the microUSB cable, then launch the Beagle Term app. It will automatically detect the necessary settings if the ESP8266 Feather is plugged in. Click ‘Connect’:

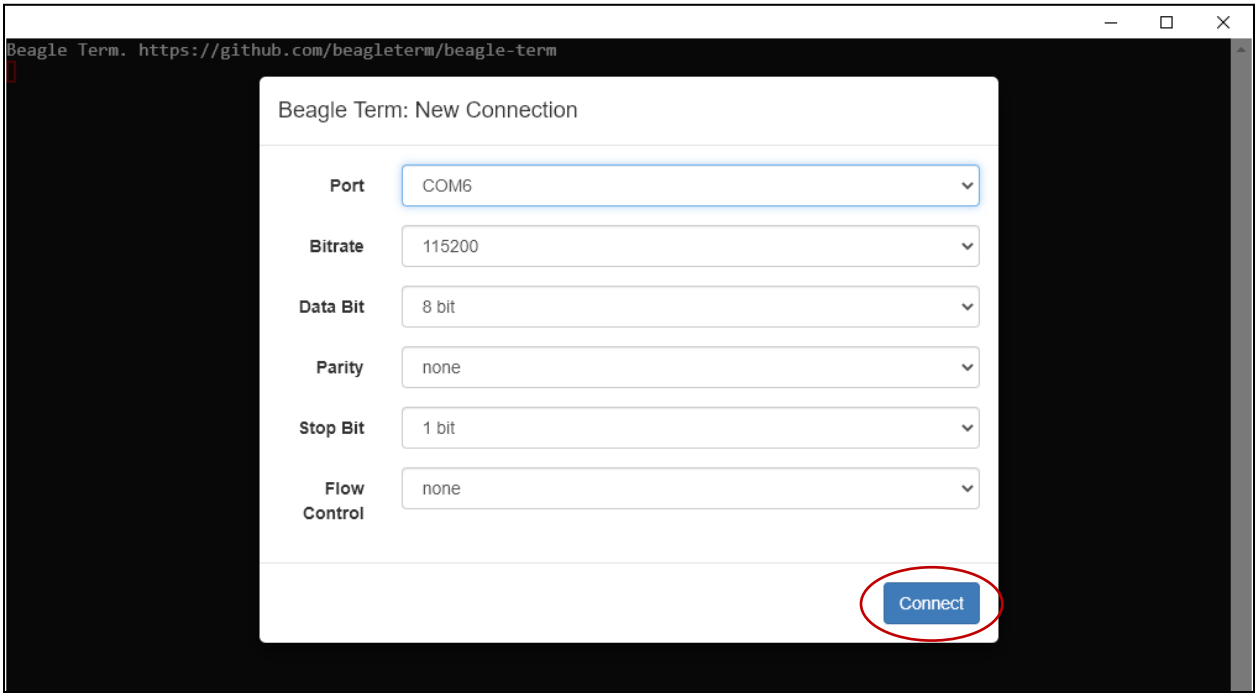

Some computers will require an additional USB to UART driver, available for Mac and Windows. Occasionally Beagle Term will not detect the correct COM port, especially if you are using a Mac. If you are not brought to the correct screen, see if there are other COM port options in the drop-down menu. If so, repeat this process using a different COM port. Often, it will be the highest number COM port. For Macs, try a COM port that contains the address: tty/USBmodem/.

4. Once you connect, click inside the Beagle Term window and press Enter. You should see a screen like the one below, which indicates you are connected to a MicroPython device:

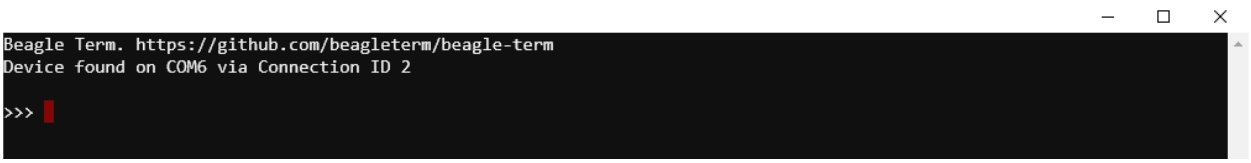

If '>>>' does not appear as shown, try selecting the terminal window with cursor and pressing 'Enter'.

5.9.1.5 Sensor operation

The assembled sensor uses the *hcsr04* library to communicate between the microcontroller and distance module. The library and the associated python script which can be used to collect measurements can be found in the microcontroller code folder of the associated GitHub repository.

The *hcsr04.HCSR04* class requires three input variables:

1. *trigger_pin*, the GPIO pin on the ESP8266 Feather corresponding to the *Trig* pin on the JSN-SR04T (Pin 12 following the instructions in section 4 above).
2. *echo_pin*, the GPIO pin on the ESP8266 Feather corresponding to the *Echo* pin on the JSN-SR04T (Pin 14 following the instructions in section 4 above).
3. *c*, the speed of sound to use to calculate distance.

Since this activity is done in water, have students choose a speed of sound appropriate for the body of water (i.e., 1480 m s^{-1} for freshwater, 1500 m s^{-1} for salt water). Values specific to the body of water being used can be determined using calculations as described in the *Activity Extensions* supplementary material or instrumentation such as conductivity, temperature, and depth (CTD) to better assess the speed of sound for the activity.

To collect a measurement, first import the *hcsr04* library, then you can initialize the sensor with the appropriate pin designations and speed of sound. You can then use the "distance" function to take a measurement (reported in centimeters):

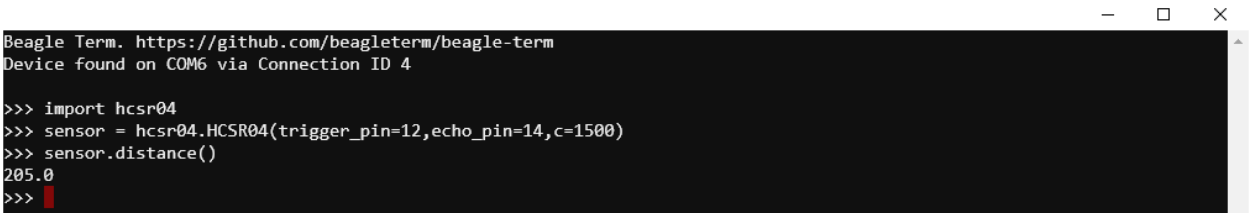

5.9.2 *Activity extensions*

5.9.2.1 Speed of sound

As described in the *Alternative Approaches and Extensions* section, students can use their sensor to identify the speed of sound in air or water by recording observations at a known fixed distance and appropriately varying the speed of sound in order to approach the correct distance in their measurements. We recommend conducting this activity in a prior class period as an opportunity for students to assemble and explore their sensors by collecting repeat measurements.

Supplementary Figure 5.3 Setup for speed of sound activity in air using the JSN-SR04T ultrasonic distance module. A tape measure should be used to set the transducer(s) a fixed distance from the target object (cardboard box).

1. Assemble the sensors according to the instructions provided in the *Sensor Assembly Guide*. In addition to the materials necessary for assembly, students will need a tape measure.
2. Using a ruler and a large object with a flat side such as a book or box, set up the sensor at a fixed distance (> 5 cm) away from the object.

3. Collect 10 measurements, starting with a c of 100 m s^{-1}, increasing c by large steps (50 m s^{-1}) with each measurement. Record and plot the values.
4. Collect another 10 measurements, this time beginning at the value of c from Step 3 which was the closest to the known distance without going over and increase c by 5 m s^{-1} with each measurement. Record and plot the value.
5. Collect another 10 measurements, this time beginning at the value of c from Step 4 which was the closest to the known distance without going over and increase c by 1 m s^{-1} with each measurement. Record and plot the value.

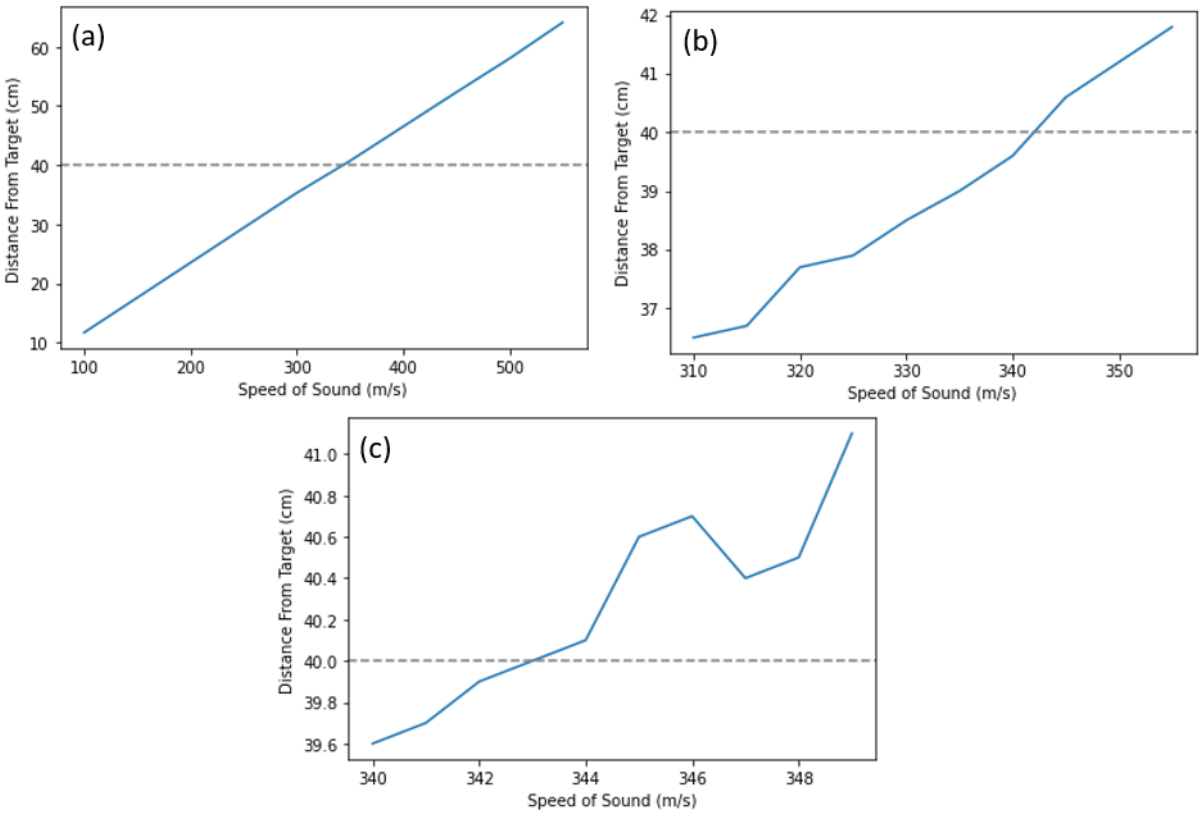

Supplementary Figure 5.4 Example figures showing distance as a function of sound speed in intervals of (a) 50 m s^{-1}, (b) 5 m s^{-1}, and (c) 1 m s^{-1}. Measurements produced by the sensor are shown in blue, with the known distance to the object indicated by the dashed horizontal line.

Students should now be able to approximate the speed of sound in air by incrementally increasing the resolution of their measurements with respect to c. When plotting the values, indicate the known distance as a horizontal line to help identify the closest measurements (Supplementary Figure 5.4).

5.9.2.2 Bathymetric contours

As described in the *Alternative Approaches and Extensions* section, students can use the sensor to take measurements at multiple fixed angles along the original transect. Measurements taken at an angle perpendicular to the transect demonstrate the operation of side-scan and multibeam echosounder systems and can be used to investigate more advanced data processing and visualization methods. While doing this activity, students could consider:

- How does the apparent depth/distance vary as a function of angle?
- What is the maximum angle at which a return echo is received?

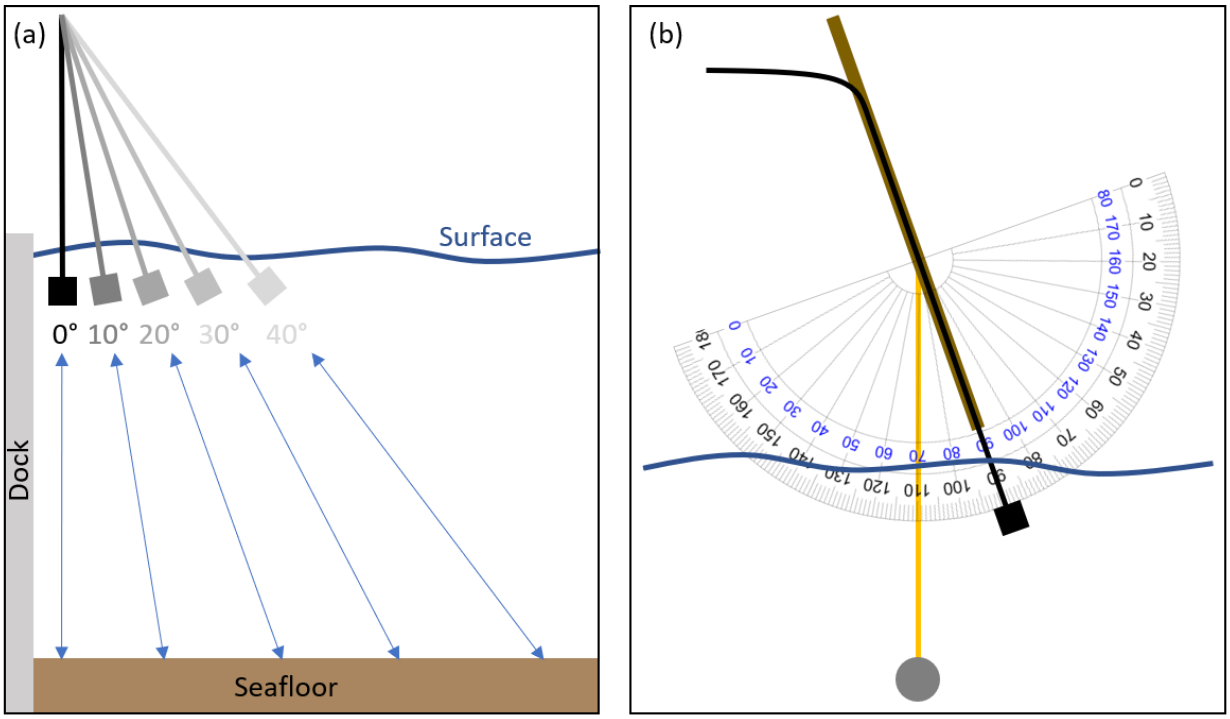

Supplementary Figure 5.5 By increasing the angle relative to a vertical measurement, students can collect distance measurements at positions further away from the dock. (b) Example sensor assembly. The transducer (black) is fixed to a pole at the 90º position on a protractor, with a weighted line attached (yellow/grey) used to indicate the angle.

At each sampling location along the transect, students should take measurements of the seafloor perpendicular to the transect with the transducer face positioned at a known angle (Supplementary Figure 5.5). As with the primary activity, repeat measurements should be collected at each location and angle position to account for potential errors and outliers.

1. Measure the depth with the transducer in a vertical position (0º) at the sampling site, collecting multiple measurements. The depth (z_1) of the seafloor is the distance reported by the sensor (d, Supplementary Figure 5.6a).
2. Setting the transducer face at a fixed angle (such as with a protractor shown in Supplementary Figure 5.5b), collect 3 distance measurements.
3. Calculate the depth (z_2, Figure S6b) at the location where the sound wave reflected off the seafloor. The depth can be calculated as $z_2 = d\sin(a)$, where d is the reported distance and a is the angle of the transducer relative to the surface of the water.
4. To map the measurements, determine the distance between z_1 and z_2 (Supplementary Figure 5.6b, c) as $x = d\cos(a)$.

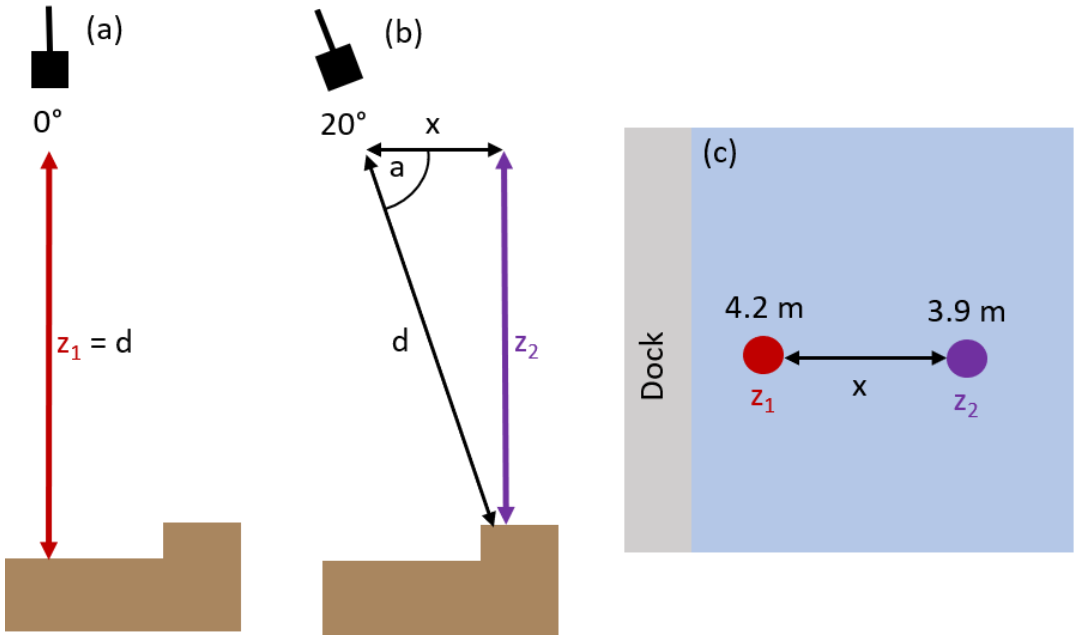

Supplementary Figure 5.6 (a) Initial measurement of depth at the sampling location with transducer in the vertical position. Water depth is the sensor-reported distance (z_1). (b) A measurement taken at the same sampling position with the transducer rotated 20º. Water depth (z_2) can be calculated from the sensor-reported distance *d* and the angle relative to the water's surface *a* using basic trigonometry. (c) Aerial view to compare locations of depths measured in (a) and (b). Using the geometry set up in (b) students can solve for *x* to determine the distance between the downward and angled measurement.

With the data collected, students can create scatter or contour plots using distance away from the dock (x), sampling location (y), and depth (z) for each of their measurements.

5.9.2.3 Additional extensions

For additional extensions, see the associated GitHub repository. These materials will be updated with activities and community suggestions.

5.9.3 *Data analysis files*

Data files for students available at: https://doi.org/10.5670/oceanog.2020.305

File: Student Data Sheet (33-3_levine_S3.xlsx)
File: Bathymetry Lab (33-3_levine_S4.ipynb)

CHAPTER 6. CONCLUSIONS

This dissertation provides new insights into the mechanisms that structure the distribution of pelagic fishes in the eastern Chukchi Sea, and the implications of environmental change on the composition of the pelagic fish community which serve as a key trophic link in the Arctic ecosystem. Rapid transitions are being observed in the physics and biology of the region, thus the timing of this research during this period of change is important to identify how increasing temperatures, decreasing sea ice and other changes are impacting pelagic fishes. This dissertation provides a snapshot of ongoing transitions in fish populations, and a methodological roadmap to assess how climate change will restructure the future Chukchi ecosystem.

6.1 ADVECTION OF AGE-0 FISHES ACROSS THE CHUKCHI SHELF

A key finding throughout Chapters 2, 3, and 4 is that advection, which is dominantly northeastward, is the primary mechanism structuring the pelagic fish community of the eastern Chukchi shelf. The distribution of age-0 Arctic cod and the recent appearance of age-0 pollock on the Chukchi shelf are found to be primarily mediated by transport, which passively displaces these fishes to the northeast over the ice-free period in summer and fall. The spawning locations of the age-0 Arctic cod and pollock are not known. However, given the northward advection of the population, both of these age-0 populations are likely to originate in the northern Bering or southern Chukchi Seas (shaded regions, Figure 6.1). Northward transport in spring and summer moves these age-0 fishes to the northeastern Chukchi shelf. There, they are observed during later-

summer and fall surveys, prior to their subsequent transport towards the Chukchi and Beaufort shelf slopes and the Arctic Basin (Figure 6.1).

I found that movement of age-0 fishes is strongly correlated with local currents, indicating that these fishes are primarily behaving as passive particles as they cross the shelf. Other modeling studies of age-0 gadid distribution have assumed the displacement of these fishes is due to passive drift (Deary et al., 2021; Vestfals et al., 2021). The displacement of fishes by currents was unverified in the field but was nonetheless the basis for the inferred locations of spawning grounds supplying the age-0 Arctic cod population to the Chukchi Sea (green shaded regions, Figure 6.1; Vestfals et al., 2021), and the transport of the age-0 Chukchi Sea population into the Beaufort Sea in fall (Chapter 2). The *in situ* observation of this relationship between fish displacement and water transport presented in Chapter 4 is a key finding in support of circulation models' ability to inform our understanding of the mechanisms that drive species distributions. My observations support the use of circulation models to explore future fish distributions and ecological transitions over longer time scales. The three (five years total) of acoustic observations of pelagic fishes presented in this dissertation provide an expansive dataset with which to refine and ground-truth predictive models.

6.2 Connectivity of Arctic cod across the Pacific Arctic

Both model and mooring observations provide strong evidence for the northeastward displacement of fishes off the Chukchi shelf towards the shelf slope and Arctic basin. For Arctic cod, their future may include recruitment to the age-1+ populations observed in Arctic waters. Age-1+ Arctic cod are found in low abundances on the Chukchi shelf, indicating that these fish may transition to

greater depths in the water column as they grow. Adult Arctic cod have been observed at > 150 m along the Chukchi (De Robertis et al., 2017) and Beaufort (Parker-Stetter et al., 2011; Rand and Logerwell, 2011) shelf slopes. Once the age-0 population of Arctic cod is displaced off the shelf, these fish may move deeper in the water column, e.g., to 150-300 m where they can reside in warmer (> 0 °C) Atlantic Water (Crawford et al., 2012). Vertical segregation by size has also been observed in the Canadian Beaufort (Geoffroy et al., 2016) with larger age-1+ Arctic cod present at depth. Low genetic differentiation between western Beaufort and Chukchi Arctic cod populations indicate that these populations are interconnected (Nelson et al., 2020), and leads us to hypothesize that the age-0 Arctic cod in the Chukchi Sea may recruit to the Beaufort and other populations along the shelf slope of the Arctic basin.

A key question remains: what is the connection between the hypothesized southern spawning grounds and the observed population of adult Arctic cod in the western Beaufort (green dashed arrow, Figure 6.1)? The work presented in this dissertation is consistent with previous studies, which, based on the egg production potential of age-1+ fishes observed in the eastern Chukchi, hypothesized that the age-0 Arctic cod population originates from a larger spawning population outside the study area (Marsh et al., 2019). Yet, adult gadids are capable of long-distance migrations of hundreds or thousands of kilometers (Robichaud and Rose, 2004; Kessel et al., 2017). Thus, the Beaufort Sea may serve as a wintering ground for age-1+ Arctic cod, with some portion of the mature population returning to the southern Chukchi and northern Bering to spawn with the seasonal advance of sea ice.

6.3 A ONE-WAY JOURNEY FOR AGE-0 POLLOCK?

Chapter 3 proposed a similar advection hypothesis for pollock: the age-0 pollock population observed on the Chukchi shelf in summer 2017 and 2019 likely originates from the large population of adult pollock observed in the northern Bering Sea (purple shaded region, Figure 6.1) that was present in both of those years (Eisner et al., 2020). The eggs and larval fish are transported north into the Chukchi Sea by the prevailing currents, where they are observed in summer. For pollock, a key piece of future work should be to address the fate of the age-0 population following their advection towards the shelf slope in late fall.

Larger age-1+ walleye pollock are highly mobile compared to age-0 pollock. In the Bering Sea, the seasonal cooling of bottom temperatures on the inner shelf during surface sea-ice formation leads to the movement of the adult population towards the outer shelf in winter to avoid the cold bottom water (Kotwicki et al., 2005). As the Bering Sea pollock population continues to expand north, even if adult pollock move north into the Chukchi Sea in summer, this dynamic, in which adult pollock retreat ahead of the formation of cold bottom waters, may happen on the Chukchi shelf as well. I.e., these larger fishes may return south to the Bering Sea to avoid the cold winter waters, rather than remaining in the Chukchi permanently. Therefore, the establishment of permanent populations in the Chukchi Sea may depend on the ability of adult pollock to seek refuge as long as seasonal ice cover persists. The age-0 fishes, however, lack the swimming ability of larger mature adults, and additional work is needed to identify the potential mortality of the population in the near future as they continue to encounter sub-zero temperatures in winter.

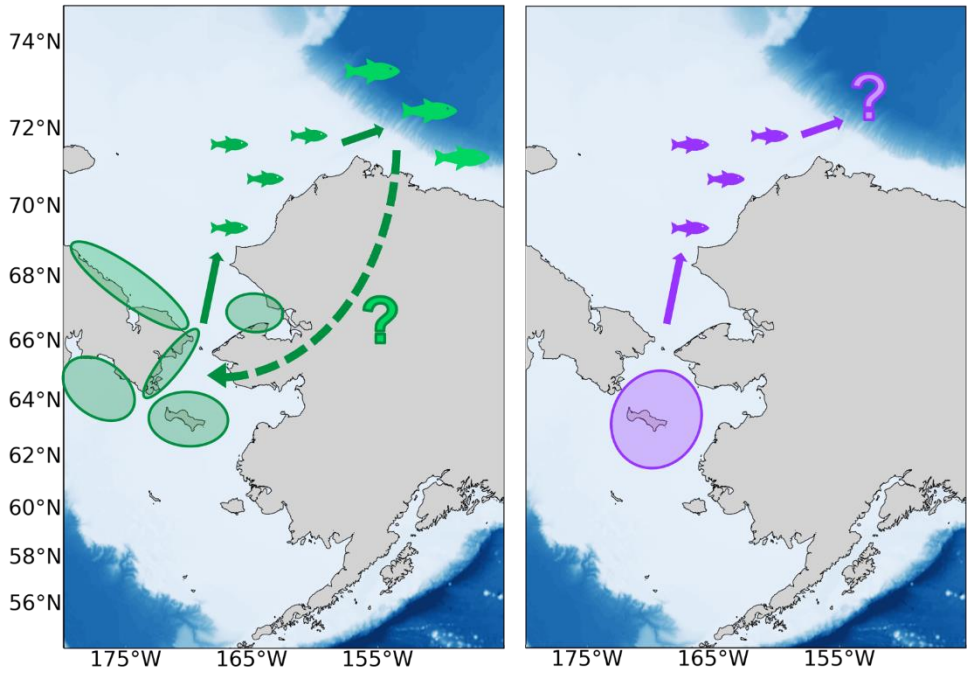

Figure 6.1 Maps of the Pacific Arctic showing the hypothesized transport pathways for Arctic cod (left, green) and walleye pollock (right, purple) and. Spawning grounds are indicated by the shaded regions (Eisner et al., 2020; Vestfals et al., 2021). The key remaining questions regarding the fate of these age-0 populations are indicated by the questions marks: (left) What is the connection between Beaufort Sea age-1+ fishes and the hypothesized spawning populations in the southern Chukchi and northern Bering Seas (dashed green arrow)? (right) What is the fate of age-0 pollock experiencing polar winter?

6.4 CONSIDERATIONS FOR FUTURE WORK

For the first time in the past 50+ years of survey observations, large numbers of southern-origin fishes are invading the Chukchi Sea, and we still know quite little about the consequences of such a shift in species distribution. A major part of the ecosystem transition being observed is the movement of Bering-origin species into the Chukchi Sea in summer, Thus, a key focus of future

work should be investigating the movement of fishes through the Bering Strait. The increases in transport through the Bering Strait over recent decades are well documented (Woodgate and Peralta-Ferriz, 2021). Given the relationship between fish and currents presented here, the implications of any potential continued increase in transport should be investigated further. If the Chukchi and Beaufort Seas serve as a sink for age-0 pollock population observed in summer, what are the implications for pollock recruitment in the northern Bering Sea? For example, does the abundance of age-0 fishes in the Chukchi represent a significant portion of the reproductive potential of adult pollock in the northern Bering Sea, and if so, what are the consequences of the potential loss of future spawning population as a result of these fishes being transported into Arctic conditions? And where did they go in prior years, before they entered the Chukchi? This further highlights the need for estimates of mortality for both Arctic cod and pollock as they enter polar winter and constraining mortality should be a key consideration for future studies.

One possible avenue of addressing these remaining questions is the continued use of moored platforms to investigate population movement. Chapter 4 demonstrates the potential for using split-beam moored echosounder systems to estimate movement and flux of fishes. Echosounders use target strength as a proxy for size, enabling them useful to distinguish age-0 fishes from adults. While we did not observe evidence of a significant number of adult fishes, the placement of the moorings in Chapter 4 was based on previous observations of age-0 fishes, intentionally capturing the movement of the juvenile population. There are likely to be a variety of pathways by which fish might return south across the Chukchi shelf, and a potential alternative

arrangement, e.g., focusing efforts across potential “gateways” such as Barrow Canyon or Bering Strait, may be more appropriate for capturing the spawning migrations of adult fish, though they may migrate within Russian waters which we do not have the ability to sample. The high interannual variability in distribution (Chapter 3) may also indicate the need for moorings to track the movement of age-0 fishes further away from the influence of the Alaskan Coastal Current such as west of Hanna Shoal or the central shelf.

A key limitation of acoustic observations is species identification. This is increasingly important in the Pacific Arctic, due to the changing species distributions as a result of the changing environment. We can no longer assume that the pelagic scatterers on the Chukchi shelf are dominated by Arctic cod. In Chapters 2 and 4, age-0 gadids as a group were assumed to be the dominant pelagic scatterers based on trawl sampling during summer ship-based surveys (Chapter 3). However, the identification of species is necessary to determine spatial and temporal variability in species distributions and abundance. Genetic analyses were necessary to identify and further ground-truth the transition in species composition between Arctic cod and pollock in the acoustic-trawl survey samples (Chapter 3). While these species were grouped together in the application of autonomous observations in this dissertation (Chapters 2 and 4), further unraveling the spatial relationships between Arctic cod and pollock will advance our understanding of how continued changes in the region will alter species distributions.

The inability to identify species is a key limitation of autonomous acoustic applications. The development of broadband signal analysis, while applicable at some taxonomic levels (Ross

et al., 2013), is less informative in differentiating among species with similar scattering properties (Bassett at el., 2018). Age-0 pollock and Arctic cod have similar target strengths (Traynor, 1996; Geoffroy et al., 2016) and the morphological similarities between age-0 gadids that make visual identification difficult are similarly confounding from an acoustic perspective. Genetic sampling and analysis were necessary to confirm species identifications in the survey samples (Wildes et al., in prep; Chapter 3), and the integration of genetics with acoustic observations offers a promising starting point to investigate how to resolve species presence at a finer resolution. Environmental DNA (eDNA) analyses, which can provide indices of species presence/absence, has been used to tease apart species composition in migrating scattering layers in other environments (Easson et a., 2020). The development of autonomous samplers that can either analyze eDNA in situ (Hansen et al., 2020) or preserve water samples for later analysis (Wietz et al., 2021) may allow for future concurrent sampling with acoustic moorings to detect transitions in species compositions and inform species assignment of acoustic data.

The need for improved species identification is particularly important to capture transitions in community structure during what appears to be a period of rapid change. The transition in pelagic fish community composition observed between 2012 and 2019 (Chapter 3) is evidence of a need for increased frequency of observations in the Pacific Arctic. This appears to be a pivotal transition period (Huntington et al., 2020; Mueter et al., 2021), however, surveys in the region are not regular occurrences, and may be conducted with varying gear types (Logerwell et al., 2015) that can introduce species-specific sampling biases (Kotwicki et al., 2017). Further, we lack

connectivity of observations across the Chukchi shelf, since only half the Chukchi is in U.S. waters. In the Russian portion of the Chukchi shelf, similar increases in boreal species have been observed (Orlov et al., 2019), and transport models indicate that there is likely east-west transport across the entirety of the shelf (Vestfals et al., 2021), potentially following the ice-edge front that forms during ice retreat (Lu et al., 2020). The movement of water and fishes is not restrained by political boundaries, thus the impact of the changing environment on the pelagic ecosystem can only be understood via observations across the entire shelf, or at least an improved knowledge of the movement of fishes between the eastern and western Chukchi shelf. This could be addressed with collaborative surveys with Russian colleagues, or direct observations of fish movement between sectors of the Chukchi (e.g., placement of moorings to estimate flux across political boundaries). Previous large-scale collaborations with Russian research groups have been successful, conducting surveys across the Russian U.S. sectors of the Bering and Chukchi Seas (O'Conner et al., 1992; Crane and Ostrovskiy, 2015). Transboundary surveys or collaborative studies that standardize and integrate survey observations between the eastern and western sectors of the Pacific Arctic would greatly enhance our understanding of continuing impacts on fish populations. In particular, surveys of the Gulf of Anadyr and the northwestern Bering Sea will help to validate the spawning regions of Arctic cod proposed by modeling studies (Vestfals et al., 2021).

6.5 FOSTERING FUTURE GENERATIONS OF ACOUSTICIANS

Given the potential of acoustics as a tool to investigate such ecological questions as those addressed in this dissertation, it is important to engage students with these acoustic methods and

technologies early in their academic careers. The final chapter in this dissertation (Chapter 5) provides students and educators with the structure to develop a low-cost, accessible activity in which to explore the principles of underwater acoustics. For many K-12 and undergraduate students, understanding the operation of and the data from oceanographic instruments can be difficult. Many of the instruments used on oceanographic surveys are expensive and may be directly integrated with research vessels, as is the case with many echosounder systems. Thus, access is limited to those with the resources and abilities to gain direct experience on research platforms. With the proliferation of ocean observing systems and the open data provided by them, we are beginning to solve one side of the equation: students now have direct access to high-resolution oceanographic observations. However, they may still lack the hands-on experience that many students need to remain engaged and to understand the calculations underlying such observations and their uncertainties. Additionally, the analysis of archived datasets may not translate to students' experiences; having agency over their own data collection gives them an opportunity to use these tools and principles in a familiar and relatable environment. The activity presented here and the additional development of the PublicSensors organization serve as examples of how active learning with simple low-cost electronics can be used to engage students in scientific concepts. Providing students with the knowledge and access to explore the tools used by oceanographers is one step towards engaging the next generation of researchers to observe and mitigate ocean change.

References

Bassett, C., De Robertis, A., Wilson, C.D., 2018. Broadband echosounder measurements of the frequency response of fishes and euphausiids in the Gulf of Alaska. ICES J. Mar. Sci. 75, 1131–1142. https://doi.org/10.1093/icesjms/fsx204

Crane, K., Ostrovskiy, A., 2015. Russian-American Long-term Census of the Arctic: RUSALCA. Oceanography 28, 18–23. https://doi.org/10.5670/oceanog.2015.54

Crawford, R.E., Vagle, S., Carmack, E.C., 2012. Water mass and bathymetric characteristics of polar cod habitat along the continental shelf and slope of the Beaufort and Chukchi seas. Polar Biol. 35, 179–190. https://doi.org/10.1007/s00300-011-1051-9

De Robertis, A., Taylor, K., Wilson, C.D., Farley, E. V., 2017. Abundance and distribution of Arctic cod (Boreogadus saida) and other pelagic fishes over the U.S. Continental Shelf of the Northern Bering and Chukchi Seas. Deep. Res. Part II Top. Stud. Oceanogr. 135, 51–65. https://doi.org/10.1016/j.dsr2.2016.03.002

Deary, A.L., Vestfals, C.D., Mueter, F.J., Logerwell, E.A., Goldstein, E.D., Stabeno, P.J., Danielson, S.L., Hopcroft, R.R., 2021. Seasonal abundance, distribution , and growth of the early life stages of polar cod (*Boreogadus saida*) and saffron cod (*Eleginus gracilis*) in the US Arctic. Polar Biol. https://doi.org/10.1007/s00300-021-02940-2

Easson, C.G., Boswell, K.M., Tucker, N., Warren, J.D., Lopez, J. V, Bolaños, L.M., 2020. Combined eDNA and Acoustic Analysis Reflects Diel Vertical Migration of Mixed Consortia in the Gulf of Mexico 7, 1–14. https://doi.org/10.3389/fmars.2020.00552

Eisner, L.B., Zuenko, Y.I., Basyuk, E.O., Britt, L.L., Duffy-Anderson, J.T., Kotwicki, S., Ladd, C., Cheng, W., 2020. Environmental impacts on walleye pollock (*Gadus chalcogrammus*) distribution across the Bering Sea shelf. Deep. Res. Part II Top. Stud. Oceanogr. 181–182, 104881. https://doi.org/10.1016/j.dsr2.2020.104881

Geoffroy, M., Majewski, A., LeBlanc, M., Gauthier, S., Walkusz, W., Reist, J.D., Fortier, L., 2016. Vertical segregation of age-0 and age-1+ polar cod (*Boreogadus saida*) over the annual cycle in the Canadian Beaufort Sea. Polar Biol. 39, 1023–1037. https://doi.org/10.1007/s00300-015-1811-z

Hansen, B.K., Jacobsen, M.W., Middelboe, A.L., Preston, C.M., Marin, R., Bekkevold, D., Knudsen, S.W., Møller, P.R., Nielsen, E.E., 2020. Remote, autonomous real-time monitoring of environmental DNA from commercial fish. Sci. Rep. 10, 1–8. https://doi.org/10.1038/s41598-020-70206-8

Huntington, H.P., Danielson, S.L., Wiese, F.K., Baker, M., Boveng, P., Citta, J.J., De Robertis, A., Dickson, D.M.S., Farley, E., George, J.C., Iken, K., Kimmel, D.G., Kuletz, K., Ladd, C., Levine, R., Quakenbush, L., Stabeno, P., Stafford, K.M., Stockwell, D., Wilson, C., 2020. Evidence suggests potential transformation of the Pacific Arctic ecosystem is underway. Nat. Clim. Chang. https://doi.org/10.1038/s41558-020-0695-2

Kessel, S.T., Hussey, N.E., Crawford, R.E., Yurkowski, D.J., Webber, D.M., Dick, T.A., Fisk, A.T., 2017. First documented large-scale horizontal movements of individual Arctic cod (*Boreogadus saida*). Can. J. Fish. Aquat. Sci. 74, 292–296. https://doi.org/10.1139/cjfas-2016-0196

Kotwicki, S., Buckley, T.W., Honkalehto, T., Walters, G., 2005. Variation in the distribution of walleye pollock (*Theragra chalcogramma*) with temperature and implications for seasonal migration. Fish. Bull. 103, 574–587.

Kotwicki, S., Lauth, R.R., Williams, K., Goodman, S.E., 2017. Selectivity ratio: A useful tool for comparing size selectivity of multiple survey gears. Fish. Res. 191, 76–86. https://doi.org/10.1016/j.fishres.2017.02.012

Logerwell, E., Busby, M., Carothers, C., Cotton, S., Duffy-Anderson, J., Farley, E., Goddard, P., Heintz, R., Holladay, B., Horne, J., Johnson, S., Lauth, B., Moulton, L., Neff, D., Norcross, B., Parker-Stetter, S., Seigle, J., Sformo, T., 2015. Fish communities across a spectrum of habitats in the western Beaufort Sea and Chukchi Sea. Prog. Oceanogr. 136, 115–132. https://doi.org/10.1016/j.pocean.2015.05.013

Lu, K., Danielson, S., Hedstrom, K., Weingartner, T., 2020. Assessing the role of oceanic heat fluxes on ice ablation of the central Chukchi Sea Shelf. Prog. Oceanogr. 184, 102313. https://doi.org/10.1016/j.pocean.2020.102313

Marsh, J.M., Mueter, F.J., Quinn, T.J., 2019. Environmental and biological influences on the distribution and population dynamics of polar cod (*Boreogadus saida*) in the US Chukchi Sea. Polar Biol. 1971. https://doi.org/10.1007/s00300-019-02561-w

Mueter, F.J., Planque, B., Hunt Jr, G.L., Alabia, I.D., Hirawake, T., Eisner, L., Dalpadado, P., Drinkwater, K.F., Harada, N., Arneberg, P., Saitoh, S.-I., 2021. Possible future scenarios in the Gateways to the Arctic for Subarctic and Arctic marine systems: Prey resources, food webs, fish, and fisheries. ICES J. Mar. Sci.

Nelson, R.J., Bouchard, C., Fortier, L., Majewski, A.R., Reist, J.D., Præbel, K., Madsen, M.L., Rose, G.A., Kessel, S.T., Divoky, G.J., 2020. Circumpolar genetic population structure of

polar cod, *Boreogadus saida*. Polar Biol. 43, 951–961. https://doi.org/10.1007/s00300-020-02660-z

O'Connor, H.J., Izrael, Y.A., Tsyban, A. V, Whitledge, T.E., McRoy, C.P., Coachman, L.K., 1992. Program on long term ecological investigations of the Bering Sea and other Pacific Ocean ecosystems (BERPAC Program), in: Results of the Third Joint US-USSR Bering & Chukchi Seas Expedition (BERPAC), Summer 1988. U.S. Fish and Wildlife Service, Washington, DC., pp. 3–6.

Orlov, A.M., Benzik, A.N., Vedishcheva, E.V., Gafitsky, S.V., Gorbatenko, K.M., Goryanina, S.V., Zubarevich, V.L., Kodryan, K.V., Nosov, M.A., Orlova, S.Y., Pedchenko, A.P., Rybakov, M.O., Sokolov, A.M., Somov, A.A., Subbotin, S.N., Taptygin, M.Y., Firsov, Y.L., Khleborodov, A.S., Chikilev, V.G., 2019. Fisheries research in the Chukchi Sea at the RV «Professor Levanidov» in August 2019: some preliminary results. Tr. VNIRO 178, 206–220. https://doi.org/10.36038/2307-3497-2019-178-206-220

Parker-Stetter, S.L., Horne, J.K., Weingartner, T.J., 2011. Distribution of polar cod and age-0 fish in the U.S. Beaufort Sea. Polar Biol. 34, 1543–1557. https://doi.org/10.1007/s00300-011-1014-1

Rand, K.M., Logerwell, E.A., 2011. The first demersal trawl survey of benthic fish and invertebrates in the Beaufort Sea since the late 1970s. Polar Biol. 34, 475–488. https://doi.org/10.1007/s00300-010-0900-2

Robichaud, D., Rose, G.A., 2004. Migratory behaviour and range in Atlantic cod: Inference from a century of tagging. Fish Fish. 5, 185–214. https://doi.org/10.1111/j.1467-2679.2004.00141.x

Ross, T., Keister, J.E., Lara-Lopez, A., 2013. On the use of high-frequency broadband sonar to classify biological scattering layers from a cabled observatory in Saanich Inlet, British Columbia. Methods Oceanogr. 5, 19–38. https://doi.org/10.1016/j.mio.2013.05.001

Traynor, J., 1996. Target-strength measurements of walleye pollock (*Theragra chalcogramma*) and Pacific whiting (Merluccius productus). ICES J. Mar. Sci. 53, 253–258. https://doi.org/10.1006/jmsc.1996.0031

Vestfals, C.D.C.D., Mueter, F.J.F.J., Hedstrom, K.S.K.S., Laurel, B.J.B.J., Petrik, C.M.C.M., Duffy-Anderson, J.T.J.T., Danielson, S.L.S.L., 2021. Modeling the dispersal of polar cod (*Boreogadus saida*) and saffron cod (*Eleginus gracilis*) early life stages in the Pacific Arctic using a biophysical transport model. Prog. Oceanogr. 196, 102571. https://doi.org/10.1016/j.pocean.2021.102571

Wietz, M., Bienhold, C., Metfies, K., Torres-Valdés, S., von Appen, W.-J., Salter, I., Boetius, A., 2021. The Polar Night Shift: Annual Dynamics and Drivers of Microbial Community Structure in the Arctic Ocean. bioRxiv 2021.04.08.436999. https://doi.org/10.1101/2021.04.08.436999

Woodgate, R.A., Peralta-Ferriz, C., 2021. Warming and Freshening of the Pacific Inflow to the Arctic from 1990-2019 implying dramatic shoaling in Pacific Winter Water ventilation of the Arctic water column. Geophys. Res. Lett. https://doi.org/10.1029/2021GL092528

VITAE

Education

2021 PhD, Oceanography, University of Washington, Seattle, WA.
2014 MS, Geological Sciences, Cornell University, Ithaca, NY.
2012 BS, Environmental Science, Cornell University, Ithaca, NY.

Professional Experience

2016–2021 Graduate Research Assistant, UW School of Oceanography, Seattle, WA.
2014–2016 Advanced Sampling Technology Contractor, Ocean Associates, Incorporated (Contracted to NOAA Alaska Fisheries Science Center), Seattle, WA.

Publications

Published

Levine R, De Robertis A, Grünbaum D, Woodgate R, Mordy C, Mueter F, Cokelet E, Lawrence-Slavas N, Tabisola H. (2021). Autonomous vehicle surveys indicate that flow reversals retain juvenile fishes in a highly advective high-latitude ecosystem. Limnology and Oceanography 66:1139–1154. dx.doi.org/10.1002/lno.11671.

Levine R, Fogaren KE, Rudzin JE, Russoniello CJ, Soule DC, Whitaker JM. (2020). Open data, collaborative working platforms, and interdisciplinary collaboration: building an Early Career Scientist community of practice to leverage Ocean Observatories Initiative data to address critical questions in marine science. Frontiers in Marine Science. dx.doi.org/10.3389/fmars.2020.593512.

Levine R, Seroy S, Grünbaum D. (2020). Sound and the Seafloor: Deter- mining bathymetry using student-built acoustic sensors. Oceanography 33:71–77. dx.doi.org/10.5670/oceanog.2020.305.

Huntington HP, Danielson SL, Wiese FK, Baker M, Boveng P, Citta JJ, De Robertis A, Dickson DM, Farley E, George JC, Iken K, Kimmel DG, Kuletz K, Ladd C, Levine R, Quakenbush L, Stabeno P, Stafford KM, Stockwell D, Wilson C. (2020). Evidence suggests potential transformation of the Pacific Arctic ecosystem is underway. Nature Climate Change 10:342–348. dx.doi.org/10.1038/s41558-020-0695-2.

De Robertis A, Levine R, Wilson CD. (2018). Can a bottom-moored echo sounder array provide a survey-comparable index of abundance? Canadian Journal of Fisheries and Aquatic Sciences 75:629–640. dx.doi.org/10.1139/cjfas-2017-0013.

In preparation

Levine R, De Robertis A, Grünbaum D, Wildes S, Farley EV, Stabeno PJ, Wilson CD. (In review). Climate-driven shifts in pelagic fish distributions in a rapidly changing Pacific Arctic. Deep-Sea Research Part II: Topical Studies in Oceanography.

Stafford K, Farley E, Ferguson M, Kuletz K, Levine R. (In review). Northward range expansion of subarctic upper trophic level animals into the Arctic. Oceanography.

Cooper D, Cieciel K, Copeman L, Emelin P, Logerwell E, Ferm N, Lamb J, Levine R, Axler K, Woodgate RA, Britt L, Lauth R, Laurel B, Orlov AM. (In review). Pacific cod or tikhookeanskaya treska (Gadus macrocephalus) in the Chukchi Sea during recent warm years: Distribution by life stage and age-0 diet and condition. Deep-Sea Research Part II: Topical Studies in Oceanography.

Wildes S, Whittle J, Nguyen H, Marsh M, Karpan K, DAmelio K, Diamond A, Cieciel K, De Robertis A, Levine R, Larson W, Guyon J. (In review). Walleye Pollock breach the Bering Strait: A change of the cods in the Arctic. Deep-Sea Research Part II: Topical Studies in Oceanography.

Levine R, De Robertis A, Grünbaum D, Wilson CD. (In prep.). Multi-year autonomous observations of seasonality in movement, behavior, and growth of pelagic fishes in the Chukchi Sea.

Non-refereed

Levine R. (2020). Environmental drivers of pelagic fish distribution in the U.S. continental shelf region of the Chukchi Sea. Electronic Journal of Applied Multivariate Statistics 10:51–65. hdl.handle.net/1773/19723.

Levine R. (2014). Temporal and Spatial Variability in Euphausiid Abundance, Biomass, and Species Composition at the Northwest Atlantic Shelf Break and Its Canyons (Thesis). Cornell University. hdl.handle.net/1813/38916.

Invited Presentations

Climate-driven changes in abundance, distribution, and composition of the pelagic fish community in the Chukchi Sea. NOAA in Alaska and the Arctic Seminar Series, Virtual. October 2021.

A multiplatform investigation of pelagic fishes in a changing Pacific Arctic. NOAA NWFSC Monster Seminar Jam 2021 Spring Seminar Series, Seattle, WA. May 2021.

Wind, Waves, and (W)robots: Autonomous vehicle surveys of Arctic cod in the Chukchi Sea. UW Program on Climate Change Spring Symposium Series, Seattle, WA. May 2020.

Are age-0 Arctic cod retained over the Chukchi Sea shelf during summer? NOAA EcoFOCI 2019 Fall Seminar Series, Seattle, WA. November 2019.

Departmental Seminars

Go with the flow: Climate-driven transition of the pelagic fish community in the Chukchi Sea. UW Biological Oceanography Lunch Seminar Spring Seminar Series, Seattle, WA. May 2021.

Are age-0 Arctic cod retained over the Chukchi Sea shelf during summer? UW Biological Oceanography Lunch Seminar Fall Seminar Series, Seattle, WA. November 2019.

The role of the Chukchi Sea as a nursery for Arctic cod (Boreogadus saida). UW Biological Oceanography Lunch Seminar Fall Seminar Series, Seattle, WA. December 2018.

Does the Chukchi Sea Serve as a Nursery for Arctic Fishes? UW Biological Oceanography Lunch Seminar Fall Seminar Series, Seattle, WA. January 2018.

Does the Chukchi Sea Serve as a Nursery for Arctic Fishes? UW Oceanography Second Year Symposium, Seattle, WA. November 2017.

Conference Abstracts

Levine R, De Robertis A, Grünbaum D, Wilson C. Where do the fish come from, and where do they go? Seasonal observations of pelagic fishes from echosounder moorings in the Chukchi Sea. Acoustical Society of America, Seattle, WA. November 2021.

Seroy S, Esparza J, Levine R, Wyeth A, Grünbaum D. PublicSensors: Integrating student- built environmental sensors for community science into the classroom. Earth Educators' Rendezvous, Virtual. July 2021.

Levine R, De Robertis A, Grünbaum D, Wilson C, Farley E, Mordy C, Stabeno P. A multiplatform acoustic-based approach to classifying abundance, distribution, and transport of age-0 gadids on the Chukchi shelf. ICES WGFAST, Virtual. April 2021.

De Robertis A, Levine R, Williams K, Wilson C. Modifying a survey trawl to better retain small Arctic fishes. ICES JFATB, Virtual. April 2021.

Levine R, De Robertis A, Grünbaum D, Wilson C, Farley E, Mordy C, Stabeno P. Where do they come from, and where do they go? Abundance, distribution, and transport of age-0 gadids on the Chukchi shelf. Alaska Marine Science Symposium, Virtual. January 2021.

Cooper D, Logerwell E, Emelin P, Cieciel K, Levine R, Axler K, Britt L, Woodgate R, Orlov A. Pacific cod or Treska (Gadus macrocephalus) in the Chukchi Sea. Alaska Marine Science Symposium, Virtual. January 2021.

Esparza J, Seroy S, Levine R, Wyteh A, Crouser D, Clay Burns T, Grünbaum D. The PublicSensors Project: Fostering community science through student-built environmental sensors. SCCS-NY, New York, NY. October 2020.

Levine R, De Robertis A, Wilson C, Grünbaum D, Farley E. Preliminary results of a 2019 acoustic-trawl survey in the U.S. Continental Shelf Region of the Chukchi Sea. Alaska Marine Science Symposium, Anchorage, AK. February 2020.

Levine R, De Robertis A, Grünbaum D, Woodgate R, Mordy C, Cokelet E, Lawrence-Slavas N, Tabisola H. Summer 2018 repeat autonomous vehicle surveys indicate age-0 Arctic cod are largely retained over the Chukchi Sea shelf. Alaska Marine Science Symposium, Anchorage, AK. February 2020.

Levine R, De Robertis A, Grünbaum D, Woodgate R, Mordy C, Cokelet E, Lawrence-Slavas N, Tabisola H. Summer 2018 repeat autonomous vehicle surveys indicate age-0 Arctic cod are largely retained over the Chukchi Sea shelf. Ocean Sciences, San Diego, CA. February 2020.

Cooper D, Cieciel K, Logerwell E, Ferm N, Levine R, Lauth R, Britt L, Ciannelli L. Distribution and Diet of age-0 Pacific Cod in the Chukchi Sea in 2012 and 2017. Alaska Marine Science Symposium, Anchorage, AK. February 2020.

Stopa J, Fogaren K, Kupchik MJ, Levine R, Philip BT, Rudzin JE, Russoniello CJ, Whitaker J. The Ocean Observatories Initiative: a catalyst for early-career, interdisciplinary research. OceanObs, Honolulu, HI. September 2019.

Deemer G, Lyons A, Bassett C, Levine R. Characterizing the high-frequency acoustic response from sea ice over one season of natural environmental forcing in the Chukchi Sea. Underwater Acoustics Conference and Exhibition, Hersonissos, Crete. July 2019.

Levine R, De Robertis A, Wilson C, Grünbaum D, Mordy C, Meinig C, Tabisola H. Observations of Fishes in the U.S. Continental Shelf Region of the Chukchi Sea from Autonomous Vehicles and Moorings. Alaska Marine Science Symposium, Anchorage, AK. January 2019.

Levine R, De Robertis A, Wilson C, Farley E, Grünbaum D. Field Studies to Investigate the Fate of Juvenile Arctic Cod in the U.S. Continental Shelf Region of the Chukchi Sea. Ecosystem Studies of Subarctic and Arctic Seas Annual Science Meeting, Fairbanks, AK. June 2018.

Levine R, De Robertis A, Wilson C, Farley E. Field Studies to Investigate the Fate of Juvenile Arctic Cod in the U.S. Continental Shelf Region of the Chukchi Sea. Alaska Marine Science Symposium, Anchorage, AK. January 2018.

De Robertis A, Levine R, Wilson C. Can a bottom-moored echosounder array provide a survey-comparable index of abundance? ICES WGFAST Annual Meeting, Nelson, New Zealand. April 2017.

Levine R, Lawson GL, Wiebe PH, Lavery AC, Greene CH, Copley NJ. Temporal and spatial variability in euphausiid abundance and species composition at the northwest Atlantic shelf break and its canyons. Ocean Sciences, Honolulu, HI. February 2014.

Ceperley E, Delatolas N, L D, Huth A, Levine R, Mnich M, Moore A, Webster D, Yost J. The Carbon-Neutral Classroom: A User's Guide. Geological Society of America Meeting, Minneapolis, MN. November 2011.

Teaching Experience

2021 Spring Guest Lecturer, Oceanography, UC Davis Earth and Planetary Sciences. Arctic circulation and ecological impact of sea ice reduction.

2021 Spring Guest Lecturer, Arctic Change, UW School of Oceanography. Role of sea ice in Pacific Arctic fisheries.

2019 Winter Guest Lecturer, Foundations of Ocean Sensors, UW School of Oceanography. Microcontroller activity to measure speed of sound and conduct bathymetric survey.

2018 Spring Guest Lecturer, Marine Zooplankton Ecology, UW School of Oceanography. Application of active acoustics for zooplankton ecology.

2018 Winter Teaching Assistant, Foundations of Ocean Sensors, UW School of Oceanography. Assisted with course activities and designed module using ultrasonic acoustic sensors.

2013 Fall Teaching Assistant, Introductory Oceanography, Cornell University. Designed and led laboratory sections, assisted with design and grading of lecture component.

2013 Summer Teaching Assistant, Marine Bioacoustics Workshop, Friday Harbor Laboratories. Classroom and field assistant, guest lecturer for forward calculations and vessel calibration.

2013 Summer Teaching Assistant, Satellite Remote Sensing Training Program, Cornell University. Assisted with computer-based exercises using NASA SeaDAS and Python.

2012 Fall Teaching Assistant, Introductory Oceanography, Cornell University. Designed and led laboratory sections, assisted with design and grading of lecture component.
2011 Summer Teaching Assistant, Satellite Remote Sensing Training Program, Cornell University. Assisted with computer-based exercises using NASA SeaDAS and IDL.

Funding and Grants

2020 Diversity Funding Award (awarded to PublicSensors), UW College of the Environment
2014 Graduate Conference Grant, Cornell University

Awards and Honors

2021 Best Student Oral Presentation Alaska Marine Science Symposium 2020 Best Student Poster Presentation, Alaska Marine Science Symposium 2018 Science Communication Fellow, Pacific Science Center
2014 Bryan Isaacks Excellence in Teaching Award, Cornell University

Workshops and Training Courses

2021 XSEDE HPC Workshop: Big Data and Machine Learning 2020 OceanHackWeek 2020, University of Washington, WA
2019 Principles and Methods of Broadband/Wideband Technologies ICES Training Course, Bergen, Norway
2019 OOI Data Labs Development Workshop, Pacific Grove, CA
2019 OOI Early Career Scientist Interdisciplinary Workshop, Washington, D.C. 2018 OOI Early Career Biology Data Workshop, Rutgers University, NJ
2018 UW Cabled Array Hack Week, University of Washington, WA
2011 Bioacoustical Oceanography Workshop, Friday Harbor Laboratories, WA

Outreach

2020–present Program Developer, PublicSensors.org. Educational initiative providing kits and instruction for hands-on learning with microcontroller-based environmental sensors.
2020 Meet a Scientist, Pacific Science Center Camps for Curious Minds. Present and answer questions on underwater acoustics and Arctic ecology.
2018–2020 Meet a Polar Scientist, Pacific Science Center. Present ecology and dynamics of the Pacific Arctic as part of a live planetarium show titled "Pole to Pole".
2019 Co-Program Leader, UW Aquatic Sciences Open House. Table activity demonstrating microcontroller-based marine sensors.
2018 Co-Program Leader, Pacific Science Center Polar Science Weekend. Hands-on activities exploring microbial life in sea ice.
2017–2018 Facilitator, UW SeaState. Conducted sensor building programs in high school chemistry and oceanography classes in Sequim and South Kitsap, WA in which the students build and use photospectrometers to explore changes in pH.

Service

University

2020 Series Organizer, UW College of the Environment Beyond Academia Speaker Series
2019–2020 UW College of the Environment Student Advisory Council Graduate Senate Liaison
2018–2020 Elections Committee, UW Graduate and Professional Student Senate
2017–2020 School of Oceanography Senator, UW Graduate and Professional Student Senate
2018–2019 Officer, UW Academic and Recreational Graduate Oceanographers

Conferences

2019 Session chair of "Arctic Fishes and Fish Habitat" at Alaska Marine Science Symposium, Anchorage, AK.

Field Experience

2019 R/V *G.O. Sars*, ICES Broadband Workshop, 7 days, Veafjorden.
2019 R/V *Ocean Starr*, NPRB Arctic IERP, 40 days, Chukchi and Beaufort Seas.
2018 USCGC *Healy*, DBO-NCIS Program, 19 days, Chukchi and Beaufort Seas.
2017 R/V *Ocean Starr*, NPRB Arctic IERP, 36 days, Chukchi and Beaufort Seas.
2016 NOAAS *Oscar Dyson*, Pollock Acoustic-Trawl Survey, 40 days, Bering Sea.
2015 NOAAS *Oscar Dyson*, Pollock Acoustic-Trawl Survey, 77 days, Gulf of Alaska.
2014 NOAAS *Oscar Dyson*, Pollock Acoustic-Trawl Survey, 38 days, Bering Sea.
2014 R/V *Tioga*, WHOI OAPS, 4 days, Gulf of Maine.
2013 R/V *Centennial*, FHL Bioacoustics Workshop, 2 days, Puget Sound.
2012 R/V *New Horizon*, WHOI OAPS, 13 days, Northeast Pacific.
2011 R/V *Centennial*, FHL Bioacoustics Workshop, 2 days, Puget Sound.

Authored Software and Datasets

Levine R, Fogaren KE, Rudzin J, Russoniello C, Soule D, Whitaker JM. (2020). Software, data, and additional documentation for: Open data, collaborative working platforms, and interdisciplinary collaboration (v1.0). dx.doi.org/10.5281/zenodo.4150102.

Levine R, De Robertis A, Wilson C. (2020). Acoustic-trawl Abundance Estimates, Arctic Integrated Ecosystem Research Program, 2019. dx.doi.org/10.24431/rw1k5b2.

Levine R, De Robertis A, Wilson C. (2020). Acoustic-trawl Abundance Estimates, Arctic Integrated Ecosystem Research Program, 2017. dx.doi.org/10.24431/rw1k5b1.

Farley E, Levine R. (2020). Surface Trawl Dataset, Arctic Integrated Ecosystem Research Program, August - September 2019. dx.doi.org/10.24431/rw1k58a.

Farley E, Levine R. (2020). Surface Trawl Dataset, Arctic Integrated Ecosystem Research Program, August - September 2017. dx.doi.org/10.24431/rw1k59h.

De Robertis A, Wilson C, Levine R. (2020). Shipboard EK60 - Fisheries Acoustics backscatter data, Arctic Integrated Ecosystem Research Program, Chukchi Sea 2017. dx.doi.org/10.24431/rw1k59l.

De Robertis A, Levine R, Wilson C. (2020). Shipboard EK60 - Fisheries Acoustics backscatter data, Arctic Integrated Ecosystem Research Program, Chukchi Sea 2019. dx.doi.org/10.24431/rw1k59k.
De Robertis A, Levine R. (2020). Midwater Trawl Catch Dataset, Arctic Integrated Ecosystem Research Program, Chukchi Sea August - September 2017. dx.doi.org/10.24431/rw1k59j.
De Robertis A, Levine R. (2020). Midwater Trawl Catch Dataset, Arctic Integrated Ecosystem Research Program, Chukchi Sea August - September 2017. dx.doi.org/10.24431/rw1k59h.
De Robertis A, Levine R. (2020). Arctic IES UTL Directional Acoustic Fish Tracker (DAFT) Platform Data, C4 Mooring Site, Chukchi Sea, August 2017 to September 2019. dx.doi.org/10.24431/rw1k59n.
De Robertis A, Levine R. (2020). Arctic IES UTL Directional Acoustic Fish Tracker (DAFT) Platform Data, C11 Mooring Site, Chukchi Sea, August 2017 to September 2019. dx.doi.org/10.24431/rw1k59m.
De Robertis A, Levine R. (2020). Arctic IES UTL Directional Acoustic Fish Tracker (DAFT) Platform Data, C1 Mooring Site, Chukchi Sea, August 2017 to September 2019. dx.doi.org/10.24431/rw1k59p.